

THE LSPA PROTEINS OF *HAEMOPHILUS DUCREYI*: EXTRACELLULAR  
VIRULENCE FACTORS

APPROVED BY SUPERVISORY COMMITTEE

---

Eric J. Hansen, Ph.D.

---

Michael Gale Jr., Ph.D.

---

Michael V. Norgard, Ph.D.

---

Kim Orth, Ph.D.

DEDICATION

*To my parents, Richard and Mary*

THE LSPA PROTEINS OF *HAEMOPHILUS DUCREYI*: EXTRACELLULAR  
VIRULENCE FACTORS

by

JASON ROBERT MOCK

DISSERTATION

Presented to the Faculty of the Graduate School of Biomedical Sciences

The University of Texas Southwestern Medical Center at Dallas

In Partial Fulfillment of the Requirements

For the Degree of

DOCTOR OF PHILOSOPHY

The University of Texas Southwestern Medical Center at Dallas

Dallas, Texas

May, 2006

Copyright

by

Jason Robert Mock, 2006

All Rights Reserved

## Acknowledgements

When considering those who have played a role during my graduate school career, I am moved by the large number of people who have guided, supported, and contributed their time and energy concerning the efforts contained within this dissertation. Dr. Eric Hansen, my supervising professor, has always provided the encouragement and numerous resources that have allowed me to pursue my work in his laboratory over the last four years. His advice and support for science and life in general, I believe, will in a large way contribute to the physician-scientist I hope to become. The members of my graduate committee (Drs. Michael Gale Jr., Michael V. Norgard, and Kim Orth) have provided their knowledge and time, and I am grateful and honored to have these three outstanding scientists serve on my committee. Two other faculty members, one here at UT Southwestern, Dr. Nicolai S. C. van Oers, and the other at Columbia University Medical Center, Dr. Steven Greenberg, have both provided major contributions to this work, and I am extremely grateful for their advice and help.

All the members of the Hansen laboratory have contributed to and made my graduate experience a positive one. So many years ago, Dr. Christine Ward was the initial member that I interacted with and who got me excited with the directions of the laboratory. She was also the first to work on the LspA proteins and her efforts provided a strong foundation for me to build on. I would like to thank Dr. Wei Wang for her help and positive attitude over the last four years. Past and present members of the *H. ducreyi* group have all been very helpful, including Drs. David Lewis, Joseph Nika, Kaiping Deng, and Merja Vakevainen. After Christine, Merja was the next to move the LspA project along by observing that the two LspA paralogs function to inhibit phagocytic activity of immune cells. Two very important lab members need special mention, Jo Latimer and Ryan Chong, both of whom I have worked closely with during my time in the Hansen laboratory. Jo taught me numerous techniques, demonstrated an unending patience, and showed through example what it takes to keep a laboratory functional. Without her help, hard work, and most importantly, her calming insight into what is important, my success and these results would not have been possible. Ryan Chong has truly been a positive factor and an

important contributor to this work. His intelligence, desire, and interest in science has kept me motivated, and always attempting to move our projects in a positive and forward direction.

I am thankful to the Medical Scientist Training Program for their financial support, as well as Dr. Robert Munford, Dr. Dennis McKearin, and Stephanie Robertson for their support and advice. Special mention should go to Dr. Rodney Ulane and Dr. Michael Brown for allowing me to experiment with how my physician-scientist training would evolve during the last seven years. I would also like to thank Robin Downing for all her supporting efforts in helping me transition smoothly from medical school to graduate school and back again.

Several individuals whom I have shared my studies with outside of the Hansen Lab have also contributed to my experiences during medical and graduate school. Drs. Steven Jennings, Sean Doyle, Marc Herr, Winston Fong, Monica Lopez, Amy Baldwin, Andrew Shulman, Kathy Sumpter, Jason Huntley, Drew Revel, Jon Blevins and Rhea Sumpter have all been my friends and/or scientific collaborators over the last several years. I thank each of them for their support and friendship. Specifically Jon, Drew, and Rhea who share my interest in science and whose help and support were critical.

Lastly, my parents, Dr. Richard Mock and Mary Mock, and my sister Cynthia have always supported my efforts throughout my education, and I know they will continue to be a fundamental part of everything that I do.

THE LSPA PROTEINS OF *HAEMOPHILUS DUCREYI*: EXTRACELLULAR  
VIRULENCE FACTORS

Publication No. \_\_\_\_\_

Jason Robert Mock, Ph.D.

The University of Texas Southwestern Medical Center at Dallas, 2006

Supervising Professor: Eric J. Hansen, Ph.D.

*Haemophilus ducreyi*, the etiologic agent of the sexually transmitted disease chancroid, has been shown to inhibit phagocytosis of both itself and secondary targets in vitro. This inhibitory activity was previously shown to be abrogated by inactivation of the *lspA1* and *lspA2* genes of this pathogen. Avoidance of phagocytosis has been suggested to be a primary method by which *H. ducreyi* persists in humans, and subsequently allows the ulcerative disease process to occur. Like other genital ulcerative diseases, chancroid is associated with an increased risk for acquisition and transmission of the human immunodeficiency virus (HIV), and is an important cofactor in HIV spread in areas where chancroid is prevalent. My studies have focused on the regulation and mechanism of action of the LspA proteins. The regulation studies have demonstrated that transcriptional

regulation of these large extracellular virulence factors does occur, and also suggest that other outer membrane proteins may be regulated by a similar method. Work elucidating the mechanism of action of the LspA proteins has identified a decrease in catalytic activity of Src family protein tyrosine kinases in macrophages exposed to wild-type *H. ducreyi*, leading to a halt in phagocytic cup formation and a subsequent decrease in uptake of opsonized targets. Additional experiments suggest a possible membrane component in immune cells may be responsible for relaying the LspA proteins' inhibitory signal. This is the first example of a bacterial pathogen that suppresses Src family protein tyrosine kinase activity to subvert phagocytic signaling in host cells.



## TABLE OF CONTENTS

	Page
Dedication .....	ii
Acknowledgements .....	v
Abstract .....	vii
Previous Publications .....	xviii
List of Figures .....	xix
List of Tables .....	xxiii
List of Abbreviations .....	xxiv
 CHAPTER ONE. INTRODUCTION .....	 1
 CHAPTER TWO. REVIEW OF LITERATURE .....	 5
I.    Historical Perspective .....	5
II.   Classification of <i>H. ducreyi</i> .....	6
III.  Identification of <i>H. ducreyi</i> .....	7
IV.  Growth and Metabolism of <i>H. ducreyi</i> .....	8
V.    Genetics of <i>H. ducreyi</i> .....	10
VI.   Clinical and Histological Features of Infection .....	12
VII.  Epidemiology .....	14
VIII. Immune Response to Chancroid .....	16

IX.	Chancroid and HIV Transmission .....	17
X.	Treatment of Chancroid .....	18
XI.	Potential Virulence Factors .....	19
	A. Hemoglobin-binding Protein .....	21
	B. Hemolysin .....	22
	C. Fine Tangled Pilus .....	23
	D. Cytolethal Distending Toxin .....	23
	E. Copper-zinc Superoxide Dismutase .....	24
	F. Lipooligosaccharide .....	25
	G. Peptidoglycan-associated Lipoprotein .....	26
	H. Major Outer Membrane Protein .....	27
	I. Porin .....	27
	J. Serum Resistance Protein .....	28
	K. Ducreyi Lectin A .....	29
	L. Tight Adherence Locus .....	29
	M. Collagen Binding Protein .....	29
	N. Large Secreted Protein A .....	30
XII.	Animal Models of Chancroid .....	31
	A. Temperature-dependent Rabbit Model .....	31
	B. Swine Ear Model .....	32
	C. Primate Model .....	32
	D. Mouse Subcutaneous Chamber Model .....	33
XIII.	Human Model of Chancroid .....	34

XIV.	Overview of Phagocytosis .....	36
XV.	FcγR-mediated Phagocytic Signaling .....	37
XVI.	Overview of Src Family Protein Tyrosine Kinases .....	39
CHAPTER THREE. MATERIALS AND METHODS.....		44
I.	Bacterial Strains and Cultivation .....	44
	A. <i>H. ducreyi</i> Strains, Plasmids, and <i>in vitro</i> Cultivation.....	44
	B. <i>E. coli</i> Strains, Plasmids, and <i>in vitro</i> Cultivation .....	45
	C. Bacterial Growth Curves.....	50
II.	Transformation of Bacterial Strains.....	50
	A. Electroporation of <i>H. ducreyi</i> .....	50
	B. Electroporation of <i>E. coli</i> .....	51
	C. Chemical Transformation of <i>E. coli</i> .....	52
III.	Mammalian Cell Lines, Media Conditions, and Protocols .....	53
IV.	DNA and RNA Isolation.....	54
	A. Plasmid Isolation.....	54
	B. Chromosomal DNA Isolation .....	54
	C. RNA Isolation .....	55
V.	Recombinant DNA Techniques .....	57
VI.	Nucleotide Sequence Analysis.....	57
VII.	Differential Display Methodology .....	57
VIII.	Molecular Genetic Techniques .....	60
	A. Construction of GFP Reporter Constructs .....	60

B.	Construction of <i>H. ducreyi</i> Mutants.....	62
I.	<i>sspA</i> Mutant .....	62
II.	HD1380 Mutant .....	65
C.	Construction of Affinity-Tagged Protein Fusion Constructs.....	67
I.	6xHis-Tagged LspA1 Fusion Proteins.....	67
II.	pMAL-Derived LspA1 Fusion Proteins.....	69
III.	pGEX-Based LspA1 YopT-like Region Fusion Proteins .....	71
D.	Construction of Site-Directed Mutations .....	72
IX.	Transposon Mutagenesis of <i>H. ducreyi</i> Constructs Containing the <i>lspB-gfp</i> Reporter Construct.....	74
A.	Tn916 Transposon Mutagenesis .....	74
B.	GFP Expression Measurements .....	75
X.	RT-PCR Analysis .....	75
XI.	Real-Time RT-PCR .....	76
XII.	DNA Affinity Purification Methods .....	77
XIII.	Bacterial Antigen Preparation.....	80
A.	Whole Cell Lysates.....	80
B.	Concentrated Culture Supernatant Fluid.....	80
C.	Preparation of Bacterial Cell Envelopes .....	81
D.	Sarkosyl Extracts of Cell Envelopes.....	81
XIV.	Sodium Dodecyl Sulfate-Polyacrylamide Gel Electrophoresis (SDS-PAGE) .....	82
XV.	Western Blot Analysis .....	83
XVI.	Protein Expression, Purification, and Analysis Methodologies.....	84

A. Agar Plate-Based Extractions for LspA1 .....	84
B. Recombinant Protein Expression and Purification .....	85
I. His-tagged Fusion Proteins .....	85
II. Maltose-Binding Protein Fusion Proteins .....	85
III. Glutathione-S-Transferase Fusion Proteins .....	86
C. Chromatographic Separations Using Ion-Exchange .....	87
XVII. Generation of Immune Sera and Monoclonal Antibodies .....	88
A. Generation of Polyclonal Antisera to Recombinant LspA1 Protein .....	88
B. Generation of a Monoclonal Antibody to Recombinant LspA1 Protein .....	89
XVIII. Phagocytosis Assays .....	90
A. Opsonization of Secondary Targets .....	90
B. Phagocytosis Assays Utilizing Fluorescent Microspheres as a Secondary Target .....	90
C. Phagocytosis Assays Utilizing Opsonized Red Blood Cells as a Secondary Target .....	91
XIX. Immunoprecipitation Methods .....	91
XX. Immunodepletion Method .....	92
XXI. Src Tyrosine Dephosphorylation Assays .....	93
A. Detection of Phosphoproteins by Western Blot Analysis .....	93
XXII. Fractionation of J774A.1 Cells for Detecting Small Rho GTPases .....	93
XXIII. Cdc42 and Rac Activation Assays .....	94
XXIV. <i>In vitro</i> Protein Tyrosine Kinase Assays .....	95
XXV. Protease Treatment of Macrophages .....	96

XXVI. <i>In vitro</i> Protein Tyrosine Phosphatase (PTPase) Assays .....	97
XXVII. Cell Staining and Fluorescent Microscopy .....	98
A. Staining of the J774A.1 Actin Cytoskeleton.....	98
XXVIII. Statistical Methods.....	100

CHAPTER FOUR. INVESTIGATION OF THE MOLECULAR BASIS FOR THE REGULATION OF EXPRESSION OF LSPA1, LSPA2, AND LSPB.....	101
I. Introduction.....	101
II. Results.....	105
A. Real-time RT-PCR Analysis.....	105
B. The <i>lspB-gfp</i> Reporter Construct .....	106
C. Identification of Putative Regulatory Gene Products by Transposon Mutagenesis .....	109
D. Stringent Starvation Protein A (SspA).....	113
E. Identification of DNA-Binding Proteins.....	117
III. Discussion.....	121

CHAPTER FIVE. USE OF DIFFERENTIAL DISPLAY TECHNOLOGY TO ANALYZE <i>HAEMOPHILUS DUCREYI</i> GENE EXPRESSION UNDER VARIOUS GROWTH CONDITIONS .....	124
I. Introduction.....	124
II. Results.....	128
A. RNA Purification .....	128

B. Differential Display cDNA Synthesis.....	129
C. Differential Display Electrophoresis.....	131
D. Differential Display Fragment Cloning .....	132
E. Fragment Sequencing and Homology Searches .....	133
III. Discussion.....	136

## CHAPTER SIX. *HAEMOPHILUS DUCREYI* TARGETS SRC FAMILY PROTEIN

TYROSINE KINASES TO INHIBIT PHAGOCYTIC SIGNALING .....	141
I. Introduction.....	141
II. Results.....	144
A. Evidence for the Involvement of the LspA Proteins in the Inhibition of Phagocytic Activity.....	144
B. Wild-type <i>H. ducreyi</i> Affects Phagocytic Cup Development.....	148
C. <i>H. ducreyi</i> Affects Macrophage Tyrosyl Phosphoproteins.....	150
D. Wild-type <i>H. ducreyi</i> Reduces the Level of Active Src Family Kinase Members .....	151
E. <i>H. ducreyi</i> Reduces the Catalytic Activity of Src Family Tyrosine Kinases...	154
III. Discussion.....	156

## CHAPTER SEVEN. CHARACTERIZATION OF THE INHIBITION OF SRC FAMILY

PROTEIN TYROSINE KINASES BY <i>HAEMOPHILUS DUCREYI</i> .....	161
I. Introduction.....	161
II. Results.....	162

A. The Effects of Chemical Inhibition of Src Protein Tyrosine Kinases on Phagocytic Activity.....	162
B. Wild-type <i>H. ducreyi</i> Reduces the Levels of Active Src Family Kinase Members in Certain Immune Cell Lineages .....	164
C. Proteinase K Treatment of Macrophages Prevents the Decrease in Active-Phospho-Src .....	166
D. Fc $\gamma$ R-Mediated Phagocytosis Signaling Events .....	168
E. Chromatographic Separation and Fractionation of J774A.1 Lysates .....	172
III. Discussion .....	176

## CHAPTER EIGHT. PROTEASE ACTIVITY OF THE LSPA PROTEINS OF

<i>HAEMOPHILUS DUCREYI</i> .....	181
I. Introduction.....	181
II. Results.....	183
A. Multiple Forms of LspA1 Can Be Detected in <i>H. ducreyi</i> Concentrated Culture Supernatant Fluid (CCS).....	183
B. Development of a Monoclonal Antibody Reactive with the Native LspA1 Protein.....	186
C. Extractions from Whole Cells.....	187
D. The LspA Proteins Contain a Region with Homology to YopT.....	190
E. Evidence that the YopT-like Region is Involved in Autocatalytic Cleavage of the C-terminal Half of LspA1.....	192
F. Identification of the Catalytic Residues in the YopT-like Region.....	196



III. Discussion.....	199
CHAPTER NINE. SUMMARY AND CONCLUSIONS .....	201
REFERENCE LIST .....	211
VITAE.....	232

### Prior Publications

- Ward, C.K., Latimer, J.L., Nika, J., Vakevainen, M. **Mock, J.R.**, Deng, K., Blick, R.J., and Hansen, E.J. 2003. Mutations in the *lspA1* and *lspA2* genes of *Haemophilus ducreyi* affect the virulence of this pathogen in an animal model system. *Infect Immun.* **71**:2478-86. Erratum in: *Infect Immun.* 2004. **72**:1221.
- Spinola, S.M., Fortney, K.R., Katz, B.P., Latimer, **Mock, J.R.**, Vakevainen, M., and Hansen, E.J. 2003. *Haemophilus ducreyi* requires an intact *flp* gene cluster for virulence in humans. *Infect Immun.* **71**:7178-82.
- Ward, C.K., **Mock, J.R.**, and Hansen, E.J. 2004. The LspB protein is involved in the secretion of the LspA1 and LspA2 proteins *Haemophilus ducreyi*. *Infect Immun.* **72**:1874-84.
- Mock, J.R.**, Vakevainen, M., Deng, K., Latimer, J.L., Young, J.A., van Oers, N.S., Greenberg, S. and Hansen, E.J. 2005. *Haemophilus ducreyi* targets Src Family protein tyrosine kinases to inhibit phagocytic signaling. *Infect Immun.* **73**:7808-16.

## LIST OF FIGURES

		Page
Figure 1	Transmission electron micrograph of the wild-type <i>H. ducreyi</i> strain 35000HP	6
Figure 2	Chancroid ulcers on the penis of a male patient	13
Figure 3	Prevalence of chancroid in the United States from 1941 – 2001 (CDC)	15
Figure 4	Schematic of key signaling effectors in FcγR-mediated phagocytosis and complement-mediated phagocytosis	39
Figure 5	Schematic of the inactive and active forms of Src family protein tyrosine kinases	42
Figure 6	Western blot analysis of CCS prepared from wild-type and mutant <i>H. ducreyi</i> strains	102
Figure 7	Gene map of the <i>lspA</i> and <i>lspB</i> genes from the 35000HP genome	103
Figure 8	Schematic of the two-partner secretion system involving the LspA and LspB proteins	104
Figure 9	Real-time RT-PCR analysis of the <i>lspA1</i> , <i>lspA2</i> , and <i>lspB</i> transcript levels in the wild-type and <i>lspA1</i> mutant strains	106
Figure 10	Plasmid map of pRB157	107
Figure 11	Outline of <i>lspB-gfp</i> transcriptional reporter construction and subsequent electroporation into wild-type and mutant <i>H. ducreyi</i> strains	108
Figure 12	Outline of Tn916 mutagenesis	110
Figure 13	Stringent starvation protein A	113

Figure 14	GFP expression measurements obtained with the <i>lspB-gfp</i> reporter in various <i>H. ducreyi</i> strains	114
Figure 15	Effect of the <i>sspA</i> mutation on LspA2 and LspB protein levels	116
Figure 16	Overview of experimental procedure for isolating DNA-binding proteins	118
Figure 17	Silver-stained gels for DNA-binding experiments	119
Figure 18	Effect of the HD1380 mutation on LspA protein levels	121
Figure 19	Effect of FCS on LspA secretion	125
Figure 20	Restriction fragment differential display-PCR (RFDD-PCR) method overview	127
Figure 21	RNA isolation and RT-PCR analysis	129
Figure 22	Agarose gel electrophoresis of cDNA	130
Figure 23	Different display profile gel	132
Figure 24	PCR-amplified differential display fragments	133
Figure 25	<i>H. ducreyi</i> inhibits the phagocytic activity of HL-60 cells in vitro	142
Figure 26	Resistance of <i>H. ducreyi</i> 35000HP and the <i>lspA1 lspA2</i> mutant 35000.12 to phagocytosis by J774A.1 macrophages	143
Figure 27	LspA1 protein schematic	145
Figure 28	LspA1-specific antibodies prevent wild-type <i>H. ducreyi</i> CCS from inhibiting phagocytosis	147
Figure 29	Wild-type <i>H. ducreyi</i> halts the progression of phagocytic cup development	149
Figure 30	Effect of wild-type <i>H. ducreyi</i> on phosphotyrosine levels	151

Figure 31	Active Src kinase levels are reduced by wild-type <i>H. ducreyi</i> in immune cell lines	153
Figure 32	The catalytic activity of Src family protein tyrosine kinases is reduced in macrophages incubated with wild-type <i>H. ducreyi</i>	155
Figure 33	Phagocytosis assays measuring the uptake of opsonized RBCs (EIgG) by J774A.1 cells incubated with chemical inhibitors of Src PTK activity	163
Figure 34	Active Src kinase levels are reduced in Jurkat T cells by wild-type <i>H. ducreyi</i>	165
Figure 35	Proteinase K pre-treatment of macrophages prevents reductions in active phospho-Src family PTKs	167
Figure 36	Western blot experiments detecting small Rho GTPases in J774A.1 cell fractions	169
Figure 37	Active small Rho GTPase levels from J774A.1 macrophages incubated with either the <i>H. ducreyi</i> wild-type or the <i>lspA1 lspA2</i> strains	171
Figure 38	Western blot analysis detecting total Hck protein levels in J774A.1 cell fractions	172
Figure 39	Anion-exchange protein separation of J774A.1 lysates incubated with either the <i>H. ducreyi</i> wild-type or <i>lspA1 lspA2</i> mutant strains	173
Figure 40	ELISA-based protein tyrosine phosphatase assays	175
Figure 41	Protein schematic for LspA1 and LspA2 showing regions of homology or interest	182
Figure 42	LspA1 protein schematic showing regions of homology or interest	184

Figure 43	Strain 35000HP CCS probed with polyclonal antisera	185
Figure 44	MAb 3H9 binds native LspA1 protein	187
Figure 45	Western blot analysis of LspA1 proteins from different sources	189
Figure 46	Sequence alignment of the <i>H. ducreyi</i> LspA proteins and the <i>Yersinia pestis</i> YopT protein	191
Figure 47	A MBP-LspA1 fusion protein undergoes autocatalytic cleavage	193
Figure 48	Schematic of MBP-LspA1 fusion proteins	194
Figure 49	Site-directed mutant data for GST-LspA1 fusion proteins	198
Figure 50	Schematic of the hypothesis for a receptor-mediated inhibition of Src PTK activity by the LspA proteins	206

## LIST OF TABLES

	Page
Table 1	CDC recommendations for the treatment of chancroid 19
Table 2	List of putative <i>H. ducreyi</i> virulence factors 20
Table 3	Bacterial strains used in this study 46
Table 4	Plasmids used in this study 47
Table 5	Primers for PCR-based amplification of <i>lspAI</i> and <i>lspB</i> promoter regions 61
Table 6	Primers used for <i>sspA</i> gene cloning and mutant construction 64
Table 7	Primers used for HD1380 gene cloning and mutant construction 66
Table 8	Primers used to amplify fragments of the <i>lspAI</i> gene for cloning into plasmid pQE-30 67
Table 9	Primers used for pMAL cloning experiments 70
Table 10	Primers used for pGEX-based cloning experiments 72
Table 11	Primers used for construction of site-directed mutations 73
Table 12	Primers used for real-time RT-PCR 77
Table 13	Primers used for DNA-binding experiments 79
Table 14	Transposon insertion mutants shown to have altered fluorescence 111
Table 15	Identification of bands excised from silver-stained gels 120
Table 16	List of sequence homology data for inserts derived from the differential display experiments 134

## LIST OF ABBREVIATIONS

aa	amino acids
ATCC	American Type Culture Collection
BHI	brain-heart infusion
bp	base pair
BSA	bovine serum albumin
CA	chocolate agar
CCS	concentrated culture supernatant
cfu	colony forming unit
ECM	extracellular matrix components
EDD	estimated delivery dose
EDTA	ethylenediamine tertracetic acid
FCS	fetal calf serum
g	gram(s)
GFP	green fluorescence protein
GUD	genital ulcer disease
h	hour(s)
HFF	human foreskin fibroblasts
HIV	human immunodeficiency virus
HSV	herpes simplex virus
IPTG	isopropylthio- $\beta$ -D-galactoside



ITAM	immunoreceptor tyrosine-based activation motifs
kb	kilobase
kDa	kilodalton
L	liter
LB	Luria-Bertani broth
LOS	lipooligosaccharide
LPS	lipopolysaccharide
LspA	large supernatant protein A
mA	milliampere
MAb	monoclonal antibody
mg	milligram
μg	microgram
mm	millimeter
MW	molecular weight
NAD	nicotinamide adenine dinucleotide
O. D.	optical density
OMP	outer membrane protein
ORF	open reading frame
PBS	phosphate-buffered saline
PAL	peptidoglycan-associated lipoprotein
PCR	polymerase chain reaction
PAGE	polyacrylamide gel electrophoresis
PMN	polymorphonuclear leukocytes

PTK	protein tyrosine kinase
RFLP	restriction fragment length polymorphism
rpm	revolutions per minute
RSV	Rous sarcoma virus
sCB	supplemental Columbia broth
SDS	sodium dodecyl sulfate
SOD	superoxide dismutase
TEM	transmission electron microscopy
V	volt
vol	volume
wt	weight
x g	times gravity

# CHAPTER ONE

## Introduction

*Haemophilus ducreyi*, a Gram-negative pleomorphic bacterium, is the etiologic agent of chancroid, a sexually transmitted genital ulcer disease (211). Each year, there are an estimated 6 million cases of chancroid worldwide (214), predominantly in sub-Saharan Africa and Southeast Asia where chancroid is a major cause of genital ulceration syndrome. Frequencies of both acquisition and transmission of HIV-1 infection are increased by the presence of chancroidal ulcers (75,83). While chancroid is extremely uncommon in the United States, outbreaks have occurred in urban areas (101).

Despite its prevalence in some countries, chancroid remains one of the least understood sexually transmitted diseases [reviewed in (191)]. Such basic issues as the causes of tissue necrosis and the retardation of healing, both characteristic features of chancroid (191), remain to be explained. Determination of the key elements in the pathogenesis of chancroid has been a difficult task, one made even more complicated by the fastidious nature of *H. ducreyi*. Nonetheless, it has been established that *H. ducreyi* cannot invade intact skin (197) and it is assumed that microabrasions sustained during sexual activity permit penetration of this bacterium into the epidermal layers. Once in this environment, *H. ducreyi* elaborates as yet unidentified virulence factors that result in ulceration.

In lesions generated in the human challenge model for experimental chancroid, *H. ducreyi* attached to phagocytes but remained extracellular, at least through the pustular stage of disease (25,27). This finding led to the hypothesis by Spinola et al. (191) that *H. ducreyi* might survive in vivo by resisting phagocytosis (191). Subsequent studies by Totten and colleagues (223) as well as by Lagergard and co-workers (6) proved that not only can wild-type strains of *H. ducreyi* resist phagocytosis in vitro, but they can also inhibit the phagocytosis of secondary targets (e.g., opsonized erythrocytes). That *H. ducreyi* can inhibit phagocytosis indicates that, in addition to production of the cytolethal distending toxin that can cause apoptosis in some immune cells (79,203), this pathogen also possesses the means to escape one of the most potent effectors of both innate and acquired immunity.

Our laboratory has determined previously that a *H. ducreyi* mutant unable to express the LspA1 and LspA2 proteins lacked the ability to inhibit phagocytic activity of macrophage-like and polymorphonuclear neutrophil (PMN)-like cell lines (215). LspA1 and LspA2 are 86% identical, have calculated masses of 456,211 Da and 542,660 Da, respectively, and are encoded by two of the largest prokaryotic ORFs (12.5 and 14.8 kb, respectively) described to date (219). Together with the LspB outer membrane protein, LspA1 and LspA2 comprise a two-partner secretion system (109) in which LspB is the essential secretion factor (220). Soluble forms of the LspA proteins with apparent molecular weights of 160-270 kDa are detectable in *H. ducreyi* culture supernatant fluid (218,219). Expression of either LspA1 or LspA2 is necessary to inhibit phagocytic activity; therefore, both *lspA1* and *lspA2* must be inactivated in order to eliminate the ability of *H.*

*ducreyi* to inhibit phagocytosis (215). In addition, a *lspB* mutant unable to secrete LspA1 or LspA2 was also unable to inhibit phagocytosis (215). Finally, a *lspA1 lspA2* mutant of *H. ducreyi* exhibited greatly reduced virulence in both the temperature-dependent rabbit model for experimental chancroid (218) and the human challenge model (112).

Herein, I provide additional evidence that the LspA proteins are involved in the inhibition of FcγR-mediated phagocytosis. More importantly, this study demonstrates that this inhibition involves one of the most proximal signaling events in phagocytosis. Incubation of wild-type *H. ducreyi* with immune cells resulted in decreased phosphorylation and reduced catalytic activity of Src family protein tyrosine kinases, leading to an inability to complete phagocytic cup development. This appears to be a novel mechanism for inhibition of phagocytosis by a bacterial pathogen.

This study also describes investigation of the regulation of expression of the LspA proteins. Wild-type *H. ducreyi* expresses more LspA1 than LspA2; however, in a *lspA1* mutant, there is a dramatic increase in LspA2 expression. Furthermore, both proteins can be detected in concentrated culture supernatant fluid (CCS) by Western blot analysis when *H. ducreyi* is grown in broth cultures containing fetal calf serum (FCS); however, when the broth cultures lack FCS, the LspA proteins cannot be detected in CCS.

Finally, efforts were made to purify recombinant LspA1 protein, and I found that a region with homology to a known cysteine protease was involved in auto-processing of the LspA proteins. This putative protease region, with homology to YopT from pathogenic

*Yersinia* species, is found near the C-terminus of the LspA1 protein and is involved in post-translational processing of the LspA proteins themselves, in a manner similar to that seen with another member of this protease family (184).

Please note that material from Chapters One, Three, and Six were previously published in *Infection and Immunity*: Mock, J.R., Vakevainen, M., Deng, K., Latimer, J.L., Young, J.A., van Oers, N.S., Greenberg, S. and Hansen, E.J. 2005. “*Haemophilus ducreyi* targets Src family protein tyrosine kinases to inhibit phagocytic signaling.” *Infect. Immun.* **73**:7808-16., and is reproduced in the dissertation with permission.

## CHAPTER TWO

### Review of Literature

#### I. Historical Perspective

Chancroid is an acute, ulcerative urogenital disease that is transmitted by sexual contact. Leon Bassereau, in 1852, was the first to clearly differentiate the soft, painful chancre of chancroid from the hard, painless chancre of syphilis (91). The etiological agent of chancroid, *Haemophilus ducreyi*, was first described by Augusto Ducrey in 1889 as a “microorganism representing a bacteria” that could be identified in purulent material from the soft chancre of patients (66). Ducrey was able to utilize pus from a chancre to inoculate the forearms of patients, and in doing so, he was able to cause similar chancre-like ulcer formation on the forearms (66). However, Ducrey was unable to grow the bacterium on artificial media. Ducrey’s work was confirmed later by Unna in 1892 who also identified short streptobacillary rods in biopsies of soft chancres (91). Later, Bezancon was the first to culture the microorganism, *Haemophilus ducreyi*, on artificial media (blood agar plates) (29,91). Furthermore, Bezancon was able to fulfill Koch’s postulates by using these media-grown organisms to reproduce chancre-like ulcers on the forearms of volunteers (29). The same organism was then re-isolated from the forearm ulcers, confirming the organism as the etiological agent of chancroid and thus satisfying Koch’s postulates.

## II. Classification of *H. ducreyi*

*Haemophilus ducreyi* is a fastidious, gram-negative coccobacillus, and an electromicrograph of the wild-type strain 35000HP is shown in Figure 1. Members of the *Haemophilus* genus require either X factor (hemin or another porphyrin) or V factor (nicotinamide adenine dinucleotide [NAD]) or both for growth (12,14,142), and these requirements are generally not seen in other bacteria outside of the *Pasteurellaceae* family. The guanine-plus-cytosine (G + C) content of *Haemophilus* species falls within 37% to 44%, and the G + C content of *H. ducreyi* is 38% (142). DNA-RNA hybridization and comparison studies have demonstrated that *H. ducreyi* is a member of the *Pasteurellaceae* family (59).



**Figure 1.** Transmission electron micrograph of the wild-type *H. ducreyi* strain 35000HP.



One report studied the 16S ribosomal RNA sequences of 54 representative strains in the *Pasteurellaceae* family including three *H. ducreyi* strains (ATCC 27722, 35000, and CIP542), and all 54 strains were demonstrated to be members of this family (61). However, DNA hybridization studies have demonstrated that *H. ducreyi* chromosomal DNA was less than 6% related to other members of the genus *Haemophilus* (44). Therefore, *H. ducreyi* is more likely a unique genus, distinct from other members of the *Pasteurellaceae* family based on comparison studies (42,45).

### **III. Identification of *H. ducreyi***

Studies have shown that accurate diagnoses of chancroid by laboratory diagnostic tests range from 33% to 80% (58). The earliest method of identification was visualization by microscopy. *H. ducreyi* is a gram-negative coccobacillus, and morphological forms seen in lesions have been described as “schools of fish” or “railroad tracks” (130). Gram-staining of clinical material has a sensitivity of only 5 – 36%, and is not recommended as a diagnostic method for chancroid (12). In vitro culture of *H. ducreyi* still remains one of the main tools for diagnosing chancroid. However, culturing of lesions caused by *H. ducreyi* has only 75% sensitivity when compared to more sensitive DNA methods, which is most likely due to the fastidious nature of *H. ducreyi* (130). Culture methods do have the advantage in that they allow for further antimicrobial resistance measurements to be performed.

Several other diagnostic methods have been established, such as antigen detection and nucleic acid probe technologies. Several monoclonal antibodies have been raised against outer membrane proteins (118) or against *H. ducreyi* lipooligosaccharide (LOS) (5,100). Sarafian et al. described ribotyping a set of clinical isolates by restriction fragment length polymorphisms (RFLP) (180). This study demonstrated that in endemic areas, such as Kenya, there are many different ribotypes, while in developed countries that have isolated chancroid outbreaks, only a few ribotypes are found (180). These methods are as sensitive as culture; however, these techniques might not be as well suited for resource-poor countries (130).

More recently, polymerase chain reaction (PCR) techniques have been established that allow better diagnosis of chancroid, and PCR has been shown to have higher sensitivity (83-96%) when compared to culture methods (48,116,130). A multiplex PCR (M-PCR) assay, which also recognizes other sexually transmitted disease agents such as *T. pallidum* and HSV types 1 and 2, has been developed and has been demonstrated to be more sensitive than culture methods (143,153). DNA amplification is now the method of choice and is being utilized in endemic areas to diagnose chancroid infections and other genital ulcer diseases.

#### **IV. Growth and Metabolism of *H. ducreyi***

Humans are the only known natural host for *H. ducreyi*, and while several animal models have been developed (see below), *H. ducreyi* is a very fastidious organism. Numerous undefined media have been shown to allow growth of *H. ducreyi* [for a complete review see ref (142)]. One of the more common media is chocolate agar made with GC agar, IsoVitalax, and lysed calf or horse red blood cells containing hemoglobin (93,211). The bacterium grows best at 33°C in a 95% air-5% CO<sub>2</sub> humidified atmosphere. The IsoVitalax is required for growth and appears to provide necessary cysteine, glucose, and glutamine (91). *H. ducreyi* colonies that form on agar are 1-2 mm in size, nonmucoid, and yellow-grey. *H. ducreyi* forms characteristically adherent colonies that are able to be pushed intact across solid media (211). The clumping of the bacteria makes quantitation difficult, and this phenotype needs to be taken into consideration when accurate quantitation of cell numbers is required.

The average doubling time for *H. ducreyi* growing in vitro ranges from 1.8 - 4 h, which is considerably slower than that of other bacteria like *E. coli*, but is consistent with the observations that it takes 48 - 72 h for visible single *H. ducreyi* colonies to form on solid media (211).

One commonly used liquid medium is Colombia broth supplemented with hemin (25 µg/mL) and fetal calf serum (FCS) (2.5% vol/vol). Although the FCS is not necessary for growth, it is probably necessary for some bacterial functions to occur—such as the release of the LspA proteins into the supernatant. It has also been suggested that the serum

binds inhibitory substances produced by the bacterium (211), resulting in the better growth rates seen in the presence of FCS.

*H. ducreyi*, like other members of the genus *Haemophilus*, requires exogenous heme since the organism is unable to synthesize porphyrins or porphobilinogen from  $\delta$ -aminoleuvulinic acid (14,92). The bacterium can utilize hemin, hemoglobin, and bovine catalase as sources of iron, and can also utilize heme and hemoglobin complexed with serum albumin or haptoglobin, respectively (126,211). The minimal heme requirements have been shown to be higher than those for other members of the genus *Haemophilus*, with requirements for *H. ducreyi* ranging from 25-50  $\mu\text{g/mL}$  on solid media and 5  $\mu\text{g/mL}$  in liquid media (211). *H. ducreyi* lacks ferrochelatase, which converts protoporphyrin IX to heme, and this may explain why this bacteria does not produce siderophores (126). *H. ducreyi* also produces a hemoglobin-binding protein (68,69,201) and a hemolysin (67,156-158,208,222), which function in assisting the organism in acquiring needed heme and both are described in further detail below.

## **V. Genetics of *H. ducreyi***

The genome of *H. ducreyi* is a single chromosome 1.7 Mb in size, and was sequenced in 2000 through a collaboration between Dr. Robert Munson at Ohio State University, and Dr. Gregory Mahairas and Dr. Leroy Hood at the Institute for Systems Biology in Seattle. The publication describing these efforts is in preparation, and the

genome sequence, with the most recent annotation, can be accessed through the STDGEN Database website (<http://www.stdgen.lanl.gov>) maintained by Los Alamos National Laboratory. A total of approximately 1,700 putative open reading frames (ORFs) have been identified (191).

There are several detailed reviews that describe the mechanisms of antimicrobial resistance in *H. ducreyi* [for review see ref (142,211)], and unlike many other members of the *Pasteurellaceae* family, this bacterium is not naturally competent for genetic transformation. Briefly, transfer of conjugative plasmids and the ability to mobilize non-conjugative plasmids have been demonstrated in *H. ducreyi* (142). There are numerous plasmids that are shared among *H. ducreyi*, *Enterobacteriaceae*, and *N. gonorrhoeae* which confer antibiotic resistance on these organisms (12). For example, a 4.9 MDa plasmid has been isolated from several clinical isolates (13). This plasmid, pLS88, has had its nucleotide sequenced published (64), and is able to replicate in *H. ducreyi*, *E. coli*, and *H. influenzae*. This plasmid has been utilized as a vector for cloning and complementation in *H. ducreyi* (98,220). More recently, Munson et al. found that several *H. ducreyi* strains contain a genetic element with homology to the *Vibrio* RS1 element that is integrated into the chromosome (144). This element confers NAD (V factor) independence and has the ability to replicate as a plasmid (144).

*H. ducreyi* has been demonstrated to be amenable to genetic manipulation by electroporation. Hansen et al. were the first to demonstrate that plasmid and linear DNA

molecules could be introduced into *H. ducreyi* by electroporation, and, furthermore, use this ability to construct isogenic mutants by allelic exchange (98). Another method for mutant construction was developed by Munson et al., in which they were able to use *lacZ* as a counter-selectable marker to construct *H. ducreyi* isogenic mutants (38). These studies have allowed for investigation of individual *H. ducreyi* genes to determine their possible role in both in vivo and in vitro virulence studies. Several laboratories, including our own, have constructed systems for generalized transposon-mediated mutagenesis of *H. ducreyi* to find virulence determinants, and several have been discovered utilizing these methods (158,198). Having available these genetic tools has allowed for further studies and a better understanding of the pathogenesis of chancroid.

## **VI. Clinical and Histological Feature of Infection**

*H. ducreyi* infects the genital skin surface and mucosal epithelium, but can also establish infections on keratinized stratified squamous epithelium (95,142). Infection is thought to be established through microabrasions that occur during sexual intercourse that allow the bacteria to enter the skin (142). There is then an incubation period which averages between 4 - 7 days, followed by formation of a tender erythematous papule (131). The papule then progresses into a pustule, which after 2 to 3 days ruptures, leading to formation of a shallow ulcer (Fig. 2) (131). The ulcers have ragged and undermined edges, and the base of the ulcer is irregular and can be partially filled with a yellowish-grey exudate (142). Chancroid ulcers are very painful and bleed easily due to the lesion being

highly vascularized and friable (142). In males, the most common sites are the distal prepuce and frenulum, while in females the majority of lesions are at the entrance to the vagina including the labia, cervix, and the perianal region (142). In the absence of antibiotic therapy, ulcers may persist for weeks to months before resolution of the infection (131). Extragenital infections occur rarely and are due to autoinoculation (131). *H. ducreyi* has not been reported to cause systemic infections even in persons who are immunocompromised, such as patients with HIV infections (211).



**Figure 2.** Chancroid ulcers on the penis of a male patient. Photograph reproduced with permission of Dr. David Lewis.

Rare phagedenic chancroid occurs when chancroidal ulcers become secondarily infected with anaerobes such as *Bacteroides* species and *Fusobacterium* species (142). In these infections, there can be acute massive tissue destruction and gangrenous ulceration of the external genitalia (142).

Painful, tender inguinal lymphadenitis can develop in up to 50% patients that allow ulcerative symptoms to persist for at least 1 - 2 weeks before treatment (131). The lymphadenitis is usually unilateral, and the lymph nodes can rapidly progress to fluctuant buboes which can rupture spontaneously, leading to secondary infections (142). Lastly, there have been no reports of *H. ducreyi* causing disease in infants born to mothers with active chancroid during delivery (174).

Chancroid ulcers have been described as having three distinct histologic zones (77,187). The first zone, at the base of the ulcer, contains a narrow layer of necrosis along with fibrin and degenerate polymorphonuclear leukocytes (PMNs). Below this is zone two, which consists of a broad edematous region that is highly vascularized. Below this is zone three, which has a large number of macrophages and CD4 and CD8 T lymphocytes (2,119).

## **VII. Epidemiology**

Each year, there are an estimated 6 million cases of chancroid worldwide (214), predominantly in sub-Saharan Africa and Southeast Asia where chancroid is a major cause of genital ulceration syndrome. The transmission rate of this pathogen is one of the highest for sexually transmitted infections, with a 70% transmission rate following a single sexual exposure (163). Chancroid infections are more often seen in males than females, and the ratio can be as high as 25:1 (male:females) (142). The disease likely persists year after year due to female commercial sex workers serving as a reservoir for *H. ducreyi* infections



(139). Frequencies of both acquisition and transmission of HIV-1 infection are increased by the presence of chancroidal ulcers (75,83). While chancroid is extremely uncommon in the United States, outbreaks have occurred in urban areas (101). The peak of chancroid infections in the United States occurred in 1947 when 9,515 cases were reported to the CDC (Fig. 3) (211).

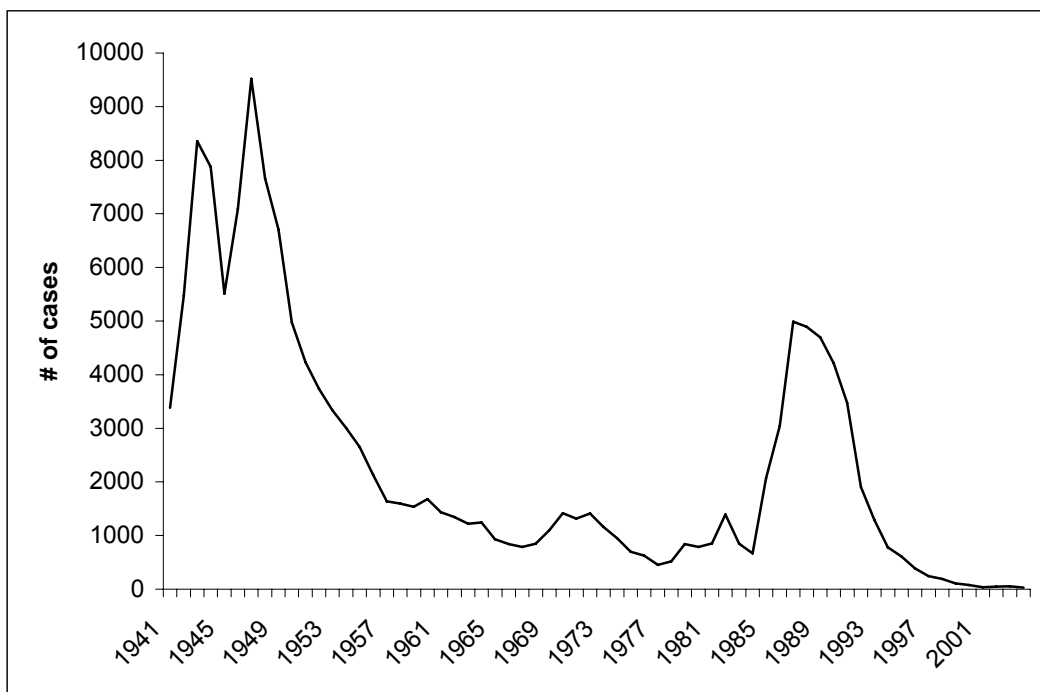


**Figure 3.** Prevalence of chancroid in the United States from 1941 – 2001 (CDC).

This number declined until the mid-1980s when there was a resurgence in the number of cases reported. The peak of this resurgence was 1987 when 4,986 cases were reported (Fig. 3) (211). The increase in number in the 1980s was due to a strong association with crack cocaine abuse in commercial sex workers (62), and likely due to the trading of crack

cocaine for sex. While the number of cases in the United States has declined dramatically, it is thought that the number of cases is still under-diagnosed and under-reported (63,139).

### **VIII. Immune Response to Chancroid**

Similar to the situation with many other sexually transmitted bacterial infections, chancroid patients do not appear to develop protective immunity to the bacterium following infection (30,95). This observation was confirmed in the human challenge model of infection (10,197). Individuals can, however, develop *H. ducreyi*-specific antibodies (41,145), which have been demonstrated in most instances to not play a protective role against infection. The likelihood of antibody production increases with ulcer duration (47). Ulcer biopsies show the presence of neutrophils, macrophages, and T cells (80,105,119), and avirulent *H. ducreyi* strains display a higher susceptibility to killing by phagocytosis and complement-mediated bactericidal activity (150)

After entering the skin through microabrasions, *H. ducreyi* stimulates keratinocytes, endothelial cells, and fibroblasts to secrete IL-6 and IL-8 (191). IL-8 recruits PMNs and macrophages to the lesion, and IL-6 induces IL-2 which leads to recruitment of CD4 cells to the site of infection (191). *H. ducreyi* LOS activates macrophages to secrete TNF- $\alpha$  and IL-12 which direct memory and effector cells to the skin within 24 h of infection (191). From the cytokines that appear in the human challenge model, it appears the human response to chancroid infection is primarily a type 1 or T<sub>H</sub>1 response, and similar to a

delayed-type (type IV) hypersensitivity reaction (159). This type of response elicits antibody production and facilitates phagocytosis and bacterial clearance of extracellular pathogens; however, this antigen-specific response does not seem to cause clearance of *H. ducreyi* (191). Spinola et al. hypothesize that chancroid is an example of immunopathogenesis, in which PMNs and macrophages fail to clear the infection and continue to release their products into the infected area thereby causing further damage to the skin (191).

## **IX. Chancroid and HIV Transmission**

It is estimated that genital ulcer diseases (GUD) increase the risk for transmission and acquisition of HIV (102,115). One epidemiological model of the initial 10-year period (1980-1990) of HIV infections in Africa estimates that 90% of heterosexually acquired HIV infections during this period may be attributed to sexually transmitted disease (173). The proposed mechanism for increased transmission is that ulcers may provide an area which has increased viral shedding (114,163), whereas the proposed mechanism for increased susceptibility to HIV infection is that lesions will have increased numbers of HIV-susceptible cells (CD4 T cells) at the point of viral entry. One study has demonstrated that GUDs increase the risk of HIV transmission from female to male by 50-300 fold and 10-50 fold for male to female (102).

Studies suggest that HIV-positive individuals have increased numbers of chancroidal lesions, which persist longer and are slower to heal (114,115). Treatment failures are also more common in HIV-infected males when compared to HIV-negative individuals (213). Therefore, those patients who are HIV-positive have GUDs that can persist longer and are less susceptible to antimicrobial therapy. This synergy increases the risk of transmitting HIV to their sexual partners.

## **X. Treatment of Chancroid**

Currently, there are no vaccines available for the prevention of chancroid. Treatment for chancroid can prevent transmission to others, resolve symptoms, and cure infection. However, scarring may still result even after successful treatment. *H. ducreyi* has acquired both chromosome-mediated and plasmid-mediated mechanisms of antibiotic resistance (142,211). Plasmid-mediated resistance to tetracycline, chloramphenicol, sulphonamides,  $\beta$ -lactams, and aminoglycosides, and chromosomal-mediated resistance to ciprofloxacin, penicillin, and trimethoprim have all been demonstrated in *H. ducreyi* (131). Table 1 lists the current Center of Disease Control (CDC) recommendation of antibiotics for the treatment of chancroid. It is also recommended that fluctuant buboes be drained to prevent possible rupture and provide patient relief from pain and discomfort (131).

**Table 1.** CDC recommendations for the treatment of chancroid.

Drug	Amount and Duration
Azithromycin	1 gram orally in a single dose
Ceftriaxone	250 milligrams intramuscularly in a single dose
Ciprofloxacin	500 milligrams orally twice a day for 3 days
Erythromycin	500 milligrams orally three times a day for 7 days

## **XI. Potential Virulence Factors**

The introduction of several animal model systems for chancroid in the early 1990s, together with the ability to construct isogenic mutants (98), provided the opportunity to test potential virulence factors for their possible role in pathogenesis. With the development of the human challenge model, these factors could again be examined in this more ideal model system. Additionally, with the completed genome sequence of *H. ducreyi* becoming available in 2000, there were numerous opportunities for further investigation into the mechanisms of *H. ducreyi* disease. Below in Table 2 is a list of potential virulence factors studied to date and the animal model system(s) where their virulence roles have been tested. In the following sections, these potential virulence factors are discussed in more detail as they relate to *H. ducreyi* and chancroid pathogenesis.

**Table 2.** List of putative *H. ducreyi* virulence factors. When appropriate, the animal model where attenuated virulence of the relevant mutant was demonstrated is marked with an X.

Gene	Function	Human Model	Rabbit Model	Pig Model	Primate Model
<i>hgbA</i> (HD2025)	Hemoglobin Receptor	X	X		
<i>hhdA</i> (HD1327)	Hemolysin				
<i>ftpA</i> (HD 0068)	Pilus				
<i>cdtC</i> (HD 0904)	Cytolethal distending toxin				
<i>sodC</i> (HD 0848)	Cu, Zn superoxide dismutase			X	
<i>lst</i> (HD 0686)	LOS sialyltransferase				
<i>losB</i> (HD 1720)	LOS biosynthesis				
<i>gmhA</i> (HD 1228)	LOS biosynthesis		X		
<i>waaF</i> (HD 0653)	LOS biosynthesis		X		
<i>pal</i> (HD 1772)	Peptidoglycan-associated lipoprotein	X			
<i>momp</i> , <i>ompA2</i> (HD 0045), (HD 0046)	Outer membrane proteins				
<i>ompP2A</i> , <i>ompP2B</i> (HD 1433), (HD 1435)	Porins				
<i>dsrA</i> (HD 0769)	Serum Resistance; Attachment	X		X	
<i>dltA</i> (HD 0746)	Serum Resistance;	Partially			

	Attachment	attenuated	
<i>tadA</i> (HD 1304)	Microcolony formation	X	X
<i>ncaA</i> (HD 1920)	Collagen binding	X	X
<i>lspA1</i> , <i>lspA2</i> (HD 1505), (HD 1156)	Inhibition of Phagocytosis	X	X

---

### A. Hemoglobin-binding Protein

Like other members of the genus *Haemophilus*, *H. ducreyi* requires exogenous heme since the organism is unable to synthesize porphyrins or porphobilinogen from  $\delta$ -aminolevulinic acid (14,92). The bacterium can utilize hemin, hemoglobin, and bovine catalase as sources of iron, and can also utilize heme and hemoglobin complexed with serum albumin or haptoglobin, respectively (126,211). *H. ducreyi* produces a hemoglobin-binding protein (68,69,201) and a hemolysin (67,156-158,208,222), which both function in assisting the organism in acquiring needed heme. The hemolysin (describe in the follow section) may affect the release of hemoglobin from erythrocytes. The 110 kDa outer membrane protein HgbA (also called HupA) has been demonstrated to be necessary for the utilization of hemoglobin and hemoglobin-haptoglobin as heme sources (68,69,71,201). An isogenic *hgbA* (HD ORF 2025) mutant was shown to have attenuated virulence in the temperature-dependent rabbit model and the human challenge model (9,201). Recently, Elkins et al. have shown that immunization of pigs with purified HgbA provides protection

against *H. ducreyi* infection in this animal model system (4). HgbA may prove to be a possible vaccine candidate.

## **B. Hemolysin**

Hemolytic activity has been identified in wild-type *H. ducreyi* (156), and two separate groups independently characterized and cloned the hemolysin gene *hhdA* (HD ORF 1327) responsible for the hemolytic phenotype (158,208). The *hhdA* ORF encodes a 125 kDa protein that is secreted by the 61 kDa HhdB protein (158). The *H. ducreyi* hemolysin has homology to the calcium-independent, pore-forming hemolysins of *Proteus mirabilis* and *Serratia marcescens*, and likely functions in a similar manner (67). Totten et al. further demonstrated that the hemolysin has cytotoxic activity on human foreskin fibroblasts (HFF) and human foreskin epithelial cells (16,222), while Munson et al. reported that an isogenic hemolysin mutant lacked the ability to produce this cytopathic effect on HFF (155). The range of cell types affected by the hemolysin include fibroblasts, epithelial cells, macrophages, B lymphocytes and T lymphocytes, and the hemolysin's cytolytic activity may contribute, at least in part, to the formation of chancroidal ulcers (67,222). In contrast to the hemoglobin-binding protein HgbA, the hemolysin does not appear to be necessary for pustule formation in the human challenge model (160,226) or lesion formation in the temperature-dependent rabbit model (67). The hemolysin appears to not play a role in papule and pustule formation in the human challenge model; however,



its possible role in ulcer formation has not been able to be assessed due to the limitations of this model (160).

### **C. Fine Tangled Pilus**

*H. ducreyi* has been shown to possess fine tangled pili which can be visualized by transmission electron microscopy (TEM), and which have a molecular mass of 24 kDa (193). The gene *ftpA* (HD ORF 0068) encoding the *H. ducreyi* pilin protein, FtpA, was cloned and sequenced and FtpA appears to not be homologous with pilin proteins from other gram-negative bacteria (40). An *ftpA* mutant lacked pili when examined by TEM (40). Additionally, the *ftpA* mutant demonstrated no attenuation in virulence in the temperature-dependent rabbit model or the human challenge model (8). To date, the function of *H. ducreyi*'s fine tangled pilus is unknown, but studies have shown that the pili are not responsible for the bacterium's binding to the extracellular matrix components (ECM) fibronectin, laminin, and type I and III collagen (26).

### **D. Cytolethal Distending Toxin**

*H. ducreyi* has been demonstrated to produce a soluble cytotoxic activity that killed HeLa and HEP-2 cells (122,167,168). Cope et al. further discovered that *H. ducreyi* has a three gene locus containing *cdtA* (HD ORF 0902), *cdtB* (HD ORF 0903), and *cdtC* (HD ORF 0904), which together encoded for the three subunits of the cytolethal distending

holotoxin (52). The cytolethal distending toxin (CDT) family members are found in many gram-negative bacteria, and they characteristically cause cell distention and cytotoxicity (162). The CdtB subunit of CDT was determined to have DNase I activity that is responsible for the cytotoxic effect on eukaryotic cells (124). Frisan et al. have further shown that the *H. ducreyi* cytolethal distending toxin induces cell cycle arrest and apoptosis. It does so by causing double-strand DNA breaks and promoting DNA damage checkpoint pathway activation (53,54,133). In the human challenge model, however, an isogenic *cdtC* mutant was found to be fully virulent (226). As with the hemolysin mutant though, an argument can be made that CDT may play an important role in ulcer formation. However, in the temperature-dependent rabbit model, both *cdtA* and *cdtB* mutants were found to be fully virulent (132). Most recently, Stebbins et al. published the crystal structure of the holotoxin from *H. ducreyi*, demonstrating that the holotoxin is a ternary complex comprised of one CdtA subunit, one CdtB subunit and one CdtC subunit (146).

### **E. Copper-zinc Superoxide Dismutase**

Copper- and zinc- superoxide dismutases ([Cu,Zn]-SODs) are metalloenzymes that convert superoxide radicals to oxygen and hydrogen peroxide, and in doing so, help prevent oxidative damage to the cell (121). The *sodC* gene was cloned and sequenced by several laboratories (123,199), and a *sodC* mutant was found to be more susceptible to killing by extracellular superoxides than wild-type *H. ducreyi*. This result suggested that this periplasmic protein may function in defense against oxidative killing by immune cells

(177). When the *sodC* mutant was tested in the pig model, the mutant was attenuated in lesion formation and a reduced number of bacteria were recovered from lesions, but when the pigs were made neutropenic by treatment with cyclophosphamide, the survival of this mutant and the number of lesions were not significantly different from wild-type (179). These data suggest that the periplasmic protein SodC plays an important role in protecting *H. ducreyi* from oxidative stress. However, when the *sodC* mutant was tested in the human challenge model of infection, no attenuation was observed with the *sodC* mutant strain. Therefore, at least through the initial stages of the disease, SodC does not play an apparent role in virulence (35). Interestingly, Battistoni et al. have published that SodC may also bind heme, suggesting another mechanism by which *H. ducreyi* can acquire necessary heme for growth and metabolism (154).

#### **F. Lipooligosaccharide**

Lipooligosaccharide is a potent inflammatory agent, and the lipid A portion of LOS is responsible for this inflammatory response in the host. The short carbohydrate side chains have been shown to have many functions including immune evasion and serum resistance. For example, it has been demonstrated that the LOS from serum-sensitive *H. ducreyi* strains allowed deposition of complement, while the LOS from serum-resistant strains did not allow complement deposition (151). This is likely due to the addition of N-acetylneuraminic acid (sialic acid) to the LOS molecule of the serum-resistant strains. Sialic acid prevents the deposition of C3b onto the bacterial surface and consequently,

sialylated gram-negative bacteria have increased serum resistance (161). *H. ducreyi* contains a novel sialyltransferase gene, *lst* (HD ORF 0686), which has been shown to not be required for pustule formation in the human challenge model (39,225). Recently, a novel sialic acid transporter was identified in *H. ducreyi* which functions to transport sialic acid via an ABC transporter-type mechanism (164).

Other studies have shown that *H. ducreyi* LOS may function in adherence to human foreskin fibroblasts and keratinocytes (15,81). An *H. ducreyi losB* (HD ORF 1720) mutant exhibited reduced attachment to a human keratinocytes cell line (81); however, the mutant was still fully virulent in the temperature-dependent rabbit model (200) and the human challenge model (225). While many different *H. ducreyi* LOS mutants have been examined only *gmhA* (HD ORF 1228) and *waaF* (HD ORF 0653) mutants were found to have decreased virulence in the temperature-dependent rabbit model (23,24). Both of these mutants produce a truncated LOS molecule.

### **G. Peptidoglycan-associated Lipoprotein**

Peptidoglycan-associated lipoproteins (PALs) help to connect the outer membrane to the peptidoglycan layer (195). *H. ducreyi* expresses a PAL protein encoded by the *pal* gene (HD ORF 1772). The *H. ducreyi pal* mutant has a smaller, more transparent colony phenotype when compared to its parent wild-type strain (76). Furthermore, this mutant is

more sensitive to antibiotics, and was found to have attenuated pustule formation ability in the human challenge model (76).

## **H. Major Outer Membrane Protein**

Two of the major outer membrane proteins in *H. ducreyi* are encoded by the *momp* gene (HD ORF 0045) and *ompA2* gene (HD ORF 0046) and are 72% identical (120). These two genes, located next to one another on the chromosome, are transcribed independently (205). Studies have demonstrated that an *E. coli ompA* mutant is more sensitive to the bactericidal effects of normal human sera than its wild-type parent (221). Similarly, the *H. ducreyi momp* mutant was sensitive to killing by normal human serum while its parent wild-type strain 35000 was serum-resistant (103). However, studies have not shown a direct correlation between the Momp protein and serum resistance, and other work has shown that another protein (DsrA) is primarily responsible for serum resistance of *H. ducreyi* (70). In the *momp* mutant, the expression of OmpA2 was increased when compared to the wild-type parent strain. This may indicate some compensatory mechanism for changes in outer membrane protein levels (205), which may indirectly affect phenotypes like serum resistance.

## **I. Porin**

The *ompP2A* gene (HD ORF 1433) and the *ompP2B* gene (HD ORF 1435) have been demonstrated to encode for the outer membrane proteins OmpP2A and OmpP2B (165). Porin analysis experiments utilizing a black lipid bilayer assay have demonstrated that both OmpP2A and OmpP2B exhibit porin activity with the ability to increase conductance across the lipid bilayer when either recombinant OmpP2A or OmpP2B was added to the bilayer (165). An *ompP2A ompP2B* mutant was found to have no change in lesion formation ability in the human challenge model when compared to its wild-type parent (111). Interestingly, in a *H. ducreyi momp* mutant, there appeared to be an increase in expression of OmpP2B (111,205), which again may indicate some compensatory mechanism for balancing outer membrane protein levels.

## **J. Serum Resistance Protein**

The *dsrA* gene (HD ORF 0769) encodes for a 30 kDa outer membrane protein, DsrA, that has been demonstrated to be necessary and sufficient for serum resistance (70). A *dsrA* mutant exhibited a 10-fold decrease in serum resistance when compared to its wild-type parent (70). The mechanism of serum resistance appears to involve blocking of the binding of IgM to the bacterium, thereby preventing initiation of the classical complement pathway (1). Further studies have shown that DsrA is also involved in attachment of *H. ducreyi* to a human keratinocyte cell line (50). Lastly, a *dsrA* mutant was shown to have decreased virulence in the human challenge model (37).

### **K. Ducreyi Lectin A**

Another outer membrane protein, DltA, encoded by the gene *dltA* (HD ORF 0746) has also been described and shown to play an apparently minor or secondary role in serum resistance (125). This protein was initially identified by its ability to bind fibronectin, and homology searches showed similarity to the ricin  $\beta$ -chain, which suggested this protein could be a lectin (125). Further experiments demonstrated that this outer membrane protein does bind lactose, and may function in binding host glycoproteins (125). In the human challenge, a *dltA* mutant was somewhat attenuated when compared to wild-type bacteria (110).

### **L. Tight Adherence Locus**

*H. ducreyi* has been shown to form microcolonies when cultured with human foreskin fibroblasts (147). A 15-gene cluster in *H. ducreyi*, with homology to the *tad* locus of *Actinobacillus actinomycetemcomitans*, has been demonstrated to be responsible for this phenotype as well as for the ability to attach to human foreskin fibroblasts and plastic in vitro (147). A *tadA* mutant was found to exhibit only a small decrease in virulence in the temperature-dependent rabbit model, while this same mutant was found to be highly attenuated in the human challenge model (147,194).

### **M. Collagen Binding Protein**

The NcaA protein has been demonstrated to be an outer membrane protein that binds collagen type I, and is also necessary for virulence in the pig model of chancroid (49). The recently published article by Janowicz et al., in which the *dltA* mutant was tested in the human challenge model, noted that inactivation of the collagen binding protein gene, *ncaA*, (HD ORF 1920) resulted in attenuation for pustule formation in the human experimental model (110). With the inclusion of this new attenuated mutant, there have been seven *H. ducreyi* mutants (counting the *lspA1 lspA2* mutant as one) that have been demonstrated to have decreased virulence in the human challenge model to date (Table 2).

#### **N. Large Supernatant Protein A**

The *lspA1* and *lspA2* genes are two large paralogs that encode secreted proteins which have been shown to have similar function (215,219). These two proteins are secreted by the outer membrane protein LspB, and are members of what has been termed a two-partner secretion system (109,220). The LspA proteins have been demonstrated to be necessary for inhibition of phagocytosis (215), and recent work has found that the presence of these proteins decreases active Src family protein tyrosine kinase levels in macrophages in vitro (141). More importantly, expression of the *lspA* genes has been demonstrated to be necessary for virulence in both the temperature-dependent rabbit model and the human challenge model (112,218). Determining the mechanism by which this occurs is the main focus of this dissertation, and this work is covered in detail in later sections.



## **XII. Animal Models of Chancroid**

Like studies of other bacterial diseases, chancroid research has benefitted greatly from several different animal models that have allowed studies of the pathogenesis of ulcer formation along with allowing potential virulence determinants to be identified. To date, these models include a temperature-dependent rabbit model, a swine ear model, a primate model, and a mouse chamber model. With the development of the human challenge model by Dr. Spinola's group, the need to use these animal models for basic mutant virulence testing has decreased in recent years. However, animal models do possess certain advantages over studies performed in human volunteers and these are discussed below.

### **A. Temperature-dependent Rabbit Model**

The temperature-dependent rabbit model was developed here at UT Southwestern by the Hansen laboratory. Purcell et al. studied the effect of lowering rabbit skin temperature on the ability of *H. ducreyi* to cause ulcer formation (166). This was based on previous work with *Treponema pallidum* that demonstrated enhanced lesion formation in rabbits by this pathogen when the ambient temperature was reduced to 15 – 17 °C (183). At this temperature, lesions are consistently produced after injection of  $1 \times 10^5$  cfu of *H. ducreyi*, and 24 h after inoculation, the site of injection appears indurated and erythematous with virulent strains of *H. ducreyi* (166). Lesions are scored on a scale of 0 to 4: 0 = no

change at injection site, 1 = erythema, 2 = induration, 3 = nodule, or 4 = necrosis (eschar). Lesions are routinely scored on days 2, 5 and 7, and this model is able to distinguish between virulent, avirulent, and attenuated strains (166,201,218). Furthermore, some level of protective immunity does develop following a single exposure (99) or after immunization with specific *H. ducreyi* components (60,67), which differs from the human, primate, and swine ear models where re-infection can readily be achieved.

### **B. Swine Ear Model**

The swine ear model for chancroid was developed by Hobbs et al. In this swine model, Landrace or Yorkshire Cross pigs develop cutaneous ulcers that are histologically similar to human chancroid lesions (104). The ears are inoculated with approximately  $1 \times 10^7$  cfu on a multi-test applicator, and lesions form 48 h after infection. The lesions are dry and crusty rather than wet and purulent like human chancroidal ulcers (104). Similar to the rabbit model, many different strains and inoculum sizes can be studied in one experiment, with up to 20 different sites on one ear being inoculated. This feature allows virulence comparisons within the same animal. Kawula et al. have also immunodepleted pigs with cyclophosphamide to allow for examination of bacterial virulence in the absence of cell-mediated immunity (178).

### **C. Primate Model**

A primate model for chancroid using adult pigtailed macaques was developed by Totten et al. (207). In this model system, the macaques were inoculated with  $10^7 - 10^8$  cfu on either the foreskin (males) or labia (females). The male macaques developed lesions that closely resembled human chancroid ulcers 6 – 12 days after inoculation, but female macaques did not develop ulcerative lesions. *H. ducreyi* could be recovered from ulcers by swab or biopsy (207). Interestingly, in lesions generated in the human challenge model for experimental chancroid, males were twice as likely to form pustules as women (192), which suggests some underlying difference in susceptibility to *H. ducreyi* infection between men and women. This animal model also allows for studies to be performed that could determine possible interactions between SIV and chancroid—work that would not be possible in humans or other animal models (129).

#### **D. Mouse Subcutaneous Chamber Model**

The mouse subcutaneous chamber model was developed by Trees et al. to provide a method to grow larger numbers of *H. ducreyi* in vivo than those recovered from the other animal models (210). This model was similar to the “Arko golf ball” model for studying *Neisseria gonorrhoeae* in which a plastic chamber was placed subcutaneously in rabbits and left to allow host connective tissue to grow around openings in the polyethylene weeks before bacteria were injected (18,19). This model allowed for a systemic immune response to be studied, and the bacteria could be injected and removed at intervals for further studies (19). The mouse chamber model involved implanting a polyethylene chamber into the

flanks of mice four weeks prior to infection with *H. ducreyi* (210). Chamber fluid could be removed easily, and it was found that infection could be sustained for one month with approximately  $2 \times 10^5$  cfu being recovered one month after inoculation with  $5 \times 10^5$  cfu (210). No other subsequent studies have been published using this model. However, it is the only in vivo model to date to that would allow the study of long-term bacterial growth. This type of model could lend itself to several types of in vivo experiments, such as IVET, RIVET, and STM, that were not available when this model was first published. This model allows for studies on growth, survival, gene transcription, and protein expression, but not on ulcer formation and pathogenesis.

### **XIII. Human Model of Chancroid**

Spinola et al. developed the human challenge model for *H. ducreyi* that involves inoculating the extension surface of the upper arm by means of multi-test applicators, and subsequently monitoring for the development of papules and pustule formation (197). In this model, the applicators are loaded with an inoculum ranging from  $1 \times 10^4$  to  $1 \times 10^6$  cfu. However, it is estimated that only 1 in 1000 cfu are actually delivered to the host by this method (196). Therefore, the estimated delivery dose (EDD) ranges from 10 – 100 cfu, which is probably similar to the dose needed to establish an infection resulting from sexual activity. However, the number of cfu required for a clinical infection is not precisely known (11,196). In this model, papules usually develop within 24 h of inoculation, which will then either progress to pustules or resolve completely. The histopathology of the

papules and pustules is similar to that seen in naturally occurring infections (119,159,197). Furthermore, Dr. Spinola's group has demonstrated that the human challenge model, much like chancroid disease, does not confer protection against re-infection (10). In this model system, papule and pustule formation frequencies have been shown to be dose-dependent. With an EDD of 30 cfu, the papule formation rate is 95%, while the pustules formation rate is only 69% (11). Interestingly, there appears to be a gender difference in pustule formation rates between men and women, with women demonstrating lower pustule formation rates (36,192). This sort of phenomenon is similarly seen in the primate model (207). The hypothesis for this difference, put forth by the Spinola group, is that *H. ducreyi* causes an immune tolerizing response in men that stops immune clearance (i.e., phagocytosis), and sustains an infection which allows for progression to pustules. In this model, women have a more pro-inflammatory response promoting clearance. The Spinola group also suggests that, since women are more prone to loss of self-tolerance (i.e., higher rates of autoimmune diseases), they might not be as susceptible to *H. ducreyi*'s efforts to tolerize itself in the female host, which would allow females to more easily clear infection. This is an interesting hypothesis and efforts to understand how *H. ducreyi* causes disease may lead to a better understanding of the interplay between disease and both innate and adaptive immunity.

In summary, the human challenge model is very useful in determining and assessing the role in virulence of specific *H. ducreyi* factors and provides one of the best methods for studying the interaction of the bacteria and the host in its natural setting. The main

limitation to this model is that the lesions (pustules) must be treated before they develop into ulcers, and consequently, factors that may be involved in ulcer formation and persistence are not as easily studied as they would be in the animal model systems.

#### **XIV. Overview of Phagocytosis**

Phagocytosis is an extremely complex process [for reviews see (3,87,204)] by which cells internalize particles/objects that are at least 1  $\mu\text{m}$  in size. Phagocytosis has evolved from a nutritional function in the amoeba to an immune process in complex organisms (117). In higher organisms, phagocytosis has many functions. In embryogenesis, phagocytosis helps to clear apoptotic cells, and in the immune response phagocytosis functions to engulf foreign organisms to protect the host. Two cellular processes occur during phagocytosis: the first involves cytoskeleton rearrangements and the second is membrane trafficking to cytosolic compartments (87). In leukocytes, phagocytosis has two main immune functions, the first of which is to ingest pathogens and target them for lysosome killing, and the second is to direct antigens to MHC I and MHC II compartments (87). In doing so, phagocytosis plays an important role in both innate immunity and adaptive immune (87).

Bacterial pathogens have devised a number of different strategies for escaping or preventing phagocytosis [for reviews see (136,175)]. These range from the expression of polysaccharide capsules, which can exert a simple physical impediment or even alter

phagocytic signaling [e.g., *Streptococcus suis* (181)], to injection of effector molecules that target signaling components [e.g., *Yersinia* YopT (185), *Pseudomonas* ExoT (202)]. The results presented below (Chapter Six and Seven) describe my initial investigation into determining how the LspA proteins of *H. ducreyi* co-opt the host machinery to down-regulate phagocytosis and subsequently avoid killing by macrophages and neutrophils. The method by which these proteins accomplish this appears to be novel for phagocytosis evasion by bacteria.

## **XV. FcγR-mediated Phagocytic Signaling**

There are two types of FcγR in leukocytes. The first are the activating receptors that contain immunoreceptor tyrosine-based activation motifs (ITAMs), and second are the inhibitory receptors that contain immunoreceptor tyrosine-based inhibition motifs (ITIMs). While binding of IgG-opsonized particles or bacteria to most FcγRs (except the inhibitory FcγRIIB) will initiate the phagocytic signaling cascade, signaling through Toll-like receptors has also recently been shown to affect phagocytosis (31,65). FcγR cross-linking (by IgG-opsonized targets) first results in clustering of FcγRs in the plasma membrane. Src family protein tyrosine kinases, with Hck, Lyn, and Fgr being predominant in murine macrophages, then associate with FcγR and recent work suggests that this association occurs in lipid microdomains in the membrane (74). These protein tyrosine kinases catalyze phosphorylation of the ITAMs (immunoreceptor tyrosine-based activation motifs) present on or associated with FcγRs. Once phosphorylated, the ITAMs become docking

sites for the SH2 domains of the tyrosine kinases Syk and ZAP-70, and type I phosphatidylinositol 3'-kinases (PI3Ks), as well as protein tyrosine phosphatases that help to control and regulate phagocytosis. Following binding to ITAMs, Syk is phosphorylated by Src kinases.

After these initial tyrosine phosphorylation events, the precise pathways and events become a little less clear. Dbp-family guanine nucleotide exchange factors are involved in the activation of the small Rho GTPase Rac and both Cdc42 and Arp6 are also activated. Once they bind GTP, both Cdc42 and Rac are involved in controlling effectors such as WASP which in turn activates the Arp2/3 complex necessary for actin filament assembly and development of the phagocytic cup (Fig. 4). Phosphatidylinositol 3,4,5-trisphosphate and phosphatidylinositol 4,5-bisphosphate accumulate locally in the phagocytic cup and the latter is involved in signaling actin assembly.



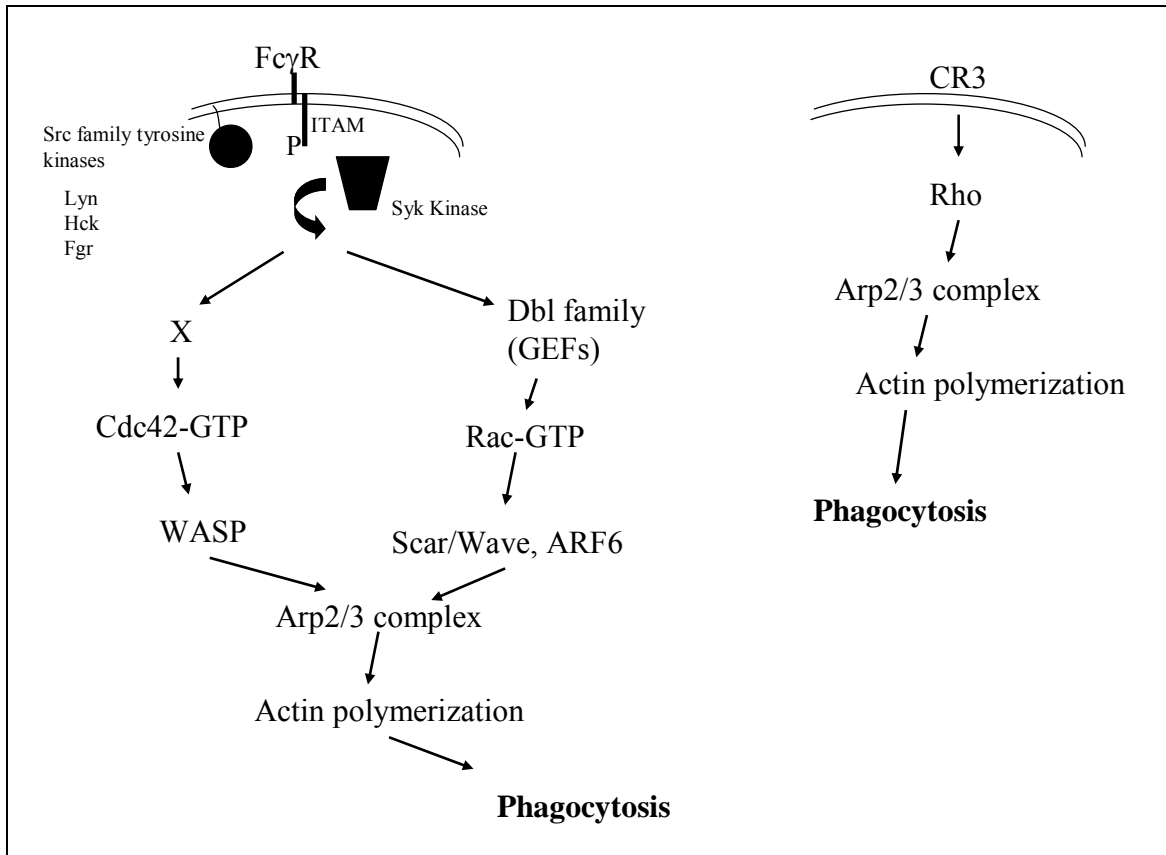


**Figure 4.** Schematic of key signaling effectors in FcγR-mediated phagocytosis and complement-mediated phagocytosis.

Less is known about complement CR3-mediated phagocytic signaling. Some of the same signaling events occur, such as RhoA activation and formation of the Arp2/3 complex to nucleate actin; however, the complement-opsonized particle appears to sink into the membrane and this differs from the pseudopod formation seen in FcγR-mediated phagocytosis (84).

## XVI. Overview of Src Family Protein Tyrosine Kinases

The Src family of protein tyrosine kinases (Src PTKs) are non-receptor tyrosine kinases that play important roles in numerous intracellular signaling pathways (137). The members of this family have been shown to function as both positive and negative regulators of immune signaling, and overall this family of intracellular signaling molecules function as rheostats or volume controls of immune cell signaling [for a review see (134)].

Src PTKs have a distinguished history when one looks at the overall research and scientists who have studied these molecules, and arguably, the investigation of Src PTKs was one of the initial areas providing an understanding into the molecular genetics of cancer. The history of Src research also eloquently demonstrates how the study of an infectious disease not only provides information on the pathogenesis of the disease process, but also provides a better understanding into how our own systems function outside the context of the disease initially studied. More specifically, the initial work on Src involved on the Rous Sarcoma virus (RSV) that was found to cause tumors in chickens (137). In the 1950s, Harry Rubin, Howard Temin and Renato Dulbecco performed work showing that each cell in a Rous sarcoma virus-induced tumor could release infectious virus. Later Temin demonstrated that the morphology of a transformed cell was controlled by a specific genetic property of the virus (137). These studies into the interaction between tumor viruses and the cell helped earn David Baltimore, Renato Dulbecco, and Howard Temin the Noble Prize in 1975. Furthermore, these studies led the way for Michael Bishop and Harold Varmus to identify and sequence the first retroviral oncogene (v-src), and to further

identify its counterpart, the first proto-oncogene (c-src) (137). It is this work that earned Bishop and Varmus the Noble Prize in 1989.

Src PTKs have been shown to be involved in cell processes such as responses to UV light, ethanol consumption, and  $\beta$ -adrenergic signaling (134). In immune cells, Src PTKs have numerous functions in innate immune signaling, antigen and integrin signaling, responses to cytokines, and phagocytosis (134). Src PTKs are found in two different conformations (Fig. 5), a closed, inactive state where a distal tyrosine residue (Y529) is phosphorylated, and an active, open conformation where a more proximal tyrosine residue (Y418) is phosphorylated. The open, active state is when the kinase domain of Src PTKs is able to phosphorylate downstream targets. All Src PTKs contain N-terminal acylation sites for myristate and often also palmitate (depending on the family member) which localize Src PTKs to cell membranes (55). The Src homology 3 (SH3) domains of Src PTKs (Fig. 5) bind polyproline motifs and are required for intracellular association of the kinase with substrates and/or binding partners (134). The Src homology 2 (SH2) domains are necessary for interactions between Src kinases and their substrates. For example, many macrophage proteins involved in phagocytic signaling have SH2 or SH3 domains that are crucial for their function. More specifically, SH2 or SH3 domains are present in some protein kinases and phosphatases involved in the regulation of phagocytosis. SH2 domains are typically about 100 aa in length and bind relatively short amino acid sequences that contain a phosphorylated tyrosine followed by 3-6 specific residues C-terminal to the phosphorylated

tyrosine. SH3 domains typically contain about 60 aa and bind the consensus sequence XPXXPPFXXP (137).

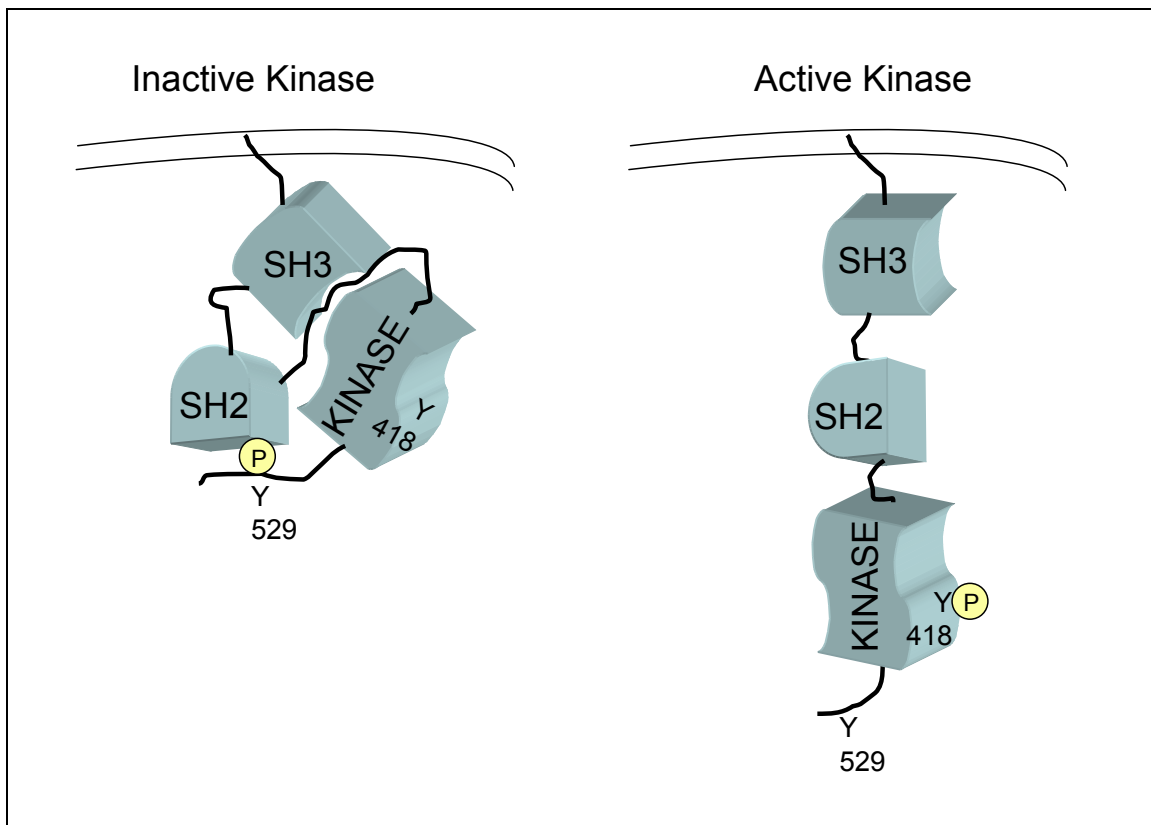


**Figure 5.** Schematic of the inactive and active forms of Src family protein tyrosine kinases. The important tyrosine residues and their phosphorylation states are indicated.

It has been established that Src PTKs are involved in a very proximal role in Fc $\gamma$ R-mediated signaling, and are important for downstream  $\gamma$ -chain and Syk phosphorylation along with subsequent actin cup formation (Fig. 4) (74). However, in the absence of Src family kinases (i.e., in knockout mouse models (74)) these signaling events still occur but

are delayed, indicating that Src family members are not absolutely required for Fc $\gamma$ R-mediated phagocytosis but enhance phagocytic activity (74). Src PTKs sensitize or “turn up the volume” by facilitating other signaling responses following immunoreceptor stimulation (134).

## CHAPTER THREE

### Materials and Methods

#### I. Bacterial Strains and Cultivation

##### A. *H. ducreyi* Strains, Plasmids, and *in vitro* Cultivation

The *H. ducreyi* strains used in this study are listed in Table 3 and were originally isolated from clinical sources. The wild-type strain used predominantly in this study, 35000HP, was provided by Dr. Stanley Spinola and was initially selected by passing the original 35000 clinical isolate strain (95) through the human challenge model (11,196). All *H. ducreyi* strains were grown as described on chocolate agar (CA) plates (112) at 33°C in a 95% air-5% CO<sub>2</sub> humidified atmosphere, and when necessary, the CA plates were supplemented with antibiotics: chloramphenicol (Sigma, St. Louis, Mo.) (0.5-2 µg/mL), kanamycin (Sigma) (30 µg/mL), spectinomycin (Sigma) (100 µg/mL) or dihydrostreptomycin sulfate (Sigma) (100 µg/mL). *H. ducreyi* strains were also grown in Columbia broth (sCB) (Difco Laboratories, Detroit, MI) supplemented with 0.1% (wt/vol) Trizma base (Sigma), hemin (25 µg/mL), 1% (vol/vol) IsoVitaleX (Becton Dickinson, Cockeysville, Md.) and 2.5% (vol/vol) heat-inactivated fetal bovine serum (FBS; Hyclone, Logan, Utah) (219) at 33°C with agitation at 120-130 rpm. In some instances, the FBS was left out of the broth medium for experimental purposes (see Chapter Five). *H. ducreyi* stocks were frozen at -80°C in LB broth containing 25% (vol/vol) sterile glycerol.

The plasmid pLS88, which is a shuttle vector able to replicate in both *H. ducreyi* and *E. coli*, was originally isolated from *H. ducreyi* and its nucleotide sequence has been published (64). This plasmid is the backbone for the GFP transcriptional reporter construct that is described in detail in a later section. A list of *H. ducreyi* plasmids and shuttle plasmids is provided in Table 4.

### **B. *E. coli* Strains, Plasmids, and *in vitro* Cultivation**

A list of *E. coli* strains used in this study is found in Table 3; these were obtained through commercial sources. In general, cultures were grown in Luria-Bertani broth (LB) with shaking at 37°C with the appropriate antibiotic at the following concentrations when necessary: ampicillin (100 µg/mL), kanamycin (50 µg/mL), chloramphenicol (15 µg/mL), spectinomycin (100 µg/mL), or dihydrostreptomycin sulfate (100 µg/mL). Solidified LB medium was prepared by adding 1.5% (wt/vol) agar (Difco) to broth media. When required for induction of recombinant proteins, the LB medium was supplemented with 0.3 mM IPTG and allowed to grow for 2-4 hours at 37°C with agitation at 225 rpm. A list of *E. coli* plasmids is provided in Table 4. All *E. coli* stocks were frozen at -80°C in LB broth containing 25% (vol/vol) sterile glycerol.

**Table 3.** Bacterial strains used in this study.

Organism	Strain	Description	Reference
<i>H. ducreyi</i>	35000	Wild type isolate from Winnipeg, Canada	(94)
	35000HP	Wild type isolate passed through human challenge model	(11,196)
	35000.12	<i>lspA1 lspA2</i> mutant, Kan <sup>r</sup> Chl <sup>r</sup>	(218)
	35000HPΩ1	<i>lspA1</i> mutant, Kan <sup>r</sup>	(112)
	35000HPΩ2	<i>lspA2</i> mutant, Chl <sup>r</sup>	(112)
	35000HPΩ12	<i>lspA1 lspA2</i> mutant, Kan <sup>r</sup> Chl <sup>r</sup>	(112)
	35000HP. <i>sspA</i>	<i>sspA</i> mutant, Chl <sup>r</sup>	This study
	35000HPΩ1. <i>sspA</i>	<i>lspA1 sspA</i> mutant, Kan <sup>r</sup> Spec <sup>r</sup>	This study
	35000HPΩ12. <i>sspA</i>	<i>lspA1 lspA2 sspA</i> mutant, Kan <sup>r</sup> Chl <sup>r</sup> Spec <sup>r</sup>	This study
	35000HP.HD1380	HD1380 mutant, Chl <sup>r</sup>	This study
<i>E. coli</i>	TOP10	Host strain	Invitrogen
	XL1-BLUE	Host strain	Stratagene



XL10-GOLD	Host strain	Stratagene
HB101	Host strain	(176)
DH5 $\alpha$	Host strain	(176)

**Table 4.** Plasmids used in this study.

Plasmid	Description	Reference
pACYC184	Cloning vector, Amp <sup>r</sup>	NEB, (46)
pUC18	Cloning vector, Amp <sup>r</sup>	NEB
pLS88	Cloning vector, Kan <sup>r</sup> Str <sup>r</sup>	(64)
pMAL-c2x	N-terminal MBP fusion expression vector, Amp <sup>r</sup>	NEB
pGEX-rTev	N-terminal GST fusion expression vector, Amp <sup>r</sup>	Dr. Kim Orth
pQE-30	N-terminal 6xHis tag cloning vector, Amp <sup>r</sup>	Qiagen
pRB157	pLS88 containing the promoterless <i>gfp</i> gene, Str <sup>r</sup>	(32)
pJM250	pRB157 with the <i>lspB</i> promoter cloned upstream of the promoterless <i>gfp</i> gene, Str <sup>r</sup>	This study
pJM251	pRB157 with the <i>lspA1</i> promoter cloned upstream of the promoterless <i>gfp</i> gene, Str <sup>r</sup>	This study
pUC18/ <i>sspA</i>	<i>sspA</i> gene region cloned into pUC18, Amp <sup>r</sup>	This study

pUC18/ <i>sspA</i> /Δ <i>Ecat</i>	<i>sspA</i> gene interrupted with the <i>cat</i> gene, Amp <sup>r</sup> Chl <sup>r</sup>	This study
pUC18/ <i>sspA</i> /spec	<i>sspA</i> gene interrupted with the nonpolar spectinomycin cassette, Amp <sup>r</sup> Spec <sup>r</sup>	This study, (135)
pLS88/HD1380	HD1380 region cloned into pLS88, Kan <sup>r</sup>	This study
pUC18/HD1380	HD1380 region cloned into pUC18, Amp <sup>r</sup>	This study
pUC18/HD1380/Δ <i>Ecat</i>	HD1380 gene interrupted with <i>cat</i> gene, Amp <sup>r</sup> , Chl <sup>r</sup>	This study
pMal1	<i>yopT</i> homology region of <i>lspA1</i> (3300 nt of <i>lspA1</i> ) in pMal-c2x, Amp <sup>r</sup>	This study
pMal2	pMal1 plus 2300 nt more 5' <i>lspA1</i> region, Amp <sup>r</sup>	This study
pMal6	pMal2 plus 3000 nt more 5' <i>lspA1</i> region, Amp <sup>r</sup>	This study
pGSTwt	<i>yopT</i> homology region of <i>lspA1</i> (1230 bp) cloned into pGEX-rTEV, Amp <sup>r</sup>	This study
pGSTwt6xHis	pGSTwt with C-terminal 6xHis	This study
pGSTwtC2837A	pGSTwt <i>lspA1</i> gene fragment with C2837A mutation	This study
pGSTwtC2841	pGSTwt <i>lspA1</i> gene fragment with C2841A mutation	This study
pGSTwtDoubleCtoA	pGSTwt <i>lspA1</i> gene fragment with C2837A and C2841A mutation	This study
pGSTwtS2842	pGSTwt <i>lspA1</i> gene fragment with S2842A mutation	This study
pGSTwtH2961A	pGSTwt <i>lspA1</i> gene fragment with H2961A mutation	This study
pGSTwtD2976A	pGSTwt <i>lspA1</i> gene fragment with D2976A mutation	This study
pQE1	pQE-30 with <i>lspA1</i> fragment from PCR with	This study

	LspA1-1 fwd and LspA1-1 rev primers	
pQE2	pQE-30 with <i>lspA1</i> fragment from PCR with LspA1-2 fwd and LspA1-2 rev primers	This study
pQE3	pQE-30 with <i>lspA1</i> fragment from PCR with LspA1-3 fwd and LspA1-3 rev primers	This study
pQE4	pQE-30 with <i>lspA1</i> fragment from PCR with LspA1-4 fwd and LspA1-4 rev primers	This study
pQE5	pQE-30 with <i>lspA1</i> fragment from PCR with LspA1-5 fwd and LspA1-5 rev primers	This study
pQE6	pQE-30 with <i>lspA1</i> fragment from PCR with LspA1-6 fwd and LspA1-6 rev primers	This study
pQE7	pQE-30 with <i>lspA1</i> fragment from PCR with LspA1-7 fwd and LspA1-7 rev primers	This study
pQE8	pQE-30 with <i>lspA1</i> fragment from PCR with LspA1-8 fwd and LspA1-8 rev primers	This study
pQE8.5	pQE-30 with <i>lspA1</i> fragment from PCR with LspA1-8.5 fwd and LspA1-8.5 rev primers	This study
pQE9	pQE-30 with <i>lspA1</i> fragment from PCR with LspA1-9 fwd and LspA1-9 rev primers	This study
pQE10	pQE-30 with <i>lspA1</i> fragment from PCR with LspA1-10 fwd and LspA1-10 rev primers	This study
pQE11	pQE-30 with <i>lspA1</i> fragment from PCR with LspA1-11 fwd and LspA1-11 rev primers	This study
pQE12	pQE-30 with <i>lspA1</i> fragment from PCR with LspA1-12 fwd and LspA1-12 rev primers	This study

---

### C. Bacterial Growth Curves

*H. ducreyi* strains were grown on CA plates containing the appropriate antibiotic overnight at 33°C. The original parent strain of each mutant was also grown alongside the mutant in broth to compare growth rates. The plate-derived bacterial growth of both the mutant and its parent strain were suspended in sCB and used to inoculate side-arm flasks (Bellco, Vineland, N. J.) containing 50 mL of sCB to a starting O.D.<sub>600</sub> of 0.1. The *H. ducreyi* strains were then incubated in a 33°C water bath with agitation at 120 rpm, and every hour for ten hours, the O.D.<sub>600</sub> was measured and recorded for each strain.

## II. Transformation of Bacterial Strains

### A. Electroporation of *H. ducreyi*

*H. ducreyi* cells were made electrocompetent by growing the selected recipient strain for 16-20 h on four CA plates and then preparing the cells as described (98). Briefly, the bacterial growth was scraped off the plates with a sterile loop and placed in 5 mL of filter-sterilized 10% (vol/vol) glycerol. The cell suspension was vortexed and then subjected to centrifugation at 6,000 x g for 10 min at 4°C and the supernatant fluid was discarded. The pellet was resuspended in another 5 mL of 10% glycerol and washed two more times as described above. Following the final wash, the pellet was resuspended in approximately 200 – 500 µL of 10% glycerol to obtain a cell paste. A 40 – 50 µL aliquot of cell paste was transferred to a 0.5 mL microcentrifuge tube and 10 µL of the appropriate

linearized DNA construct, previously desalted and suspended in water, was added and mixed gently with the cell paste. Desalting was performed by placing the DNA onto a type VS 0.025  $\mu\text{m}$  filter (Millipore, Billerica, MA) floating in sterile water. The total volume of the DNA/cell paste mixture was then transferred to an Eppendorf Electroporation cuvette (Fisher Scientific, Pittsburg, PA), and electroporated in the *E. coli* Pulser electroporator (Bio-Rad Laboratories., Hercules, CA) at a setting of 1.5 kV. After electroporation, the solution was diluted with 100  $\mu\text{L}$  of Brain Heart Infusion (BHI) (Difco) broth and the total volume was spread onto a CA plate which was incubated for approximately 5 – 6 h at 33°C in a 95% air – 5% CO<sub>2</sub> incubator. Following this recovery incubation, the CA plate was washed and the growth scraped into BHI broth. Three consecutive 1 mL volumes were used for this purpose. The washes were combined and subjected to centrifugation at 6,000 x g for 10 min at room temperature. The supernatant fluid was discarded and the cell pellet resuspended in 500  $\mu\text{L}$  of BHI. The suspension was then plated onto CA plates containing the appropriate antibiotic to select for the desired *H. ducreyi* mutant or recombinant strain. The CA plates containing the appropriate antibiotics were incubated as described above for 48 – 96 h. Transformants were further patched to CA plates containing the appropriate antibiotics and single colony passaged twice to ensure that a single strain (i.e., pure culture) was obtained.

### **B. Electroporation of *E. coli***

Transformations of *E. coli* cells were performed by electroporation. Large batches of electrocompetent cells were made by taking an overnight 50 mL LB culture of the *E. coli*

strain, diluting it (1:50) in fresh LB media, and then allowing the cells to grow to an O.D.<sub>600</sub> of 0.6. The culture was then placed at 4°C for 30 min. and then subjected to centrifugation at 6,000 x g for 10 min. at 4°C. The supernatant fluid was discarded and the cell pellet was resuspended to ¼ of the original culture volume in sterile, ice-cold water. The suspension was again subjected to centrifugation at 6,000 x g for 10 min. at 4°C. The cells were resuspended and washed several more times as above, decreasing the total volume of water to 1/10 and then 1/50 of the original culture volume. After the last water wash, the cell pellet was resuspended in 10 mL of sterile 10% (vol/vol) glycerol. The suspension was subjected to another round of centrifugation and the cell pellet was resuspended in 2 mL of sterile 10% (vol/vol) glycerol. Aliquots of 40 µL were prepared and flash frozen in liquid N<sub>2</sub> and stored at -80°C. For transformation, an aliquot was thawed and mixed with a 10 µL portion of desalted DNA. Desalting was performed by placing the DNA onto a type VS 0.025 m filter (Millipore) floating on sterile water. The competent cell/DNA mixture was then transferred to an Eppendorf Electroporation cuvette (Fisher Scientific). The competent *E. coli* were electroporated in the *E. coli* Pulser (Bio-Rad) at a setting of 1.6 kV. The cells were then immediately suspended in 0.25 mL of SOC medium (Invitrogen, Carlsbad, CA) and incubated at 37°C with agitation for 45 min to 1 h before being spread onto a LB agar plate containing the appropriate antibiotics.

### **C. Chemical Transformation of *E. coli***

Transformation of the *E. coli* strain XL10 – Gold (Stratagene) was performed as per manufacturer's instructions. After transformation, the cells were recovered in SOC

medium (Invitrogen) for 1 h at 37°C and then plated on agar plates with the appropriate antibiotic.

### **III. Mammalian Cell Lines, Media Conditions, and Protocols**

Cell lines utilized in this study were cultivated as described in detail below. All cell lines were used only at low passage number and maintained in culture for less than one month. The human PMN-like HL-60 cell line (CCL-240; American Type Culture Collection [ATCC], Manassas, VA), the T cell-like Jurkat cell line (ATCC TIB-153), and the B cell-like Daudi cell line (ATCC CCL-213) were cultured in RPMI 1640 (BioWhittaker, Walkersville, Md) supplemented with 4 mM GlutaMAX (GIBCO-BRL, Rockville, Md.) and 20% (vol/vol) heat-inactivated FBS at 37°C in a humidified atmosphere of 95% air/5% CO<sub>2</sub>. The HL-60 cell line was differentiated as previously described (215) into granulocytes by supplementing the same medium described above with 100 mM N,N-dimethylformamide (Sigma) for 5 days. After differentiation, the HL-60 cells were collected by centrifugation at 160 x g for 5 min and suspended in RPMI media lacking FBS immediately prior to use in phagocytosis assays.

The mouse monocyte-macrophage cell lines J744A.1 (ATCC TIB-67) and RAW264.7 (ATCC TIB-71), the DC2.4 dendritic cell line (kindly provided by Dr. Kenneth Rock, Dana-Farber Cancer Institute, Boston, MA), the RBL-1 (ATCC CRL-1378) B cell-like cell line, HeLa cells (ATCC CCL-2), and COS-7 cells (ATCC CRL-1651) were all cultivated in Dulbecco's Modified Eagle's Medium (BioWhittaker) supplemented with

10% (vol/vol) heat-inactivated FBS, 4 mM GlutaMAX, and 1 mM sodium pyruvate. For experiments involving the staining of J774A.1 cells, the macrophages were placed in 24-well tissue culture plates and allowed to adhere to glass coverslips ( $1 \times 10^5$  cells/well) twenty hours before infection. For assays determining cellular localization and phosphorylation states of proteins, these murine macrophage cell lines were grown in 75 cm<sup>2</sup> tissue culture flasks to confluency and approximately 12 hours prior to use in experiments, fresh media lacking FBS was added to the cells in place of the media described above containing FBS. This was done to remove possible interfering immune complexes (present in FBS) from the media prior to all assays.

#### **IV. DNA and RNA Isolation**

##### **A. Plasmid Isolation**

Plasmids were isolated from *E. coli* or *H. ducreyi* by using the Wizard *Plus* SV Minipreps DNA Purification System (Promega, Madison, WI) according to the manufacturer's protocol.

##### **B. Chromosomal DNA Isolation**

Chromosomal DNA was isolated from *H. ducreyi* by two different methods. The first used the Easy-DNA Kit (Invitrogen) following the manufacturer's protocols. For the second method, *H. ducreyi* cells were harvested from 2 – 4 CA plates after overnight



growth by scraping the cells from the plate with a loop and suspending these cells in 2 mL of TE (10 mM Tris (pH 8.1), 1 mM EDTA) buffer. A 200  $\mu$ L volume of 10% (wt/vol) SDS was then added. The mixture was then incubated for 10 – 15 min at 37°C. Next, 200  $\mu$ L of RNase (Sigma) (10 mg/mL stock) was added and the solution was incubated at 37°C for 1 h. Then, 50  $\mu$ L of 5 M NaCl and 20  $\mu$ L of Proteinase K (Sigma) (5 mg/mL stock) were added and the solution allowed to incubate at 37°C for 2 h. The solution then underwent equal volume extractions, first two times with phenol (Sigma), then three times with phenol/chloroform/isoamyl alcohol (25:24:1) (Fisher), and then twice with chloroform (Sigma). After the final extraction, the aqueous phase was placed into a microcentrifuge tube and chromosomal DNA was precipitated by adding 5 M NaCl to bring the final NaCl concentration to 0.2 M. Then two times the solution volume of 100% ethanol was added and the tube was mixed gently. The precipitated chromosomal DNA was spooled out of the solution with a glass Pasteur pipet and placed in 70% ethanol for washing. The DNA was then removed from the 70% ethanol and placed in a microcentrifuge tube and rehydrated with 200 – 500  $\mu$ L of sterile water.

### **C. RNA Isolation**

Total *H. ducreyi* RNA was isolated using two different procedures. For the RNA used in the differential display experiments, the Ultraspec RNA Isolation System (Biotecx Laboratories Inc., Houston, TX) was used per the manufacturer's protocol. The concentration of the RNA was then determined by spectrophotometry using an Ultraspec 2000 spectrophotometer (Amersham Pharmacia, Cambridge, UK). Next, 20  $\mu$ g of the RNA

sample was subjected to DNase treatment with the MessageClean Kit (GeneHunter Inc., Nashville, TN) as per the manufacturer's protocol. After DNase treatment, the RNA was used as the template in the differential display experiments.

The other method used to isolate RNA involved the RNeasy Midi Kit (Qiagen, Valencia, CA) and was performed following the manufacturer's protocol with several modifications, including the RNase-Free DNase Set (Qiagen) DNase reaction on the column as recommended by the protocol. The other modification to the protocol was that, after the final elution of RNA with RNase-free water, the RNA was precipitated by adding 1/10 the elution volume of 3 M sodium acetate (pH 5.2) and three times the elution volume of 100% ethanol, followed by standing overnight at -80°C. The tube was then thawed on ice and centrifuged at 14,000 x g for 15 min at 4°C. The RNA pellet was washed twice with 75% ethanol and centrifuged at 14,000 x g for 15 min at 4°C, and after the final wash, the RNA pellet was rehydrated in 500 µL of sterile RNase-free water. The concentration of the RNA was then determined by using the NanoDrop instrument (NanoDrop Technologies, Wilmington, DE). Next, 40 µg of the RNA sample was subjected to two more rounds of DNase treatment with the MessageClean Kit (GeneHunter Inc.) as per the manufacturer's protocol. After two more rounds of DNase treatment, approximately 20 µg of RNA was recovered for downstream applications such as RT-PCR, real-time PCR, or DNA microarray analysis.

## **V. Recombinant DNA Techniques**

Recombinant DNA techniques such as restriction enzyme digestion, agarose gel electrophoresis, ligation reactions, and polymerase chain reactions (PCR) were performed as described (176) or following the manufacturer's protocols. DNA restriction enzymes, T4 ligase and *Taq* polymerase were purchased from New England Biolabs, Beverly, MA. *ExTaq* DNA polymerase was purchased from Takara Mirus Bio, Otsu, Shiga, Japan. *Pfu* polymerase and the QuikChange II XL Site-Directed Mutagenesis Kit were purchased from Stratagene Corp., La Jolla, CA. Oligonucleotides primers (Tables 5 – 16) were synthesized by Integrated DNA Technologies, Inc., Coralville, IA. PCR reactions were performed with a Peltier-effect cycler with a heated lid (MJ Research, Inc., Incline Village, NV).

## **VI. Nucleotide Sequence Analysis**

Nucleotide sequence analysis of plasmids, PCR products, or chromosomal DNA was performed through the McDermott Center DNA sequencing core facility at UT Southwestern Medical Center using Big Dye Terminator 3.1 chemistry (Applied Biosystems, Foster City, CA) and ABI capillary instruments (Applied Biosystems). DNA sequence data was analyzed by using the DNASTAR Lasergene analysis package (version 5.03, DNASTAR, Inc. Madison, WI).

## **VII. Differential Display Methodology**

The displayPROFILE Kit (Display Systems Biotech, Inc., Copenhagen, DK) was utilized to detect possible transcriptional changes in *H. ducreyi* grown in both sCB containing FCS and sCB without FCS. In both media, *H. ducreyi* wild-type strain 35000 was grown to mid-log phase ( $\text{O.D.}_{600} = 0.6$ ) and RNA was isolated as described above. The RNA (after DNase treatment) was then used with the displayPROFILE Kit as per the manufacturer's protocol to determine if there were differences in transcription between the two growth conditions. The overall method is described below. The isolated RNA from the two growth conditions was used as a template for cDNA synthesis. The cDNA pool was then digested with the *TaqI* restriction enzyme which is a 4-base-cutter (TCGA) that leaves 5' overhanging ends on the cDNA fragments. Next, two different DNA adaptors are ligated onto the sticky ends of the cDNA fragments; the EP-adaptor (extension-protection) and the standard adaptor. For the technique to work properly, the digested cDNA must have both adaptor types ligated to its cDNA ends—the EP-adaptor onto one end of the cDNA and the standard adaptor on the other cDNA end. The standard adaptor will allow the displayPROBE primers (64 different primers in total) to anneal to the cDNA. There are 64 different displayPROBE primers that have the same 5' primer sequence but vary in the sequence of their last three nucleotides. (To have all three variations of nucleotides represented;  $4^3 = 64$ .) It is these last three 3' bases that make the displayPROBE specific for certain cDNA sequences, because based on design the 3' end of these primers extend into the cDNA sequence so only a certain primer (in theory) should anneal to the standard adaptor and the cDNA region containing the complementary 3 nucleotides that match the one exact 64 displayPROBE primer. The other adaptor, the EP-adaptor, has a modification on its 3' end to prevent  $3' \rightarrow 5'$  synthesis to fill in the 5' overhang, the presence of which is

necessary for the O-extension 5' primer to anneal. Therefore, the primer used to amplify off this new adaptor, the O-extension 5' primer, must have the template replicated first off of a displayPROBE primer annealed to the standard adaptor so that the primer that is complementary to the EP adaptor can then anneal and allow for production of a PCR product. This is how both adaptors are used to amplify selected cDNAs based on the 64 different displayPROBE primers. Therefore, each fragment that has the EP adaptor ligated onto one of its ends and the standard adaptor ligated onto its other end is able to be amplified in further downstream steps using PCR. So, after ligation of both adaptors, the 64 high-stringency PCR reactions are carried out with the O-extension 5' primer and one or a mixture of several of the 64 different displayPROBE 3' primers. For visualization of the PCR products, the O-extension 5' primer was end-labeled with radioactive phosphate from [ $\gamma$ - $^{32}\text{P}$ ]ATP (specific activity = 10  $\mu\text{Ci}/\mu\text{L}$ ) as per the manufacturer's instructions to allow detection of the PCR products by autoradiography. The amplified gene fragments were separated on a 6% Long Ranger sequencing gel (Cambrex Inc., East Rutherford, NJ) as per the manufacturer's instructions. A 50 mL gel solution contained 39 mL of 52.5% (wt/vol) solution of urea (Sigma), 5 mL 10x TBE (0.89 M Tris (Sigma), 0.02 M sodium EDTA salt (Sigma), 0.89 M boric acid (Sigma)), 6 mL of Long Ranger Gel Solution (50%) (Cambrex), 250  $\mu\text{L}$  10% (wt/vol) ammonium persulfate (APS) (Bio-Rad) and 40  $\mu\text{L}$  tetramethylethylenediamine (TEMED) (Bio-Rad). The solution was mixed well before casting. The gel was set to solidify for 30 min and then warmed by running the gel in 1X TBE at 30W for 30 min. Next, the wells were washed with 1X TBE and then the  $^{32}\text{P}$ -cDNA samples were loaded on the gel and run for 2 h at 30W. After electrophoresis, the gel was mounted on Whatman paper, covered with plastic wrap, and dried on a gel dryer

(Bio-Rad model 583). The dried gel was then exposed to Bio Max X-Ray film (Kodak, Rochester, NY) for 12 – 48 h in a radiographic cassette containing a BioMax Transcreen-LE intensifying screen (Kodak) at -70°C, and then developed. The autoradiograph was then visualized and cDNA bands of interest were excised by aligning the autoradiograph with the dried gel, cutting out the desired gel area with a scalpel, and placing the excised region in a microcentrifuge tube. Next, 50 µL of TE buffer was added to the excised gel piece and the tube was heated to 95°C for 10 min. The dissolved cDNA fragment was then used as a template for amplification in a PCR reaction as per the displayPROFILE protocol (Display Systems Biotech Inc.). The amplified PCR products were then subcloned into a TOPO TA cloning vector (Invitrogen) as per the manufacturer's instructions. The plasmids from the clones were then isolated and the inserts sequenced using the primers provided with the TA cloning kit to determine DNA sequence. Finally, the DNA sequences were analyzed by BLAST (NCBI) search to determine possible cDNA identity or homology.

## **VIII. Molecular Genetic Techniques**

### **A. Construction of GFP Reporter Constructs**

A GFP transcriptional reporter was previously constructed for differential fluorescence induction (DFI) by a former student, Robert Blick, in the Hansen laboratory, and is described in detail in his M.S. thesis (33). Briefly, the plasmid was constructed by amplifying the origin of replication and streptomycin resistance gene from plasmid pLS88 by PCR using the primers pLS88IVET-3 (5'-

CCAAAGGTACCAAGCGTGTCTGTATCCCAC-3') and pLS88IVET-4 (5'-GGGGATATCATTAAATACAAGGTCAATGCTCGGC-3'). These primers contain *Kpn*I, *Eco*RV, and *Swa*I sites (underlined). This 3.2 kb PCR product was then digested with *Kpn*I and ligated to a *Kpn*I/*Sma*I fragment from pGreenTIR (140) containing a promoterless *gfp* cartridge to construct pRB153. Next, to stop possible plasmid promoter-based transcription into the promoterless *gfp*, an  $\Omega$ Amp cartridge from pKT254 $\Omega$ -Ap (72) was inserted into the *Swa*I site upstream of the *gfp* ORF to obtain pRB155. Then, a *Bgl*II linker, consisting of dimers of the oligonucleotide 5'-CAGATCTG-3' was ligated into the *Eco*RV site of pRB155 to yield pRB157 which contains the promoterless *gfp* construct in which DNA fragments with *Bgl*II-compatible ends could be inserted in front of the promoterless *gfp* ORF. The putative promoter regions for *lspA1* and *lspB* were PCR-amplified with the following primers (listed in Table 5): LspA1 GFP 5' and LspA1 GFP 3' for the *lspA1* promoter region (~500 bp) and LspB GFP 5' and LspB GFP 3' for the *lspB* promoter region (~300 bp). These PCR products were cloned into the *Bgl*II site in pRB157. The constructs were then screened for correct orientation by PCR using the GFP primer to confirm orientation and two constructs containing the correct orientation were designated pJM250 and pJM251 for the *lspB-gfp* and *lspA1-gfp* transcriptional reporters, respectively.

**Table 5.** Primers for PCR-based amplification of the *lspA1* and *lspB* promoter regions

Primer	Primer Sequence 5' – 3' (restriction sites underlined)
LspA1 GFP 5'	GAAGATCTATATACAACGCAGACAATCCTTAT
LspA1 GFP 3'	GAAGATCTGAACCATTCACTTGATATGATAGC
LspB GFP 5'	GGAAGATCTCGCTACATCAGTTA

LspB GFP 3'	GGA <u>AGATCT</u> ATTTGTTAAAGTGCTCAC
GFP primer	CCTTCACCCTCTCCACTGACAG

---

## B. Construction of *H. ducreyi* Mutants

### I. *sspA* mutants

The *sspA* gene was inactivated in the strains 35000HP, 35000Ω1, and 35000Ω12. Briefly, the *sspA* gene and flanking DNA were PCR-amplified with the primers SspA 5' *Bam*HI and SspA 3' *Bam*HI (Table 6). The PCR reaction was placed onto a Montage column (Millipore) to remove unincorporated primers and salt by washing with 4 times the PCR reaction volume of dH<sub>2</sub>O. The washed PCR product and the vector, pUC18, were both digested with *Bam*HI for 2 h and then run on an agarose gel for 1 h to separate digested DNA bands by size. The desired DNA products were then gel-purified (Promega). Ligations reactions were performed according to the manufacturer's instructions with T4 DNA ligase (New England Biolabs). The ligations were then transformed by electroporation into *E. coli* TOP10 cells. Clones were confirmed by PCR analysis and a plasmid containing the *sspA* gene was designated pUC18/*sspA*. The plasmid was then digested with *Nsi*I which cuts twice within the *sspA* ORF and the digested plasmid was gel-purified. After purification, the linearized plasmid's *Nsi*I overhangs were blunt-ended by treatment with *Pfu*. Next, the Δ*Ecat* chloramphenicol resistance gene was PCR-amplified



with the primer set E Cat 5' *Pst*I and E Cat 3' *Pst*I (Table 6) and ligated to the blunted *Nsi*I sites. The resultant plasmid was designated pUC18/*sspA*/Δ*Ecat*. This plasmid was used to transform *E. coli* HB101, and then the plasmid was isolated and linearized with *Bsp*HI and used to electroporate 35000HP. Transformants resistant to chloramphenicol were single colony passed twice and then genomic DNA was isolated from these and the primers SspA KO primer and E Cat 3' *Pst*I were used in PCR to confirm the interruption of the *sspA* gene. This *H. ducreyi* *sspA* mutant was designated 35000HP.*sspA*.

Nonpolar *sspA* mutations were also constructed in the 35000HPΩ1 and 35000HPΩ12 strains by interrupting the *sspA* ORF with nonpolar spectinomycin resistance cassettes (135). This was the first time that the spectinomycin resistance cartridge was used to construct mutants in *H. ducreyi*. The pUC18/*sspA* plasmid digested with *Nsi*I and *Pfu*-blunted as described above was used in ligation reactions with one of the three different nonpolar spectinomycin gene cassettes that had been digested with *Sma*I and then gel-purified. The ligations were transformed into *E. coli* TOP10 cells and selection was accomplished using LB-spectinomycin plates. Plasmids from the clones were isolated and used in DNA sequencing with the SspA nonpolar 3' spec primer (Table 6) to confirm which clone had the spectinomycin gene in the same reading frame as the *sspA* gene. The plasmid that had the correct reading frame was designated pUC18/*sspA*/spec. This plasmid was then propagated in *E. coli* HB101, linearized with *Bsp*HI, and electroporated into either 35000HPΩ1 or 35000HPΩ12. Spectinomycin-resistant transformants were single colony passed twice, confirmed by PCR, and designated as 35000HPΩ1.*sspA* and 35000HPΩ12.*sspA*, respectively.

These *sspA* mutants were later transformed with the *lspB-gfp* reporter plasmid pJM250 and GFP expression was measured and compared to that of their parent strains as described below. It should be noted that growth curves comparing the *sspA* mutants to their parent strains were performed as described above. A complementation plasmid was also constructed by PCR-amplifying the *sspA* gene region with the primers SspA complement 5' *Bam*HI and SspA complement 3' *Xba*I, digesting the PCR product and the pACYC184 vector with *Bam*HI and *Xba*I, and ligating the two DNA fragments together. Ligations were transformed into *E. coli* TOP10 and clones were screened for presence of the *sspA* gene region in the pACYC184 vector.

**Table 6.** Primers used for *sspA* gene cloning and mutant construction.

Primer	Primer Sequence 5' – 3' (restriction sites underlined)
SspA 5' <i>Bam</i> HI	CGC <u>GGATCCT</u> TGGTAAGTCAAGTAACGCACG
SspA 3' <i>Bam</i> HI	CGC <u>GGATCCA</u> ATCCCGCACCTTTACGAAG
SspA KO primer	GGCCTACTTTGCGCCCTGAGC
E Cat 5' <i>Pst</i> I	AA <u>ACTGCAGC</u> ACACGGTCACACTGCTTCC
E Cat 3' <i>Pst</i> I	AAT <u>CTGCAGT</u> GATGTCCGGCGGTGCTTTTG
SspA 3' nonpolar spec	CACATAAACATCGCGCAACATACC
SspA Complement 5' <i>Bam</i> HI	CGC <u>GGATCCC</u> ACTTTTTGAACCATTACGAC
SspA complement 3' <i>Xba</i> I	TGCT <u>TCTAGAA</u> ACATACCTTGGAACGAGCAT

## II. HD1380 mutants

A mutation in the HD1380 gene was constructed in the 35000HP strain and confirmed by PCR analysis with the primers listed below in Table 7. Briefly, the HD1380 gene and flanking DNA were PCR-amplified with primers HD1380 5' *Xba*I and HD1380 3' *Kpn*I and the PCR reaction was placed onto a Montage column (Millipore) to remove unincorporated primers and salt. The washed PCR product and the vector, pUC18, were both digested with *Xba*I and *Kpn*I for 2 h and then electrophoresed on agarose gel for 1 h to separate DNA bands by size. The desired DNA products were then gel-purified (Promega). Ligations reactions were performed according to the manufacturer's instructions with T4 DNA ligase (New England Biolabs). A plasmid containing the HD1380 gene was designated as pUC18/HD1380. The plasmid was then digested with *Spe*I and *Pac*I (which both cut within the HD1380 ORF) and the digested plasmid was gel-purified. The  $\Delta Ecat$  chloramphenicol resistance gene was then ligated to the *Spe*I and *Pac*I sites; the resultant plasmid was designated pUC18/HD1380/ $\Delta Ecat$ . The plasmid insert was PCR-amplified with the HD1380 primer set originally used to clone this region into pUC18 and was used to electroporate 35000HP; transformants were selected on CA-chloramphenicol plates. The colonies were single colony passed twice and then genomic DNA was isolated and PCR analysis using the primer pair HD1380 5' PCR and HD1380 3' PCR was performed to confirm the interruption of the HD1380 ORF. The mutant was designated 35000HP.HD1380.

The HD1380 gene region was also cloned into pLS88 as a PCR product obtained by using the primers HD1380 5' *Nco*I and HD1380 3' *Bsp*EI. This construct was designated pLS88/HD1380, and used for complementation studies.

**Table 7.** Primers used for HD1380 gene cloning and mutant construction.

Primer	Primer Sequence 5' – 3' (restriction sites underlined)
HD1380 5' <i>Nco</i> I	CATGCCATGGGATTTACCGGGGTTTGATGTTG
HD1380 3' <i>Bsp</i> EI	CATGTCCGGAAATAATGCCGCTTTTGCTGAT
HD1380 5' <i>Xba</i> I	GCTCTAGAGCTAGTGGCACAAGGATA
HD1380 3' <i>Kpn</i> I	GCGGTACCCTGCAATACGCGTAATAGGA
E CAT 5' <i>Spe</i> I	GGTACTAGTCACACGGTCACACTGCTTCC
E CAT 3' <i>Pac</i> I	CGGTTAATTAATGATGTCCGGCGGTGCTTTTG
HD1380 5' PCR	CGTTTATTTTCGTTTAGCCGTTTTA
HD1380 3' PCR	AAAAACACCCGCTTCATCTTG

## C. Construction of Affinity-Tagged Protein Fusion Constructs

### I. 6xHis-Tagged LspA1 Fusion Proteins

The plasmid pQE-30 (Qiagen Inc.) was used as the vector for constructing genes expressing 6xHis-tagged fusion proteins. Briefly, oligonucleotide primers (Table 8) were used in PCR with *Pfu* polymerase (Stratagene Corp., La Jolla, Calif.) to obtain their respective gene fragments of *lspA1*. PCR products were digested with *Bam*HI and *Ava*I (New England Biolabs Inc., Beverly, Mass.) and ligated, using T4 DNA ligase, (New England Biolabs Inc.) into pQE-30, which had also been digested with the same restriction enzymes. Nucleotide sequence analysis was performed on all thirteen constructs to confirm sequence and reading frame before expressing and purifying fusion proteins as per the manufacturer's specifications (Qiagen Inc.).

**Table 8.** Primers used to amplify fragments of the *lspA1* gene for cloning into plasmid pQE-30.

Primer	Primer Sequence 5' – 3' (restriction sites underlined)
LspA1-1 fwd	CGGGATCCATGAACAACAAACGTTATAA
LspA1-1 rev	CGCTCGAGTTAACCAGAAGAAATAGGTGTAGC
LspA1-2 fwd	CGGGATCCGTAATATTCAAGGCGCA
LspA1-2 rev	CGCTCGAGTTAGTGTAATAATGATTTCATA
LspA1-3 fwd	CGGGATCCGGGAATGTTACCTTGAATGCA
LspA1-3 rev	CGCTCGAGTTACTCTAATTTATTCTTAACATTGA

LspA1-4 fwd	CGGGATCCGAGTATGGTTCAAATGTGGAT
LspA1-4 rev	TTCTCGAGTTAATTAAAGAAATATTTAGCGCC
LspA1-5 fwd	CGGGATCCCAACTAGATACAGAAGACGAT
LspA1-5 rev	TTCTCGAGTTAGCCACTGGCAGATGCTGAGTA
LspA1-6 fwd	CGGGATCCGGCGGACAATCAGCGGGCATT
LspA1-6 rev	CGCTCGAGTTATACATTACATTATCTCTGGC
LspA1-7 fwd	CGGGATCCGCCGGAGCGAGTTCTGGTTGT
LspA1-7 rev	CGCTCGAGTTATAAACGCGGTGAATCAACTCC
LspA1-8 fwd	CGGGATCCGTGGATGAGAGCCCTTATGCT
LspA1-8 rev	CGCTCGAGTTACTTACCACGAGACTTAGGCGT
LspA1-8.5 fwd	CGGGATCCCGTGGTATTTCTGAGGAG
LspA1-8.5 rev	CGCTCGAGTTATAATTTGCGCAAAGTTAGGG
LspA1-9 fwd	CGGGATCCGATAAGAAAAGCTTCGAAAAA
LspA1-9 rev	CGCTCGAGTTATTCTACTTGTTGCCCTCTGAT
LspA1-10 fwd	CGGGATCCCATCATCGTTGTATGCGAAA
LspA1-10 rev	CGCTCGAGTTATTTGCGGATAAATTCGTCTT
LspA1-11 fwd	CGGGATCCGGACAGCTTTACTTTGCATTA
LspA1-11 rev	CGCTCGAGTTAATCAAGAGACACCGGTGCTAA
LspA1-12 fwd	CGGGATCCGCAGCAAATATTCTATCTTCA
LspA1-12 rev	CGCTCGAGTTACTGAGTCTATCTAACCGACTT

---

## II. pMAL – Derived LspA1 Fusion Proteins

The plasmid pMAL-c2x (New England Biolabs) was used as the vector to construct LspA1 fusions involving the maltose-binding protein. Briefly, oligonucleotide primers (Table 9) were used in PCR with *Pfu* polymerase (Stratagene Corp., La Jolla, Calif.) to obtain their respective gene fragments of *lspA1*. PCR products were digested with *Bam*HI and *Ava*I (New England Biolabs Inc., Beverly, Mass.) and ligated, using T4 DNA ligase, (New England Biolabs Inc.) into pMAL-c2x which had also been digested with the same restriction enzymes. The construction of the pMal constructs was based on sequentially increasing the size of the *lspA1* gene fragment, starting with the *yopT* homology region located near the 3' end of the *lspA1* ORF and working toward the 5' of the ORF. The first region cloned into the pMal-c2x vector was the *lspA1* region that had been amplified (~3300 bp) with the primers MBP-LspA1-I-5' *Bam*HI and MBP-LspA1-I-3' *Xba*I. The full size of the fusion protein was estimated at 166 kDa and the plasmid was designated pMal1. The next fusion construct was formed by cloning, in frame, the next 2300 nt of *lspA1* directly upstream of the *lspA1* sequence in pMal1. The primer pair used for PCR was pMal-c2x-LspA1 extend A 5' and pMal-c2x-LspA1 extend 3', and this PCR product and the pMal1 construct were separately digested with *Bam*HI and *Pac*I. The 5' primer had a *Bam*HI site (used to clone into the *Bam*HI site of pMal1) and the 3' primer sequence was based on the *lspA1* sequence which itself contained the *Pac*I restriction site and could be utilized to ligate, in frame, with the *lspA1* sequence in pMal1. The full size of this fusion protein was estimated to be 247 kDa and this plasmid was designated pMal2. The next fusion construct was formed by cloning, in frame, the next 3000 nt of *lspA1* directly

upstream of the *lspA1* sequence in pMal2. The primer pair used for PCR was pMal-LspA1 *Bam*HI 5' 3kb and pMal-LspA1 *Nhe*I 3'; the PCR product and the pMal2 construct were separately digested with *Bam*HI and *Nhe*I. The 5' primer had a *Bam*HI site (used to clone into the *Bam*HI site of pMal2) and the 3' primer sequence was based on the *lspA1* sequence which contained the *Nhe*I restriction site and could be utilized to ligate, in frame, with the *lspA1* sequence in pMal2. The full size of this fusion protein was estimated to be 356 kDa and this plasmid was designated pMal6. Nucleotide sequence analysis was performed on all DNA constructs to confirm correct sequence and reading frame before expressing and purifying fusion proteins as described below.

**Table 9.** Primers used for pMAL cloning experiments.

Primer	Primer Sequence 5' – 3' (restriction sites underlined)
MBP-LspA1-I- 5' <i>Bam</i> HI	CGC <u>GGATCC</u> GTTGATTCACCGCGTTTA
MBP-LspA1-I- 3' <i>Xba</i> I	TGCT <u>CTAGAC</u> TATCCATTAGTTTGAGATT
pMAL-c2x- LspA1 extend A 5'	CGC <u>GGATCC</u> GTCGATCTTACTGCTAGCGAATTG
pMAL-c2x- LspA1 extend 3'	CGGCTTCACCT <u>TTAATTAA</u> ACGCGGTG
pMAL-LspA1 <i>Nhe</i> I 3'	CAATTC <u>GCTAGC</u> AGTAAGATC
pMAL-LspA1 <i>Bam</i> HI 5' 500	CGC <u>GGATCC</u> GTTTACATGATATTGCTTTAGTG



pMAL-LspA1 <i>Bam</i> HI 5' 2kb	CGC <u>GGATCC</u> GGTGAAATTTATAGCCAAGCAGGT
pMal-LspA1 <i>Bam</i> HI 5' 3kb	CGC <u>GGATCC</u> GGCACTATTGCCGGCCTTACC

---

### III. pGEX - Based LspA1 YopT-like Region Fusion Proteins

The plasmid pGEX4T-3 (Amersham) was modified to include the rTev cleavage site; this plasmid construct was provided by Dr. Kim Orth, UT Southwestern Medical Center and designated pGEX-rTEV. Briefly, this construct was prepared by digesting the pGEX4T-3 plasmid with *Bam*HI and *Not*I and ligating in an adaptor constructed by annealing the rTEV 5' and rTEV 3' primers (see table 10) that had been digested with *Bgl*II and *Not*I. The new construct was designated pGEX-rTev and this plasmid was utilized for subsequent experiments involving GST fusion proteins. The oligonucleotide primer pairs of either GST-LspA1 *Bam*HI 5' and GST-LspA1 *Xho*I 3' or GST-LspA1 *Bam*HI 5' and GST-LspA1-*Xho*I 6xHis 3' (Table 10) were used in PCR with *Pfu* polymerase (Stratagene Corp., La Jolla, Calif.) to obtain their respective fragments of the *yopT* homology region of *lspA1*. PCR products were digested with *Bam*HI and *Xho*I (New England Biolabs Inc., Beverly, Mass.) and ligated using T4 DNA ligase (New England Biolabs Inc.) into pGEX-rTev which had also been digested with the same restriction enzymes. The resultant constructs were designated pGSTwt and pGSTwt6xHis, respectively. Nucleotide sequence analysis was performed on all DNA constructs to confirm correct sequence and reading frame before expressing and purifying fusion proteins as described below.

**Table 10.** Primers used for pGEX-based cloning experiments

<b>Primer</b>	<b>Primer Sequence 5' – 3' (restriction sites underlined)</b>
rTEV 5'	GATCTGAAAACGTGTATTTTCAGGGCGGATCCCC GAATTCCCGGGTCGACTCGAGCTGCAGC
rTEV 3'	GGCCGCTGCAGCTCGAGTCGACCCGGGAATTCGGGGATC CGCCCTGAAAATACAGGTTTTCA
GST-LspA1 <i>Bam</i> HI 5'	CGC <u>GATCC</u> GTGAGAAGCAAAATTAACGAT
GST-LspA1 <i>Xho</i> I 3'	CCG <u>CTCGAG</u> CTAACCTAACTCCGGCAATTTTGATTG
GST-LspA1- <i>Xho</i> I 6xHis 3'	CCG <u>CTCGAG</u> CTAGTGATGGTGATGGTGATGCG ATCCTCTACCTAACTCCGGCAATTTTGATTG

#### D. Construction of Site-Directed Mutations

The site-directed mutagenesis kit QuikChange II XL (Stratagene) was used according to the manufacturer's instructions. The templates for mutagenesis were either the pMAL1 or pGSTwt plasmids containing the *yopT* homology region of the *lspA1* gene. A list of site-directed primers used to generate nucleotide changes is contained below in Table 11. After digestion with *Dpn*I, these reaction mixtures were transformed into *E. coli* XL10 – Gold (Stratagene) or *E. coli* TOP10 (Invitrogen) and the resultant clones are described in Table 4 above.

**Table 11.** Primers used for construction of site-directed mutations.

<b>Primer</b>	<b>Primer Sequence 5' – 3'</b>
YopT C2837A 5'	GCAGAGACACAAAATGGCGTAGCTGAAGCGACTTGTTCACTGG
YopT C2837A 3'	CCAGTGTGAACAAGTCGCTTCAGCTACGCCATTTTGTGTCTCTGC
YopT C2841A 5'	GCAGAGACACAAAATGGCGTATGTGAAGCGACTGCTTCACACTGG
YopT C2841A 3'	CCAGTGTGAAGCAGTCGCTTCACATACGCCATTTTGTGTCTCTGC
YopT doubleCtoA 5'	GCAGAGACACAAAATGGCGTAGCTGAAGCGACTGCTTCACACTGG
YopT doubleCtoA 3'	CCAGTGTGAAGCAGTCGCTTCAGCTACGCCATTTTGTGTCTCTGC
YopT S2842A 5'	GGCGTATGTGAAGCGACTTGTGCACACTGGATAGCGAAGAAAGTC
YopT S2842A 3'	GACTTTCTTCGCTATCCAGTGTGCACAAGTCGCTTCACATACGCC
YopT doubleCandS 5'	GGCGTAGCTGAAGCGACTGCTGCACACTGGATAGCGAAGAAAGTC
YopT doubleCandS 3'	GACTTTCTTCGCTATCCAGTGTGCAGCAGTCGCTTCAGCTACGCC
YopT H2961A 5'	ATAAACTTAGAGGGCGGCTCAGCCACCGTATCAGCAAGTATAGAA
YopT H2961A 3'	TTCTATACTTGCTGATACGGTGGCTGAGCCGCCCTCTAAGTTTAT
YopT D2976A 5'	GGGCAAAAAGTTGTATTCTTTGCACCTAACTTTGGCGAAATTACC
YopT D2976A 3'	GGTAATTTTCGCCAAAGTTAGGTGCAAAGAATACAACCTTTTGGCCC

## **IX. Transposon Mutagenesis of *H. ducreyi* Constructs Containing the *lspB-gfp* Reporter Construct**

### **A. Tn916 Transposon Mutagenesis**

Tn916 mutagenesis has been previously reported to yield transposon insertion mutants of *H. ducreyi* (158). To determine the identity of gene products possibly involved in the regulation of the *lspA1* and *lspB* genes, this mutagenesis scheme was utilized. The basis for this mutagenesis was to screen for mutants that had GFP expression levels that had changed relative to the levels of their parent strain. Both the wild-type 35000HP strain and the *lspA1 lspA2* mutant strain 35000Ω12 containing the plasmid pJM250 (i.e., the *lspB-gfp* reporter) were made electrocompetent as described above. The plasmid pAM120, which contains the transposable element Tn916, was isolated as previously described (158) and 1 – 2 µg of plasmid DNA was electroporated into these two strains. Mutants harboring transposon insertions were selected on CA containing tetracycline (5 µg/mL) along with streptomycin (100 µg/mL) to maintain the *lspB-gfp* reporter plasmid pJM250. Putative mutant colonies were picked and patched onto large CA plates containing both antibiotics listed above and each mutant's GFP expression level was compared to that of their respective parent strains. Those mutants that had visibly detectable differences in GFP expression were single colony passed two times and their chromosomal DNA was isolated. Plasmids isolated from these mutants were compared to pJM250 by gel electrophoresis to confirm that no obvious changes had occurred in the reporter construct. The chromosomal

DNA was then used as a template for nucleotide sequence analysis to determine the *H. ducreyi* genomic DNA region where the Tn916 transposon had been inserted. The two primers used for sequencing reactions were Tn916-L 5' – GATAAATCGTCGTATCAAAG – 3' and Tn916-R 5' – GAAATATGCAAAGAAACGTG – 3'. The sequence data were then used in BLAST searches against the *H. ducreyi* genome to determine the gene region(s) that had been disrupted by the transposon.

## **B. GFP Expression Measurements**

For quantitative measurement of GFP expression by *H. ducreyi* constructs, relevant strains were grown overnight on CA plates containing streptomycin (100 µg/mL), the cells were harvested into 1 mL of PBS, and vortexed. These suspensions were added to 3 – 5 mL PBS to an OD<sub>600</sub> = 0.3. Aliquots of these standardized suspensions were then placed in a 96-well plate and GFP fluorescence was determined using a SPECTRAFluor Plus fluorometer (Tecan, Research Triangle Park, NC) at a wavelength of 590 nm.

## **X. RT-PCR Analysis**

To determine the transcriptional unit and possible operonic nature of the *lspB* and *lspA2* genes, reverse transcriptase-PCR was performed. RNA prepared and DNase-treated as described above was reverse-transcribed with the SuperScript II reverse transcriptase (Invitrogen) Kit for two hours at 42°C using the *H. ducreyi* genome-directed

primer set (57 6-mer primers) to initiate cDNA synthesis. Then the primer set RT LspA2 5' – GAGGGCAACAAGTAGAAGTAGATG – 3' and RT LspA2 5' – TTTGCCGCGTTGGTAAT – 3' was used to determine the presence of the *lspA2* transcript by PCR analysis. This primer set was designed to only amplify cDNA derived from the *lspA2* transcript. The PCR amplicons were then electrophoresed in an agarose gel.

## **XI. Real-Time RT-PCR**

To quantitate RNA transcript levels, real-time RT-PCR was performed. For determination of the transcriptional levels of the *lspA1* and *lspB* genes, RNA was prepared as described above and was DNase-treated to remove any DNA contamination. Primers were designed using Primer Express software (Applied Biosystems, Foster City, CA), and primers designed to measure 16S rRNA levels were used as an internal control and to normalize all data. The primers designed and used in real-time RT-PCR analysis are listed in Table 12. All assays were performed in triplicate. A master mix for each transcript was prepared and each well contained 12.5  $\mu$ L of 2X SYBR Green Master Mix (Applied Biosystems), 1  $\mu$ L of 2.5  $\mu$ M of each primer, 0.1  $\mu$ L of MultiScribe Reverse Transcriptase (50 U/ $\mu$ L) (Applied Biosystems), and dH<sub>2</sub>O to bring the final volume to 20  $\mu$ L. Next, 5  $\mu$ L portions of the RNA samples (20 ng/ $\mu$ L) were added to each well. The ABI 7500 Sequence Detection System (Applied Biosystems) was used to perform the real-time RT-PCR analysis and the 7500 System SDS v.13 software was used to analyze the raw data. The relative quantitation method ( $\Delta\Delta C_T$ ) was used to determine possible transcriptional differences.

**Table 12.** Primers used for real-time RT-PCR.

Primer	Primer Sequence 5' – 3'
LspB 5' realtime	TGACGATAGCGGTGAAACGAC
LspB 3' realtime	TCGTCCCCGATTGAGAATTG
16S rRna 5' realtime	GCGGCAGGCTTAACACATG
16S rRna 3' realtime	TCCCCCTCCATAAGCCAGAT

## XII. DNA Affinity Purification Methods

To identify possible transcriptional factors that could be involved in the regulation of the *lspA1* and *lspB* genes, DNA promoter “pull-down” experiments were performed. Primers used in this study are listed in Table 13 below. The 5' primer for each set was modified with a biotin group which, during PCR amplification, would be incorporated into the 5' region of the putative promoter region. The presence of the biotin would then allow for binding of the amplified promoter region to magnetic strepavidin M-270 Dynabeads (Invitrogen). The primers were used in standard PCR reactions and the products were electrophoresed on agarose gels and gel-purified (Promega) according to the manufacturer's instructions. A 200  $\mu$ L aliquot (2 mg) of magnetic Dynabeads were placed in a microcentrifuge tube and washed three times in 2X B&W buffer (10 mM Tris-HCl, pH 7.5, 1 mM EDTA, 2 M NaCl) and after the final wash, the beads were resuspended in 400  $\mu$ L of B&W buffer. The washes were accomplished by placing the microcentrifuge tube in a

magnet holder to pellet the beads and then carefully removing the supernatant fluid with a pipet. Next, an equal volume of gel-purified and biotinylated PCR product was added to the magnetic beads and incubated with gentle rotation for 15 min at room temperature. The beads were separated from the fluid phase by placing the tube in the magnetic holder for 2 min and then the beads with the biotinylated PCR products were washed three times as described above with 1 mL of 1X B&W buffer. After the final wash, the biotinylated PCR-bead complex was resuspended in 400  $\mu$ L of 1X B&W buffer. The beads were then incubated with lysates prepared from *H. ducreyi* strains 35000HP or 35000HP $\Omega$ 12. Lysates from these two strains were obtained by harvesting the growth from 10 CA plates grown overnight and suspending the cells in 3 mL of PBS. The suspension was then placed in metal sonication tubes held in a ice water slurry, and the suspension was subjected to sonication using a model 450 sonifier (Branson Sonic Power Co., Danbury, CT) with settings at 70% duty, setting 6 – 7, and 30 seconds per sonication with a 30 sec rest period between sonications. This was repeated five times for each sample. After sonication, 400  $\mu$ L of 1 M KCl (Sigma) and 800  $\mu$ L of 5% streptomycin sulfate (Sigma) were added to the sonicate to precipitate DNA and to dissociate DNA-binding proteins from genomic DNA. The sonicate was then centrifuged at 12,000 x g for 15 min at 4°C. The supernatant fluid was transferred to a new centrifuge tube and centrifuged at 46,000 x g for 1 h at 4°C. The suspension was then concentrated to 500  $\mu$ L using an Amicon Ultra centrifugal filter device (10,000 MWCO) (Millipore, Inc., Bedford, MA). Then the concentrated lysate was incubated with the biotinylated PCR-bead complex for 30 min at room temperature. Utilizing the magnetic holder, the bead complex was washed two times with 1X B&W buffer containing 10 mg/mL of needle-sheared salmon sperm DNA, followed by two



washes with 1X B&W buffer. The beads were then washed twice with 1X B&W buffer containing 0.15 M NaCl and then DNA-bound proteins were eluted with 100  $\mu$ L of elution buffer (1X B&W buffer containing 0.5 M NaCl). To each elution, 50  $\mu$ L of 3X Digestion buffer was added and the eluted proteins were resolved on SDS-PAGE and silver stained (Bio-Rad). The recovered protein bands were compared between the control promoter (the *H. ducreyi g6pd* gene) and the experimental promoters from *lspA1* or *lspB*. Bands recovered only with the experimental promoters were excised from the gel, subjected to tryptic digest, and then to HPLC - mass spectrometry (performed by the UT Southwestern Protein Sequencing Core) to determine protein identities when compared to *H. ducreyi* genome BLAST data.

**Table 13.** Primers used in DNA-binding experiments.

Primer	Primer Sequence 5' – 3'
LspA1 5' Biotin	/5Bio/ATTTTACCGCATGATCACCATAA
LspA1 3'	TATAACGTTTGTTCATAATG
LspB 5' Biotin	/5Bio/TTTCGCTACATCAGTTAAACCATC
LspB 3'	ATGTTGCAACACCTGAAAGCATAA
G6PD 5' Biotin	/5Bio/ATAATTCGCCCGCTTACTCCTCAC
G6PD 3'	ATGTTTCGCCTAACCGACCTACTTT

### **XIII. Bacterial Antigen Preparation**

#### **A. Whole Cell Lysates**

For analysis of total cellular proteins of either *H. ducreyi* or *E. coli*, whole cell lysates were prepared. The overnight growth from one agar plate of *H. ducreyi* or *E. coli* bacteria was harvested and suspended in 1 mL of PBS by vortexing. The suspension was then diluted in PBS to an OD<sub>600</sub> reading of 0.3 to standardize for biomass between samples and 200 µL was removed and placed in a microcentrifuge tube. Next, 100 µL of 3X digestion buffer (0.15 M Tris-HCl (pH 6.8), 6% (wt/vol) glycerol and 0.015% (wt/vol) pyronin Y tracking dye) was added. The solution was vortexed to mix thoroughly and the sample heated to 100°C for 5 min. before being subjected to SDS-PAGE.

#### **B. Concentrated Culture Supernatant Fluid**

Concentrated culture supernatant fluids (CCS) were prepared from broth-grown *H. ducreyi* as described (215). Briefly, the culture supernatant fluid was first subjected to centrifugation at 6,000 x g for 10 min at 4°C to remove the bacteria. The resultant supernatant fluid was passed through a 0.22 µm (pore-size) filter and then subjected to ultracentrifugation at 125,000 x g for 1 h at 4°C to remove membrane fragments. Lastly, this fluid was concentrated 40-fold by using an Amicon Ultra centrifugal filter device (100,000 MWCO) (Millipore, Inc., Bedford, Mass) and used immediately in the

phagocytosis assays, or mixed with 3X digestion buffer for SDS-PAGE or Western blot analysis.

### **C. Preparation of Bacterial Cell Envelopes**

*H. ducreyi* strains were grown overnight on 10 – 30 CA plates. The cells were harvested in 10 mL of ice-cold PBS (pH 7.4) and kept on ice. The cells were then homogenized (in a Dounce homogenizer) on ice by gently (avoiding the formation of foam or bubbles) pressing back and forth 30 times with the plunger. The suspension was then placed in a metal sonication tube and the suspension was subjected to sonication using a model 450 sonifier (Branson Sonic Power Co., Danbury, CT) with settings at 70% duty, setting 6 – 7 and 30 seconds per sonication with a 30 sec rest period between sonications. This was repeated five times for each sample. The sonicate was then centrifuged at 12,000 x g for 15 min at 4°C. The supernatant was transferred to a new centrifuge tube and centrifuged at 38,700 x g for 1 h at 4°C. The resultant pellet was then suspended in 500 µL of H<sub>2</sub>O and had an amber appearance. A Lowry or Bradford protein assay was then performed to determine protein concentration of the sample which was stored at -20°C.

### **D. Sarkosyl Extracts of Cell Envelopes**

To prepare cell fractions enriched for outer membrane proteins, the Sarkosyl method with modification was used (73). The cell envelope preparations described above were diluted with 10 mM Hepes buffer (pH 7.4) to a final protein concentration of 3 mg/mL.

Then, to a 2.5 mL volume of this diluted suspension, 2.5 mL of 10 mM HEPES buffer and 5 mL of 2% (wt/vol) sodium N-lauroylsarcosine (Sigma) in 10 mM HEPES (Sarcosyl detergent) were added. This mixture was placed on a rotator and agitated for 35 min at room temperature to solubilize cytoplasmic membrane proteins. The sample was then centrifuged at 363,000 x g for 1 h at 25°C. The supernatant was removed and the pellet was suspended in 500 µL of dH<sub>2</sub>O and, if necessary, homogenized to facilitate resuspension. A Lowry protein assay was performed to determine protein concentration and the sample was stored at -20°C.

#### **XIV. Sodium Dodecyl Sulfate-Polyacrylamide Gel Electrophoresis (SDS-PAGE)**

Protein samples were mixed with 3X digestion buffer (as described above) and heated for 100°C for 5 min. prior to loading onto the gel. Several different gels were utilized depending on the application. Routinely, the Mini-PROTEAN 3 cell or the Criterion cell were used (Bio-Rad). However, for better separation, the Hoefer SE 600 electrophoresis unit (Amersham Pharmacia Biotech, Piscataway, NJ) was used. All polyacrylamide gels were made using a 30% acrylamide/bis solution, 37.5:1 (Bio-Rad). The stacking gel consisted of 4% (wt/vol) polyacrylamide, 0.125 M Tris-HCl (pH 6.8) and 0.1 % (wt/vol) SDS. Depending on the application, the separating gels consisted of either 5%, 7.5%, 10%, 12.5%, 15% or 17.5% (wt/vol) polyacrylamide, 0.375 M Tris-HCl (pH 8.8), and 0.1% (wt/vol) SDS. The gels were polymerized with 0.1% (wt/vol) APS (Bio-Rad) and 0.1% (wt/vol) TEMED (Bio-Rad). The running buffer was composed of 0.025 M Tris-HCl (pH 8.3), 0.192 M glycine, and 0.1% (wt/vol) SDS.

Routinely, gels were subjected to electrophoresis using a constant current of 25 – 40 mA and run until the dye front reached the bottom of the gel. High molecular weight range Rainbow markers (Amersham) were run in one lane of every gel as a standard for protein separation.

To visualize proteins in the gel, several staining methods were used. Routinely, gels were stained with 0.1% (wt/vol) Coomassie Brilliant Blue R-250 stain (Sigma) dissolved in 10% (vol/vol) acetic acid (Sigma) and 25% (vol/vol) methanol (Sigma) for 20 min. with agitation. Gels were then destained using destain solution (10% (vol/vol) acetic acid, 10% (vol/vol) methanol, 6% (vol/vol) glycerol) until protein bands could be visualized and images could be obtained with the AlphaImager (Alpha Innotech Corporation, San Leandro, CA), or the gel itself was dried and encased in cellophane using a drying frame (Research Products International Corp., Mount Prospect, IL). To detect smaller amounts of protein, silver staining of protein was performed with the Bio-Rad Silver Staining Kit (Bio-Rad) as per the manufacturer's instructions.

## **XV. Western Blot Analysis**

Proteins resolved by SDS-PAGE were transferred to Immobilon-P Transfer Membrane (polyvinylidene difluoride (PVDF)) as per standard methods (209) in Tris-glycine transfer buffer (20 mM Tris-HCl (pH 8.3), 150 mM glycine, 20% (vol/vol) methanol). Proteins were transferred at constant voltage (120 V) for 1 h. The membranes

were then blocked for one hour with either 4% (wt/vol) BSA (Sigma) or 3% skim milk in PBS (1.1 M NaCl, 21 mM KCl, 83 mM Na<sub>2</sub>HPO<sub>4</sub>, 12 mM KH<sub>2</sub>PO<sub>4</sub>, (pH 7.4) containing 0.05% (vol/vol) polyoxyethylenesorbitan monolaurate (Tween 20). Next, the membranes were incubated with the primary antibody either for 2 – 4 h at room temperature or overnight at 4°C. Membranes were then washed with PBS-Tween three times for 15 min. each and subsequently incubated with a secondary antibody conjugated to horseradish peroxidase for 1-2 hours at room temperature. The blots were again washed three times with PBS-Tween and the horseradish peroxidase-antibody conjugates were detected by chemiluminescence by using the Western Lightning Chemiluminescence Reagent Plus (New England Nuclear, Boston, MA) followed by exposure to Fuji Medical X-ray film (Fujifilm/Diagnostic Imaging, Dallas, TX).

## **XVI. Protein Expression, Purification, and Analysis Methodologies**

### **A. Agar Plate-Based Extractions for LspA1**

To obtain a larger amount of the LspA1 protein than could be obtained from the concentrated culture supernatant method, a rapid extraction method was performed using whole cells of the *H. ducreyi* 35000HPΩ2 *lspA2* mutant strain (which expresses only LspA1) that had been grown overnight on 40 chocolate agar plates. The bacterial growth was harvested into a mixture (sCB-FCS) of supplemented Columbia broth with 2.5% (vol/vol) of a dialysate containing fetal bovine serum components with a molecular weight

of less than 10 kDa. This mixture also contained a protease inhibitor cocktail (Roche). The suspended cells were incubated in this mixture for 30 min. at 37°C. The bacterial cells were then removed by low-speed centrifugation (4,000 x g for 10 min) at room temperature, and the resultant supernatant fluid was filter-sterilized through a 0.22 µm filter (Millipore). The filtered supernatant was then subjected to ultracentrifugation at 60,000 x g for 1 h at 4°C to remove membrane blebs and fragments. The cleared supernatant was then probed in Western blot analysis with the LspA-reactive MAb 11B7 to determine the presence and amount of LspA1 protein present in the preparation.

## **B. Recombinant Protein Expression and Purification**

### **I. His-tagged Fusion Proteins**

The 12.5 kb *lspA1* ORF was segmented into thirteen, approximately 1 kb fragments which were then amplified by PCR and cloned into the plasmid vector pQE-30 (Qiagen, Inc., Valencia, CA) to obtain fusion proteins consisting of LspA1 protein segments with an N-terminal 6XHis tag as described above. To induce the expression of the 6xHis-LspA1 fusion proteins, isopropylthio-β-D-galactoside (Invitrogen, Carlsbad, CA) was added to a final concentration of 1 mM. Each His-LspA1 fusion protein was purified as per the Qiagen protocol.

### **II. Maltose-Binding Protein Fusion Proteins**

As described above, the pMal constructs containing regions of the *lspA1* gene were expressed in *E. coli* TOP10 cells and the MBP-LspA1 fusion proteins were purified according to the manufacturer's instructions (New England Biolabs).

### **III. Glutathione-S-Transferase Fusion Proteins**

As described above, the pGEX constructs containing fragments of the *lspA1* gene were expressed in *E. coli* TOP10 cells and the GST-LspA1 fusion proteins were purified as detailed below. Cell cultures were grown at 37°C with agitation at 250 rpm to an OD<sub>600</sub> of 0.6 – 0.8 and then induced with IPTG (at a final concentration of 3 mM) for 2 – 4 h. The cells were harvested by centrifugation at 6,000 x g for 10 min at room temperature. The supernatant fluid was discarded and the pellet resuspended in lysis buffer (PBS [pH 7.4], 1% Triton X-100 [Sigma], 0.1% 2-mercaptoethanol) containing a protease inhibitor cocktail (Roche). The suspension was then sonicated as described previously and centrifuged at 20,000 x g for 30 min at 4°C. The supernatant was incubated with 1 – 2 mL of GSH agarose beads (Sigma) for 1 h at 4°C with gentle agitation. The beads were then centrifuged at 150 x g for 2 min at room temperature and the supernatant fluid removed. The beads were washed four times with 5 mL of PBS (pH 7.4) containing 1% Triton X-100 and 0.1% 2-mercaptoethanol. After the final wash, 1.5 mL of elution buffer (50 mM Tris [pH 7.6], 150 mM NaCl, 0.1% 2-mercaptoethanol and 10 mM glutathione [Sigma]) was added to the beads to elute the GST-LspA1 fusion protein, which was stored at -70°C.



### C. Chromatographic Separations Using Ion-Exchange

Chromatographic separation of proteins in homogenates derived from macrophages that had been incubated with either the wild-type *H. ducreyi* strain or the *lspA1 lspA2* mutant was performed as previously described (190). Briefly, the mammalian cell line J774A.1 (ATCC – TIB 67) was incubated with either the wild-type 35000HP or the *lspA1 lspA2* mutant 35000HP $\Omega$ 12 strain at 33°C for 4 h as described below. After decanting the fluid from the flasks, the monolayers were washed once with 10 mL of ice-cold PBS (pH 7.4) and then the cell monolayer was scraped and suspended in 40 mL of ice-cold PBS (pH 7.4). The suspension was then subjected to centrifugation at 150 x g for 5 min. at room temperature to pellet the mammalian cells. The cell pellets were resuspended in 40 mL of PBS (pH 7.4) and washed two more times as above. After the third wash, the cell pellets were resuspended in 4 mL of cold Buffer B (20 mM Tris-HCl, 2 mM EDTA, and 2 mM 2-mercaptoethanol, pH 7.6) containing a protease inhibitor cocktail (Roche), and incubated on ice for 15 min. The J774A.1 cells were then disrupted with a Dounce homogenizer on ice by gently (avoiding the formation of foam or bubbles) pressing back and forth 30 times with the pestle. The homogenate was incubated on ice for 20 min. and then subjected to centrifugation at 60,000 x g for 1 h at 4°C. The supernatant fluid was then filtered through a 0.22  $\mu$ m pore filter (Millipore) and a Bradford assay was performed to determine the protein concentrations of the two samples. If necessary, the more concentrated homogenate was diluted so that the protein concentrations loaded onto the ion-exchange column would

be equivalent between the two samples. The samples (2 mL) were applied to a 5 mL HiTrap Q-sepharose column (Amersham Biosciences) linked to an AKTA FPLC system (Amersham Biosciences). Proteins that were retained on the column were eluted with a linear NaCl gradient (Buffer C: Buffer B plus 1 M NaCl) at a flow rate of 1.0 mL/min. For each chromatography run, forty fractions of 3 mL each were taken and each was tested in the ELISA-based protein-tyrosine phosphatase (PTPase) assay as described below.

## **XVII. Generation of Immune Sera and Monoclonal Antibodies**

### **A. Generation of Polyclonal Antisera Raised to Recombinant LspA1 Protein**

Purified, denatured 6xHis-tagged LspA1 fusion proteins were obtained as per the Qiagen protocol and used to immunize 8-week-old female BALB/c mice (Charles River Laboratories Inc., Wilmington, MA). Five mice were immunized with each of the 13 separate N-terminal, His-tagged fusion proteins described above. Briefly, BALB/c mice were first injected intraperitoneally (IP) with 30 µg of purified protein mixed 1:1 with Freund's Complete Adjuvant (FCA). Then, 4 weeks following the primary injection, mice were injected IP with 10 µg of purified denatured protein mixed 1:1 with Freund's Incomplete Adjuvant (FIA). Serum was prepared from blood drawn two weeks after the booster immunization. These LspA1 antisera were used in Western blot analysis to probe *H. ducreyi* concentrated culture supernatant (CCS) fluids, prepared as previously described

(4). Western blot analysis demonstrated that 10 of the 13 6xHis-tagged proteins induced the synthesis of polyclonal antibodies against the LspA proteins.

### **B. Generation of a Monoclonal Antibody to Recombinant LspA1 Protein**

Nucleotides 7045-7929 (in the *lspA1* gene) encoding amino acids 2349-2639 from the *H. ducreyi* LspA1 protein were amplified from *H. ducreyi* 35000HP chromosomal DNA by PCR using the oligonucleotide primers 5'-CGGGATCCGTGGATGAGAGCCCTTATGCT-3' (*Bam*HI site underlined) and 5'-CGCTCGAGTTACTTACCACGAGACTTAGGCGT-3' (*Ava*I site underlined). After digestion with *Bam*HI and *Ava*I, this fragment was ligated into plasmid pQE-30 (Qiagen, Valencia, CA) to generate a 6XHis-LspA1 fusion protein that was then purified and provided to Dr. Wayne Lai in the Department of Pathology at the University of Texas Southwestern Medical Center who used the purified protein preparation to immunize three BALB/c mice for production of lymphocyte hybridoma secreting monoclonal antibodies. Culture supernatant fluid from the hybridoma fusion clones were screened in an ELISA assay for reactivity with the purified 6xHis-LspA1 protein. Those that showed reactivity were then further screened by taking the individual hybridoma supernatant fluid (2 -5 mL) and using these in immunoprecipitation reactions to determine if the monoclonal antibody would precipitate the native LspA proteins from concentrated culture supernatant fluid preparations. Hybridoma culture supernatant fluid from the hybridoma cell line 3H9 bound an approximately 270 kDa LspA antigen present in *H. ducreyi* CCS.

## **XVIII. Phagocytosis Assays**

### **A. Opsonization of Secondary Targets**

Opsonization of streptavidin-coated green fluorescent microspheres (Bangs Laboratories, Inc. Fisher, Ind.) and sheep erythrocytes (Colorado Serum Co. Denver, Co.) was performed as reported previously, with the only change being that the fluorescent microspheres were opsonized with rabbit anti-streptavidin IgG (Rockland Immunochemicals, Gilbertsville, Pa) (215).

### **B. Phagocytosis Assays Utilizing Fluorescent Microspheres As a Secondary Target**

Portions (100  $\mu$ l volume) of CCS from wild-type 35000HP and the 35000 $\Omega$ 12 mutant were added to a 96-well tissue culture plate containing differentiated HL-60 cells at a concentration of  $5 \times 10^5$  cells/well. Similarly, 100  $\mu$ l volumes of immunodepleted CCS fluids (described below) prepared from both wild-type 35000HP and the 35000HP $\Omega$ 12 mutant were added to HL-60 cells. The supernatant fluids were incubated with HL-60 cells at 33°C for 1 hr. Then, a 10  $\mu$ l portion of opsonized fluorescent microspheres ( $\sim 5 \times 10^7$  particles) was added to each well and incubated at 37°C for 1 hr with gentle shaking. After 1 hr, the HL-60 cells were transferred from the 96-well plate to microcentrifuge tubes and

washed two times (130 x g, 7 min) with PBS containing 1 % (w/v) bovine serum albumin. The washed cells were then suspended in 100 µl PBS, transferred into a 96-well microtiter plate, and centrifuged at 150 x g for 5 min. Then, the percentage of HL-60 cells containing fluorescent microspheres was determined by fluorescent microscopy to measure phagocytic activity.

### **C. Phagocytosis Assays Utilizing Opsonized Red Blood Cells As a Secondary Target**

These assays were performed using J774A.1 cells attached to glass coverslips in 24-well plates ( $1 \times 10^5$  cells/well) in tissue culture medium without FBS. The cells were incubated for 1 h at 33°C with *H. ducreyi* cells (MOI=25). Sheep erythrocytes opsonized with rabbit IgG (EIgG) were added to each well and incubated for 30 min at 37°C as described (85). To measure ingestion, extracellular erythrocytes were lysed with 0.2% saline for 1 min. The cells were fixed with 2% glutaraldehyde for 10 min at room temperature and viewed by light microscopy. For each well, 100 cells were counted from at least 5 separate high-power fields that were selected at random.

## **XIX. Immunoprecipitation Methods**

In general, immunoprecipitation reactions were performed by first preparing protein-standardized lysates or homogenates and then adding the appropriate antibody

(approximately 2-5 µg total antibody/reaction) to the lysate or homogenate. The reactions were routinely allowed to incubate overnight with rotation at 4°C. Then, 30 µL of Protein A/G agarose (Santa Cruz Biotechnology, Santa Cruz, CA) was added to each reaction and the suspension was mixed for 1 h at 4°C and then subjected to centrifugation at 12,000 x g for 5 sec to pellet the antigen-antibody-agarose complexes. The antigen-antibody-agarose complexes were washed 3 – 4 times with RIPA buffer (Santa Cruz Inc.). The immunoprecipitated complexes were then resuspended either in 50 µl of 3X digestion buffer for SDS-PAGE analysis or in the appropriate reaction buffer for subsequent applications.

## **XX. Immunodepletion Method**

CCS from the wild-type strain 35000HP and the *lspA1 lspA2* mutant 35000HPΩ12 were incubated with heat-inactivated LspA1 mouse antiserum or with heat-inactivated normal BALB/c mouse serum for 2 h at 4°C. Protein A/G agarose (Santa Cruz Biotechnology, Santa Cruz, CA) was then added and the suspension was mixed for 1 h at 4°C and then subjected to centrifugation at 12,000 x g for 5 sec to remove antigen-antibody-agarose complexes. The resultant supernatant fluids were used in phagocytosis assays with HL-60 cells.

## **XXI. Src Tyrosine Dephosphorylation Assays**

### **A. Detection of Phosphoproteins by Western Blot Analysis**

Mammalian cell lines were incubated with cells of wild-type 35000HP and the *lspA1 lspA2* mutant 35000HP $\Omega$ 12 at 33°C for 4 hours. After decanting the fluid from the flasks, the monolayers were lysed with RIPA buffer (Santa Cruz Biotechnology, Inc). The protein content of the lysates was measured and standardized by using the Bradford method (Bio-Rad). These lysates were heated at 100°C for 5 min in digestion buffer (89) and proteins present in the lysates were resolved by SDS-PAGE using 10% (wt/vol) polyacrylamide separating gels and transferred to polyvinylidene difluoride (PVDF) membrane (Millipore Inc., Billerica, Mass.) The membranes were blocked with PBS containing 0.05% (vol/vol) Tween-20 and 4% (wt/vol) bovine serum albumin prior to incubation with primary antibodies. MAb 4G10 (Upstate Biotechnology Inc, Lake Placid, NY) was used to detect phosphotyrosine residues whereas the rabbit polyclonal antisera pY418 and pY529 (BioSource International, Inc., Camarillo, CA) were used to detect specific phosphorylated forms of Src family protein tyrosine kinases. Total Src protein was detected with MAb 327 (Calbiochem, San Diego, CA) and glyceraldehyde-3-phosphate dehydrogenase was detected with MAb 6C5 (Abcam, Cambridge, MA).

## **XXII. Fractionation of J774A.1 Cells for Detecting Small RhoGTPases**

J774A.1 cells were incubated with cells of wild-type 35000HP and the *lspA1 lspA2* mutant 35000HPΩ12 at 33°C for 3 – 4 h. After decanting the fluid from the flasks, the monolayers were washed once with 10 mL of ice-cold PBS (pH 7.4) and once with 10 mL of cold Tris buffer (20 mM Tris-HCl, 10mM EDTA, and 1 mM DTT, pH 7.4). The cell monolayer was then scraped and suspended in 10 mL of Tris buffer. The J774A.1 cells were disrupted with a Dounce homogenizer on ice by gently (avoiding the formation of foam or bubbles) pressing back and forth 20 – 30 times with the pestle. The homogenate was then subjected to centrifugation at 400 x g for 10 min. at 4°C to remove cellular debris. The supernatant fluid was then ultracentrifuged at 60,000 x g for 1 h at 4°C. The supernatant fluid (cytosolic fraction) was concentrated with Amicon (Millipore) 10,000 MWCO columns to a final volume of 200 – 400 µL. The pellet from the ultracentrifugation step was dissolved in 100 – 200 µL of Tris buffer. The protein content of the fractions was measured by using the Bradford method (Bio-Rad) and then standardized before resolving samples by SDS-PAGE and then transferring to polyvinylidene difluoride (PVDF) membrane (Millipore). The membranes were blocked with PBS containing 0.05% (vol/vol) Tween-20 and 4% (wt/vol) bovine serum albumin for 1 h prior to incubation with primary antibodies. The membrane and cytosolic fractions were probed with antibodies to Cdc42, Rac, and Rho to determine relative levels of these three proteins in these fractions.

### **XXIII. Cdc42 and Rac Activation Assays**



The mammalian cell line J774A.1 was incubated with either the wild-type *H. ducreyi* or *lspA1 lspA2* mutant strains as described above and then the amounts of active Cdc42 or Rac were determined by using the Cdc42 Activation Assay (Cat. # BK034, Cytoskeleton Inc., Denver, CO) per the manufacturer's instructions. Briefly, this kit involves a "pull-down" assay utilizing a GST-CRIB fusion that binds only the active GTP-bound form of Cdc42 or Rac. These precipitates can then be probed in Western blot analysis to determine the concentrations of Cdc42 or Rac present, representing the amount of active protein in the lysate.

#### **XXIV. *In vitro* Protein Tyrosine Kinase Assays**

J774A.1 macrophages were incubated with medium (control), wild-type *H. ducreyi* 35000HP, or the *lspA1 lspA2* mutant 35000HP $\Omega$ 12 for 4 hrs and then lysed with RIPA Buffer. The protein content of the lysates was measured and standardized by using the Bradford method (Bio-Rad). Polyclonal antibodies to Lyn (sc-15, Santa Cruz) and Hck (06-833, Upstate) were added and allowed to incubate overnight at 4°C to bind these macrophage kinases in the standardized lysates. Protein A/G agarose (Santa Cruz) was then added and the suspension mixed for 1 hr, followed by several washes with kinase buffer [32.5 mM Tris-HCl (pH 7.6), 6.25 mM MnCl<sub>2</sub> and 0.0625% (vol/vol) Triton X-100]. The immunoprecipitated complexes were resuspended in 40  $\mu$ l of kinase buffer and 1  $\mu$ g of a purified GST fusion protein containing the cytoplasmic region of the T cell receptor  $\zeta$  (zeta) subunit (190) was added along with unlabeled ATP to a final concentration of 0.024 mM.

This fusion protein was obtained from Dr. Nicolai S. C. van Oers in the Center for Immunology at UT Southwestern Medical Center. A 1  $\mu$ l portion of [ $\gamma$ - $^{32}$ P]ATP (specific activity = 10  $\mu$ Ci/ $\mu$ l) was added and the reactions were incubated at 30°C for 45 min. The kinase reaction was terminated by addition of 20  $\mu$ l of loading buffer followed by heating at 95°C for 5 min. Proteins in the reaction mixture were resolved by SDS-PAGE and transferred to PVDF membrane. Phosphorylated GST- $\zeta$  protein was detected by autoradiography. Additional Western blot analysis involving different antibodies to Lyn (sc-7274, Santa Cruz), Hck (sc-1428, Santa Cruz) and  $\zeta$  (MAb 6B10.2) (216) was used to verify that equivalent amounts of the immunoprecipitated protein tyrosine kinases and purified GST- $\zeta$  were loaded and transferred to the PVDF membrane. Relative quantitation of phosphorylated GST- $\zeta$  was achieved by using an Amersham Biosciences Storm 820 Phosphorimager.

## **XXV. Protease Treatment of Macrophages**

A 6 ml portion of tissue culture medium containing 3.3 mg/ml proteinase K, 1 mM CaCl<sub>2</sub>, and 5 mM MgCl<sub>2</sub> was added to monolayers of J774A.1 cells in 75 cm<sup>2</sup> tissue culture flasks and incubated for 45 min at 37°C. After the monolayers were washed twice with medium lacking FBS, medium containing 10% FBS was added and the monolayers incubated for 20 min at 37°C, followed by several washes with medium lacking FBS. The monolayers were then incubated with wild-type *H. ducreyi* or the *lspA1 lspA2* mutant for 4

hr at 33°C and the levels of active phospho-Src were determined by Western blot analysis using the anti-Src [pY418] phosphospecific antibody as described above.

J774A.1 monolayers were similarly treated with bovine pancreatic trypsin (6.7 mg/ml; Calbiochem) for 45 min-1 hr at 37°C followed by two washes with medium lacking FBS. Soybean trypsin inhibitor (Calbiochem) was then added to a final concentration of 2 mg/ml for 20 min. The monolayers were washed once with medium containing FBS followed by incubation for 20 min in this same medium. Following a final wash with tissue culture medium lacking FBS, the bacteria were added as described above for the proteinase K experiments.

## **XXVI. *In vitro* Protein Tyrosine Phosphatase (PTPase) Assays**

The ELISA-based protein tyrosine phosphatase assays (PTPase assay) were performed as previously described (190). Briefly, a 96-well plate (Corning CoStar, Cambridge, MA) was coated overnight at 4°C with purified phospho-src (pY418) at a 1/10000 dilution (100 µL/well) in a 0.2 M sodium carbonate (pH 9.1) buffer supplemented with sodium orthovanadate (Sigma), sodium fluoride (Sigma) and PMSF (Sigma). The purified phospho-src was a generous gift from Dr. Nicolai S. C. van Oers in the Center for Immunology at UT Southwestern Medical Center. The plate was washed four times with Tris-buffered salt solution containing 0.05% Tween-20 (TBST), and then blocked for 1 h with 300 µL of 4% BSA (Sigma) in TBST. The plate was then rinsed two times with TBST

and, following these two washes, the plate was then washed two more times in PTPase assay buffer consisting of 10 mM Tris-Cl (pH 8.0), 2 mM EDTA, and 2 mM 2-mercaptoethanol. Next, 100  $\mu$ L of PTPase assay buffer (50 mM Tris (pH 7.6), 0.1% Triton X-100, 2 mM EDTA, 2 mM 2-mercaptoethanol) was added to each well. Then 40 – 80  $\mu$ L of each fraction from the J774A.1/*H. ducreyi* homogenate from the anion exchange chromatography procedure described above was added to the individual wells and incubated at 37°C for 1 h with agitation. The plate was then washed four times with TBST. Then, 100  $\mu$ L of anti-phosphotyrosine MAb (4G10, 1  $\mu$ g/mL) was added for 30 min. to each well with agitation at room temperature. Then the plate was washed four times with TBST and then 100  $\mu$ L goat anti-mouse IgG-conjugated HRP antibody (Zymed Laboratories, San Francisco, CA) was added for to each well, followed by agitation at room temperature for 30 min. The plate was then washed two times with TBST and then two times with PBS. The assay was then developed with the ABTS (2,2'-axino-di-(3-ethylbenz-thiazoline sulfonic acid) Solution Substrate Kit (Zymed) according to the manufacturer's instructions.

## **XXVII. Cell Staining and Fluorescent Microscopy**

### **A. Staining of the J774A.1 Actin Cytoskeleton**

Bacteria were grown for 15 hr in liquid culture, harvested by centrifugation for 10 min at 4,000 x g, and suspended in tissue culture medium lacking fetal bovine serum (FBS)

to an optical density at 600 nm ( $OD_{600}$ ) of 0.5. These assays were performed using J774A.1 cells attached to glass coverslips in 24-well plates ( $1 \times 10^5$  cells/well) in tissue culture medium without FBS. The J774A.1 cells were incubated for 1 hr at 33°C with *H. ducreyi* cells (MOI = 25). Sheep erythrocytes opsonized with rabbit IgG (EIgG) were added to each well and incubated for 3-6 min at 37°C. The J774A.1 cells were washed twice with PBS and then fixed with 3.7% formaldehyde for 10 min at room temperature. The cells were then permeabilized with 0.1% (vol/vol) Triton X-100 in PBS for 3-5 min at room temperature. To reduce nonspecific background, 1% (wt/vol) bovine serum albumin was incubated with the coverslips for 30 minutes prior to adding staining solution. The staining solution consisted of 5  $\mu$ L of methanolic stock solution of rhodamine-phalloidin (Molecular Probes, Eugene, Oreg.) and 0.5  $\mu$ L of Oregon Green 488 goat anti-rabbit IgG (Molecular Probes) in 200  $\mu$ L of PBS for each coverslip to be stained. The staining solution was placed on the coverslip for 20 min at room temperature. The coverslips were washed two times with PBS and mounted on a slide (cell-side down) in Vectashield mounting medium solution (Vector Laboratories, Inc., Burlingame, Calif.). Slides were viewed using a CFI Plan Apochromat DM60X (NA 1.4) objective and a Nikon TE-200 inverted microscope equipped with epi-fluorescence. Imaging was performed using MetaMorph software (v. 6.1) and Nearest Neighbors digital deconvolution (Universal Imaging Corp., Downingtown, PA). This microscopy was performed by Steven Greenberg, M.D., at Columbia University Medical Center.

**XXVIII. Statistical Methods**

The paired Student *t* test was utilized to determine significance for experiments when necessary and *p* values less than 0.05 were considered statistically significant. In those instances, the method is mentioned in the relevant sections and *p* values are presented.

## CHAPTER FOUR

### Investigation of the Molecular Basis for the Regulation of Expression of LspA1, LspA2, and LspB

#### I. Introduction

While *H. ducreyi* is an obligate human pathogen, it is likely that this organism encounters several different environments within the host as the disease state progresses. Furthermore, as this pathogen encounters these varying conditions, it would benefit from regulating gene expression to allow for optimal growth, persistence, and immune evasion. Many pathogens regulate gene expression based on different environmental conditions and disease stages. By regulating gene expression, these pathogens can conserve energy by expressing only those factors necessary for survival and growth in a certain environment. To date, there are no published studies involving genetic regulation in *H. ducreyi*; however, experiments performed in this laboratory have determined that expression of the LspA proteins is indeed regulated by *H. ducreyi*. Examination of wild-type *H. ducreyi* CCS using MAbs specific for either LspA1 or LspA2 has shown readily detectable amounts of LspA1 protein (Fig. 6, panel A, lane 1) but only barely detectable quantities of LspA2 (Fig. 6 panel B, lane 1) (218). [Please note that Figure 6 is adapted from the publication by Ward et al (218).] Inactivation of the *lspA1* gene resulted in a dramatic increase in the amounts of detectable LspA2 protein in CCS (Fig. 6, panel B, lane 2) (218).

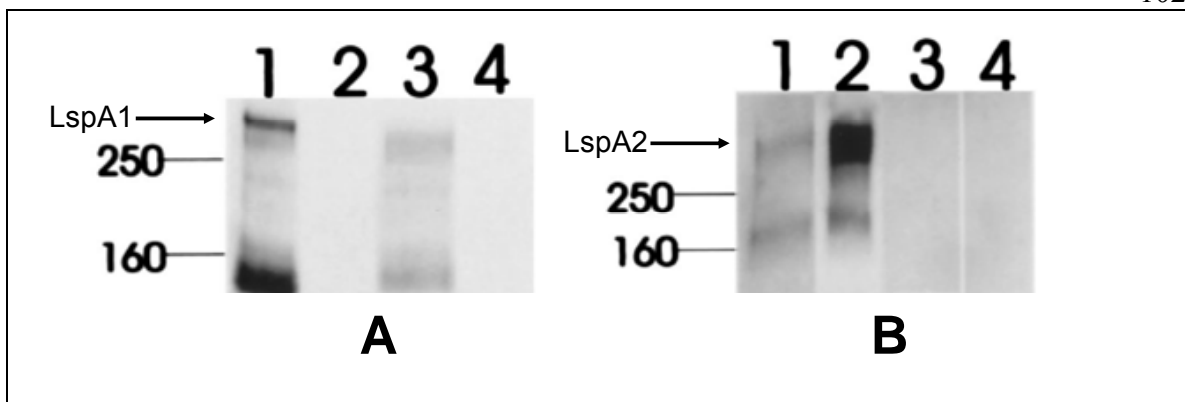


**Figure 6.** Western blot analysis of CCS prepared from wild-type and mutant *H. ducreyi* strains probed with (A) MAb 20A2 (LspA1-specific MAb) or (B) MAb 1H9 (LspA2-specific MAb). Lanes: 1, 35000HP; 2, *lspA1* mutant 35000HP.1; 3, *lspA2* mutant 35000HP.2; 4, *lspA1 lspA2* mutant 35000HP.12.

It should also be noted that LspB protein expression is apparently up-regulated in a *lspA1* mutant (Fig. 15), and this result would be expected in view of the fact that *lspB* and *lspA2* are co-transcribed as a single mRNA (Fig. 7) (220). These results demonstrate that regulation of these virulence factors of *H. ducreyi* is occurring. The overall extent of regulation of genes in *H. ducreyi* is unknown, but efforts to discover regulatory pathways should lead to a better understanding of the pathogenesis of disease caused by this organism. The observed up-regulation of LspA2 upon inactivation of LspA1 directly led to the work described herein to elucidate the molecular mechanism(s) that regulate the expression of the LspA and LspB proteins. How *H. ducreyi* “senses” that LspA1 is not being expressed and consequently up-regulates expression of LspA2 is not known. Experiments designed to determine the mechanism(s) that controls expression of the LspA proteins are described below; however, as a review for the reader, a brief summary of what is known about these proteins is provided directly below.



The LspA1 and LspA2 proteins of *H. ducreyi* are encoded by two of the largest prokaryotic ORFs (12.5 kb and 14.8 kb, respectively) described to date (Fig. 7). The predicted LspA1 and LspA2 proteins have calculated masses of approximately 456,000 Da and 542,000 Da, respectively, and 86% identity. Smaller forms of these two proteins, which likely represent processed products, can be detected in both *H. ducreyi* whole cell lysates and *H. ducreyi* CCS.

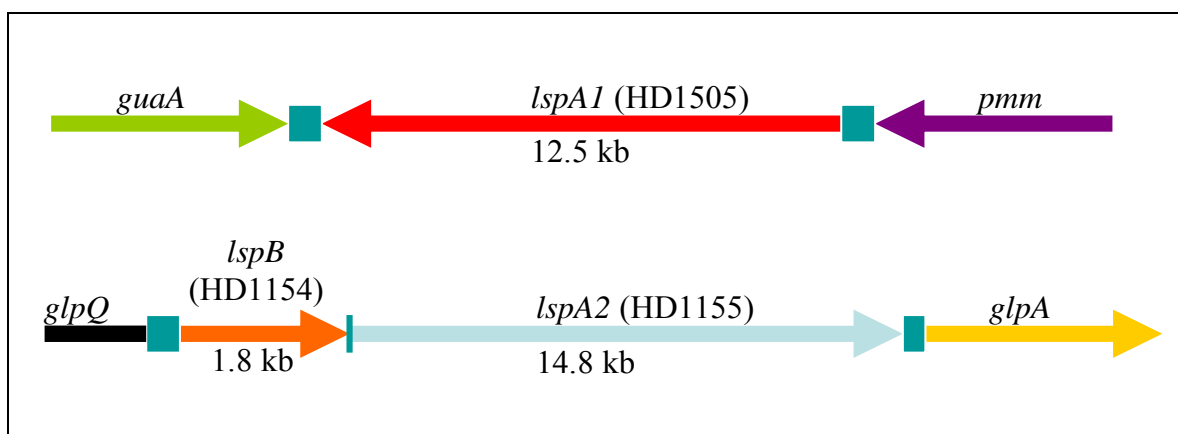


**Figure 7.** Gene map of the *lspA* and *lspB* genes from the 35000HP genome sequence with HD ORF numbers listed for the *lspA* and *lspB* genes.

Together with the LspB outer membrane protein, LspA1 and LspA2 comprise a two-partner secretion system (109) in which LspB is the secretion factor (220) (Fig. 8). To date, however, the active form of the LspA proteins has not been defined. Over the past several years, this laboratory has focused on the LspA1 and LspA2 proteins to assess their role in virulence expression. Both *lspA1* and *lspA2* have been shown to be transcribed *in vivo*, based on RT-PCR experiments performed in both animal (219) and human (206) models of experimental chancroid. Mutant analysis has shown that lack of expression of

both LspA1 and LspA2 results in much reduced lesion formation in a rabbit model (218) and a greatly reduced ability to form pustules in the human challenge model (112). Similarly, a *lspB* mutant that was unable to secrete either of these proteins was attenuated in the rabbit model (220). At the time when these studies were performed, however, the molecular basis for this attenuation of the *lspA1 lspA2* and *lspB* mutants was not known.

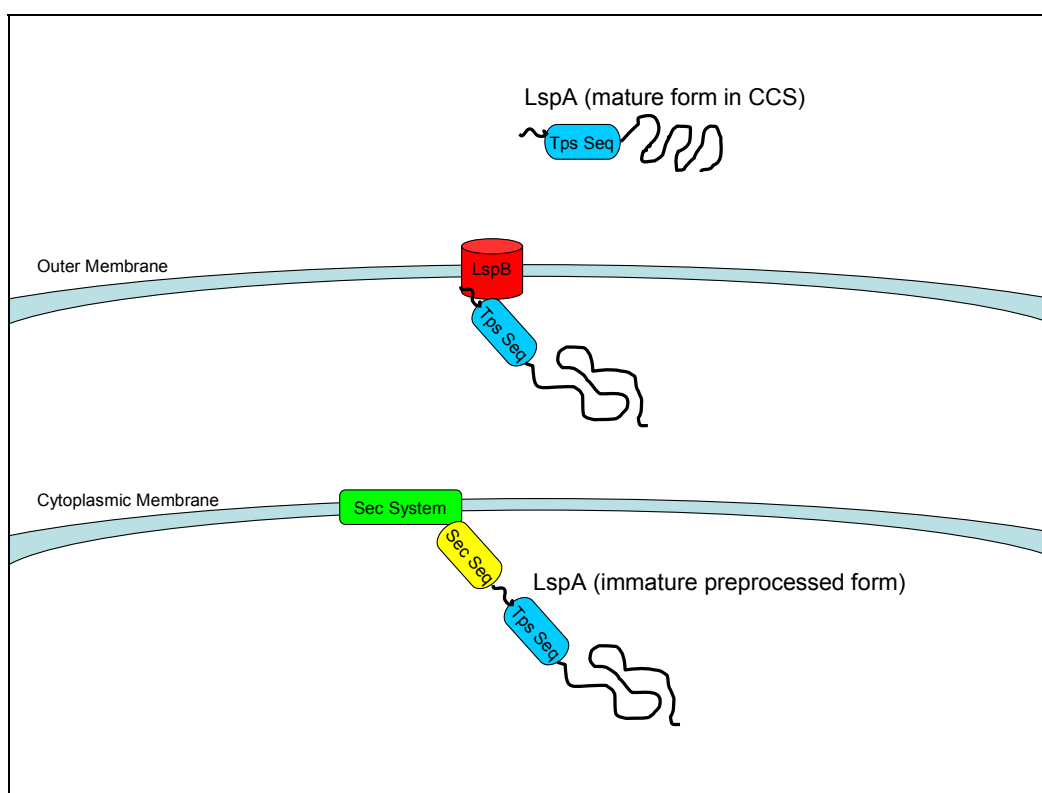


**Figure 8.** Schematic of the two-partner secretion system involving the LspA and LspB proteins.

Recently, this laboratory has established that expression of the LspA1 and LspA2 proteins by *H. ducreyi* is essential for this bacterium's ability to inhibit phagocytic activity. It has further been established that expression of either LspA1 or LspA2 individually is

sufficient for *H. ducreyi* to inhibit the phagocytic activity of PMN-like and macrophage-like cell lines *in vitro* (215). Precisely how the LspA proteins inhibit phagocytic activity is not apparent, but I have already identified one important effect exerted by the LspA proteins on macrophages. Incubation of wild-type *H. ducreyi*, but not the *lspA1 lspA2* mutant, with macrophages results in a dramatic reduction in the levels of the active form of Src family protein tyrosine kinases (presented in detail in Chapter Six). These protein tyrosine kinases are some of the most proximal effectors in the phagocytic signaling pathway.

## **II. Results**

### **A. Real-Time RT-PCR Analysis**

Using real-time RT-PCR, Dr. Kaiping Deng in this laboratory showed that the levels of both *lspB* and *lspA2* mRNA were increased in a *lspA1* mutant relative to those found in the wild-type parent strain (Fig. 9). The level of increase for *lspB* mRNA in the *lspA1* mutant was approximately 5-fold, while the level of increase for *lspA2* mRNA in the *lspA1* mutant was approximately 10-fold. These results correlated with the increased protein expression of the LspA2 protein seen in CCS by Western blot analysis (Fig. 6). Preliminary DNA microarray analysis of the transcriptomes from the wild-type parent strain 35000HP and the *lspA1* mutant 35000HP $\Omega$ 1 grown *in vitro* showed that *lspB* transcripts were approximately 7-fold more abundant in the *lspA1* mutant (data not shown).

I was not able to detect any *lspA2* transcripts using these DNA microarrays for reasons that are not apparent (but may be related to probe design).

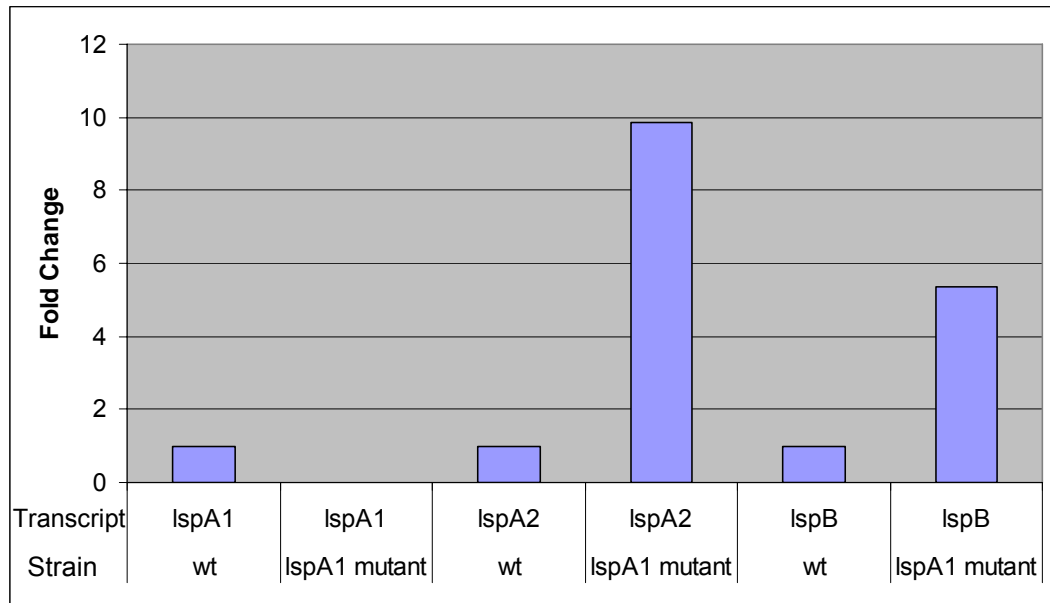


**Figure 9.** Real-time RT-PCR analysis of the *lspA1*, *lspA2* and *lspB* transcript levels in the wild-type and *lspA1* mutant strains.

These two different experimental methods provide confirmation of the changes in protein expression observed with the initial mutant analysis (Fig. 6), and warranted further studies into understanding the underlying regulation that is occurring with these virulence gene products.

## B. The *lspB-gfp* Reporter Construct

This laboratory has previously constructed a pLS88-derived plasmid (pRB157) (32) that contains a promoterless green fluorescent protein (GFP) gene, and also a constitutively expressed GFP construct (pRB157K) by cloning a kanamycin promoter upstream of the GFP ORF in pRB157 (215). The plasmid map for the promoterless GFP construct, pRB157, is shown below in Figure 10 and was reproduced from Robert Blick's M.S. thesis (32).

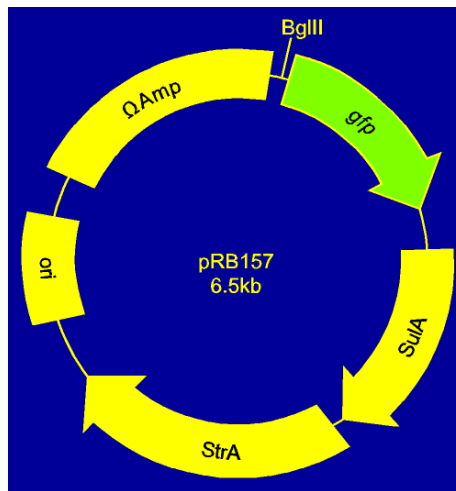


**Figure 10.** Plasmid map of pRB157.

I modified this plasmid by inserting a 300-bp fragment containing the *lspB* promoter region to construct a *lspB-gfp* transcriptional fusion (Fig. 11). The resultant plasmid pJM250 was used to electroporate both the wild-type strain 35000HP and the *lspA1 lspA2* mutant 35000HPΩ12 (Fig. 11). The level of GFP expressed by this reporter construct in the wild-type parent strain was five-fold lower than that expressed by this same reporter in the *lspA1 lspA2* mutant (Fig. 11 and Fig. 12). This finding suggests that the

*lspA1* mutation causes *H. ducreyi* to increase transcription of the *lspB-lspA2* operon. It should be noted that I used the *lspA1 lspA2* mutant here solely for the purpose of having a *lspA1* mutation. Furthermore, the same regulatory event is most likely occurring in both the *lspA1* mutant and *lspA1 lspA2* mutant based on the finding that the increase in GFP fluorescence is similar between these two strains and actually greater for the *lspA1 lspA2* mutant.

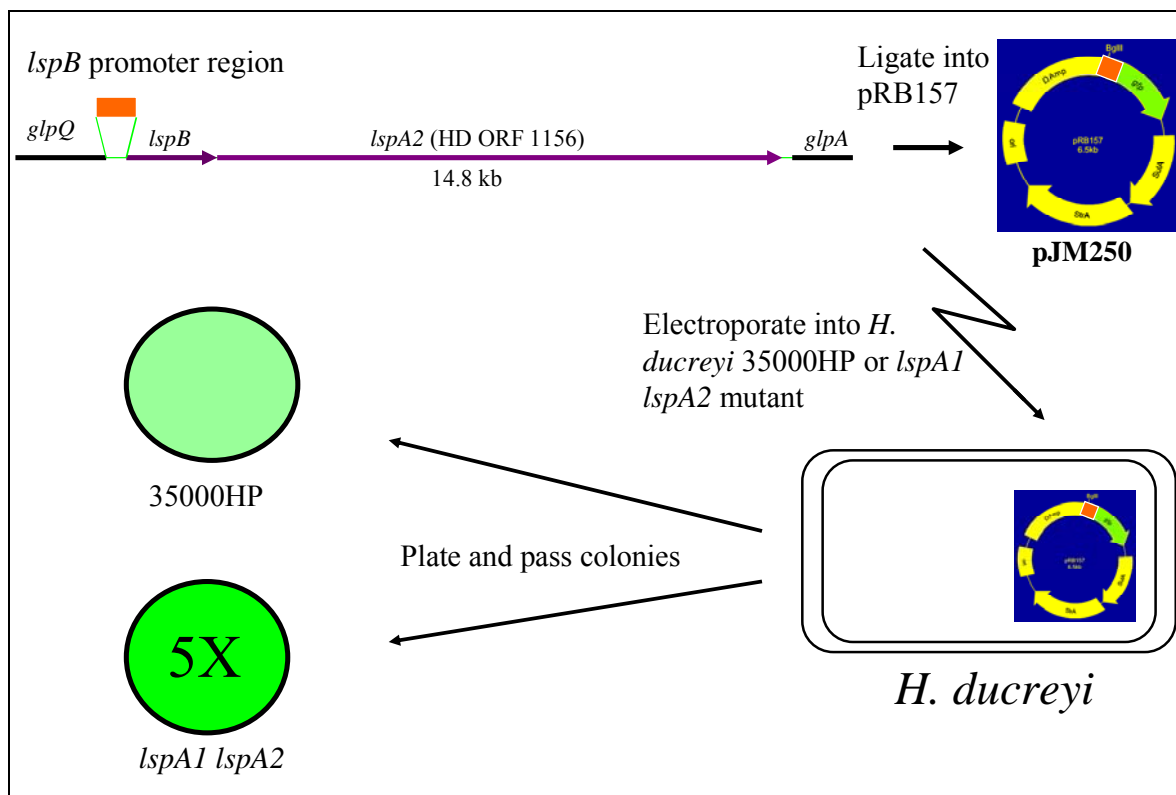


**Figure 11.** Outline of *lspB-gfp* transcriptional reporter construction and subsequent electroporation into wild-type and mutant *H. ducreyi* strains.

By cloning this *lspB-gfp* transcriptional reporter construct into both strains and obtaining readily visible differences in GFP expression, this provided a foundation for a set

of transposon mutagenesis experiments to be attempted. These experiments were intended to identify potential regulatory gene candidates involved in the observed *lspB-lspA2* transcriptional regulation.

### **C. Identification of Putative Regulatory Gene Products by Transposon**

#### **Mutagenesis**

Both 35000HP(pJM250) and 35000HP $\Omega$ 12(pJM250) were mutagenized with Tn916 from pAM120 as shown below (Fig. 12) and previously described (158). Tetracycline-resistant colonies were screened for an increase or decrease in fluorescence relative to that of the immediate parent strain. For example, if the insertion had interrupted a putative transcriptional repressor, I could screen for insertional mutants in the 35000HP(pJM250) parent strain that had increased fluorescence when compared to the parent strain (Fig. 12, orange bar graph). Similarly, if the insertion had interrupted a putative transcriptional activator (Fig. 12, blue bar graph), then I could screen for tetracycline-resistant colonies of 35000HP $\Omega$ 12(pJM250) that had a decrease in fluorescence when compared to the parent strain. It must be noted that, with any mutants found to have a change in fluorescence relative to its parent, I confirmed that the transposon had not inserted itself into the *lspB-gfp* reporter plasmid.

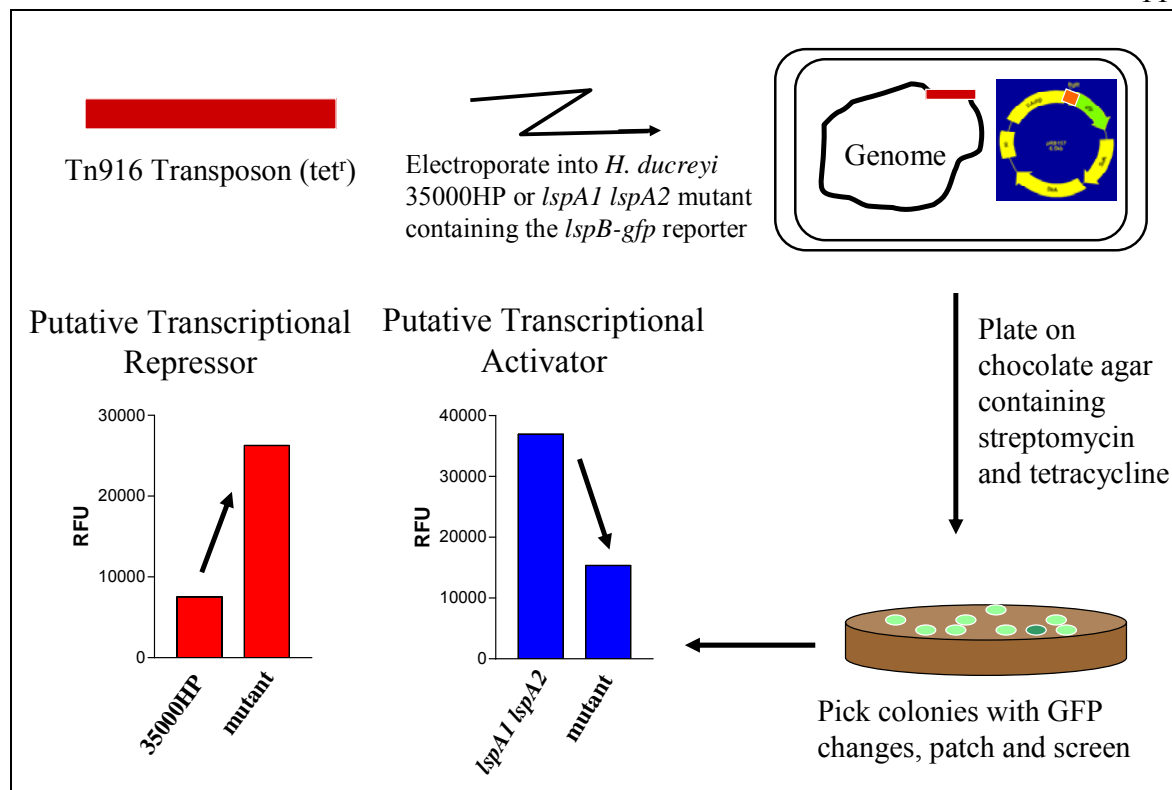


**Figure 12.** Outline of Tn916 mutagenesis.

In all, about 1,000 tetracycline-resistant colonies were screened for the 35000HP(pJM250) parent and 2,500 were screened for the *lspA1 lspA2* 35000HPΩ12(pJM250) parent. To date, four mutants have been shown to have a transposon insertion that altered fluorescence when compared to that of their respective parent strain. Two insertional mutants from each of the two different parent strains are listed in Table 14.



**Table 14.** Transposon insertion mutants shown to have altered fluorescence.

<b>35000HP(pJM250) Transposon Insertions</b>	<b>35000HP<math>\Omega</math>12(pJM250) Transposon Insertions</b>
<i>ompA2</i> (HD ORF 0046)	<i>nusG secE</i> (HD ORF 1886)
<i>serS</i> (HD ORF 1133)	<i>sspA</i> (HD ORF 1425)

The first mutant in the 35000HP(pJM250) parent strain had increased fluorescence relative to 35000HP(pJM250) and was found to contain a transposon in the promoter region upstream of the *ompA2* gene (HD ORF 0046). This gene product has previously been studied in this laboratory and found to be an outer membrane protein (120). Based on the observation that there are detectable differences in the expression levels of several outer membrane proteins when comparing the *H. ducreyi* wild-type strain to the *lspA1 lspA2* mutant strain (112), this finding is perhaps not surprising and may lend further support to the hypothesis that *H. ducreyi* can “sense” outer membrane perturbations and regulate and vary expression of these different proteins.

The second mutant in the 35000HP(pJM250) parent strain had increased fluorescence relative to 35000HP(pJM250) and was found to contain a transposon in a gene (HD ORF 1133) with homology (85% identity) to the *serS* gene of *Actinobacillus pleuropneumoniae*. The *serS* ORF is predicted to encode a serine tRNA synthetase. While tRNA synthetases can be involved in the regulation of certain biosynthetic genes or operons

(e.g., *trp*) (224), it is not immediately apparent how a mutation in *serS* could affect *lspB-lspA2* expression. It is more likely the transposon insertion in *serS* may have had a polar effect on expression of a downstream ORF. This could be determined by reconstructing a *serS* mutation with a nonpolar cartridge, and then determining this *serS* mutant's effect on *lspB* transcript levels.

The first mutant in the 35000HP $\Omega$ 12(pJM250) parent strain had decreased fluorescence relative to 35000HP $\Omega$ 12(pJM250) and was found to contain a transposon in the promoter region upstream of the *secE* gene (HD ORF 1886). It has been reported for the HMW proteins of *H. influenzae* that *secE* is necessary for secretion of the HMW proteins via a two-partner secretion system (82). This mutant again lends further support to the idea that transcription of outer membrane genes in *H. ducreyi* may be regulated in response to changes in the protein composition of the outer membrane.

The second mutant in the 35000HP $\Omega$ 12(pJM250) parent strain had decreased fluorescence relative to 35000HP $\Omega$ 12(pJM250) and its transposon was found within a gene (HD ORF 1425) with homology (71% identity) to *sspA* from *P. multocida*. Stringent starvation protein A (SspA) is a transcriptional activator (96,97) and has been shown to affect expression of virulence factors of other pathogens including *Yersinia enterocolitica* and *Francisella tularensis* (20,21). This was the most interesting insertional mutant obtained to date and further work to confirm the possible involvement of this gene product in regulation of expression of the LspA proteins is discussed below.

### D. Stringent Starvation Protein A (SspA)

With the transposon inserted into the *sspA* gene (HD ORF 1425) in the 35000HPΩ12(pJM250) parent strain resulting in decreased fluorescence of the *lspB-gfp* reporter, the *sspA* gene product could possibly be a transcriptional activator of the *lspB-lspA2* operon. In *E. coli*, SspA has been shown to bind RNA polymerase to facilitate transcription (97). Figure 13 illustrates the quantitative decrease in GFP expression caused by the transposon insertion in the *sspA* gene along with a gene map of the region containing the *sspA* gene in the 35000HP genome.

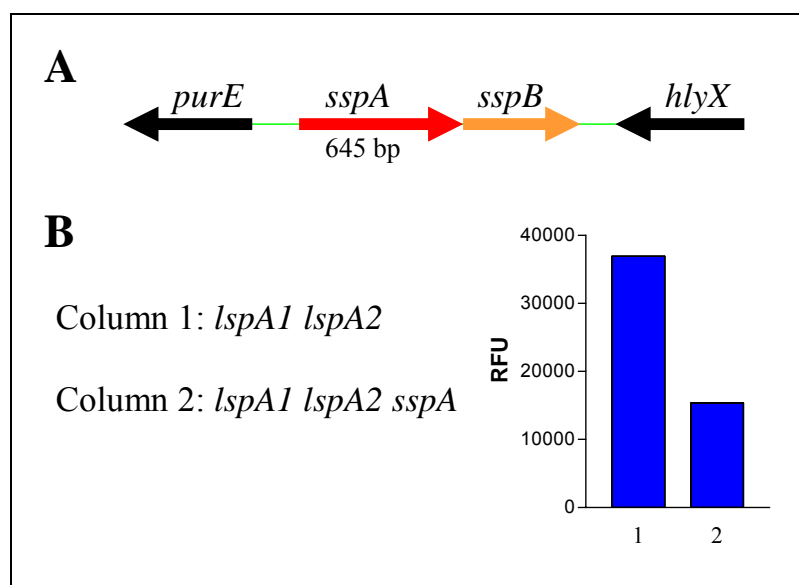


**Figure 13.** Stringent starvation protein A. (A) Gene map of the region containing the *sspA* gene in the 35000HP genome. (B) Relative fluorescence unit measurements for the *lspB-gfp* transcriptional reporter construct in the *lspA1 lspA2* mutant parent strain (column 1) and the mutant with the Tn916 insertion in the *sspA* gene (column 2).

To verify that the insertional mutation in the *sspA* gene does result in a decrease in *lspB* promoter-driven GFP expression and was not caused by polar effects of the transposon insertion, the *sspA* ORF was inactivated in several *H. ducreyi* strains by insertion of a non-polar spectinomycin resistance cartridge (135) or a potentially polar chloramphenicol resistance cartridge (98). Then, the *lspB-gfp* transcriptional reporter was transformed into these mutant strains and their levels of GFP expression were measured as illustrated in Figure 14 below.

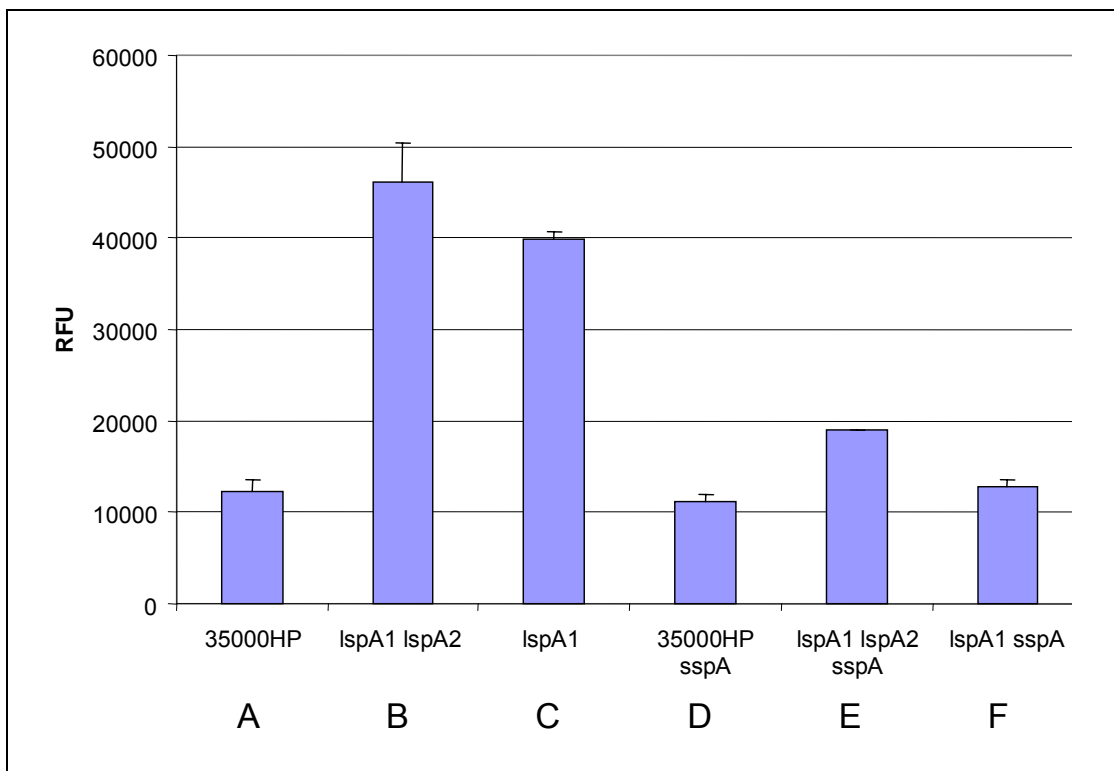


**Figure 14.** GFP expression measurements obtained with the *lspB-gfp* reporter in various *H. ducreyi* strains.

In Figure 14, columns A and B are the *lspB-gfp* reporter expression levels of the two parent strains used for transposon mutagenesis. The GFP expression level of the *lspB-gfp*

reporter construct in the *lspA1* mutant is shown in Figure 14, column C. When compared to 35000HP, both the *lspA1* mutant and the *lspA1 lspA2* have a 4-5 fold increase in GFP expression. While the original insertion mutation for *sspA* was obtained in the *lspA1 lspA2* mutant strain, a *sspA* insertion mutant was also constructed in the 35000HP wild-type strain background (35000HP.*sspA*), and then the *lspB-gfp* reporter construct was transformed into this new mutant to determine if there was a change in GFP expression (Fig. 14, column A and D). There was no appreciable difference between these two strains. Two more *sspA* mutations were constructed in the *lspA1* and the *lspA1 lspA2* strains with a nonpolar spectinomycin resistance cartridge as described in Chapter Three and designated 35000HP $\Omega$ 1.*sspA* and 35000HP $\Omega$ 12.*sspA*, respectively. After construction of the *sspA* mutation in these two strains, the *lspB-gfp* reporter was then transformed into these strains and the level of GFP expression was measured to determine possible decreases in expression when compared to their respective parent strains. For both the 35000HP $\Omega$ 1.*sspA* and 35000HP $\Omega$ 12.*sspA* mutants, the GFP expression levels decreased when compared to their respective parent strains (Fig. 14, compare column B with column E and column C with column F). So, after reconstructing the *sspA* mutations independently, the levels of GFP expression decreased as seen with the original *sspA* transposon mutant. These results provide support for the possibility that *sspA* might encode a transcriptional activator for the *lspB-lspA2* operon. GFP is not an optimal choice for measurement of transcriptional levels. However, this is the only system available currently for use in *H. ducreyi*. One other unexplained observation was made during these studies. As the strains were passaged *in vitro*, the GFP levels tended to increase, and this made

interpreting the data more difficult. Therefore, further transcriptional measurements (i.e., using real-time RT-PCR) are in progress to confirm and better quantitate the putative transcriptional difference observed in these different mutants.

I also examined the effect of the *sspA* gene product on LspB and LspA2 protein expression. Western blot analysis was performed to measure the levels of expression of LspA1, LspA2, and LspB in the 35000HP, 35000HP $\Omega$ 1, and 35000HP $\Omega$ 1.*sspA* strains (Fig. 15).

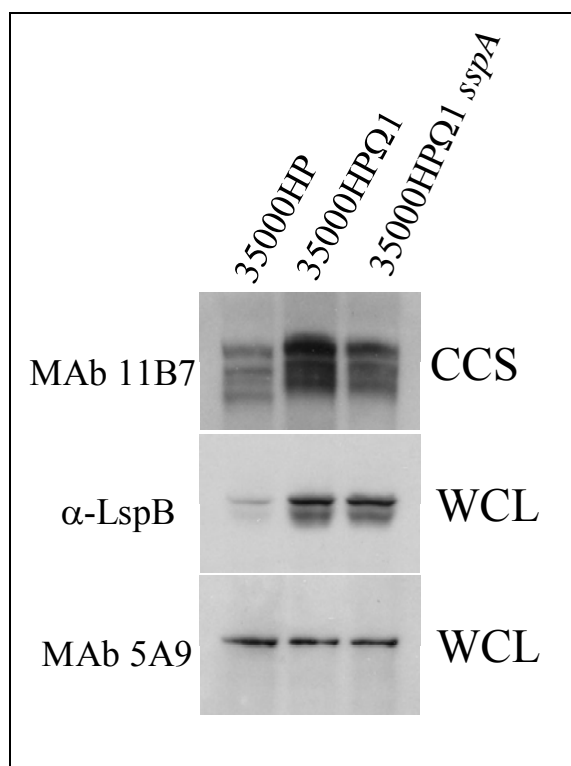


**Figure 15.** Effect of the *sspA* mutation on LspA2 and LspB protein levels. Western blot analysis of CCS from *H. ducreyi* strains 35000HP, 35000HP $\Omega$ 1, and 35000HP $\Omega$ 1.*sspA* using MAb 11B7 which recognizes both LspA1 and LspA2. Whole-cell lysates from these same three strains were probed with antiserum against LspB or with the MAb 5A9 (which recognizes HgbA) and were used here as a loading control.

There appeared to be a slight decrease in LspA2 expression in the 35000HP $\Omega$ 1.*sspA* strain when compared to the 35000HP $\Omega$ 1 strain. It is difficult to standardize the CCS; however, this experiment was repeated multiple times with similar results. When looking at LspB expression in whole cell lysates prepared from these three strains, there appeared to be no appreciable difference in the levels of LspB between the 35000HP $\Omega$ 1 and 35000HP $\Omega$ 1.*sspA* strains. This result, showing no change in LspB levels, does not correspond with the slight decrease in the level of LspA2 expression in CCS seen in the 35000HP $\Omega$ 1.*sspA* strain when compared to the 35000HP $\Omega$ 1 strain.

#### **E. Identification of DNA-Binding Proteins**

Another method to identify possible transcriptional factors that could be involved in the regulation of the *lspA1* and *lspB* genes involved the use of DNA promoter “pull-down” experiments as outlined in Figure 16. Promoter regions were amplified by PCR and the 5’ primer for each set was modified with a biotin group which, during PCR amplification, would be incorporated into the 5’ region of the putative promoter region. The presence of the biotin would then allow for binding of the amplified promoter region to magnetic streptavidin beads (Fig 16). The beads, now with the promoter region DNA bound to them, were then incubated with lysates prepared (as described in Chapter Three) from *H. ducreyi* strains 35000HP or 35000HP $\Omega$ 12 (Fig. 16). The beads were then washed several times to remove proteins not associated with the bead-bound DNA, and then the bead-bound DNA-

protein complex was placed in a concentrated salt solution to elute the DNA-binding proteins (Fig. 16).

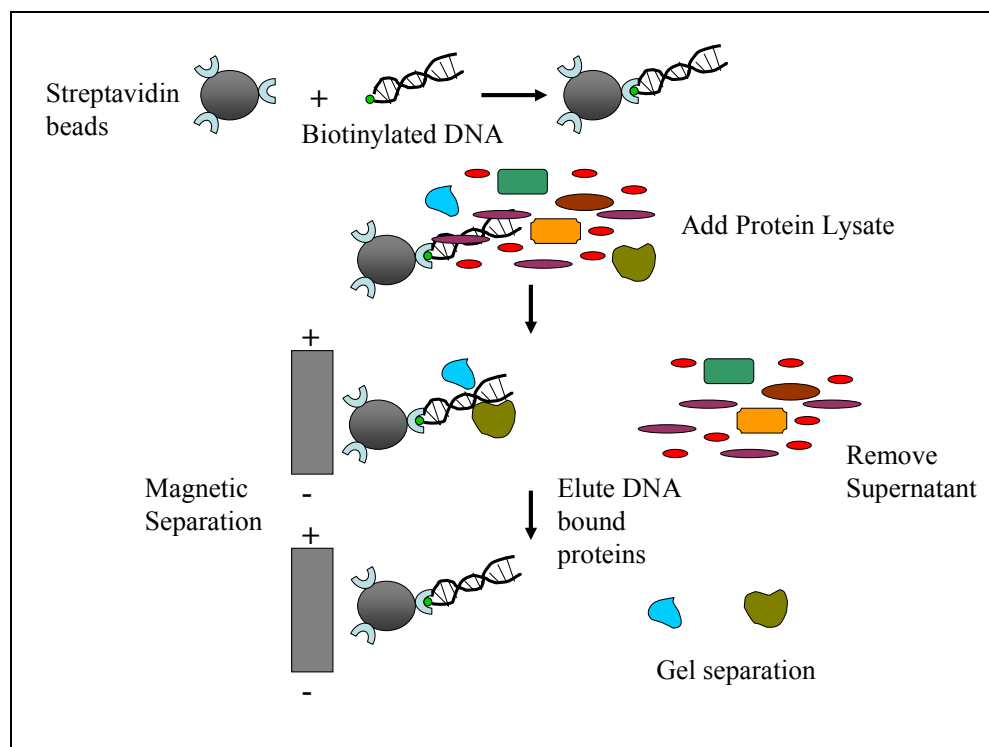


**Figure 16.** Overview of experimental procedure for isolating DNA-binding proteins.

The eluted proteins were resolved by SDS-PAGE and silver-stained (Fig. 17). The recovered protein bands were compared between the control promoter (from the *H. ducreyi* *g6pd* gene) and the experimental promoters for *lspA1* or *lspB*. Bands recovered and present only with the *lspA1* or *lspB* promoters were excised from the gel, subjected to tryptic digest, and then to HPLC - mass spectrometry (performed by the UT Southwestern Protein Sequencing Core) to determine protein identities when compared to *H. ducreyi* genome BLAST data. The results are listed in Table 15.



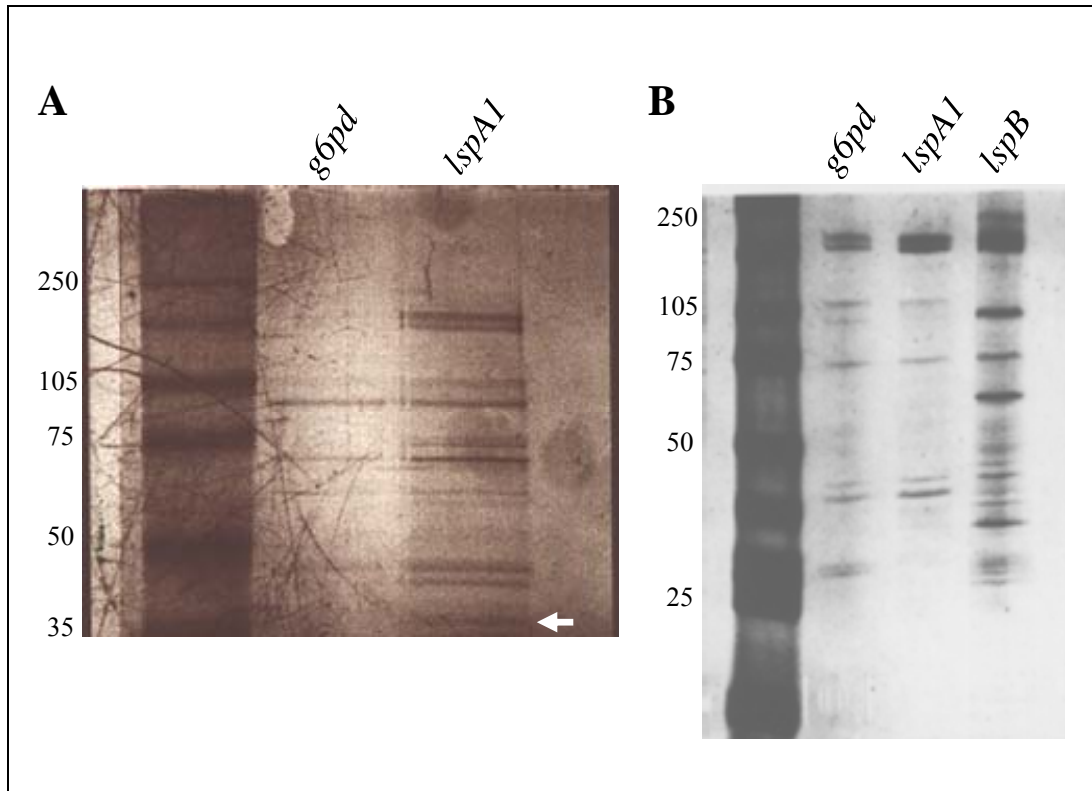


**Figure 17.** Silver-stained gels for DNA-binding experiments. (A) Gel showing DNA-binding proteins from wild-type 35000HP lysates obtained by using either the control *g6pd* promoter or the *lspA1* promoter regions. The white arrow shows the band that was excised and whose sequence was found to correspond to the amino sequence of HD1380. (B) Gel showing DNA-binding proteins from the *lspA1 lspA2* mutant (35000HP $\Omega$ 12) lysates obtained by using either the control *g6pd*, *lspA1*, or *lspB* promoter regions.

The vast majority of the excised bands from the gel came back with sequence matches to RNA polymerase subunits or DNA topoisomerase I. While these results confirmed that I was purifying DNA-binding proteins by using this experimental method, only one band proved to be of interest for further study. This band (Fig. 17, white arrow) had homology to a putative transcriptional regulator (encoded by HD ORF 1380) based on the 35000HP genome annotation.

**Table 15.** Identification of bands excised from silver-stained gels.

Protein Name	Molecular Weight	Peptide Sequence
DNA topoisomerase I (TopA)	98.0 kDa	KADHIYLATDLDR
DNA-directed RNA polymerase, alpha chain (RpoA)	36.4 kDa	AATILAEQLDAFVDLR
Unknown ( <i>Pasteurella multocida</i> ) (HD1380)	31.4 kDa	IFLFGVGSSGITAEDAK
Unknown ( <i>Haemophilus ducreyi</i> ) (TadZ)	41.4 kDa	LGSQDLDLLFDK
Serum resistance protein ( <i>Haemophilus ducreyi</i> ) (DsrA)	30.1 kDa	WTWSNEGGFDIK
Unknown( <i>Haemophilus ducreyi</i> ) (TadD)	28.2 kDa	GISSAQQGELAK

The predicted protein product of the HD1380 ORF had homology to two distinct domains. Its N-terminal region has homology to a helix-turn-helix motif and its C-terminus has homology to SIS domains which have been reported (22) to be phosphosugar-binding domains found in proteins that regulate metabolic genes involved in phosphosugar synthesis. The gene map of HD1380 is shown in Figure 13A. HD1380 has homology to the *rpiR* gene in *E. coli* which has been demonstrated to be involved in the regulation of *rpiB*, a gene involved in ribose catabolism (189). Homologous members of this RpiR

family of regulators that were inactivated by mutation in *Brucella melitensis* have been shown not to be required for virulence (90).

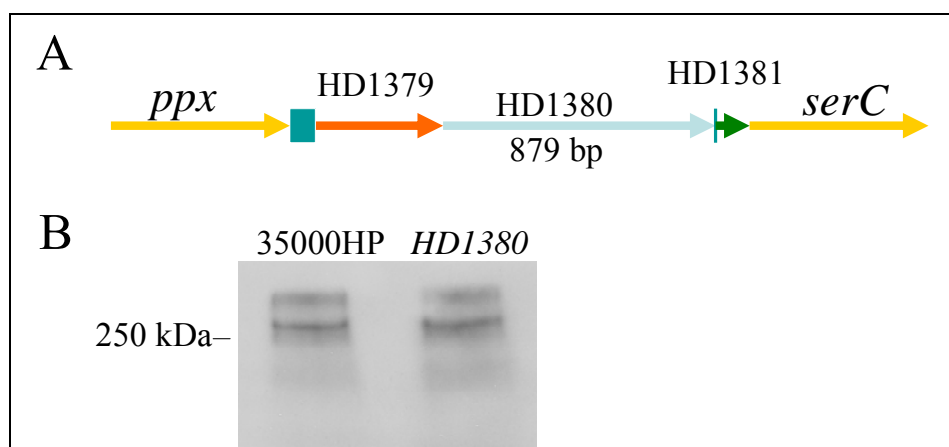


**Figure 18.** Effect of the HD1380 mutation on LspA protein levels. (A) Gene map of the region containing the HD1380 gene in the 35000HP genome. (B) Western blot analysis of CCS prepared from wild-type and HD1380 mutant *H. ducreyi* strains probed with MAb 11B7 (recognizing LspA1 and LspA2).

I next constructed a *H. ducreyi* mutant lacking the ability to express the HD1380 gene product (as described in Chapter Three) and prepared CCS and examined expression levels of LspA proteins by Western blot analysis (Fig. 18B). By Western blot analysis, there appears to be no noticeable difference in LspA protein expression between this mutant and the wild-type parent strain.

### III. Discussion

The work presented in this chapter focused on determining the possible role that genetic regulation may have in contributing to the expression of virulence factors involved

in the pathogenesis of chancroid. This work was performed during the first year of my graduate work. Several techniques were developed and may, in the future, be useful in determining possible regulatory mechanisms involved with the *lspA* and *lspB* genes. Two potential candidate regulatory genes (*sspA* and HD1380) were identified using these methods; however, the latter gene product appeared to have no effect on expression of the LspA proteins.

For the *sspA* gene, its apparent lack of effect on expression of the LspB protein (Fig. 15) could be due to several factors including membrane protein stoichiometry. It is difficult to reconcile the GFP data on transcript levels with the protein expression data above, and further experiments using real-time RT-PCR need to be performed to determine the possible role of SspA in *lspB* and *lspA2* regulation. It is also possible that up-regulation of LspB-LspA2 protein expression in response to the *lspA1* mutation could be the result of a cell envelope stress response. As studied in *E. coli*, there are two cell envelope stress response pathways – one controlled by the alternative sigma factor  $\sigma^E$  (encoded by *rpoE*) and the other regulated by the CpxAR two-component system (56,57,169,170). Inspection of the *H. ducreyi* genome indicated that it encodes predicted  $\sigma^E$ , CpxA, and CpxR orthologs, so both pathways could be functional. It is unlikely that the alternative sigma factor  $\sigma^E$  is involved here, however, because this pathway is normally activated by peptides ending with OMP-like C-terminal sequences (170) and the 35000HPQ1 *lspA1* mutant does not make any LspA1 protein. Nonetheless, to formally exclude this possibility, we could attempt to construct a *H. ducreyi rpoE* mutant and assess the effect of this mutation on expression of

LspA1 and LspB-LspA2. Similarly, both I and others have attempted to construct an isogenic *H. ducreyi* *cpxR* mutant to determine whether this mutation affects expression of LspA1 or LspB-LspA2; however, I have had little success in this endeavor, and it is likely that this mutation is lethal in *H. ducreyi*.

## CHAPTER FIVE

### Use of Differential Display Technology To Analyze *Haemophilus ducreyi* Gene Expression Under Various Growth Conditions

#### I. Introduction

Humans are the only known natural host for *H. ducreyi*, and therefore little bacterial gene regulation would be thought to occur in this organism. However, other strict human pathogens like *Bordetella pertussis* have numerous regulatory elements and, indeed, do vary and coordinate expression of important gene products involved in pathogenesis (138). Based on results from the previous chapter, and the observation that the LspA1 protein was released into the culture supernatant fluid only when *H. ducreyi* was grown in the presence of fetal calf serum (FCS) (Fig. 19), I performed differential display analysis to study possible transcription changes in *H. ducreyi* grown in the presence and absence of FCS. Since it appears that the appearance of one known virulence factor (i.e., the LspA protein paralogs) in the culture supernatant fluid depends on some factor provided by FCS, this raised the possibility that other virulence factors are regulated or controlled by the presence of FCS. Therefore, utilizing a method that would help to identify the possible gene product(s) responsible for regulating the effects of FCS could lead to a better understanding of *H. ducreyi* disease pathogenesis. Even though humans are the only natural host for this pathogen, the different biological niches that *H. ducreyi* comes in contact with (i.e., skin, immune cells, lymph node) may require the organism to vary expression of gene products to allow for optimal growth and persistence in the host.

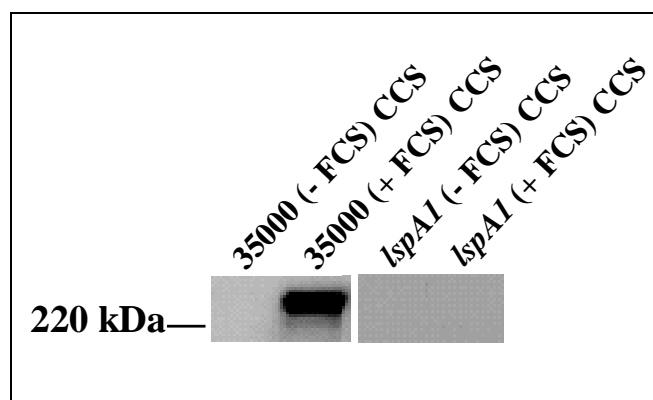


**Figure 19.** Effect of FCS on LspA secretion. Western blot analysis determining levels of the LspA1 protein in CCS fluid from either the wild-type 35000 or the *lspA1* mutant strains grown in the presence or absence of FCS. MAb 20A2 was used to detect LspA1.

Differential display RT-PCR (DD-PCR) was originally developed for analyzing expression in eukaryotic cells (217). This experimental procedure provides a quick and sensitive method for determining differential transcriptional expression. This method has appeared to become secondary to DNA microarray analysis for determining transcriptional levels and changes on a whole-genome scale; however, in eukaryotic studies, a similar number of papers utilizing differential display are published each year when compared to papers involving DNA microarray analysis.

The original differential display-PCR was designed for eukaryotic analysis and relied on polyadenylated RNA for first-strand cDNA synthesis. This was a significant limitation when this methodology was used with prokaryotes, because the vast majority of prokaryotic mRNAs are not polyadenylated. After production of cDNA from mRNA by reverse transcription, a set of arbitrary primers are used to allow for parts of the cDNA to be amplified by PCR. Then the amplified products are resolved by acrylamide electrophoresis

to make comparisons between paired conditions. As with all gene expression-based methodologies, the technique and results obtained are only as reliable as the quality of the RNA isolated from the samples to be studied. The technique used for the experiments below was a variation of DD-PCR termed Restriction Fragment Differential Display-PCR (RFDD-PCR) and the displayPROFILE kit purchased from Display Systems Biotech was utilized. This technique helps to solve some of the limitations of basic DD-PCR for prokaryotes. The main modification in this method is that, after the cDNA is synthesized, it is then fragmented by digestion with a restriction enzyme and specific adaptors are then ligated onto the digested cDNA fragments. The overall method is diagrammed below (Fig. 20) and the experimental procedures are described in detail in Chapter Three above.



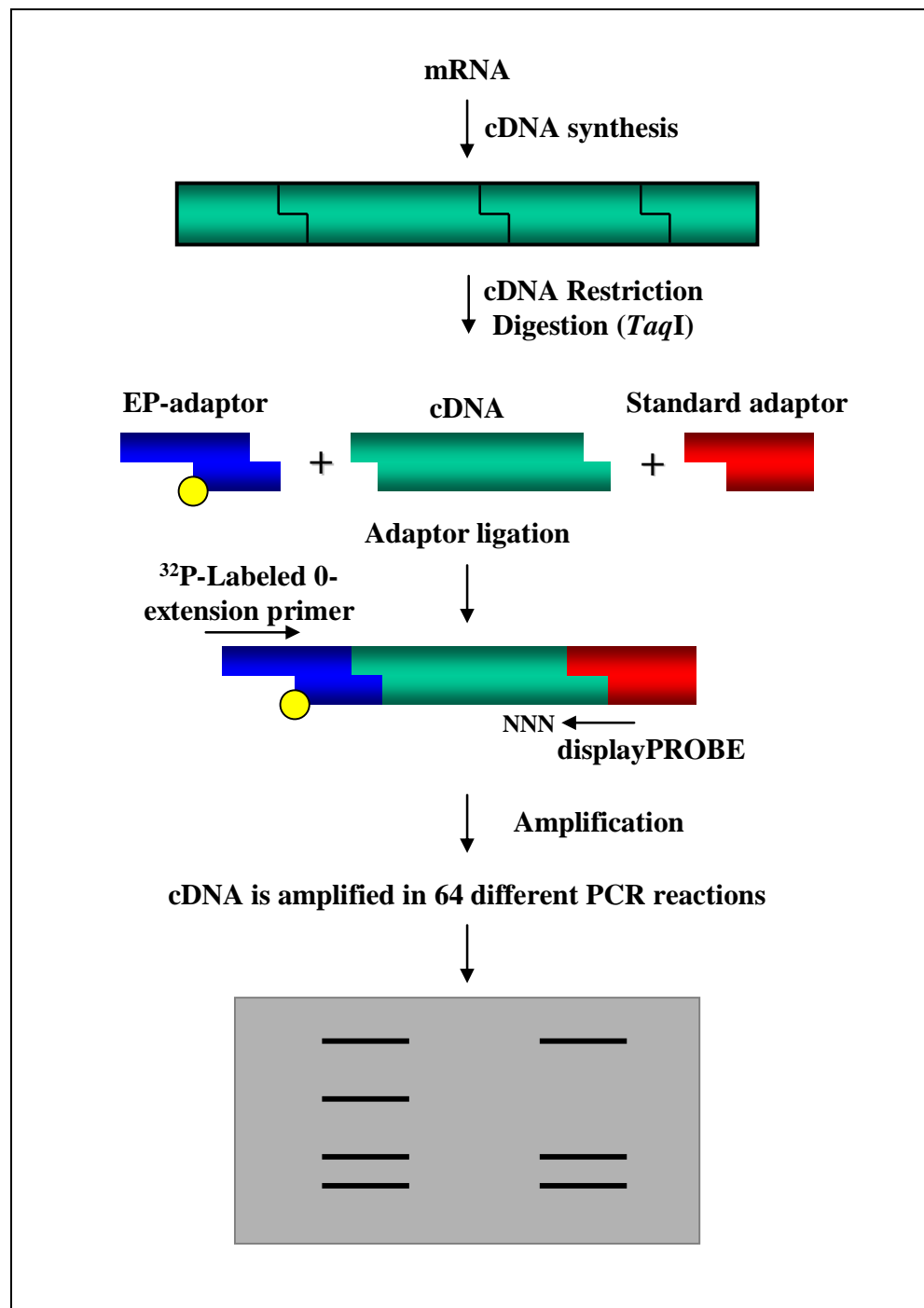


**Figure 20.** Restriction fragment differential display-PCR (RFDD-PCR) method overview.

## II. Results

### A. RNA Purification

The wild-type strain 35000 was grown to mid-logarithmic phase ( $OD_{600}=0.6$ ) in supplemented Columbia Broth both in the presence and absence of 2.5% (vol/vol) heat-inactivated FCS. Total *H. ducreyi* RNA was isolated using either the Ultraspec RNA Isolation System or a Boehringer Mannheim (BM) RNA Isolation Kit. The quantity and quality of the RNA, both before and after DNase treatment, were checked by agarose gel electrophoresis (Fig. 21A). The overall quality of RNA before and after DNase-treatment was similar for RNA obtained by using the Ultraspec method. This RNA also appeared to be of a higher quality than that prepared by using the Boehringer Mannheim kit. To detect possible DNA contamination, RT-PCR analysis was performed on the isolated RNA samples before and after DNase treatment (Fig. 21B). RNA isolated by the Ultraspec method that had also been DNase-treated had no detectable DNA contamination by RT-PCR analysis in the no reverse transcriptase (No RT) reactions (Fig. 21B, lanes 10-11). Therefore, RNA isolated by using the Ultraspec RNA Isolation System that had also been DNase-treated was used in the differential display experiments to determine if there were differences in transcription between the two growth conditions under study.

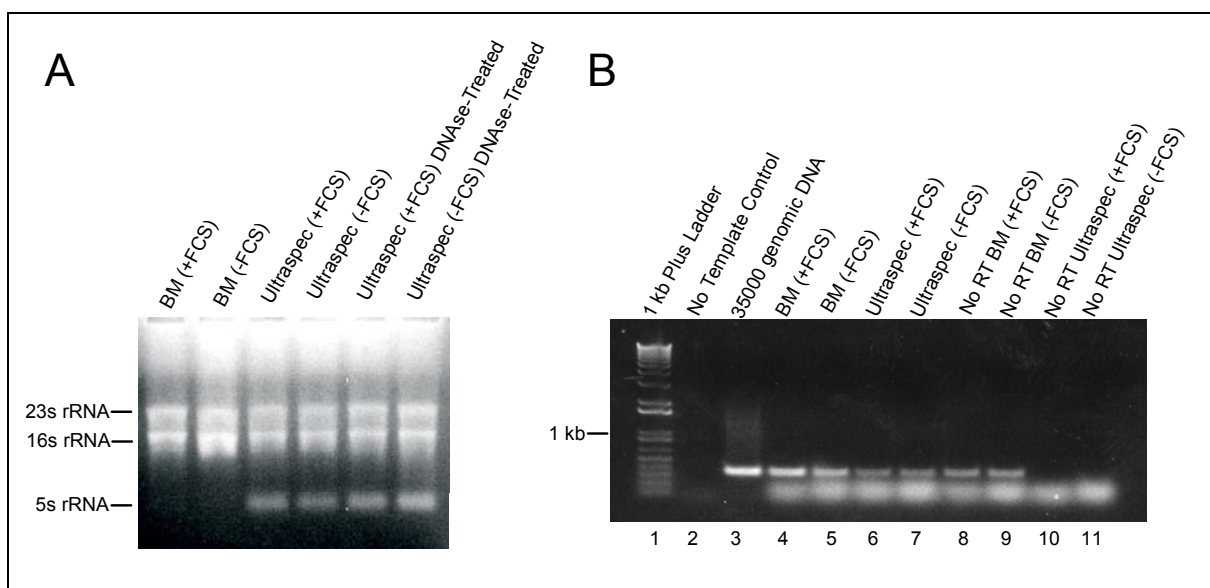


**Figure 21.** RNA isolation and RT-PCR analysis. (A) Agarose gel electrophoresis of total RNA isolated from 35000 comparing RNA integrity between the two preparation procedures. (B) RT-PCR analysis of RNA to detect DNA contamination.

## B. Differential Display cDNA Synthesis

After RNA quality had been determined, cDNA synthesis was performed as described in the displayPROFILE kit, and the efficiency of cDNA synthesis was confirmed by checking the cDNA in agarose gel electrophoresis (Fig. 22). A cDNA smear containing products ranging from 100-bp to approximately 2000-bp is expected for a high quality cDNA synthesis reaction, and this was seen for the cDNA samples produced from the RNA prepared above. This cDNA pool was then digested with the *TaqI* restriction enzyme, a 4-base-cutter (TCGA) that leaves 5' overhanging ends on the cDNA fragments. Then the two different DNA adaptors were ligated onto the sticky ends of the cDNA fragments; the EP-

adaptor (extension-protection) and the standard adaptor as shown above (Fig. 20). Therefore, each fragment that has the EP adaptor ligated onto one of its ends and the standard adaptor ligated onto its other end is able to be amplified in further downstream steps using PCR (Fig. 20). After ligation of both adaptors, the 32 high-stringency PCR reactions were carried out with the 0-extension 5' primer and one or a mixture of several of the 64 different displayPROBE 3' primers. For visualization of the PCR products, the 0-extension 5' primer was end-labeled with radioactive phosphate from [ $\gamma$ - $^{32}$ P]ATP. There are 64 different displayPROBE primers and, in the reactions that I performed, I pooled 2 primers for each reaction. Therefore, 32 total reactions had to be performed for RNA from both growth conditions to use all of the primers.

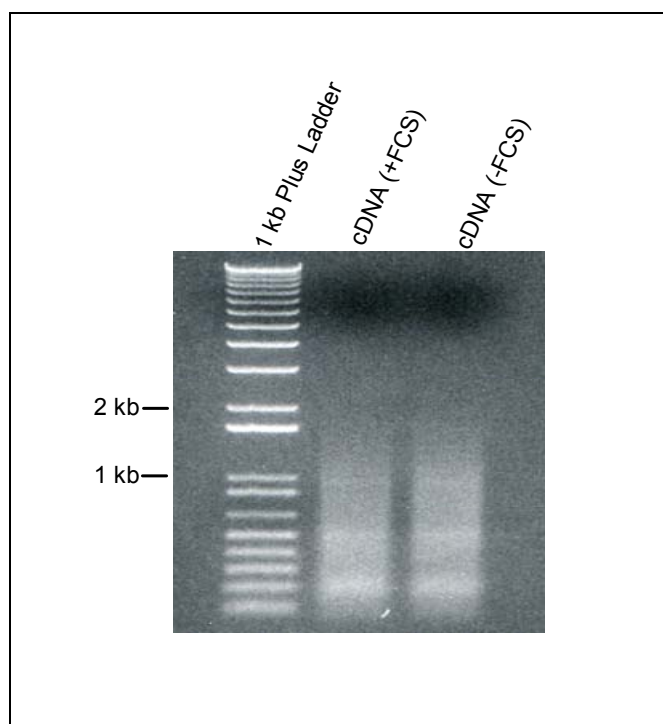


**Figure 22.** Agarose gel electrophoresis of cDNA. The cDNA derived from RNA samples obtained from strain 35000 cells grown both in the presence and absence of FCS.

### **C. Differential Display Electrophoresis**

The amplified gene fragments were separated in a polyacrylamide sequencing gel, and after electrophoresis, the gel was mounted on Whatman paper, covered with plastic wrap, and dried on a gel dryer. The dried gel was then exposed to film for 12 – 48 h in a radiographic cassette at -70°C, and then developed. The autoradiograph was then visualized (Fig. 23) and cDNA bands of interest were excised by aligning the autoradiograph with the dried gel, cutting out the desired gel area with a scalpel, and placing the excised region in a microcentrifuge tube. In Figure 23, there are 13 different reactions from both conditions (+ or – FCS).

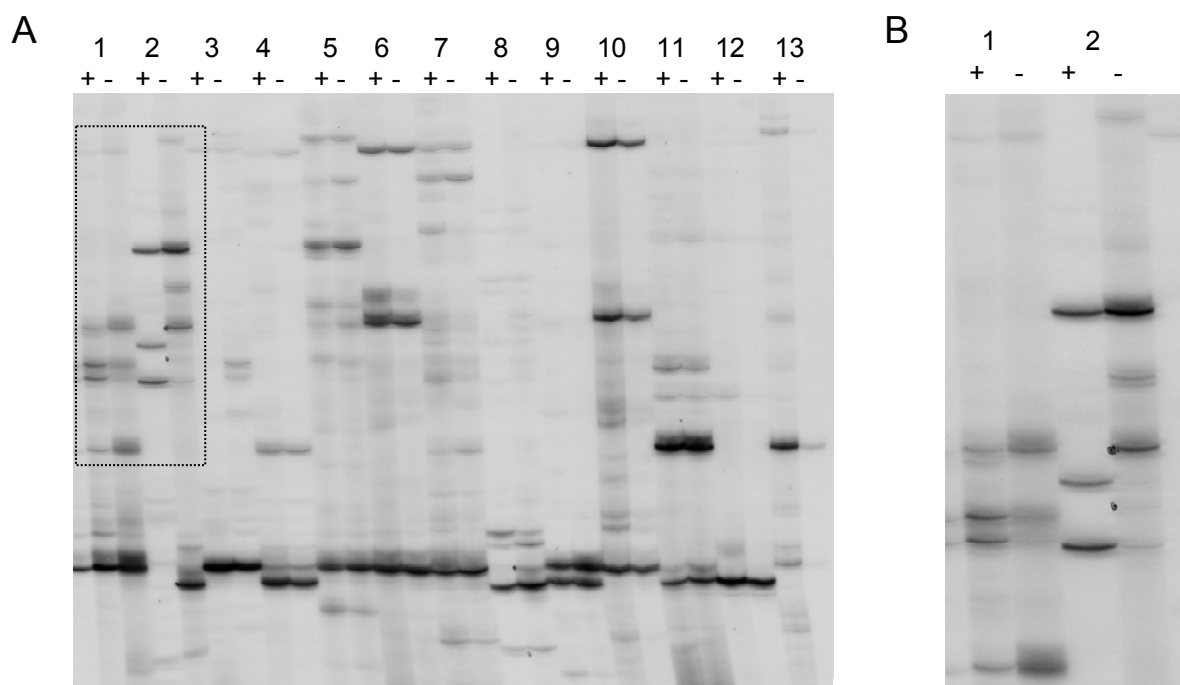


**Figure 23.** Differential display profile gel. (A) Differential display profile obtained with 13 different displayPROBE primers for both growth conditions [(+) with FCS and (-) without FSC]. Hatched box is enlarged and shown in (B).

#### D. Differential Display Fragment Cloning

The dissolved cDNA fragments were then used as a template for amplification in a PCR reaction as per the displayPROFILE protocol. The amplified PCR products (Fig. 24A) were then subcloned into a TOPO TA cloning vector. The plasmids were then isolated and the inserts (Fig. 24B) sequenced using the primers provided with the TA cloning kit. Finally, the DNA sequences were analyzed by BLAST (NCBI) search to determine possible cDNA identity or homology.

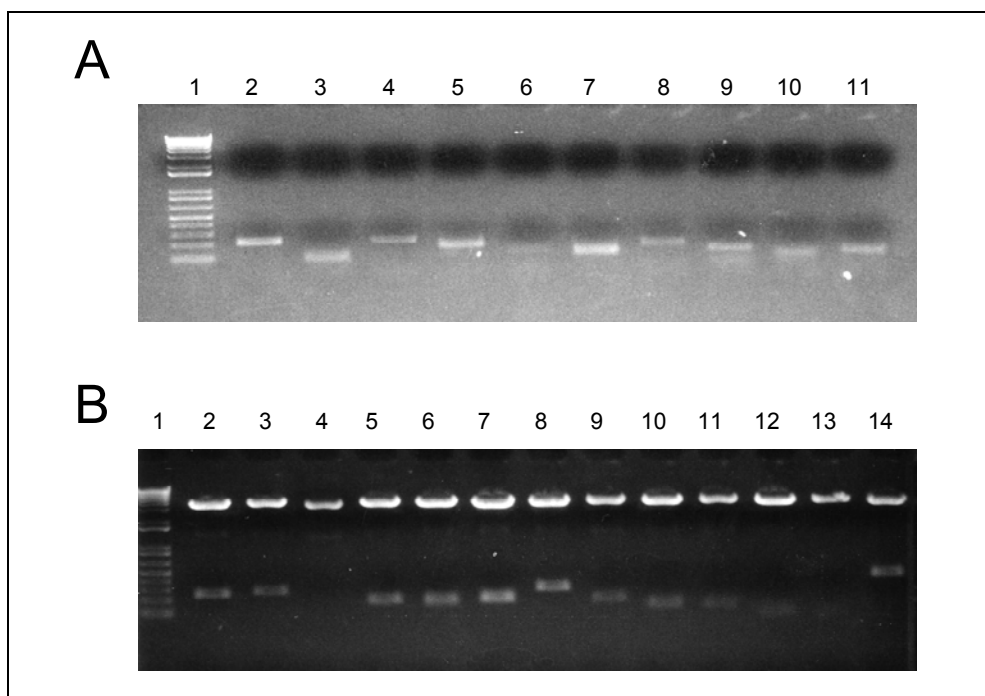


**Figure 24.** PCR-amplified differential display fragments. (A) PCR-amplified fragments from the excised gel areas. (B) Fragments were cloned into TA cloning vectors and the insert sizes determined by digestion of the plasmids with *EcoRI*.

### E. Fragment Sequencing and Homology Searches

All 34 clones listed below were sequenced and their corresponding *H. ducreyi* ORF ID numbers are listed in Table 16. In several cases where a DNA sequence did not match any putative *H. ducreyi* ORF, the most significant homology and the relevant organism are provided. It should be noted that the homology results were derived from recent (February 2006) BLAST searches.

**Table 16.** List of sequence homology data for inserts derived from the differential display experiments.

Plasmid	Homology	HD ORF Designation
pJM101	Phosphoglycerate mutase ( <i>pgam-I</i> )	<i>Hordeum vulgare</i> (Barley)
pJM102	<i>lspA2</i>	HD1156
pJM103	rRNA-23S	rRNA
pJM104	rRNA-23S	rRNA
pJM105	rRNA-23S	rRNA
pJM106	rRNA-23S	rRNA
pJM107	Not enough sequence for homology	
pJM108	Methyl-accepting chemotaxis protein	<i>Pseudomonas sp.</i>
pJM109	rRNA-23S	rRNA
pJM110	Polynucleotide phosphorylase ( <i>pnp</i> )	HD1588
pJM111	Polynucleotide phosphorylase ( <i>pnp</i> )	HD1588
pJM112	<i>lspB</i>	HD1155
pJM113	rRNA-23S	rRNA
pJM114	rRNA-23S	rRNA
pJM115	1-hydroxy-2-methyl-2-(E)- butenyl 4-diphosphate synthase ( <i>gcpE</i> )	HD1037
pJM116	NifU family	<i>Yersina pestis</i>



pJM117	rRNA-23S	rRNA
pJM118	rRNA-23S	rRNA
pJM119	Not enough sequence for homology	
pJM120	<i>dsrA</i>	HD0769
pJM121	Not enough sequence for homology	
pJM122	rRNA-23S	rRNA
pJM123	rRNA-23S	rRNA
pJM124	Not enough sequence for homology	
pJM125	rRNA-23S	rRNA
pJM126	Hypothetical protein, tmRNA	HD0085
pJM127	rRNA-23S	rRNA
pJM128	rRNA-16S	rRNA
pJM129	rRNA-23S	rRNA
pJM130	Not enough sequence for homology	
pJM131	rRNA-23S	rRNA
pJM132	Hypothetical protein, tmRNA	HD0085
pJM133	Primosomal protein N'	HD0623
pJM134	Primosomal protein N'	HD0623

---

### III. Discussion

This work was performed during my rotation period in the Hansen laboratory in the summer of 1999. At that time, the genome of *H. ducreyi* was in the process of being sequenced by another laboratory and, therefore, DNA microarrays were not available. Therefore, differential display technology, with the modifications made by Display Systems Technology in their displayPROFILE kit, was an attractive alternative based on the options available at that time. It should be noted again that the homology results are from recent (February 2006) BLAST searches. When of interest or importance, the initial homologies based on the 1999 NCBI database search are discussed below. At the time, most of the homologies obtained were to other organisms' genes; however, the majority of the cloned DNA fragments do correspond to an *H. ducreyi* ORF from the recently available *H. ducreyi* 35000HP genome sequence.

Using this method, known *H. ducreyi* virulence factors were found to have transcriptional changes between the two growth conditions. First, both the *lspA* and *lspB* genes were identified in this analysis, demonstrating that this method could be used in determining possible transcriptional changes that affect protein expression (see Fig. 19). Second, one of the most interesting sequences identified by using this method matched the *dsrA* transcript (HD0769); however, at the time these experiments were performed, the cloned DNA sequence most closely matched that of the *uspA2* gene of *Moraxella*

*catarrhalis*. The *dsrA* gene was not identified or described until half a year later, in March 2000, by another laboratory which demonstrated that the *dsrA* gene product was involved in serum resistance (70). A year later, a *dsrA* mutant was shown to have decreased virulence in the human challenge model (37). DsrA is now a putative major virulence determinant. Therefore, these differential display experiments had, at the time, identified an unknown virulence factor further demonstrating (with some hindsight now) that this technique could be useful in elucidating potential differential regulation of virulence genes.

Three of the DNA inserts obtained in these experiments still do not have matches to annotated *H. ducreyi* sequences. They match instead to a phosphoglycerate mutase (*pgam-I*) from *Hordeum vulgare* (Barley), a methyl-accepting chemotaxis protein from *Pseudomonas sp.*, and the *nifU* gene family from *Yersina pestis*. Possibly the small size of the cloned insert (~70-100 nt) along with poor sequencing reactions may explain the lack of direct matches to the *H. ducreyi* genome.

Two of the DNA inserts matched *H. ducreyi* ORF HD0085 which has homology to *ssrA*. This ORF encodes for a RNA molecule (tmRNA) which functions to recognize ribosomes stalled on defective messages and then adds a peptide tag which marks the incomplete polypeptide for proteolysis (128). A tmRNA encoded by *smpB* from *Salmonella typhimurium*, when disrupted by transposon mutagenesis, decreases virulence in mice and reduces survival of this pathogen within macrophages (28). Furthermore, there has been a demonstrated interaction between tmRNA-tagged proteins and the *smpB* gene

product which binds to ribosomes and helps to facilitate degradation by the ClpXP protease (34). *E. coli* cells with an *sspB* mutation are defective in degrading SsrA-tagged proteins (128). This result is interesting with regard to our mutagenesis data in the chapter above concerning the *sspA* gene product, and its possible affect on transcription of the *lspB-lspA2* operon because the *sspA* and *sspB* genes likely form an operon in *H. ducreyi*. Another DNA insert matched *H. ducreyi* genome ORF HD1588 which has homology to polynucleotide phosphorylase, an enzyme that has been shown to also be involved in mRNA degradation (113).

Two DNA inserts had homology with the *priA* gene which encodes for the primosomal protein N' involved in the DNA replication fork and serves as part of the helicase-primase replication machine in lagging-strand synthesis (127,148). Isogenic mutations of *priA* in *E. coli* have been demonstrated to activate the SOS response and also affect, in some cases, plasmid copy numbers (148).

One DNA insert had homology to HD1037 (*gcpE*); however, the function of this gene product has not been well-characterized, but is thought to be essential and involved in isoprenoid and cell wall biosynthesis (17). Homology of *gcpE* to the *aarC* gene in *Providencia stuartii* has been shown. The *aarC* gene product is involved in the acetylation of peptidoglycan, and may act in a pathway that is regulated by quorum sensing (172).

Five of the clones had relatively small DNA inserts which together with questionable nucleotide sequence results did not allow for any specific homology matches.

Nearly half of the DNA inserts were cDNAs from ribosomal RNA. If these experiments were to be scaled-up and used with numerous different growth conditions, then the large number of false-positive results would have become a significant burden, specifically with the cloning and sequencing aspects of these experiments. There are now available methods and procedures to remove or selectively amplify mRNA species from total isolated RNA, of which rRNA makes up the vast majority. One of these methods used in the Hansen laboratory is to employ genome-directed primers that would allow for selective amplification of *H. ducreyi* mRNA species (33). Had this method been available at the time these differential display experiments were performed, the large number of clones that contained 23S rRNA genes might have been reduced and I would have been able to bias or skew the experiments more towards selecting for mRNAs.

In summary, the differential display technique identified numerous transcripts that appeared to be differentially regulated between the two tested growth conditions (media either containing or lacking FCS). More importantly, despite the relatively short amount of time spent on these experiments, a previously unknown virulence factor (i.e., DsrA) was found to be differentially expressed between these two conditions. Currently, the laboratory has available full *H. ducreyi* DNA microarrays and numerous experiments are planned. Based on the initial results from this differential display analysis, there is a good

likelihood that some *H. ducreyi* virulence genes are regulated in a serum-dependent manner. One hypothesis is that materials present in serum may regulate expression of certain gene products, and this differential expression of bacterial proteins may help the bacterium to establish or maintain infection. The putative regulation demonstrated above may not be independent of the *lspA* and *lspB* regulation discussed in Chapter 4, and these two systems may be part of a global regulatory pathway. Performing these types of studies may help to identify and characterize mechanisms responsible for modulating virulence, and provide valuable insight regarding the pathogenesis of *H. ducreyi* disease.

## CHAPTER SIX

### ***Haemophilus ducreyi* Targets Src Family Protein Tyrosine Kinases To Inhibit Phagocytic Signaling**

#### **I. Introduction**

In lesions generated in the human challenge model for experimental chancroid, *H. ducreyi* attached to phagocytes but remained extracellular at least through the pustular stage of disease (25,27). This finding led to the hypothesis by Spinola et al. (191) that *H. ducreyi* might survive in vivo by resisting phagocytosis (191). Subsequent studies by Totten and colleagues (223) as well as by Lagergard and co-workers (6) proved that not only can wild-type strains of *H. ducreyi* resist phagocytosis in vitro, but they can also inhibit the phagocytosis of secondary targets (e.g., opsonized erythrocytes). That *H. ducreyi* can inhibit phagocytosis indicates that, in addition to production of the cytolethal distending toxin that can cause apoptosis in some immune cells (79,203), this pathogen also possesses the means to escape one of the most potent effectors of both innate and acquired immunity.

This laboratory had previously shown that a *H. ducreyi* mutant unable to express the LspA1 and LspA2 proteins lacked the ability to inhibit phagocytic activity of macrophage-like and polymorphonuclear neutrophil (PMN)-like cell lines (215). LspA1 and LspA2 are 86% identical, have calculated masses of 456,211 Da and 542,660 Da, respectively, and are encoded by two of the largest prokaryotic ORFs (12.5 and 14.8 kb, respectively) described

to date (219). Together with the LspB outer membrane protein, LspA1 and LspA2 comprise a two-partner secretion system (109) in which LspB is the essential secretion factor (220). Expression of either LspA1 or LspA2 is necessary to inhibit phagocytic activity; therefore, both *lspA1* and *lspA2* must be inactivated in order to eliminate the ability of *H. ducreyi* to inhibit phagocytosis (Fig. 25). Illustration of *H. ducreyi*'s inhibitory effect on the phagocytic activity of J774A.1 macrophages is shown below in an image provided by Dr. Merja Vakevainen (Fig. 26) (215). In addition, a *lspB* mutant unable to secrete LspA1 or LspA2 was also unable to inhibit phagocytosis (215). Finally, a *lspA1 lspA2* mutant of *H. ducreyi* exhibited greatly reduced virulence in both the temperature-dependent rabbit model for experimental chancroid (218) and the human challenge model (112).

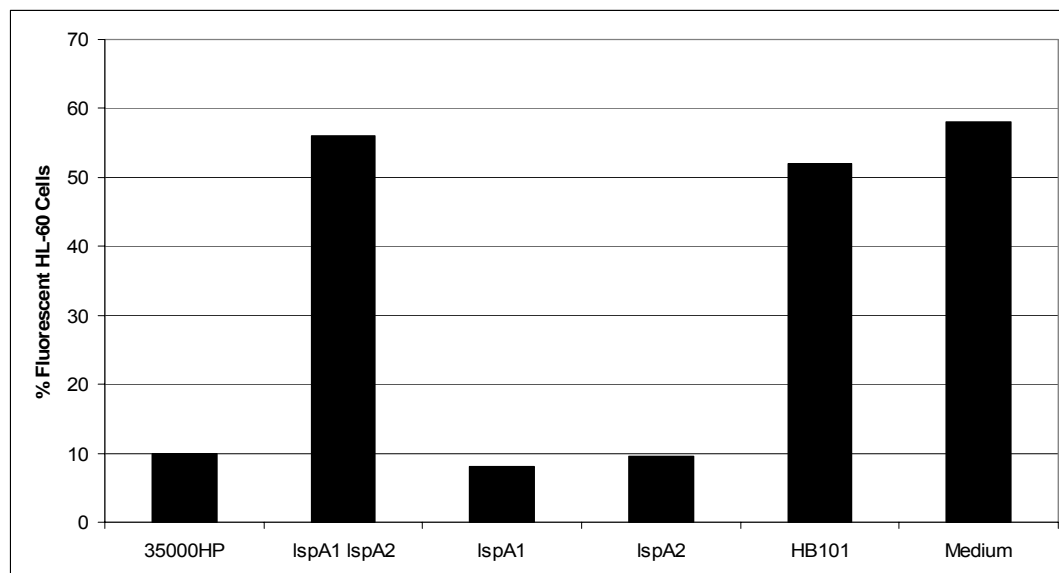


**Figure 25.** *H. ducreyi* inhibits the phagocytic activity of HL-60 cells in vitro. *H. ducreyi* wild-type and mutant strains, *E. coli* HB101 or medium only (RPMI-F) were incubated for 1 h with differentiated HL-60 granulocytes at 33°C. Then opsonized fluorescent microspheres were added and the cells incubated at 37°C for 1 h. The percentage of HL-60 cells containing intracellular fluorescent microspheres is shown.



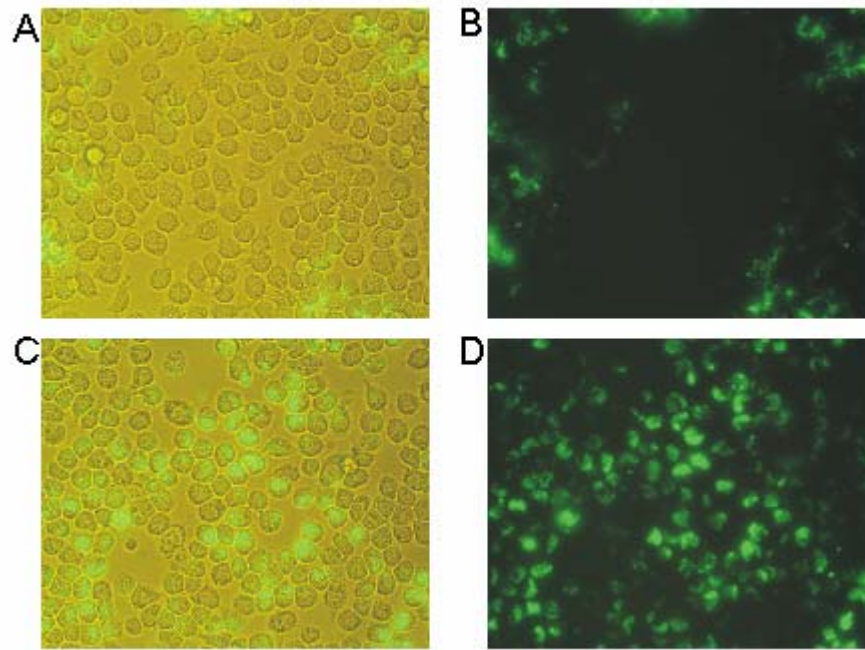


**Figure 26.** Resistance of *H. ducreyi* 35000HP and the *lspA1 lspA2* mutant 35000.12 to phagocytosis by J774A.1 macrophages. These macrophages were incubated with antiserum-opsonized *H. ducreyi* 35000HP(pRB157K) (A [light microscopy] and B [fluorescence microscopy]) or the *lspA1 lspA2* mutant 35000.12(pRB157K) (C [light microscopy] and D [fluorescence microscopy]) for 40 min at 33°C [From (215)].

Herein is provided additional evidence that the wild-type *H. ducreyi* LspA proteins are involved in the inhibition of FcγR-mediated phagocytosis. More importantly, this study demonstrated that this inhibition involves one of the most proximal signaling events in phagocytosis. Incubation of wild-type *H. ducreyi* with immune cells resulted in decreased phosphorylation and reduced catalytic activity of Src family protein tyrosine kinases, leading to an inability to complete phagocytic cup development. This appears to be a novel mechanism for inhibition of phagocytosis by a bacterial pathogen.

## II. Results

### A. Evidence for the Involvement of the LspA Proteins in the Inhibition of Phagocytic Activity

It has been previously reported that a *lspA1 lspA2* mutant of *H. ducreyi* was unable to inhibit phagocytosis (215). Efforts to clone full-length *H. ducreyi lspA* genes into *E. coli* have been unsuccessful to date, thus precluding the use of a genetic approach to prove that the LspA proteins are directly involved in the inhibition of phagocytosis. Therefore, to obtain additional evidence that the LspA proteins are necessary for the inhibition of phagocytosis by *H. ducreyi*, immunodepletion experiments were performed with *H. ducreyi* concentrated culture supernatant fluid (CCS). His-tagged LspA1 fusion proteins were used to raise mouse polyclonal antibodies to different regions of the LspA1 protein for use in these immunodepletion experiments (Fig. 27). We were successful in obtaining antibodies against 10 of the 13 LspA1 segments depicted in Fig. 27B.

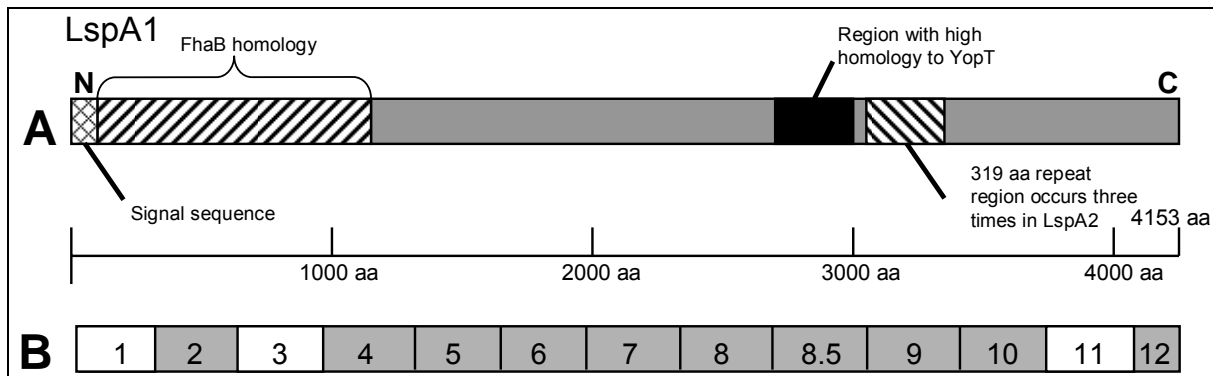


**Figure 27.** LspA1 protein schematic. (A) LspA1 protein schematic showing regions of homology or interest. (B) His-tagged LspA1 fusion proteins used to raise polyclonal mouse antibodies to different regions of LspA1. The numbered segments denote the ~1 kb fragments from the *H. ducreyi* 35000HP *lspA1* ORF used to construct pQE30-based recombinant plasmids that expressed His-LspA1 fusion proteins. Polyclonal mouse antisera were successfully raised against His-LspA1 proteins represented by the 10 shaded segments; antisera were not raised to the 3 white segments.

As reported previously (215), wild-type 35000HP CCS (Fig. 28, column A) readily inhibited phagocytosis whereas CCS from the *lspA1 lspA2* mutant 35000HP $\Omega$ 12 (Fig. 28, column B) did not inhibit phagocytic activity. To confirm the involvement of the LspA proteins in this inhibition, polyclonal mouse antibodies raised against some of the His-LspA1 fusion proteins (Fig. 27B) were incubated with CCS from wild-type *H. ducreyi* and the *lspA1 lspA2* mutant. [LspA1 is the vastly predominant form of LspA protein in wild-type *H. ducreyi* CCS; the amount of LspA2 is almost undetectable (218).] After removal of the immune complexes, the CCS were incubated with HL-60 cells which were then used in phagocytosis assays with opsonized fluorescent microspheres. In initial immunodepletion experiments, I used a pool of antisera to His-LspA1 fusion proteins 4-10 (Fig. 27B) and successfully removed the ability of wild-type *H. ducreyi* CCS to inhibit phagocytosis by

HL-60 cells (data not shown). Subsequent experiments were then performed using polyclonal antibody to only the His-LspA1 fusion protein 8 (Fig. 27B). Incubation with these LspA1 antibodies caused the wild-type CCS (Fig. 28, column C) to lose its ability to inhibit phagocytic activity. Normal mouse serum (i.e, a negative control) (Fig. 28, column E) did not eliminate this inhibitory effect. As expected, the lack of inhibition observed with CCS from the *lspA1 lspA2* mutant (Fig. 28, column B) was not affected by either of these antibody preparations (Fig. 28, columns D and F). These results provide additional evidence for the LspA proteins' involvement in the phagocytic inhibition phenotype of wild-type *H. ducreyi* 35000HP.

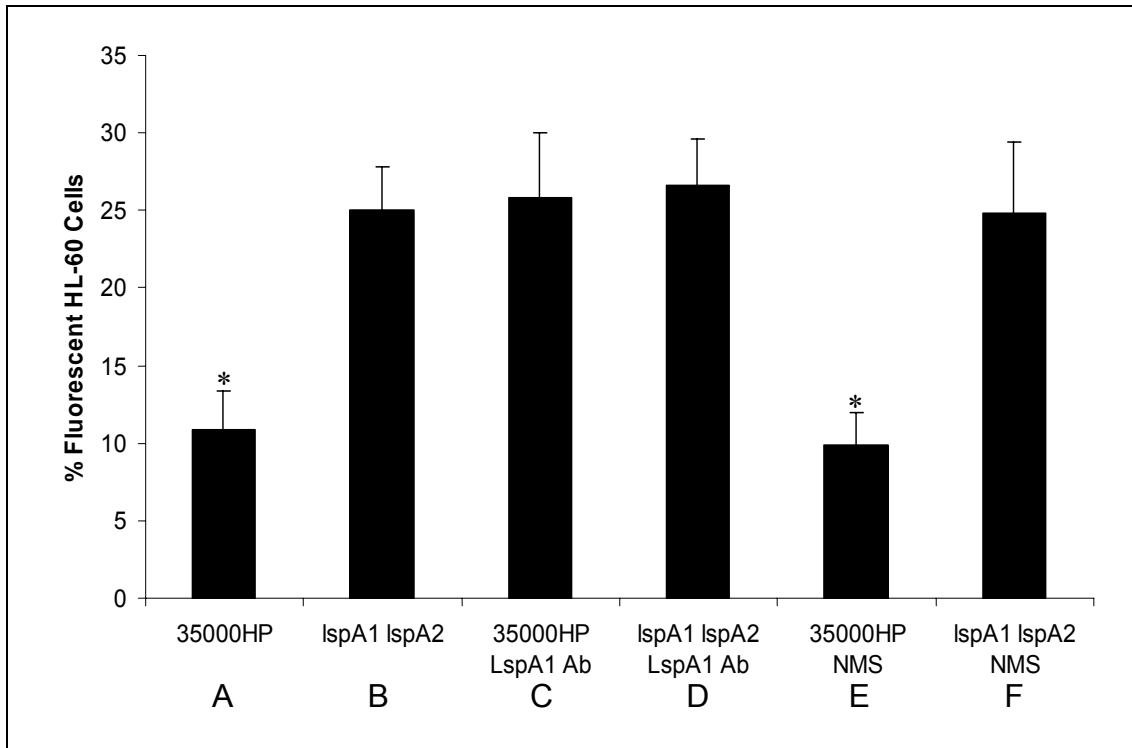


**Figure 28.** LspA1-specific antibodies prevent wild-type *H. ducreyi* CCS from inhibiting phagocytosis. CCS from the wild-type strain 35000HP (columns A, C, and E) and the *lspA1 lspA2* mutant 35000HP $\Omega$ 12 (columns B, D, and F) were incubated with antiserum (LspA1 Ab) (columns C and D) raised against His-LspA1 fusion protein 8 (Fig. 2B) or normal mouse serum (NMS) (negative control) (columns E and F). The complement system in both sera had been heat-inactivated by incubation at 56°C for 30 min. After removal of immune complexes with Protein A/G agarose, the resultant supernatant fluids were incubated with HL-60 cells that were subsequently mixed with opsonized fluorescent microspheres to measure phagocytic activity. These data represent the mean with standard deviation from two independent experiments. Asterisks indicate significance ( $p < 0.001$  using paired Student's *t* test) for the difference between column A and column B and the difference between column E and column F.

## **B. Wild-type *H. ducreyi* Affects Phagocytic Cup Development**

FcγR-mediated phagocytosis normally involves localized actin assembly, which drives pseudopod extension, forming a “cup-like” structure. This culminates in complete target engulfment and eventual actin depolymerization (86). Cytoskeleton staining was performed and viewed by indirect immunofluorescence to detect possible differences in FcγR-induced actin assembly in macrophages exposed to wild-type *H. ducreyi* 35000HP and the *lspA1 lspA2* mutant 35000HP.12. This method allows visualization of both phagocytic cups and IgG-opsonized particles (86).

J774A.1 macrophages were incubated for 1 hr with either strain prior to the addition of IgG-opsonized erythrocytes (EIgG). After a 3 min incubation with EIgG, the cells were fixed, permeabilized, and stained with rhodamine-phalloidin to detect F-actin and an Oregon green-conjugated sheep anti-rabbit IgG to detect the opsonized erythrocytes. Macrophages incubated with the *lspA1 lspA2* mutant (Fig. 29, lower panels, white arrows) showed normal phagocytic cup development and engulfment of opsonized erythrocytes. In contrast, exposure to wild-type *H. ducreyi* apparently halted progression of phagocytic cup formation around the opsonized erythrocytes which remained extracellular (Fig. 29, upper panels, white arrowheads). It should also be noted here that it was previously shown that exposure to wild-type *H. ducreyi* does not affect binding of IgG-opsonized targets to these macrophages (215).

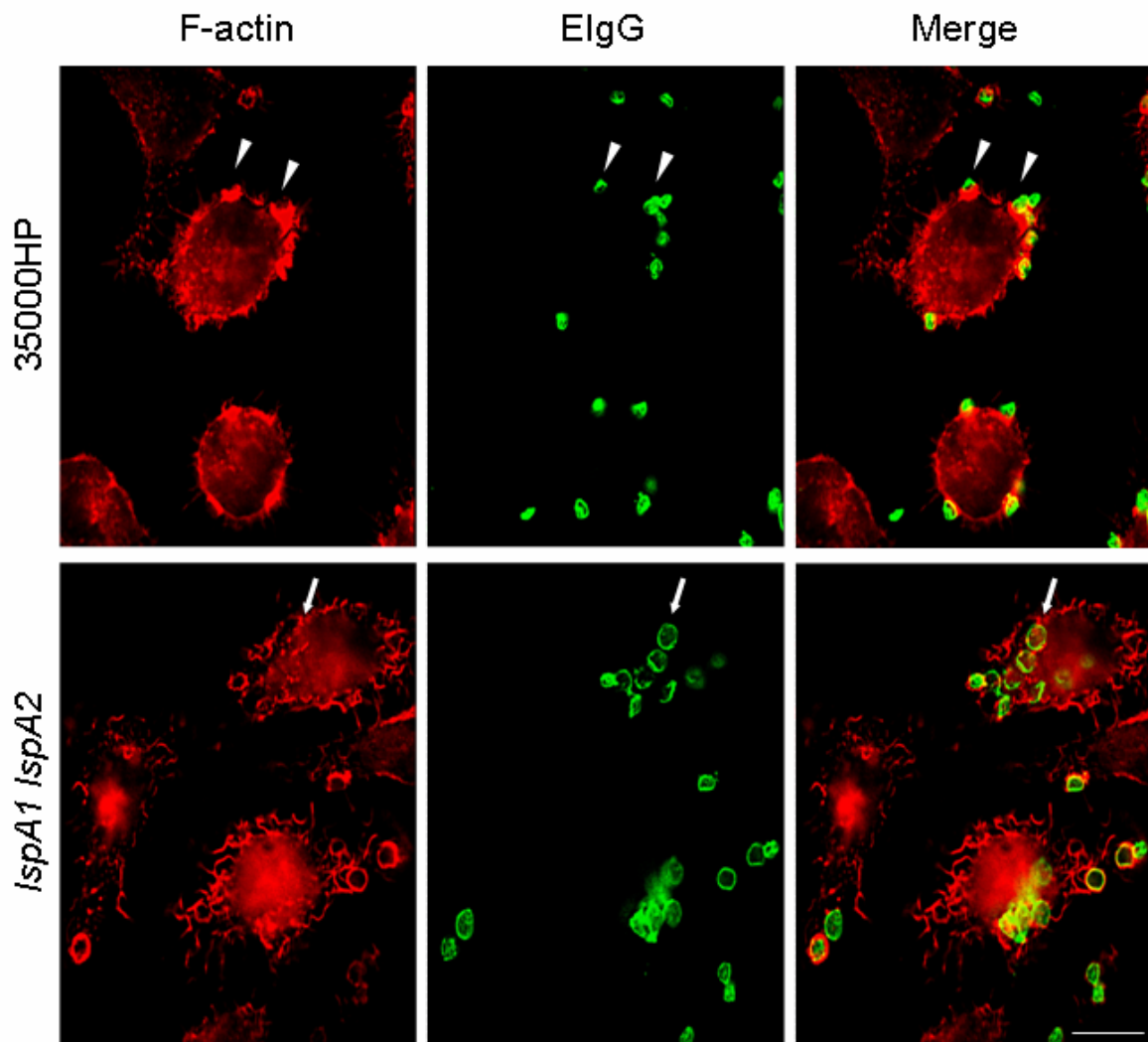


**Figure 29.** Wild-type *H. ducreyi* halts the progression of phagocytic cup development. J774A.1 macrophages were first incubated with wild-type *H. ducreyi* 35000HP or the *lspA1 lspA2* mutant 35000HP.12 and then ElgG were added. The cells were then permeabilized and stained with rhodamine-phalloidin to detect F-actin (red) and Oregon Green-conjugated sheep anti-rabbit IgG to detect ElgG (green). These images represent a 3 min incubation with the opsonized erythrocytes. Arrowheads in upper panels indicate incomplete phagocytic cups indicative of partially ingested ElgG. Arrows in the lower panels indicate a fully ingested ElgG target. Note absence of associated rhodamine-phalloidin staining in the lower panels, consistent with actin depolymerization following complete internalization.

### C. *H. ducreyi* Affects Macrophage Tyrosyl Phosphoproteins

The fact that wild-type *H. ducreyi* had the ability to apparently halt the development of the phagocytic cup suggested a direct inhibition of phagocytic signaling and prompted us to examine the level of phosphoproteins in these macrophages. The most proximal events in the phagocytic signaling pathway involve protein phosphorylation events (e.g., Src kinase activation, immunoreceptor tyrosine-based activation motif (ITAM) phosphorylation, etc.) catalyzed by tyrosine protein kinases (Fig. 30A) [for reviews see (134,204)]. To determine whether the LspA proteins were involved in perturbing these signaling events, J774A.1 macrophages were incubated with wild-type *H. ducreyi* 35000HP or the *lspA1 lspA2* mutant 35000HPQ12. These phagocytes were then lysed and their solubilized proteins were probed in Western blot analysis with the phosphotyrosine-specific MAb 4G10. The levels of several macrophage phosphotyrosine proteins were found to be drastically reduced in lysates from J774A.1 macrophages incubated with wild-type *H. ducreyi* (Fig. 30B, lane 1) relative to those incubated with the mutant (Fig. 30B, lane 2). These included prominent phosphotyrosine proteins with an apparent molecular weight of approximately 55,000. This effect of wild-type *H. ducreyi* 35000HP on phosphoproteins was not limited to J774A.1 macrophages and was observed with RAW 264.7 macrophages as well (Fig. 30B, compare lanes 3 and 4). The levels of phosphoproteins were equivalent between macrophages incubated with media only (control) or the *lspA1 lspA2* mutant (data not shown). Furthermore, decreases in these phosphoproteins were also observed when



IgG-opsonized erythrocytes were added to the macrophages after incubation with wild-type *H. ducreyi* (data not shown). This decrease in phosphoprotein levels due to the wild-type *H. ducreyi* strain could be detected after only 1 hour of incubation (data not shown).

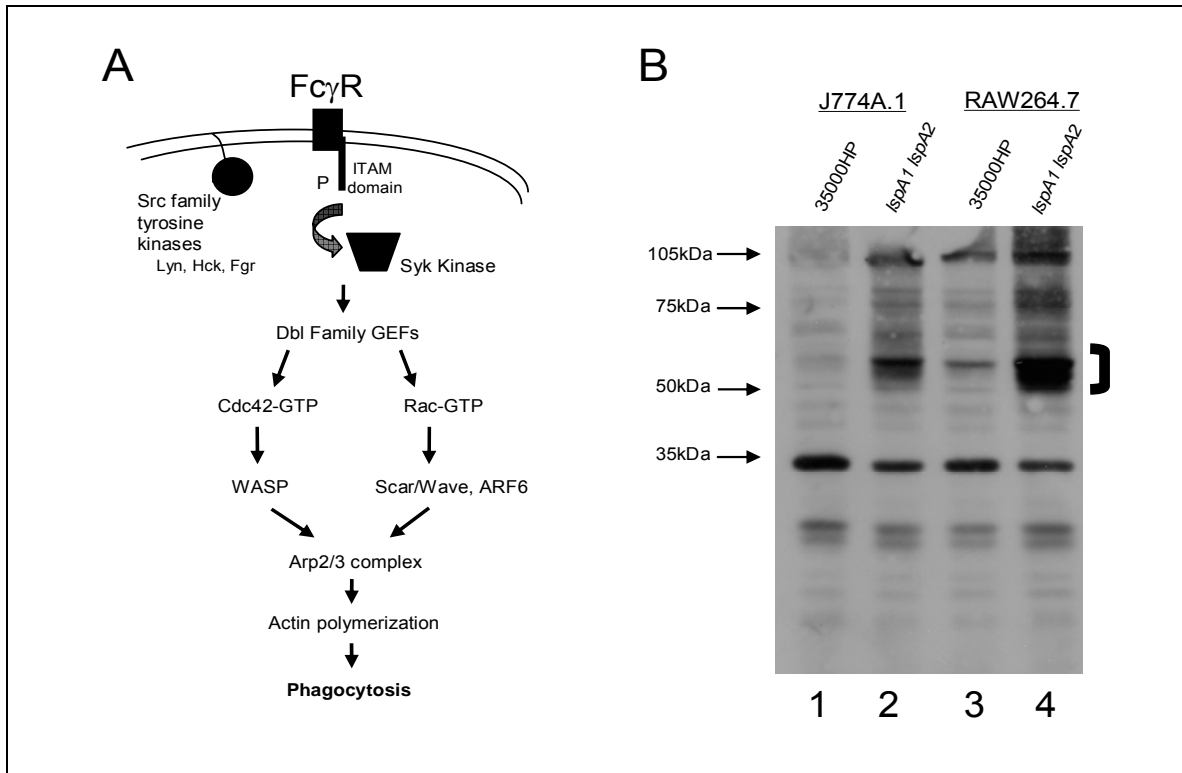


**Figure 30.** Effect of *H. ducreyi* on phosphotyrosine levels. (A) Schematic of key signaling effectors in FcγR-mediated phagocytosis. (B) Effect of *H. ducreyi* on levels of phosphotyrosine proteins in murine macrophages. J774A.1 (lanes 1 and 2) and RAW 264.7 (lanes 3 and 4) macrophages were incubated with wild-type *H. ducreyi* 35000HP (lanes 1 and 3) and the *lspA1 lspA2* mutant 35000HP $\Omega$ 12 (lanes 2 and 4) at 33°C for 4 hr. Macrophage lysates were probed in Western blot analysis with the phosphotyrosine-specific MAbs 4G10. Src family protein tyrosine kinases (indicated by bracket) migrate near the 50 kDa marker.

#### D. Wild-type *H. ducreyi* Reduces the Levels of Active Src Family Kinase

##### Members

The apparent molecular weights of the phosphoprotein(s) affected by incubation with wild-type *H. ducreyi* (Fig. 30B) corresponded to the approximate sizes of Src family protein tyrosine kinases which are essential for normal phagocytic activity (Fig. 30A) (74,134). To determine whether these phosphoproteins were Src family kinases, I prepared cellular extracts from four different cell lines that had been incubated with either wild-type *H. ducreyi* 35000HP or the *lspA1 lspA2* mutant 35000HP $\Omega$ 12 and probed these in Western blot analysis with antibodies specific for the two different tyrosine phosphorylated forms of Src family members. To detect the active form of Src family kinases, we used a polyclonal antiserum ( $\alpha$ -pY418) reactive with the phosphorylated form of Src tyrosine residue Y418; this tyrosine is phosphorylated when Src kinases are catalytically active. To detect the inactive phosphorylated form of Src kinases, I used an antibody ( $\alpha$ -pY529) that recognizes the Src tyrosine residue which, when phosphorylated, holds Src kinases in an inactive state. Extracts from the three immune cell lineages (J774A.1 macrophages, PMN-like HL-60 cells, and DC2.4 dendritic cells) that had been incubated with wild-type *H. ducreyi* (Fig. 31A, panel A, lanes 2, 5, and 8, respectively) showed a dramatic decrease in reactivity with the pY418 antibody specific for active phospho-Src kinases. In contrast, extracts from cells of the same types that had been incubated with the *lspA1 lspA2* mutant (Fig. 31A, panel A, lanes 3, 6, and 9) or with tissue culture medium (control) (Fig. 31A, panel A, lanes 1, 4, and 7) showed little or no reduction in reactivity with this same antibody. Interestingly, extracts from the non-immune HeLa cell line (Fig. 31A, panel A, lanes 10, 11, and 12) showed no apparent difference in reactivity with this same antibody. In these same four cell lines

incubated with wild-type *H. ducreyi*, we found modest and variable changes in the level of phosphorylation of the distal Src tyrosine residue Y529 (Fig. 31A, panel B). The levels of total Src tyrosine kinases were relatively unchanged within each group of different cell types (Fig. 31A, panel C). Additional experiments indicated that a decrease in activated phospho-Src could be detected by Western blot analysis after just 1 hr of incubation with wild-type *H. ducreyi* 35000HP in the presence or absence of opsonized targets (i.e. opsonized sheep erythrocytes) (Fig. 31B).

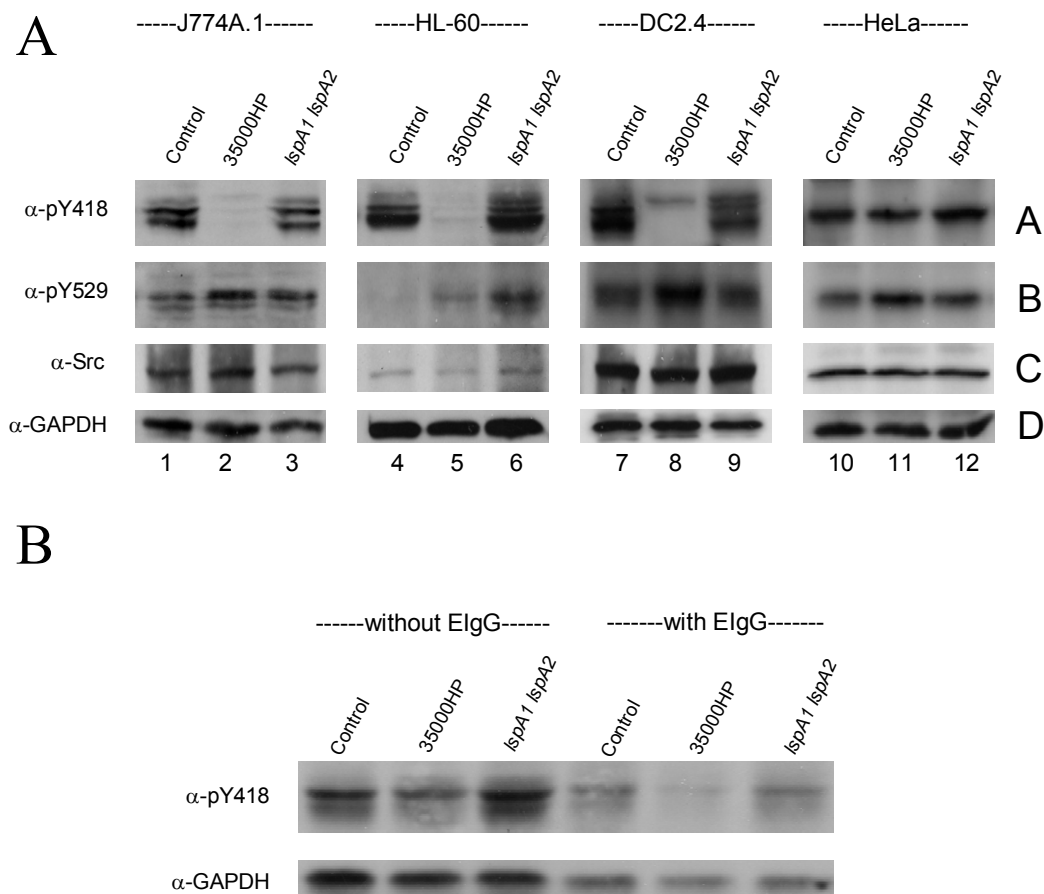


**Figure 31.** Active Src kinase levels are reduced by wild-type *H. ducreyi* in immune cell lines. (A) Active Src kinase levels are reduced by *H. ducreyi*. J774A.1 macrophages (lanes

1-3), PMN-like HL-60 cells (lanes 4-6), DC2.4 dendritic cells (lanes 7-9), and HeLa cells (lanes 10-12) were incubated with medium (control), wild-type *H. ducreyi* 35000HP, or the *lspA1 lspA2* mutant 35000HP $\Omega$ 12 for 4 hr at 33°C. The mammalian cells were then lysed with RIPA buffer, the proteins in the lysates resolved by SDS-PAGE, and then transferred to PVDF membrane. Antibodies to pY418 (active phospho-Src family kinases; panel A) and to pY529 (inactive phospho-Src kinases; panel B) were used to detect active and inactive Src family kinases, respectively. Antibody to Src (panel C) was used to detect total Src protein. Antibody to glyceraldehyde-3-phosphate dehydrogenase (GAPDH) (panel D) was used to verify equal loading. (B) J774A.1 macrophages were incubated with medium (control), wild-type *H. ducreyi* 35000HP, or the *lspA1 lspA2* mutant 35000HP $\Omega$ 12 for 1 hr at 33°C either in the presence or absence of sheep erythrocytes opsonized with rabbit IgG (EiG). Cells were lysed with RIPA buffer and probed with antibodies to pY418 and GAPDH as described above.

#### **E. *H. ducreyi* Reduces the Catalytic Activity of Src Family Tyrosine Kinases.**

The Western blot data (Figs. 30B and 31A) clearly demonstrated a reduction in the levels of the active forms of Src kinases. The Src family kinases Hck, Lyn, and Fgr are the predominant Src kinases present in macrophages (134); the former two tyrosine kinases are required for normal phagocytic activity whereas Fgr plays an important negative regulatory role (88). Our Western blot data suggested that Hck and Lyn would exhibit a decrease in catalytic activity. To examine this possibility, J774A.1 macrophages were incubated with *H. ducreyi* strains as described for Figure 31 and then, after lysis of the macrophages, antibodies to Hck and Lyn were used to immunoprecipitate these Src family members for use in tyrosine kinase reactions. These in vitro kinase assays utilized a physiological substrate, the immunoreceptor tyrosine-based activation motif (ITAM)-containing T cell receptor  $\zeta$  (zeta) subunit (in the form of a GST fusion protein). As can be seen from the levels of phosphorylated GST- $\zeta$ , there was a decrease in the catalytic activity of both Hck (Fig. 32, panel A, lane 2) and Lyn (Fig. 32, panel A, lane 5) in macrophages incubated with

wild-type *H. ducreyi* but not in macrophages incubated with the *lspA1 lspA2* mutant (Fig. 32, panel A, lanes 3 and 8, respectively). Phosphorimager analysis indicated an 84% reduction in Hck activity and a 47% reduction in Lyn activity; these differences were significant (Student's paired *t* test;  $p=0.045$  for Hck and  $p=0.012$  for Lyn). Equivalent amounts of total Hck and Lyn kinases (panel B) and total GST- $\zeta$  protein (panel C) were present in these samples as determined by Western blot analysis. These data indicate that the reduced levels of active Src kinases seen in Fig. 31 in the J774A.1 cells are reflected by a decrease in the enzymatic activity of both Hck and Lyn.

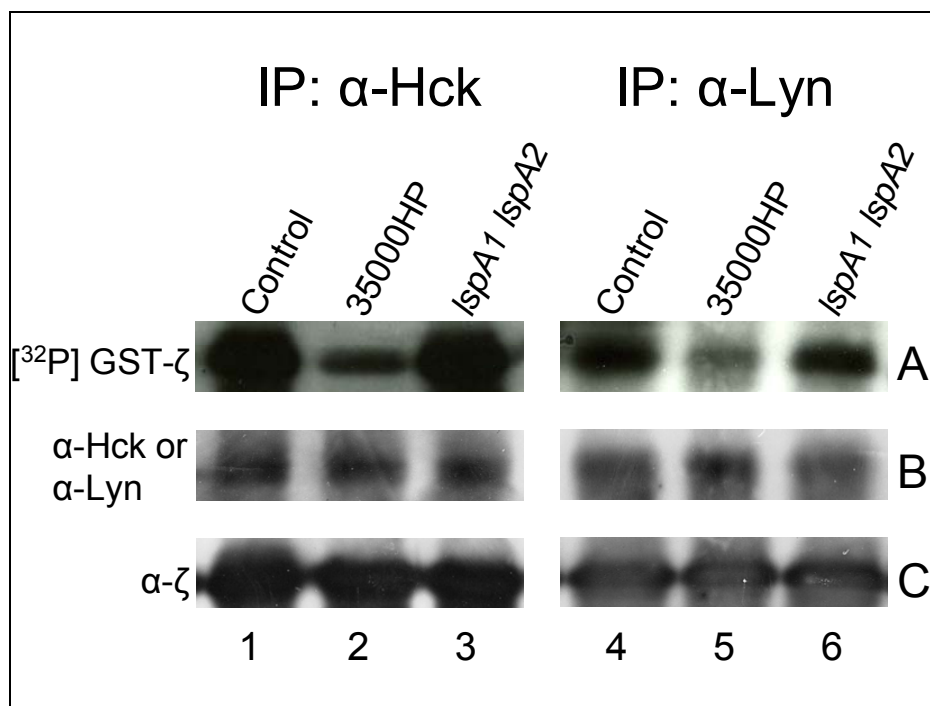


**Figure 32.** The catalytic activity of Src family protein tyrosine kinases is reduced in macrophages incubated with wild-type *H. ducreyi*. J774A.1 macrophages that had been incubated with medium (lanes 1 and 4) (control), wild-type *H. ducreyi* 35000HP (lanes 2 and 5), or the *lspA1 lspA2* mutant 35000HP $\Omega$ 12 (lanes 3 and 6) as described for Fig. 5 were lysed and then polyclonal antibodies to Lyn and Hck were used to immunoprecipitate these Src family kinases. Enzymatic activity was measured by using a GST- $\zeta$  fusion protein as the substrate for phosphorylation; radiolabeled GST- $\zeta$  was detected by autoradiography (panel A). Western blot analysis using antibodies to Hck (panel B, lanes 1, 2, and 3) and

Lyn (panel B, lanes 4, 5, and 6) and  $\zeta$  ( $\alpha$ - $\zeta$ ; panel C) was used to confirm the presence of equivalent amounts of the different protein tyrosine kinases and GST- $\zeta$ . The Hck and Lyn antibodies used in panel B were different from the antibodies used for immunoprecipitation of these kinases.

### III. Discussion

A large number of putative virulence factors of *H. ducreyi* have been identified to date, including both proteins and lipooligosaccharide (LOS) [see (191) for a review]. In addition, *H. ducreyi* has been shown to synthesize at least two toxins (52,156,208) and a copper-zinc superoxide dismutase (177). However, when tested in the human challenge model for experimental chancroid (11,197), only a few of these gene products have been shown to be required for full virulence of *H. ducreyi*. These include the peptidoglycan-associated lipoprotein (76), the hemoglobin-binding outer membrane protein HgbA (7), the DsrA outer membrane protein (37), the *flp* gene cluster (194), and the LspA1 and LspA2 proteins (112). These latter two proteins have been shown, by both earlier mutant analysis (215) and the present study, to be involved in the ability of this pathogen to inhibit phagocytosis in vitro. The findings in the present study have also revealed a novel and previously unreported capacity of *H. ducreyi* to affect the phosphorylation state of Src family protein tyrosine kinases.

Bacterial pathogens have devised a number of different strategies for escaping or preventing phagocytosis [for reviews see (136,175)]. These range from the expression of polysaccharide capsules, which can exert a simple physical impediment or even alter

phagocytic signaling [e.g., *Streptococcus suis* (181)], to injection of effector molecules that target signaling components [e.g., *Yersinia* YopT (185), *Pseudomonas* ExoT (202)]. Phagocytosis is an extremely complex process (Fig. 6A) [for a review see (204)]. While binding of IgG-opsonized particles or bacteria to most Fc $\gamma$ R (except Fc $\gamma$ RIIB) will initiate the phagocytic signaling cascade, signaling through Toll-like receptors has also recently been shown to affect phagocytosis (31,65). Fc $\gamma$ R cross-linking (by IgG-opsonized target particles) results in activation of Src family protein tyrosine kinases, with Hck, Lyn, and Fgr being predominant in murine macrophages (74). These protein tyrosine kinases catalyze the phosphorylation of ITAMs present on or associated with Fc $\gamma$ R. Once phosphorylated, Fc $\gamma$ R-associated ITAMs become docking sites for the SH2 domains of Syk and Src family protein tyrosine kinases. ITAM-bound Syk is catalytically activated by a combination of autophosphorylation and trans-phosphorylation by Src family protein tyrosine kinases. Activated Syk subsequently phosphorylates a number of intracellular substrates, initiating a series of downstream events, including small Rho GTPase activation, which culminate in actin filament assembly and development of the phagocytic cup (Fig. 30A). As activation of Src family protein tyrosine kinases is a very proximal event in Fc $\gamma$ R signaling, it is likely that multiple cellular events relevant to phagocytosis (e.g., altered membrane trafficking) are also affected by the LspA proteins, in addition to actin assembly (Fig. 29).

We have established that expression of either LspA1 or LspA2 individually is necessary for *H. ducreyi* to inhibit phagocytic activity in vitro (215). Efforts to clone full-

length *H. ducreyi* *lspA* genes into *E. coli* or purify functional LspA proteins from spent *H. ducreyi* culture medium have been unsuccessful to date, so I used LspA-specific antibodies to provide additional proof that this inhibitory effect required these *H. ducreyi* proteins (Fig. 28). Other experiments showed that incubation of wild-type *H. ducreyi*, but not the *lspA1 lspA2* mutant, with macrophages resulted in a dramatic reduction in the levels of active Src protein tyrosine kinases (Figs. 30B and 31A). These kinases are involved in some of the most proximal events of the phagocytic signaling pathway (Fig. 30A). This reduced enzymatic activity of the Src protein tyrosine kinases is consistent with the inability of the former macrophages to complete the development of phagocytic cups (Fig. 29). We hypothesize that either (1) the LspA proteins bind to a receptor on the macrophage surface and thereby initiate a signaling cascade that abolishes phagocytic activity or (2) the LspA proteins enter or penetrate into the phagocyte and therein cause derangement of the normal phagocytic signaling pathway. The level of active phospho-Src kinases in all three immune cell types tested in this study was reduced by exposure to wild-type *H. ducreyi*, whereas phospho-Src kinase levels in HeLa cells appeared unaffected (Fig. 31A). This finding raises the possibility that a surface component present in immune cell lineages may interact with the LspA proteins, resulting in a negative signaling event. At this time, however, we cannot exclude the possibility that LspA proteins enter the macrophage via an endocytic process and exert their function in the cytoplasm, but it is unclear how these proteins would survive endosomal proteolysis and exit into the cytoplasm. An equivalently large bacterial exoprotein (i.e., RtxA) synthesized by *Vibrio cholerae* has been shown to



directly cross-link actin intracellularly but the method of entry or penetration of this protein into the host cell cytoplasm remains to be determined (186).

Only two regions of the LspA proteins have significant homology to known bacterial virulence factors. The N-terminal one-quarter of LspA1 (Fig. 27A) contains several features associated with secretion of other soluble virulence factors including the *Bordetella pertussis* filamentous hemagglutinin (109). There is also a 230-aa region in the C-terminal half of the LspA proteins that has 36% identity with the YopT protein from pathogenic *Yersinia* species (185) (Fig. 27A). YopT is the prototype of a family of cysteine proteases involved in virulence expression and cleaves small Rho GTPases from the eukaryotic cell membrane (185), thereby altering signaling and inhibiting phagocytosis. Western blot signaling (43) showed a reduction in the level of membrane-bound Cdc42 in macrophages incubated with wild-type *H. ducreyi* relative to that in macrophages exposed to the *lspA1 lspA2* mutant (Chapter Seven, Fig. 36). It is likely that this change is simply a downstream effect related to the greatly decreased levels of Src family kinase activity. Moreover, we have established that the level of membrane-bound Hck is unchanged whether the macrophages are incubated with wild-type *H. ducreyi* or the *lspA1 lspA2* mutant (Chapter Seven, Fig. 38). This latter finding indicates that the YopT-like region is not cleaving Hck from the membrane. Our recent data indicate that this YopT-like region may be involved in auto-processing of the LspA proteins (Chapter Eight), in a manner similar to that catalyzed by the *Pseudomonas syringae* AvrPphB protein, another member of this cysteine protease family (184).

To date, there is only one other example of a bacterial gene product that affects Src family protein tyrosine kinases. The CagA protein of *Helicobacter pylori*, after injection into macrophages via a type IV secretion system, is phosphorylated by Src kinase (182) and in turn causes a reduction in active phospho-Src kinase by increasing the activity of the protein tyrosine phosphatase SHP-2 (212). However, two independent studies indicate that CagA is not involved in the inhibition of phagocytosis caused by *H. pylori* (149,171). It should be noted here that efforts to detect possible phosphorylation of the *H. ducreyi* LspA proteins after their interaction with macrophages have been unsuccessful to date (data not shown).

Exactly how the LspA proteins are involved in the observed reduction in the catalytic activity of the Src family protein tyrosines kinases remains to be determined. At this time, we cannot formally exclude the possibility that another, as yet unidentified *H. ducreyi* gene product works in concert with the LspA proteins to inhibit phagocytosis. Efforts to elucidate the precise mechanism of action of these secreted virulence factors are in progress and may provide additional insight into the pathogenesis of chancroid as well as a valuable biologic tool for further dissection of Src family kinase function, regulation, and activity.

## CHAPTER SEVEN

### Characterization of the Inhibition of Src Family Protein Tyrosine Kinases by *Haemophilus ducreyi*

#### I. Introduction

Having determined that the LspA proteins of *H. ducreyi* are necessary for inhibition of phagocytosis due, at least in part, to their ability to decrease the catalytic activities of the Src family protein tyrosine kinases, I next set out to determine the mechanism by which the LspA proteins cause the downregulation of active signaling events to occur in host immune cells.

Members of the Src family of protein tyrosine kinases (Src PTKs) are involved in some of the most proximal events of the phagocytic signaling pathway. The reduced enzymatic activity of the Src PTKs in macrophages exposed to wild-type *H. ducreyi* is consistent with the inability of these macrophages to complete the development of phagocytic cups (Chapter Six, Fig. 29). I propose two main hypotheses to explain these events. Either (1) the LspA proteins bind to a receptor on the macrophage surface and thereby initiate a signaling cascade that abolishes phagocytic activity or (2) the LspA proteins enter or penetrate into the phagocyte and therein cause derangement of the normal phagocytic signaling pathways. The experiments performed below in this section were

done in an attempt to further elucidate the mechanism of immune cell modulation by the LspA proteins of *H. ducreyi*.

## **II. Results**

### **A. The Effects of Chemical Inhibition of Src Protein Tyrosine Kinases on Phagocytic Activity**

It has been established that Src PTKs are involved in a very proximal role in Fc $\gamma$ R-mediated signaling, and are important for downstream  $\gamma$ -chain and Syk phosphorylation along with subsequent actin cup formation (74). However, in the absence of Src family kinases these signaling events still occur but are delayed, indicating that Src family members are not absolutely required for Fc $\gamma$ R-mediated phagocytosis but enhance phagocytic activity (74). To examine the relationship between Src kinase activity and phagocytic uptake of opsonized particles, I performed phagocytosis assays with IgG-opsonized RBCs (EIgG) and J774A.1 macrophages that had been incubated with the *H. ducreyi* wild-type and *lspA1 lspA2* mutant strains. For these experiments, chemical inhibitors of Src kinases were added to determine their effect on phagocytosis. The chemical inhibitors genistein [100  $\mu$ M] and PP2 [20  $\mu$ M] were added 40 minutes before the opsonized targets were incubated with the macrophages and then phagocytic uptake of EIgG targets was measured by determining the phagocytic index levels for each set of conditions (Fig. 33). Genistin [100  $\mu$ M], an inactive form of genistein that is not able to

inhibit Src catalytic activity, was used as a negative control for genistein. The phagocytic index was calculated by counting the number of engulfed targets (i.e., EIgG) per macrophage. For example, a phagocytic index value of 3 means that, on average, there were approximately 3 EIgG engulfed per macrophage.

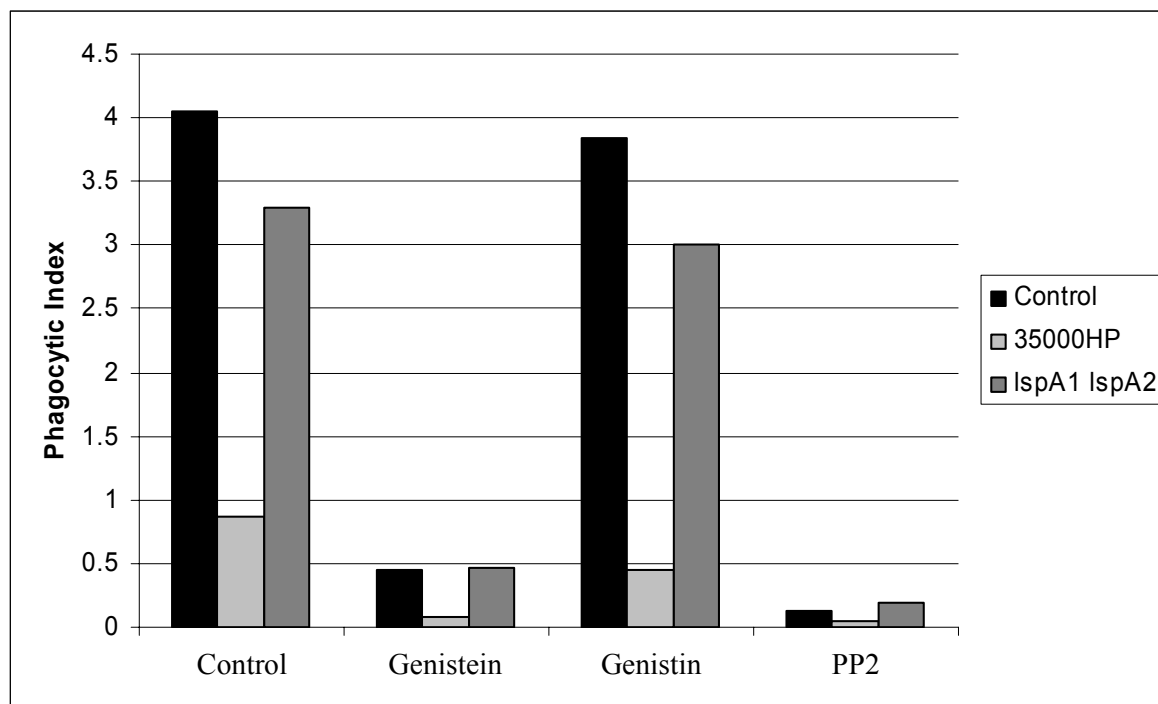


**Figure 33.** Phagocytosis assays measuring the uptake of opsonized RBCs (EIgG) by J774A.1 cells incubated with chemical inhibitors of Src PTK activity.

The two chemical inhibitors genistein and PP2 dramatically inhibited phagocytosis of opsonized particles regardless of which *H. ducreyi* strain had been incubated with the macrophages (Fig. 33). Interestingly, there was an additional decrease in phagocytic index values in those macrophages that were incubated with both the wild-type *H. ducreyi* strain

and the chemical inhibitors. These results reaffirm the important role that Src tyrosine kinases play in Fc $\gamma$ R-mediated phagocytosis.

### **B. Wild-type *H. ducreyi* Reduces the Levels of Active Src Family Kinase Members in Certain Immune Cell Lineages**

Having seen the decrease in active Src PTK levels caused by *H. ducreyi* in several immune cell lineages (i.e., J774A.1, RAW264.7, DC2.4, and HL-60 cells) but not in other cell types such as like HeLa and COS7 cells, I set about to further characterize the effect the LspA proteins may have on Src kinase levels in several other immune cell lines. The Jurkat T cell-like line, the Daudi B cell-like line, and the RBL-1 mast cell-like line were incubated with either the wild-type 35000HP strain or the *lspA1 lspA2* mutant strain as described previously for the other cell lines above. The lysates were prepared and probed with antibodies recognizing active Src kinases along with an antibody recognizing total Src protein (to confirm equivalent Src protein levels) (Fig. 34).

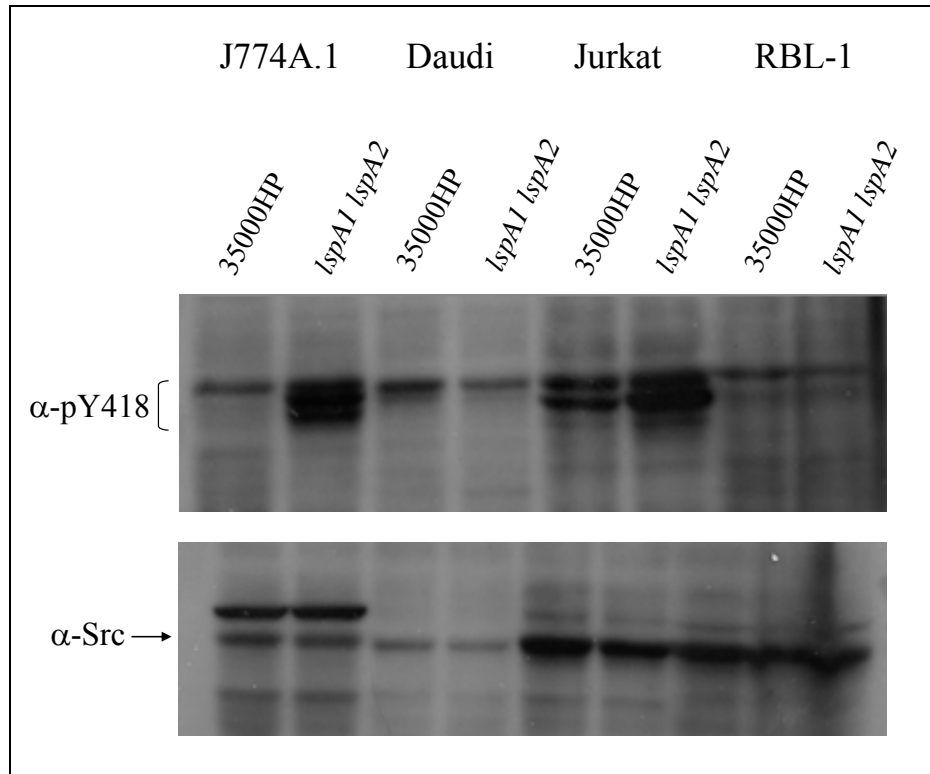


**Figure 34.** Active Src kinase levels are reduced in Jurkat T cells by wild-type *H. ducreyi*. J774A.1 macrophages, B cell-like Daudi cells, T cell-like Jurkat cells, and mast cell-like RBL-1 cells were incubated with wild-type *H. ducreyi* 35000HP or the *lspA1 lspA2* mutant 35000HPQ12 strains for 4 hr at 33°C. The mammalian cells were then lysed with RIPA buffer, the proteins in the lysates resolved by SDS-PAGE, and transferred to PVDF membrane. Antibodies to pY418 used to detect active phospho-Src family kinases and antibodies to Src were used to detect levels of total Src protein.

Only the Jurkat cells showed a decrease in active Src kinase levels when incubated with the wild-type strain when compared to cells that had been incubated with the *lspA1 lspA2* mutant. The Daudi and RBL-1 cells had lower baseline levels of active Src kinases when compared to the J774A.1 and Jurkat cell lines, and furthermore, did not have any appreciable difference in active Src levels after incubation with either the wild-type 35000HP or *lspA1 lspA2* mutant strains. In the mammalian cell lines examined to date, the decrease in active Src kinase levels caused by wild-type *H. ducreyi* appears to be specific to

immune cell lines. The most pronounced decrease in active Src kinase levels appears in professional phagocytic cells (i.e., J774A.1, RAW264.7, HL-60 and DC2.4 cells); however, there is also a detectable decrease in the T cell-like Jurkat cells.

### **C. Proteinase K Treatment of Macrophages Prevents the Decrease in Active-Phospho-Src**

While the inhibitory effect of *H. ducreyi* on phagocytosis can be detected within 15 min after exposure of macrophages to this pathogen (223), the nature of the molecular interaction between the LspA proteins and the macrophage remains to be determined. The very large size of these proteins, together with the absence of a type III secretion system in *H. ducreyi*, make it unlikely that these macromolecules are introduced directly into the macrophage. In addition, a strain of *H. ducreyi* with a mutation in the putative type IV secretion system (147) still inhibited phagocytosis like the wild-type parent strain (data not shown). The LspA proteins could bind a macrophage surface moiety that then transmits a signal inhibiting phagocytosis, similar to the interaction between CD47 and SIRP $\alpha$  (152). To address this possibility, J774A.1 macrophages were first treated with either proteinase K or trypsin and then exposed to wild-type *H. ducreyi* or the *lspA1 lspA2* mutant. Macrophages pretreated with proteinase K and incubated with the wild-type strain (Fig. 35, lane 1) exhibited levels of activated phospho-Src equivalent to those found in macrophages incubated with the *lspA1 lspA2* mutant, regardless of whether they were treated with proteinase K (Fig. 35, lanes 2 and 4).



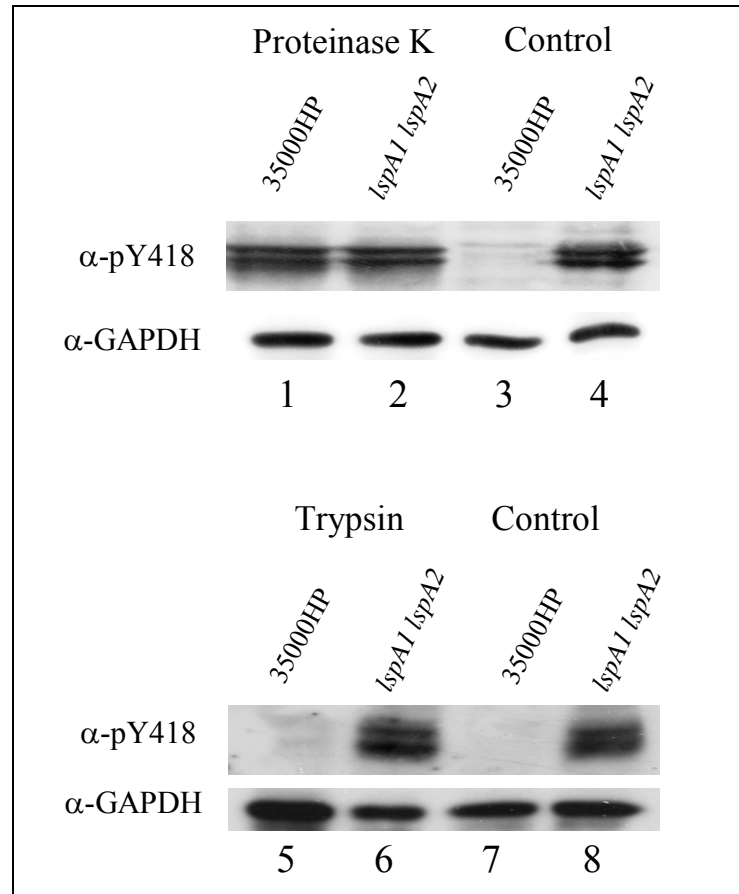


**Figure 35.** Proteinase K pre-treatment of macrophages prevents reductions in active phospho-Src family PTKs. J774A.1 macrophages were first treated with proteinase K (lanes 1 and 2), trypsin (lanes 5 and 6), or tissue culture medium (control) (lanes 3, 4, 7 and 8) as described in Materials and Methods and then incubated with wild-type *H. ducreyi* and the *lspA1 lspA2* mutant 35000HPΩ12. These macrophages were then lysed and processed to detect activated phospho-Src levels. Antibody to GAPDH was used to verify equivalent loading of samples.

In contrast, when the macrophages were pretreated with trypsin, incubation with the wild-type *H. ducreyi* strain caused the characteristic decrease in active phospho-Src levels (Fig. 35, lane 5). This latter result suggests the possible existence of a proteinaceous surface component or receptor for LspA proteins which is proteinase K-sensitive but

trypsin-insensitive. This phenomenon is not uncommon; for example, the Fc $\gamma$ RII and Fc $\gamma$ RIII in mouse macrophages are trypsin-insensitive (51). One caveat to this experiment is that, even though the cells were washed several times, there remains the possibility that some proteinase K was still present which could degrade the LspA proteins, leading to the incorrect conclusion that some surface component was necessary for Src kinase inhibition. The results obtained from the proteinase K experiments do raise the possibility, however, that a surface component present in immune cell lineages may interact with the LspA proteins, resulting in a negative signaling event. However, attempts to detect an interaction between the LspA proteins and selected macrophage components (e.g., SIRP $\alpha$ ) known to down-regulate phagocytic activity have been unsuccessful to date.

#### **D. Fc $\gamma$ R-Mediated Phagocytosis Signaling Events**

Only two regions of the LspA proteins have significant homology to known bacterial virulence factors. The N-terminal one-quarter of LspA1 contains several features associated with secretion of other soluble virulence factors including the *Bordetella pertussis* filamentous hemagglutinin (109). There is also a 230-aa region in the C-terminal half of the LspA proteins that has 36% identity with the YopT protein from pathogenic *Yersinia* species (185) (Chapter Six, Fig. 27). YopT is the prototype of a family of cysteine proteases involved in virulence expression and cleaves small Rho GTPases from the eukaryotic cell membrane (185), thereby altering signaling and inhibiting phagocytosis. The presence of the YopT-like region in the LspA proteins prompted me to examine

whether small GTPases in macrophages could be affected by wild-type *H. ducreyi*. I performed Western blot experiments targeting the small Rho GTPases known to be involved in FcγR-mediated signaling (43), using both lysates and cell fractions from macrophages that had been incubated with either wild-type 35000HP or the *lspA1 lspA2* mutant 35000HPΩ12 for 3 hrs. These experiments showed a reduction in the level of total membrane-bound Cdc42 in macrophages incubated with wild-type *H. ducreyi* relative to that in macrophages exposed to the *lspA1 lspA2* mutant (Fig. 36). There consistently appeared to be a decrease in the amount of membrane-bound total Cdc42 caused by the wild-type strain, although there was no apparent difference in the amount of activated Cdc42 (data not shown). Membrane-bound Cdc42 appeared to be reduced, while the levels of Rac and RhoA appeared unchanged (Fig. 36).

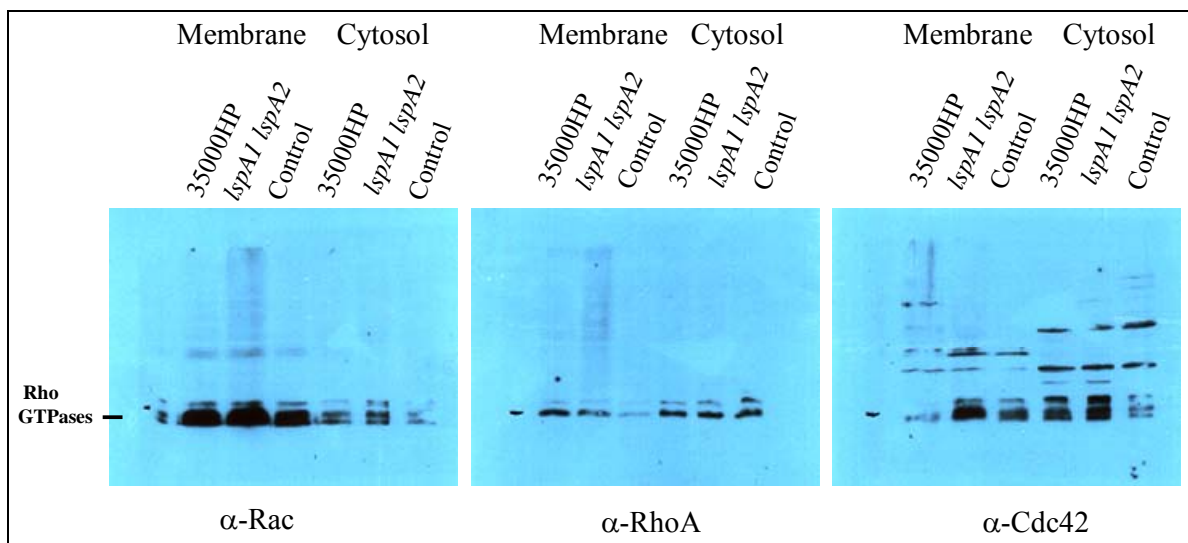


**Figure 36.** Western blot experiments detecting small Rho GTPases in J774A.1 cell fractions. Western blot experiments detecting the small Rho GTPases in cell fractions from macrophages that had been incubated with media only control, wild-type 35000HP, or the *lspA1 lspA2* mutant 35000HPΩ12 for 3 hrs. Membrane and cytosol fractions were standardized by the Bradford assay.

As stated above, the mammalian cell line J774A.1 was incubated with either the wild-type *H. ducreyi* 35000HP strain or the *lspA1 lspA2* mutant strain, and then the amounts of active Cdc42 or Rac were determined by using the Cdc42 Activation Assay Kit (Cytoskeleton Inc.). Briefly, this kit involves a “pull-down” assay utilizing a GST-CRIB fusion protein that binds only the active GTP-bound form of Cdc42 or Rac. These precipitates can then be probed in Western blot analysis to determine the concentrations of Cdc42 or Rac present, representing the amount of active protein in the lysate. There was little difference seen in activated Cdc42 levels in macrophages incubated with either the 35000HP or *lspA1 lspA2* mutant strain (data not shown). There appeared to be a very modest decrease in active GTP-bound Rac in J774A.1 cells that had been exposed to 35000HP when compared to those cells exposed to the *lspA1 lspA2* mutant (Fig. 37). If these changes are a direct result of enzymatic activity expressed by the YopT-like region in the LspA protein, then this would argue that the LspA proteins somehow enter or penetrate into the macrophage. Alternatively and perhaps more likely, these may simply be downstream effects related to the decreased level of active phospho-Src.

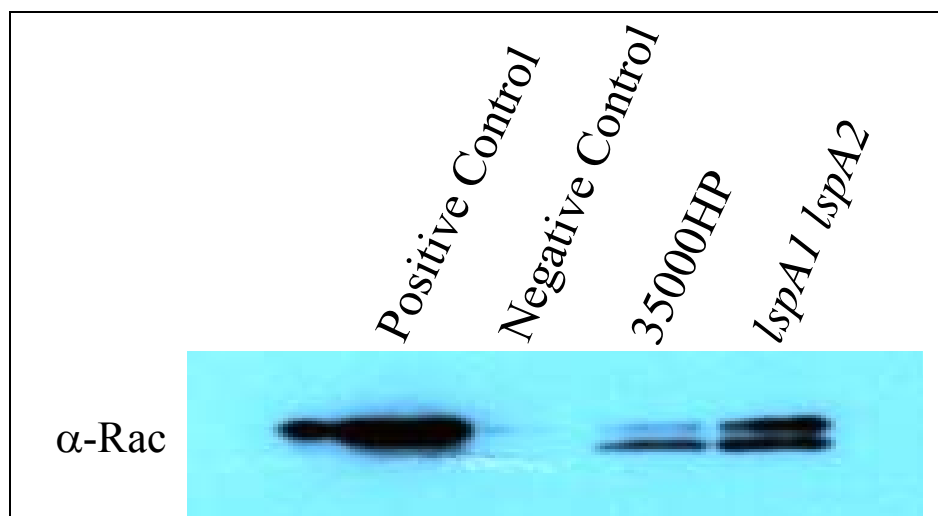


**Figure 37.** Active small Rho GTPase levels from J774A.1 macrophages incubated with either the *H. ducreyi* wild-type or the *lspA1 lspA2* strains. The activation of small Rho GTPases was measured by using the Cdc42 Activation Assay kit from Cytoskeleton Inc. The level of active GTP-bound Rac was measured in J774A.1 cells incubated with the wild-type 35000HP strain and the *lspA1 lspA2* mutant. The positive and negative controls were performed by either adding a high concentration of GTP or GDP respectively.

Considering that Src family members are also associated with the cytoplasmic side of the cell membrane by myristylation in their N-terminal region, the possibility that the LspA proteins may cleave and release Src kinases away from the membrane was also examined. I found that the level of membrane-bound Hck was apparently unchanged whether the macrophages were incubated with wild-type *H. ducreyi* or the *lspA1 lspA2* mutant (Fig. 38). Based on these results, the LspA proteins are not cleaving the small Rho GTPases or Src PTKs from the membrane to perturb phagocytic signaling. These findings indicate that, while both the YopT and LspA proteins inhibit phagocytosis, the LspA proteins are apparently not functioning like the YopT protein and cleaving small Rho GTPases from the membrane.

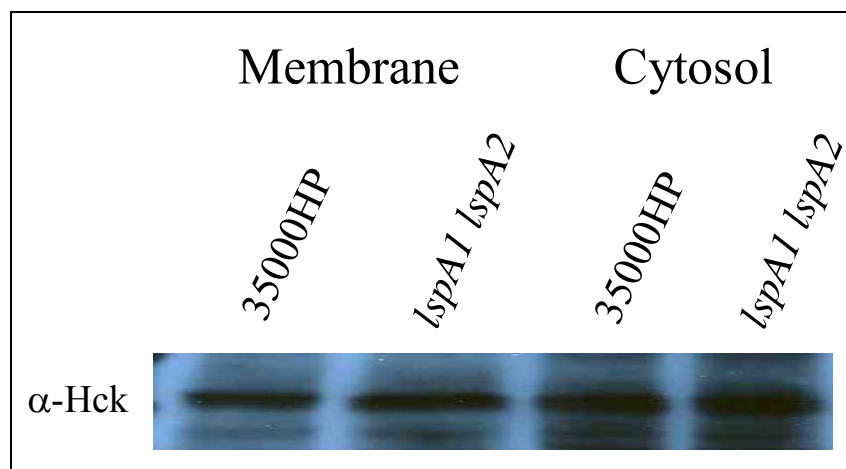


**Figure 38.** Western blot analysis detecting total Hck protein levels in J774A.1 cell fractions. Western blot analysis using cell fractions from macrophages that had been incubated with wild-type 35000HP or the *lspA1 lspA2* mutant 35000HPΩ12 for 3 hrs and then probed with an anti-Hck antibody.

Furthermore, I have additional data which indicate that this YopT-like region may be involved in auto-processing of the LspA proteins (discussed in Chapter Eight), in a manner similar to that catalyzed by the *Pseudomonas syringae* AvrPphB protein, another member of the YopT cysteine protease family (184).

### E. Chromatographic Separation and Fractionation of J774A.1 Lysates

The mammalian cell line J774A.1 was incubated with either the wild-type 35000HP or the *lspA1 lspA2* mutant 35000HPΩ12 strains at 33°C for 4 h as described (141) and then total protein homogenates for each were subjected to chromatographic separation as previously described (190). The lysate samples were applied to a HiTrap Q-Sepharose column linked to an AKTA FPLC system. Proteins that were retained on the column were

eluted with a linear NaCl gradient (an example is shown in Figure 39). For each chromatography run, forty fractions were taken.

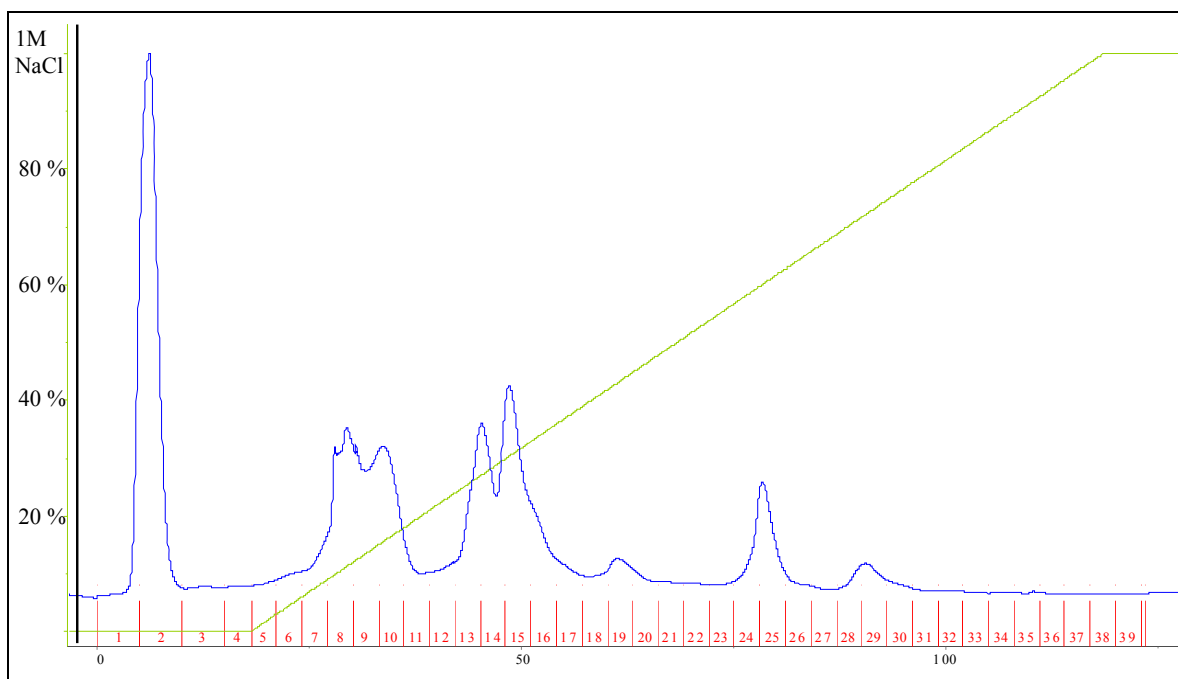


**Figure 39.** Anion-exchange protein separation of J774A.1 lysates incubated with either the *H. ducreyi* wild-type or *lspA1 lspA2* mutant strains. Chromatographic separation graph demonstrating the elution of proteins (blue line) by a linear NaCl gradient (green line). The fractions taken are shown in red. The x-axis represents the milliliter volume during the separation, while the y-axis is the percentage of the 1M NaCl in the linear gradient.

These individual fractions were used in an ELISA-based protein tyrosine phosphatase PTPase assay as previously described (190). A 96-well plate was coated overnight with either purified phosphor-  $\zeta$  or purified phospho-Src (pY418). Then, a 40 – 80  $\mu$ L volume of each fraction (from either the J774A.1/*H. ducreyi* 35000HP strain homogenate or the J774A.1/*H. ducreyi lspA1 lspA2* strain homogenate) from the anion exchange chromatography was added to the individual wells and incubated at 37°C for 1 h

with agitation. Then, the anti-phosphotyrosine MAb 4G10 was added to detect levels of phosphorylated Src, and a goat anti-mouse IgG-conjugated HRP secondary antibody was added to each well. The assay was then developed and optical density readings were performed with a spectrophotometer. The optical density readings from each fraction were graphed and compared between the two sample fraction sets (35000HP and *lspA1 lspA2*) (Fig. 40A and 40B).

In Figure 40A, the substrate was phosphor- $\zeta$  and phosphatase activity was detected in fractions 8 and 9, with the fractions from J774A.1/35000HP having increased phosphatase activity (Fig. 40A, blue line) when compared to those same fraction numbers from the J774A.1/*lspA1 lspA2* mutant set (Fig. 40A, pink line). The activity in fractions 8 and 9 was also seen when the substrate was phosphor-Src (Fig. 40B). The J774A.1/35000HP samples (Fig. 40B, blue line) again also had increased PTPase activity (Fractions 8 and 9) when compared to the J774A.1/*lspA1 lspA2* mutant fractions (Fig. 40B, pink line). Based on the results from the two different PTPase assays, fractions 8 and 9 from the J774A.1/35000HP lysates consistently had increased PTPase activity when compared to the same fractions from the J774A.1/*lspA1 lspA2* mutant fractions. When these two fractions were probed by Western blot analysis for the presence of various known PTPases such as SHP-1, CD45, PTP $\alpha$ , and SIRP $\alpha$ , only SHP-1 was found to be present in these two fractions (Fig. 40C).



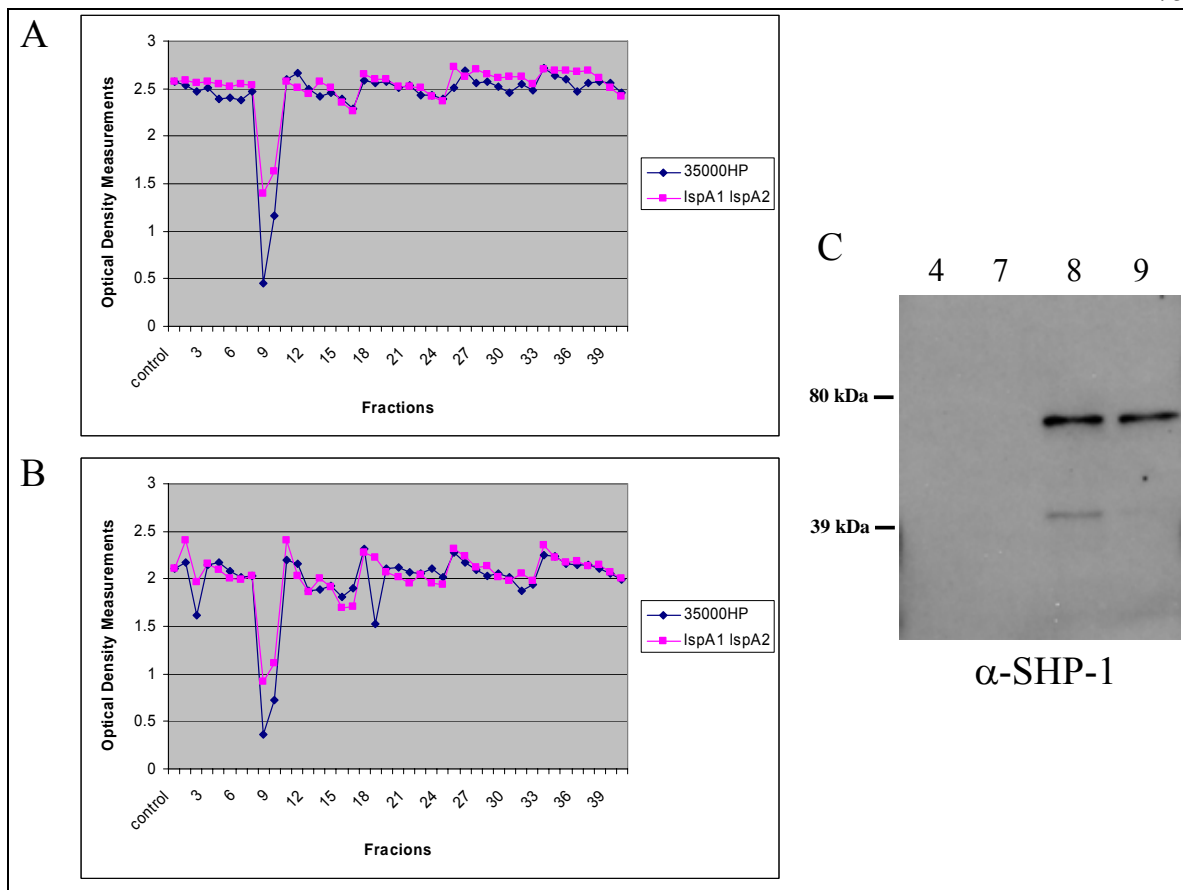


**Figure 40.** ELISA-based protein tyrosine phosphatase assays. ELISA-based protein tyrosine phosphatase assays (PTPase assays) using fractionated J774A.1 lysates with either phospho- $\zeta$  (A) or phospho-Src (B) as the substrate. (C) Western blot experiment probing fractions 4, 7, 8, 9 with antibody to SHP-1.

SHP-1 is present in hematopoietic cells and functions as a modulator of cell signaling events (190). This phosphatase has been demonstrated to preferentially dephosphorylate the inhibitory (Y529) phosphotyrosine site of Src when compared to the active phosphotyrosine residue (Y418) (188).

### III. Discussion

Src protein tyrosine kinases (PTKs) are involved in some of the most proximal events of the phagocytic signaling pathway. The reduced enzymatic activity of the Src PTKs in macrophages incubated with wild-type *H. ducreyi* is consistent with the inability these macrophages to complete the development of phagocytic cups (Chapter Six, Fig. 29). I have hypothesized that either (1) the LspA proteins bind to a receptor on the macrophage surface and initiate a signaling event that abolishes phagocytic activity or (2) the LspA proteins enter or penetrate into the phagocyte and therein cause derangement of the normal phagocytic signaling pathways. It is also a possibility that these hypotheses are not mutually exclusive because, after binding to a surface receptor, the LspA proteins could be endocytosed or otherwise engulfed.

Two lines of evidence support the former hypothesis in which the LspA proteins interact with an immune cell specific receptor, leading to a negative signal for phagocytosis. The level of active phospho-Src PTKs in all four phagocytic cell types (J774A.1, RAW264.7, HL-60 and DC2.4) tested in this study were reduced by exposure to wild-type *H. ducreyi*, whereas phospho-Src PTK levels in HeLa cells appeared to be unaffected (Chapter Six, Fig. 30). Further characterization of other immune cell types demonstrated that the effect of the LspA proteins was only found in the T cell-like Jurkat cells and not in the B cell-like Daudi cells or mast cell-like RBL-1 cells. These findings raise the possibility that a surface component present in some immune cell lineages may

interact with the LspA proteins, resulting in a negative signaling event. This possibility is reinforced by the finding that proteinase K treatment of J774A.1 macrophages eliminated the ability of wild-type *H. ducreyi* to reduce levels of active phospho-Src PTKs (Fig. 35). At this time, we cannot exclude the possibility that LspA proteins enter the macrophage via an endocytic process and exert their function in the cytoplasm, but it is unclear how these proteins would survive endosomal proteolysis and exit into the cytoplasm. An equivalently large bacterial exoprotein (i.e., RtxA) synthesized by *Vibrio cholerae* has been shown to directly cross-link actin but the method of entry or penetration of this large protein into the host cell cytoplasm remains to be determined (78,186).

The presence of the YopT-like region in the LspA proteins led us to examine whether small Rho GTPases in macrophages could be affected by wild-type *H. ducreyi*. However, if the LspA proteins acted similarly to YopT from *Yersinia* species, then this would support the other hypothesis in which the LspA proteins somehow enter or penetrate into the macrophage. The observed changes in total membrane-bound Cdc42 (Fig. 36) and decreased active Rac levels (Fig. 37) are most likely downstream effects related to the decreased level of active phospho-Src. I also considered that the YopT-like region may cleave Src family members in a manner similar to how YopT cleaves the small Rho GTPases Rho, Rac and Cdc42. However, experiments intended to test this hypothesis showed no change in the level of membrane-bound Hck regardless of whether the macrophages were incubated with wild-type *H. ducreyi* or the *lspA1 lspA2* mutant (Fig. 38). Taken together with the small Rho GTPase data, these findings indicate the LspA proteins

likely use a mechanism to inhibit phagocytosis that is different from that used by YopT from *Yersinia* species.

How the LspA proteins reduce the catalytic activity of the Src PTKs remains to be determined, but based on some of the data described above, it is possible that a specific immune cell inhibitory receptor is involved. Furthermore, the finding that only the active phosphotyrosine (pY418) level is decreased in macrophages, and not the levels of inactive phosphotyrosine (pY529) (Chapter Six), suggests that a specific phosphatase activity is upregulated in macrophages exposed to the LspA proteins via a membrane receptor. Protein-tyrosine phosphatases (PTPases) function in regulating phosphorylation levels in mammalian cells, and their activity in balancing these levels plays an important role in cell signaling. I have attempted to determine if there is an increase in some type of PTPase activity in macrophages exposed to the wild-type *H. ducreyi* strain when compared to macrophages exposed to the *lspA1 lspA2* mutant. Macrophage cellular fractions were prepared and utilized in assays measuring PTPase activity. In two fractions from macrophages incubated with the wild-type *H. ducreyi* strain, there appeared to be a two-fold increase in PTPase activity when compared to the equivalent fractions from macrophages that had been incubated with the *lspA1 lspA2* mutant (Fig. 40A and 40B). When these fractions were probed with antibodies to known PTPases (i.e., CD45, PTP $\alpha$ , SIRP $\alpha$ , and SHP-1), only SHP-1 appeared to be present in these two fractions (Fig. 40C). While it has been reported that SHP-1 functions mostly in the dephosphorylation of the inactive phosphotyrosine (pY529) residue (188), it is possible that SHP-1 activity toward

the active pY418 residue is increased by the immune cell's interaction with the LspA proteins. Further experiments measuring SHP-1 activity in *in vitro* PTPase assays are planned and should hopefully answer these questions. It is also possible that another PTPase is responsible for this increase in activity and further biochemical characterization will be necessary to address this. Preliminary experiments have been performed in an effort to determine the effects of both chemical phosphatase inhibitors, such as sodium orthovanadate, and chemical cysteine protease inhibitors, such as E64 or N-ethylmaleimide (NEM), on J774A.1 macrophages co-incubated with wild-type *H. ducreyi* to determine whether chemically inhibiting phosphatase or protease activity would have an effect on the LspA proteins' ability to decrease active Src PTK levels. These experiments have been inconclusive to date. Further work needs to be performed to confirm whether these inhibitors can affect the interaction between the LspA proteins and immune cell lines.

If the LspA proteins do interact with a specific receptor then, there are many experimental options available to determine the exact receptor; however, the majority of these approaches will require purified LspA protein. Attempting to purify recombinant LspA1 has been a major focus of my work during the last several years, and is described in detail in Chapter Eight. Having purified protein will permit a precise determination of whether the LspA proteins are directly responsible for phagocytic inhibition by *H. ducreyi*, and will also allow more precise experiments to be performed. The availability of purified LspA1 will also allow biochemical characterization, including experiments to determine

possible membrane receptor involvement by measuring membrane saturability and specific binding.

Work is ongoing to elucidate the precise mechanism of action of these secreted *H. ducreyi* virulence factors. These efforts will hopefully increase our knowledge about a major virulence mechanism of *H. ducreyi*, provide additional insight into the pathogenesis of chancroid, and should also contribute to our understanding of phagocytosis and the signaling pathways involved in this crucial host defense mechanism.

## CHAPTER EIGHT

### Protease Activity of the LspA Proteins of *Haemophilus ducreyi*

#### I. Introduction

Currently, there are no data to suggest that the LspA1 and LspA2 proteins, which are 86% identical, have different functions. The predicted size of the intact LspA2 protein is larger than that of LspA1, and this is mainly due to the presence of a 319-aa repeat that occurs three times in LspA2 but only once in LspA1 (Fig. 41). In fact, this laboratory has already established that expression of either LspA1 or LspA2 is sufficient to inhibit phagocytosis (215). As mentioned in the previous chapter, having purified LspA1 would greatly facilitate my efforts to determine the mechanism of action of these *H. ducreyi* virulence factors. For this reason, I initiated efforts to obtain and purify either native or recombinant LspA1 protein.

The LspA1 and LspA2 proteins of *H. ducreyi* are encoded by two of the largest prokaryotic ORFs (12.5 kb and 14.8 kb, respectively) described to date (Chapter Four, Fig. 7). The predicted LspA1 and LspA2 proteins have calculated masses of approximately 456,000 Da and 542,000 Da, respectively. Smaller forms of these two proteins, which likely represent processed products, can be detected in both *H. ducreyi* whole cell lysates and *H. ducreyi* concentrated culture supernatant (CCS) and are described later in this chapter. Only two regions of the LspA proteins have significant homology to known

bacterial virulence factors. The N-terminal half (Fig. 41) contains several features associated with secretion of other soluble virulence factors including the *Bordetella pertussis* filamentous hemagglutinin (107-109). There is also a 230-aa region in the C-terminal half of the LspA proteins that has 36% identity with the YopT protein from pathogenic *Yersinia* species (184) (Fig. 41). YopT is the prototype of a family of cysteine proteases involved in virulence and has been shown to cleave small Rho GTPases from the eukaryotic cell membrane (184,185), thereby altering signaling and inhibiting phagocytosis. However, as described in the previous chapter, the LspA proteins do not function in a similar manner to the *Yersinia* species YopT proteins.

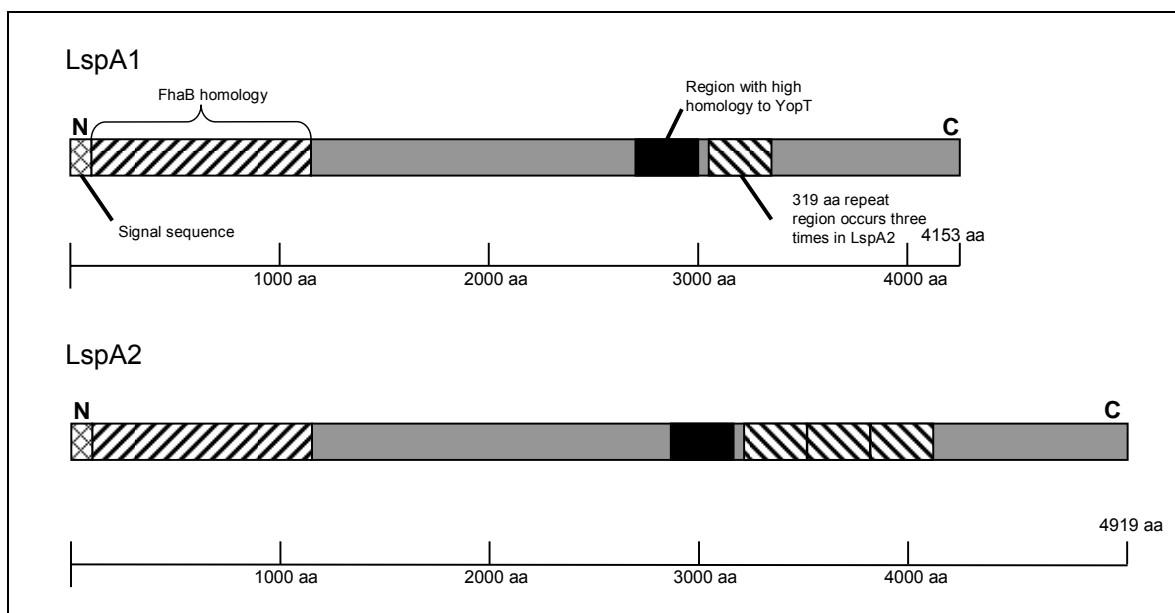


**Figure 41.** Protein schematic for LspA1 and LspA2 showing regions of homology or interest.

As experiments attempting to purify a recombinant version of the YopT-like region of LspA1 were being performed, I found that this region was involved in auto-processing of



the LspA proteins, in a manner similar to that catalyzed by at least one other member of this cysteine protease family (184,227).

## **II. Results**

### **A. Multiple Forms of LspA1 Can Be Detected in *H. ducreyi* Concentrated Culture Supernatant Fluid (CCS)**

Soluble LspA1 and LspA2 proteins can be detected in CCS from the wild-type strain 35000HP and the *lspA1* mutant, respectively, by using specific monoclonal antibodies (MAbs) in Western blot analysis. Both the LspA1-specific MAb 40A4 and the LspA2-specific MAb 1H9 bind epitopes located in the N-terminal half of these two proteins; this means that these MAbs will not allow detection of other, perhaps more truncated LspA proteins that lack this region. These MAbs bind two forms of both LspA1 and LspA2 – one with an apparent molecular weight of approximately 270 kDa and the other with an apparent molecular weight of about 160 kDa (Chapter Four, Fig. 6) (218). Clearly, these two forms must represent processing products derived from the precursor proteins which have calculated molecular weights of 456 kDa (LspA1) and 542 kDa (LspA2).

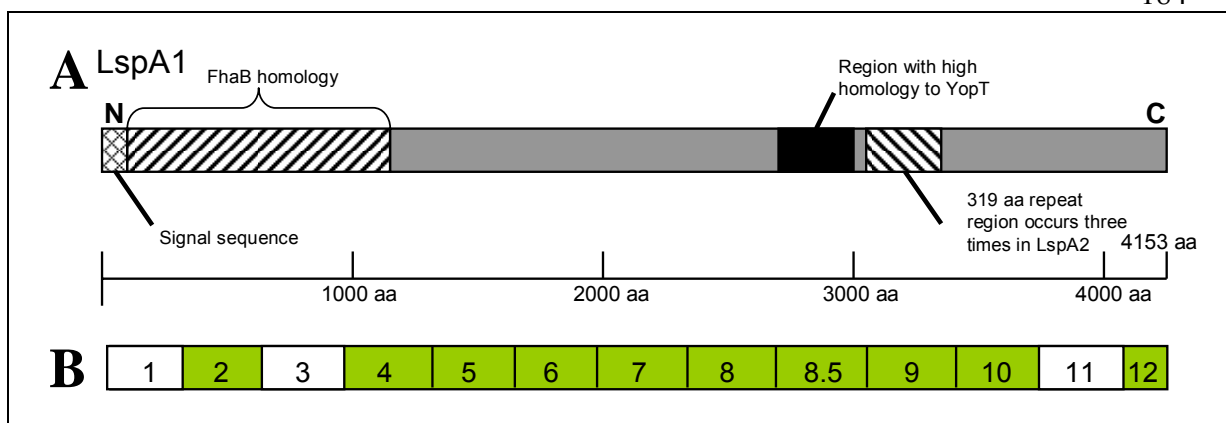


**Figure 42.** LspA1 protein schematic. (A) LspA1 protein schematic showing regions of homology or interest. (B) His-tagged LspA1 fusion proteins used to raise polyclonal mouse antibodies to different regions of LspA1. The numbered segments denote the ~1 kb fragments from *lspA1* used to make His-LspA1 fusion proteins. Polyclonal mouse antisera were successfully raised against His-LspA1 proteins represented by the 10 green segments; antisera were not raised to the 3 white segments.

To obtain antibodies to the other regions in the LspA1 protein, our laboratory divided the *lspA1* gene into 13 separate (approx. 1 kb) regions and constructed fusions that expressed 6xHis-tagged fusion proteins (Fig. 42) which were used to immunize mice. The antisera raised against the His-LspA1 fusion proteins were then utilized in Western blot analysis of CCS to determine the sizes of the LspA protein fragments (Fig. 43A). The majority of the fusion proteins (Fig. 42B, green boxes) were able to induce the synthesis of antibodies that would detect LspA proteins in Western blot analysis, with the exceptions of numbers 1, 3, and 11 shown in Figure 42B in white. A select set of Western blot data are provided in Figure 43B that demonstrate the four main fragments detected by these antisera. A schematic compiled from all of the Western blot data is provided in Figure 43C for clarity. In the N-terminal region encompassing the His-LspA1 fusion proteins 1 – 5, there were two major fragments, 270 kDa and 160 kDa, detected by Western analysis (Fig. 43B

and 43C). In the middle region of the protein, covering fusion proteins 6 – 8.5, there was only one predominant fragment around 270 kDa in size (Fig. 43B and 43C). In the C-terminal region encompassing fusion proteins 9 – 12, the fragments detected were greater than 270 kDa and less than 500 kDa in size (Fig 43B and 43C). From these experiments, it appears that there are several different processed forms of the LspA proteins, and two of the areas where these cleavage events appear to occur are contained in regions 5-6 and regions 8.5-9 (Fig 43B and 43C).

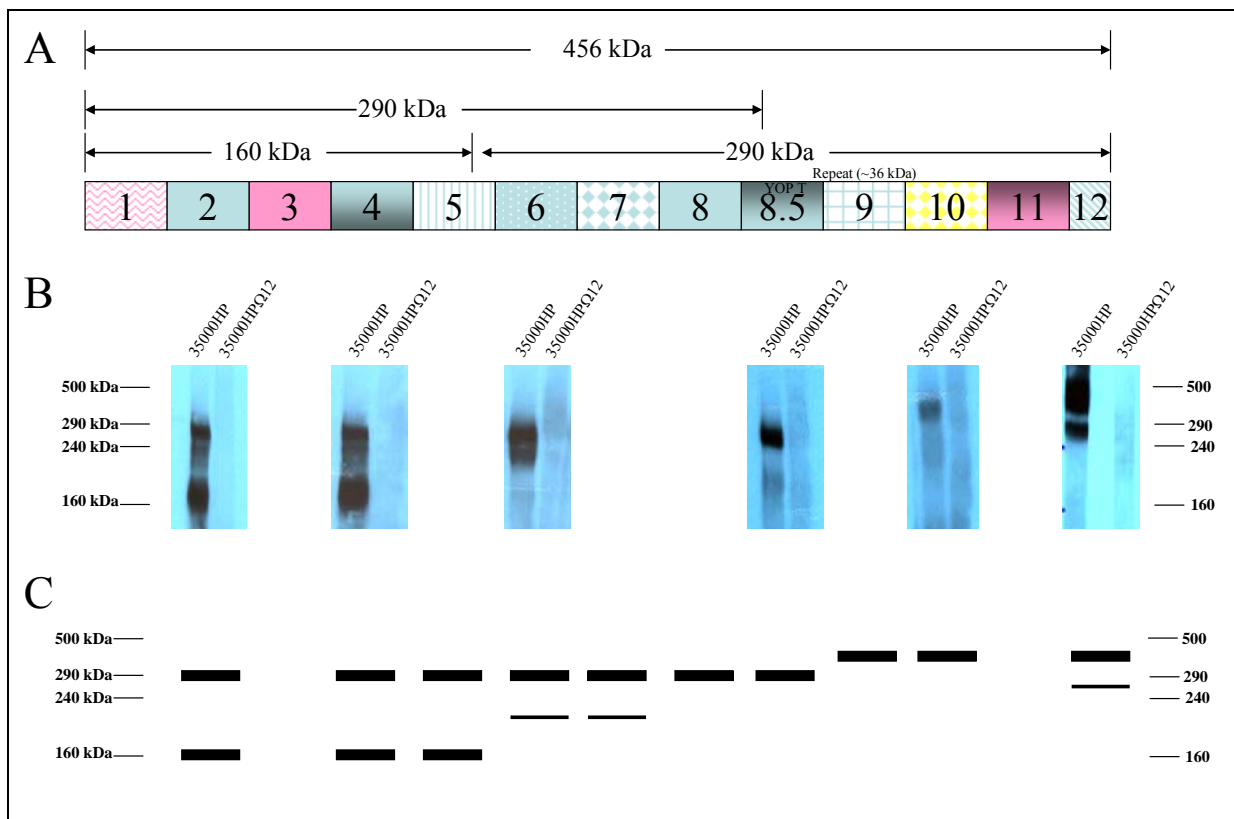


**Figure 43.** Strain 35000HP CCS probed with polyclonal antisera. (A) Schematic showing the 13 His-LspA1 fusion proteins used to immunize mice for polyclonal antisera. (B) Western blot data showing *H. ducreyi* 35000HP CCS probed with polyclonal antisera raised against the respective His-LspA1 fusions. (C) Schematic representing the Western blot data for all 10 antisera that recognized the LspA proteins.

These antisera were also used in the immunodepletions experiments performed in Chapter Six. In these immunodepletion experiments (Chapter Six, Fig. 28), I proved that the soluble LspA1 protein is necessary for the inhibition of phagocytosis. The antiserum used to immunodeplete the CCS of LspA1 was that raised against region 8. These data suggest that the active form of LspA1 contains the area around this region, and is possibly the 270 kDa fragment detected in Western blot analysis (Fig. 43B).

### **B. Development of a Monoclonal Antibody Reactive with the Native LspA1 Protein**

The previously available MAbs for LspA1 and LspA2 (i.e., 11B7, 40A4, and 1H9) bind only the denatured form of these proteins in Western blot analysis. By testing the polyclonal antisera raised against the different His-LspA1 fusion proteins, I found that the number 8 fusion protein (Fig. 43) was able to raise antibodies that would bind native LspA1 protein. It was also this same antiserum that was used in immunodepletion experiments. Additional mice were immunized with this fusion protein to induce the synthesis of antibodies that would be used for lymphocyte hybridoma production. Of the twelve hybridoma lines tested for their production of a monoclonal antibody that could bind native LspA1 protein in CCS from the 35000HP $\Omega$ 2 strain, only one, 3H9, was found to react with the native LspA1 protein (Fig. 44).

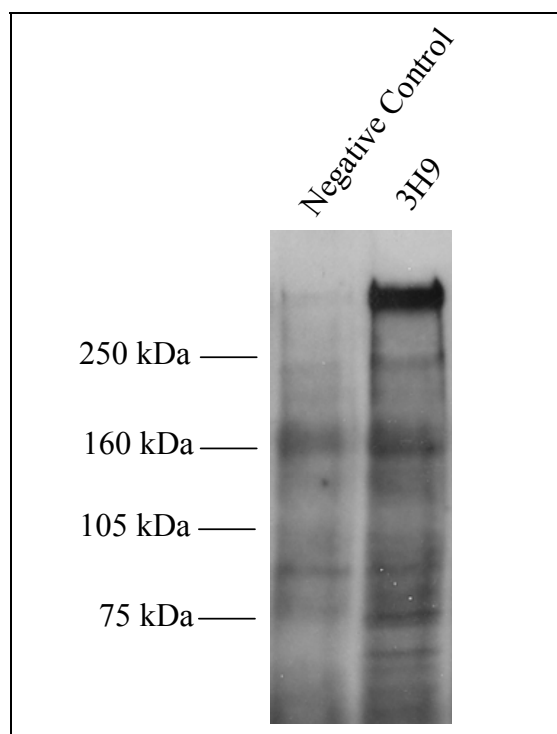


**Figure 44.** MAb 3H9 binds native LspA1 protein. Western blot analysis was performed using immune precipitates derived from wild-type 35000HP CCS that had been incubated with either MAb 3H9 or buffer (negative control). The resultant antigen-antibody complexes were bound to Protein A/G Agarose, washed, eluted into 3X digestion buffer, and resolved by SDS-PAGE. The LspA protein-reactive MAb 11B7 was used to probe these samples in Western blot analysis. A control with an irrelevant MAb yielded a result similar to that obtained with the buffer negative control.

This type of MAb able to recognize native LspA protein will not only help further our laboratory's efforts to purify LspA1 protein, but will also allow additional studies to be performed, such as determining protein-protein interactions with possible surface components if a macrophage receptor for LspA1 is found.

### C. Extractions from whole cells

One initial method by which I attempted to purify LspA1 involved extracting the protein from *H. ducreyi* itself. The 35000HPΩ2 *lspA2* mutant, which expresses only LspA1, was grown overnight on 40 chocolate agar plates. The bacterial growth was harvested into a mixture of supplemented Columbia broth with 2.5% (v/v) of a dialysate containing fetal bovine serum components with a molecular weight of less than 10 kDa. This mixture also contained a protease inhibitor cocktail (Roche). The suspended cells were incubated in this mixture for 10 min at 37°C. The bacterial cells were then removed by low speed centrifugation, the resultant supernatant fluid was filter-sterilized, and membrane blebs were removed by ultracentrifugation. Probing of this preparation with the LspA-reactive MAB 11B7 in Western blot analysis showed one predominant protein with an apparent molecular mass of approximately 270 kDa (Fig. 45, lane 5). In contrast, a whole cell lysate (Fig. 45, lane 1) and CCS (Fig. 45, lane 3) from this same strain contained many more antibody-reactive bands.

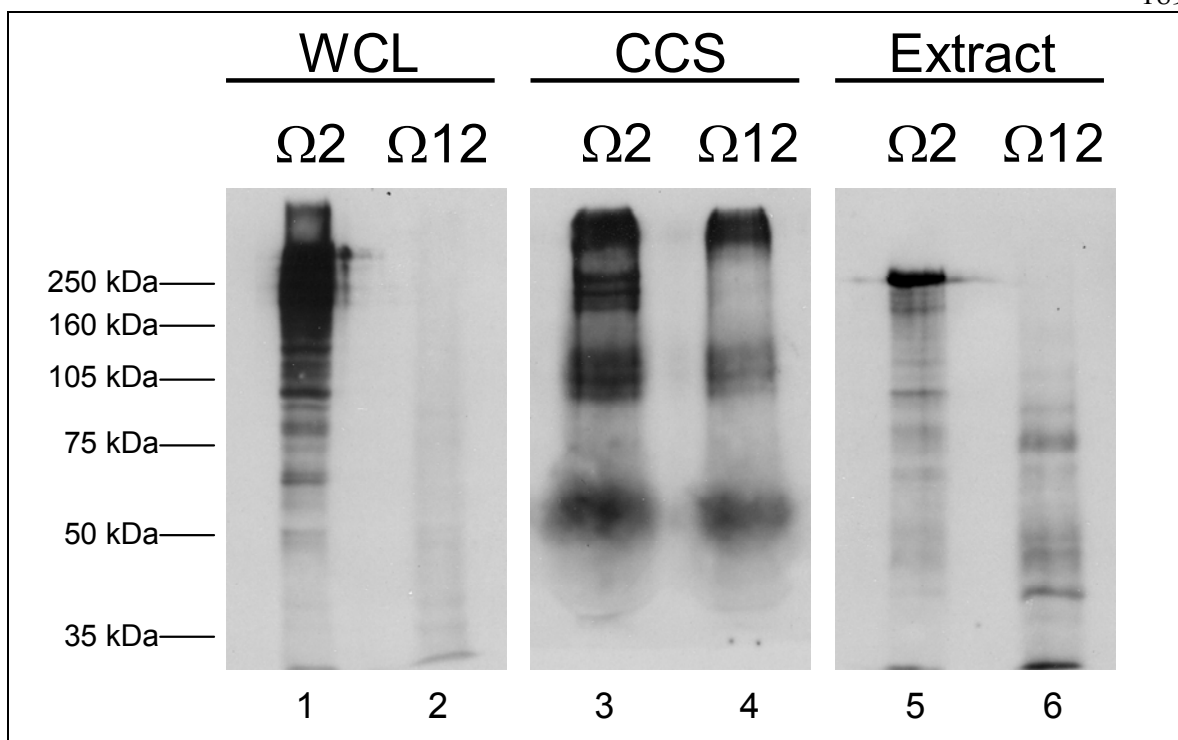


**Figure 45.** Western blot analysis of LspA1 proteins from different sources. The 35000HPΩ2 *lspA2* mutant and the 35000HPΩ12 *lspA1 lspA2* mutant (negative control) were grown in broth and whole cell lysates (WCL) and CCS were prepared from these cultures. These same two strains were grown on 40 chocolate agar plates each and the proteins extracted from these cells (Extract) into SCB-FCS. The LspA1-reactive MAb 11B7 was used as the primary antibody to detect LspA1.

I scaled-up this chocolate agar growth-based extraction method to 500 plates with the *lspA2* mutant 35000HPΩ2 in an attempt to determine the N-terminal amino acid (aa) sequence for LspA1. Preliminary N-terminal aa sequence analysis of LspA1 protein prepared in this manner yielded several short sequences [G(P/A)AGP and (G/S)IPL] that did not perfectly match the predicted aa sequence in the N-terminal half of LspA1. These results raised the possibility that the N-terminus of the mature LspA1 protein could be blocked (similar to the blocked N-terminus of the *Bordetella pertussis* FhaB protein, another very large protein secreted by a two-partner secretion system) (106).

#### **D. The LspA Proteins Contain a Region with Homology to YopT**

The YopT proteins of pathogenic *Yersinia* species are cysteine proteases that cleave small GTPases from the eukaryotic cell membrane. This enzyme has a well-defined set of conserved residues (C/H/D) which have been shown to be essential for its activity (184,185) and these same conserved residues are present in a 230-aa region in LspA1 and LspA2 that has 36% identity with YopT. The YopT-like region of the LspA proteins, while appearing not to function in a manner similar to its *Yersinia* counterparts, provided a starting point for constructing LspA recombinant proteins. The LspA1 region with homology to *Yersinia* YopT is approximately 230 aa in size and corresponds to the last two-thirds of the *Yersinia* YopT protein (YopT aa 102 – 317). The amino acids of LspA1 and LspA2 that comprise this homology region are aa 2800 – 3019 and aa 2929 – 3148, respectively (Fig. 46). The cysteine protease catalytic triad consists of a cysteine, a histidine, and an aspartic acid residue, and these are highlighted in Figure 6 in green, red and blue, respectively, for all three proteins (184). These three residues in LspA1 are C2837, H2961, and D2976. While efforts to clone a full-length *lspA1* gene into *E. coli* have not been successful to date, I have designed several different recombinant DNA-based approaches based on the YopT-like region as a starting point.



	10	20	30	40	
VRS - - - - -	S	V E E Y G G E V T F K Y A Q S K G E V Y N E I V K H A E T	LspA1		
VRS KI ND VRS	S	V E E Y G G E V T F K Y A Q S K G E V Y N E I V K H A E T	LspA2		
- - - - -	VRE	S V A N Y G G N I N E K F A Q T K G A F L H K L I K H S D T	YopT <i>Y. pestis</i>		
	50	60	70	80	
QNGV	C E A T C S H W I A K K V N D E N I W T D L Y K D G Q K G R K G G L N K	LspA1			
QNGV	C E A T C S H W I A K K V N D E N I W T D L Y K D G Q K G R K G G L N K	LspA2			
ASGV	C E A L C A H W I R S H A Q G Q S L F D Q L Y V G G - - - R K G K F Q I	YopT <i>Y. pestis</i>			
	90	100	110	120	
DAI E S I E K L Q T E F I N A G T A T Q Q F K L T N T W L E E Q G V V P K Q K		LspA1			
DAI E S I E K L Q T E F I N A G T A T Q Q F K L T N T W L E E Q G V V P K Q K		LspA2			
DTLY	S I K Q L Q I D G C K A D V D Q D E V T L - - D W F K K N G I S E R M I	YopT <i>Y. pestis</i>			
	130	140	150	160	
Y F G K L S R A D E V A G T V S K N D V S A L V K A I L D T G N E S S A V K K I		LspA1			
Y F G K L S R A D E V A G T V S K N D V S A L V K A I L D T G N E S S A V K K I		LspA2			
ERHC	L L R P V D V T G T T E S E G L D Q L L N A I L D T H G I G Y G Y K K I	YopT <i>Y. pestis</i>			
	170	180	190	200	
S I N L E G G S H T V S A S I E G Q K - V V F F D P N F G E I T F K D K K S F E		LspA1			
S I N L E G G S H T V S A S I E G Q K - V V F F D P N F G E I T F K D K K S F E		LspA2			
HLSGQMS	A H A I A A Y V N E K S G V T F F D P N F G E F H F S D K E K F R	YopT <i>Y. pestis</i>			
	210	220	230		
K W M K N A F W K K S G Y A G K K D T K R F F N V V N Y		LspA1			
K W M K N A F W K K S G Y A G K K D T K R F F N V V N Y		LspA2			
K W F T N S F W D N S M Y H Y P L G V G Q R F R V L T F D S K E V		YopT <i>Y. pestis</i>			

**Figure 46.** Sequence alignment of the *H. ducreyi* LspA proteins and the *Yersinia pestis* YopT protein. The cysteine protease catalytic triad consists of a cysteine, histidine, and aspartic acid and these are highlighted in Figure 6 in green, red and blue, respectively. A second cysteine residue is marked with a purple arrow and a serine residue is marked with a black arrow.

### **E. Evidence that the YopT-like Region is Involved in Autocatalytic Cleavage of the C-terminal Half of LspA1**

The first recombinant fusion that I successfully constructed consisted of a 3.5 kb fragment of the *lspA1* ORF containing the YopT-like region that was cloned into the maltose binding protein (MBP) fusion vector pMAL-c2x. This plasmid was designated pMAL1 (Fig. 47A). Interestingly, the predicted size of this MBP-LspA1 fusion protein (containing LspA1 aa 2307 – 3420) was 166 kDa, but when this protein was expressed in *E. coli*, it had an apparent size of about 135 kDa in SDS-PAGE (Coomassie blue stain) (Fig. 47B), suggesting that a small portion of this fusion protein had been processed or removed. Western blot analysis of a whole cell lysates from this recombinant *E. coli* strain revealed that antisera to His-tagged LspA1 fragments 8, 8.5, and 9 (Fig. 47A) bound proteins with apparent molecular weights of about 135 kDa and 166 kDa (Fig. 47C). In contrast, antibodies to His-tagged LspA1 fragment 9 bound to both of these same proteins and to several smaller proteins, including one with an apparent molecular weight of about 34 kDa (Fig. 47C). Antibodies to His-tagged LspA1 fragment 10 bound the 166 kDa protein and some smaller proteins including the 34 kDa protein (Fig. 47C). It should be noted that the MBP-LspA1 fusion protein contained only a small region of the aa sequence from His-tagged LspA1 fragment 10. If this region (and a portion of fragment 9) was removed by cleavage, then the antibodies to His-tagged LspA1 fragment 10 would not bind to the resultant 135 kDa fragment; it can be seen that these antibodies do not bind the 135 kDa

fragment (Fig. 47C, lane 10). The reactivity of the 166 kDa fragment seen in all four lanes in Figure 47C presumably represents binding of these antibodies to the intact MBP-LspA1 fusion protein.

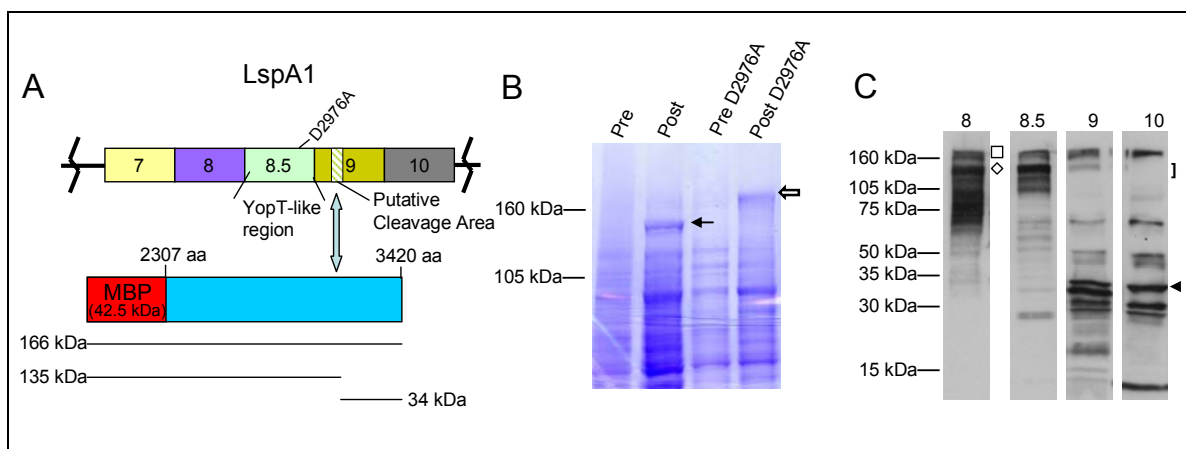


**Figure 47.** A MBP-LspA1 fusion protein undergoes autocatalytic cleavage. (A) Schematic of the LspA1 protein regions contained in the MBP-LspA1 fusion protein; numbering corresponds to the *lspA1* DNA fragments in Fig 2. The YopT-like region is indicated as is the putative cleavage region. (B) Coomassie blue-stained SDS-PAGE gel showing the 135 kDa MBP-LspA1 fusion protein (black arrow) expressed by pMAL1 after IPTG induction. The 166 kDa MBP-LspA1 fusion protein expressed by the D2976A mutant pMAL1-D is indicated by the white arrow. (C) Western blot analysis of the whole cell lysates from *E. coli* (pMAL1) probed with antisera raised against His-LspA1 fusion proteins 8, 8.5, 9, and 10. The bracket indicates the region containing the 135 kDa protein (present in lanes 8, 8.5, and 9 but missing in lane 10). The open box between lanes 8 and 8.5 marks the position of the 166 kDa protein and the diamond marks the position of the 135 kDa protein.

The removal of the 34 kDa fragment from this 166 kDa fusion protein was likely the result of the YopT-like region expressing its potential cysteine protease activity. In this regard, autocatalytic processing of another YopT-like protein has been described (184). Analysis of these Western blot data would suggest that the cleavage point is located within the aa sequence (aa 3095-3394) encoded by *lspA1* fragment 9 (Fig. 47A).

I addressed this possibility further by performing site-directed mutagenesis on pMAL1 to change the invariant (conserved) D residue found in YopT family cysteine proteases (184). When the aspartate (D) residue at position 2976 (i.e., using LspA1 aa sequence numbering) was converted to an alanine (A), the resultant MBP-LspA1 fusion protein expressed by pMAL1-D no longer underwent cleavage into the 135 kDa and 34 kDa from but instead migrated with an apparent molecular weight of 166 kDa (Fig. 47B). These results suggest that one function of the YopT-like region in LspA1 is to process the LspA1 protein.

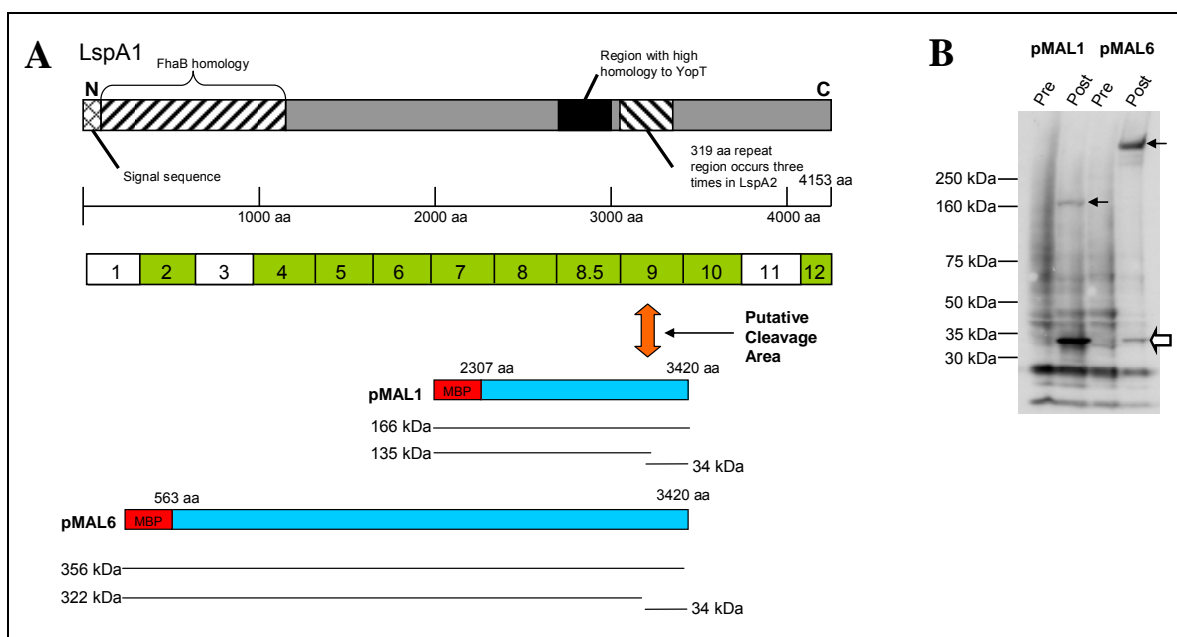


**Figure 48.** Schematic of MBP-LspA1 fusion proteins. (A) Schematic of the *lspA1* DNA regions used to make the MBP-LspA1 fusion construct contained in pMAL6. The YopT-like region is indicated as is the putative cleavage region. (B) Western blot analysis of the whole cell lysates from *E. coli* (pMAL1) and *E. coli* (pMAL6) probed with antiserum raised against His-LspA1 No. 10. The black arrows indicate the full-length, uncleaved fusion proteins, while the white arrow indicates the 35 kDa cleavage product.

The apparent molecular weight of the native LspA1 protein in Figure 45, lane 5 is approximately 270 kDa. Using the data on autocatalytic cleavage of the MBP-LspA1 fusion protein described above (Fig. 47), a mature 270 kDa LspA1 protein with a C-terminus located somewhere within the aa sequence (aa 3095-3394) encoded by *lspA1* fragment 9 (Fig. 47A) would have to have an N-terminus located somewhere between aa 600-1000. It can also be inferred from these data that the N-terminus of LspA1 must undergo post-translational processing beyond the simple removal of a leader peptide. These data have been used in the design of LspA1 fusion proteins which will be assayed for their ability to inhibit phagocytic activity. I continued to increase the size of this *lspA1* recombinant gene in the 5' direction, adding additional *lspA1* DNA in 1 kb increments, with the goal of obtaining a functional MBP-LspA1 fusion protein that inhibits phagocytic activity. These individual MBP-LspA1 fusion proteins of increasing size have been purified and tested individually for their ability to inhibit the phagocytic activity of J774A.1 macrophages. The largest, sequence-confirmed MBP-LspA1 fusion protein that I have constructed to date is shown in Figure 48 and designated pMAL6. The full length fusion protein is approximately 356 kDa in size, while the estimated cleavage product is 322 kDa (Fig. 48A). Western blot analysis utilizing antiserum to region 10 confirmed the expression and cleavage of pMAL6 (Fig 48B). Unfortunately, preliminary experiments in which *E. coli* (pMAL6) lysates containing this fusion protein were incubated with J774A.1 macrophages have not shown inhibition of Src family PTKs detectable by Western blot

analysis. Furthermore, I have had difficulty purifying these fusions by amylose affinity chromatography.

## **F. Identification of the Catalytic Residues in the YopT-like Region**

Having demonstrated that the YopT-like region is involved in post-translational processing of LspA1, I wanted to determine if the active site residues were identical to those from the *Yersinia* YopT protein. I constructed a smaller GST-LspA1 fusion protein that contained the YopT-like region from LspA1 together with the immediate C-terminal region where the putative cleavage was predicted to occur (Fig. 49A and 49B). This was done because I had difficulty purifying the MBP-LspA1 fusion constructs with affinity chromatography and, furthermore, I wanted to determine if the YopT-like region alone was sufficient for proteolytic activity. The GST-LspA1 fusion contained LspA1 aa 2800 – 3195 which represented 44 kDa of LspA1 (Fig. 49B). The YopT-like region was contained within this area and included aa 2800 – 3019, comprising 24.6 kDa (Fig. 49B). The remaining 19 kDa is the immediate C-terminal region which contains the predicted cleavage region. Upon expression of this GST-LspA1 fusion, the predicted full length size is 72 kDa; however, if the fusion undergoes autoprocessing in the predicted cleavage region, then I expected to detect a processed product of around 60 kDa. Western blot analysis of whole cell lysates from *E. coli* containing this fusion construct demonstrated (Fig. 49C) that the GST-LspA1 fusion protein did indeed undergo processing similar to that seen with the pMAL fusions seen in Figures 47 and 48. Site-directed mutagenesis was

performed on the residues shown in Figure 49B. The three invariant residues (C, H, and D) required for cysteine protease activity (184) in *Yersinia* YopT were first changed to alanines. Interestingly, changing the H and D residues appeared to affect the autoprocessing of the fusion protein (Fig. 49C), while changing the C residue to an A appeared to have no effect on cleavage. This was an interesting finding and led to my changing the only other C residue (C2841) in the fusion protein to determine its possible involvement in autoprocessing (Fig. 46, purple arrow and Fig. 49C). As demonstrated in Figure 49C, changing this second C residue or changing both C residues to an A (Fig. 49C) had no effect on cleavage. Therefore, it is unlikely that the LspA1 YopT-like region is a cysteine protease. When comparing the LspA proteins' YopT-like region to the other putative 19 proteins in this family of cysteine proteases (184) the LspA proteins were the only members to have a serine residue in close proximity to the cysteine residues (184). These results led to further experiments to change S2842 (Fig. 46, black arrow) to an alanine to determine its possible involvement in protease activity (Fig. 49C). Based on the S2842A mutation, it appears that the serine is necessary for auto-processing to occur. Other fusion proteins containing the LspA1 YopT-like region are being constructed to determine the exact cleavage site and the same residues described above will be mutated again in a different fusion protein to confirm their potential involvement in proteolytic activity. Further experimentation with cysteine and serine protease inhibitors may help to further elucidate the exact mechanism of proteolysis. Therefore, it is very likely that this YopT-like region is involved in processing but this ongoing work will be necessary to determine the exact aa residues necessary for this activity as well as those in the cleavage region.

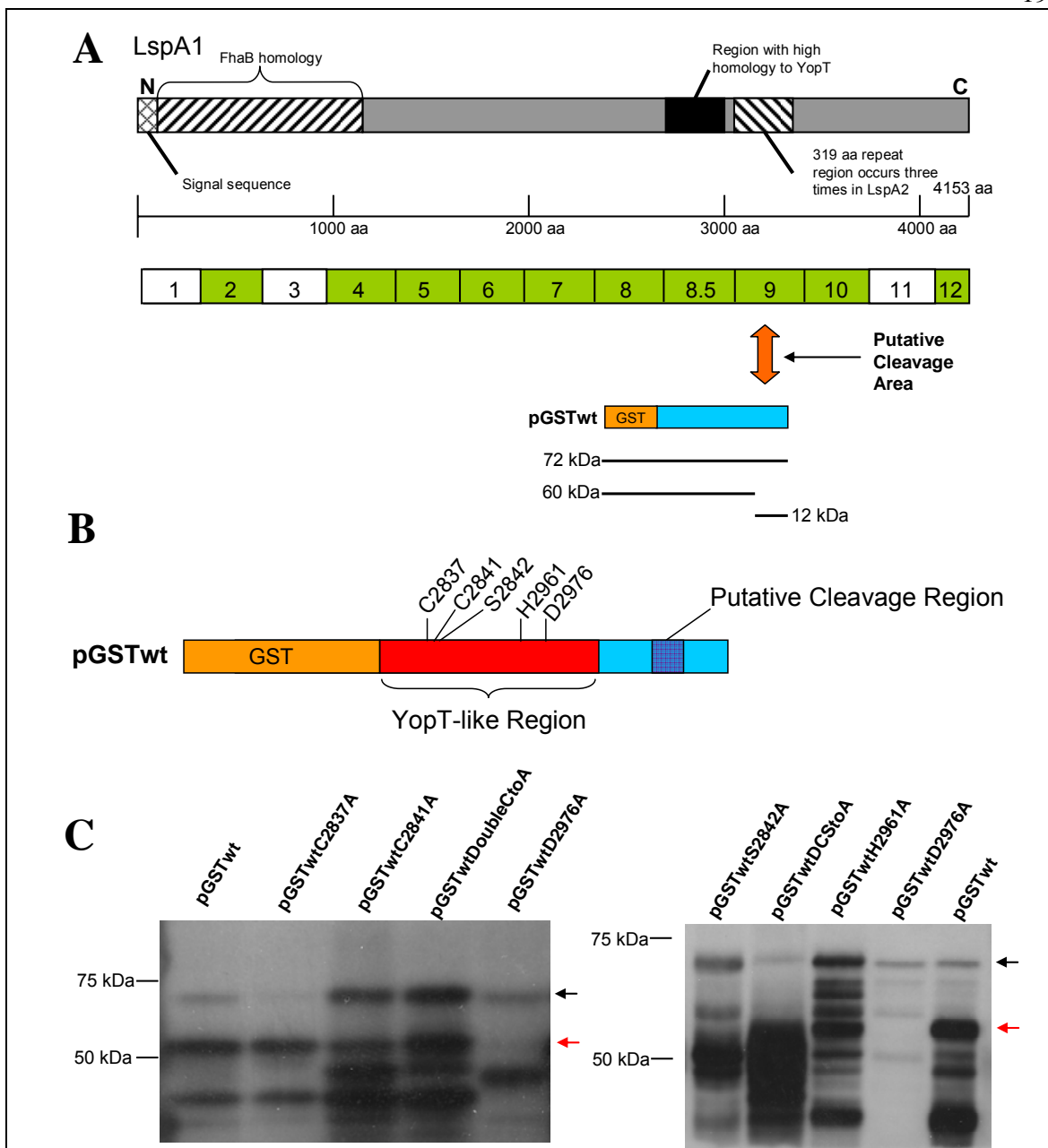


**Figure 49.** Site-directed mutant data for GST-LspA1 fusion proteins. (A) Schematic of the *lspA1* DNA regions used to make the GST-LspA1 fusion construct contained in pGSTwt. The YopT-like region is indicated as is the putative cleavage region. (B) The fusion protein expressed by the pGSTwt construct, the YopT-like region, and the putative cleavage region are indicated. (C) Western blot analysis of the whole cell lysates from *E. coli* (pGSTwt) and GST-LspA1 site-directed mutants probed with anti-GST antibody. The black arrows represent the uncleaved fusion proteins while the red arrow represents the 60 kDa cleavage product.



### III. Discussion

Efforts to clone full-length *H. ducreyi* *lspA* genes into *E. coli* or purify LspA proteins from spent *H. ducreyi* culture medium have been unsuccessful to date. However, the efforts described herein have brought our laboratory closer to obtaining purified LspA1 protein. My finding that the YopT-like region likely functions in autocatalytic cleavage of LspA1 suggests that the soluble LspA1 protein is the ultimate functional end-product of this gene system. However, this finding does raise the question of which is the most active form of LspA1. Is it the soluble supernatant form or is some cell-bound form of LspA1 more active? My published experiments using PMN-like HL-60 cells showed that wild-type *H. ducreyi* CCS could inhibit the phagocytic activity of these cells (141). This finding indicated that active (i.e., inhibitory) LspA1 was present in soluble form in CCS. I further confirmed that this soluble LspA1 protein was responsible for the observed inhibition of phagocytosis by performing the immunodepletion experiments (141).

It is also unclear whether the LspA proteins are members of the YopT cysteine protease family because the C2937 residue and the other C2941 residue are apparently not involved in the observed processing. It is possible that the LspA proteins are serine proteases and may be members of a novel protease family. Further work is necessary to determine this. Also, it is important to remember that, once the specific type of protease is determined, then work will need to be performed with inhibitors to determine if this

protease activity is necessary for phagocytic inhibition. Lastly, work is also ongoing to determine the exact cleavage site by determining the N-terminal sequence of the C-terminal cleaved product. Determining the exact cleavage point will help facilitate efforts to further purify correctly processed parts of the LspA1 proteins which can then be tested to determine if they inhibit Src family PTK activity in immune cells.

## CHAPTER NINE

### Summary and Conclusions

The work presented herein focuses on one of the major virulence factors of *H. ducreyi*, the LspA proteins. The LspA proteins have previously been demonstrated to be necessary for phagocytic inhibition (215) and furthermore, necessary for disease progression in the human challenge model of infection (112). The LspA proteins' involvement in *H. ducreyi* virulence and disease progression are paramount. This work focuses on our laboratory's continuing endeavors to better understand the LspA proteins' mechanism of action, and the factors that regulate expression of these proteins. While encompassing two broad areas of study, I have devised methods to (1) study the regulation of the *lspA* and *lspB* genes and (2) determine the mechanism by which the LspA1 and LspA2 proteins inhibit phagocytosis and allow the bacteria to evade engulfment by immune cells. I have found that the LspA proteins inhibit phagocytosis in a novel method previously undescribed for any other bacterial pathogen. The outcome of this work has provided further knowledge to the field, and has also initiated studies that will provide further understanding of *H. ducreyi* disease pathogenesis.

The work presented in Chapters Four and Five focused on determining the possible role that genetic regulation may have in contributing to the expression of the LspA and LspB proteins and other potential other virulence factors involved in the pathogenesis of chancroid. The majority of these studies were performed during the first several years of my graduate work. Initially, when I began working in the laboratory, the genome of *H.*

*ducreyi* was in the process of being sequenced by another laboratory and, subsequently, DNA microarrays were not available. Therefore, differential display technology was an attractive alternative based on the options available at that time. The differential display technique identified numerous transcripts that appeared to be differentially regulated between the two tested growth conditions. Using this method, known *H. ducreyi* virulence factors were found to have transcriptional changes between the two growth conditions. First, both the *lspA* and *lspB* genes were identified in this analysis, demonstrating that this method could be used in determining possible transcriptional changes that affect protein expression. Second, one of the most interesting sequences identified by using this method matched the *dsrA* transcript (HD0769). The *dsrA* gene was not identified or described until half a year later, in March 2000, by another laboratory which demonstrated that the *dsrA* gene product was involved in serum resistance (70). A year later, a *dsrA* mutant was shown to have decreased virulence in the human challenge model (37). DsrA is now a putative major virulence determinant. Therefore, these differential display experiments had, at the time, identified a previously unknown virulence factor, further demonstrating that this technique could be useful in elucidating potential differential regulation of virulence genes. With the recently available *H. ducreyi* 35000HP genome sequence, the laboratory now has available full *H. ducreyi* DNA microarrays and numerous experiments are planned. Based on the initial results from this differential display analysis, there is a good likelihood that some *H. ducreyi* virulence genes are regulated. Performing these types of studies may help to identify and characterize mechanisms responsible for modulating virulence, and provide valuable insight regarding the pathogenesis of *H. ducreyi* disease.

Several other techniques, such as DNA-binding pull-down experiments and a GFP reporter-based transposon mutagenesis system, were developed that may, in the future, be useful in determining possible regulatory mechanisms involved with the *lspA* and *lspB* genes. Two potential candidate regulatory genes (*sspA* and HD1380) were identified using these methods; however, the latter gene product appeared to have no effect on expression of the LspA proteins. As regards to the *sspA* gene, the apparent lack of effect of a *sspA* mutation on expression of the LspB protein (Chapter Four, Fig. 15) could be due to several factors including membrane protein stoichiometry. Further experiments using real-time RT-PCR need to be performed to determine the possible role of SspA in *lspB* and *lspA2* regulation.

When compared to the large difference in protein expression initially seen with the *lspA* mutants (Chapter Four, Fig. 6), I think the gene product(s) responsible is still yet to be identified, and further screening is necessary and ongoing to determine the mechanism of this interesting regulation. Other experimental procedures may be helpful to complement the efforts in elucidating this regulation mechanism. I think the ability, methods, and tools are in place for these questions to be answered in the near future.

The findings in Chapters Six, Seven, and Eight have revealed a novel and previously unreported capacity of the *H. ducreyi* LspA proteins to affect the phosphorylation state of Src family protein tyrosine kinases, along with providing further

results suggesting how this mechanism occurs. Recent data also indicates that the YopT-like region of the LspA proteins has protease activity and is involved in the auto-processing of the LspA proteins themselves.

Experiments in Chapter Six showed that incubation of wild-type *H. ducreyi*, but not the *lspA1 lspA2* mutant, with macrophages resulted in a dramatic reduction in the levels of active Src protein tyrosine kinases (Chapter Six, Figs. 30B and 31A). These kinases are involved in some of the most proximal events of the phagocytic signaling pathway (Chapter Six, Fig. 30A). This reduced enzymatic activity of the Src protein tyrosine kinases is consistent with the inability of the former macrophages to complete the development of phagocytic cups (Chapter Six, Fig. 30). As activation of Src family protein tyrosine kinases is a very proximal event in FcγR signaling, it is likely that multiple cellular events relevant to phagocytosis (e.g., altered membrane trafficking) are also affected by the LspA proteins (Chapter Six, Fig. 29).

My hypotheses for the mechanism by which Src PTK activity is decreased are either (1) the LspA proteins bind to a receptor on the macrophage surface and thereby initiate a signaling cascade that abolishes phagocytic activity or (2) the LspA proteins enter or penetrate into the phagocyte and therein cause derangement of the normal phagocytic signaling pathway. It is also a possibility that these hypotheses are not mutually exclusive because, after binding to a surface receptor, the LspA proteins could be endocytosed or otherwise engulfed.

The presence of the YopT-like region in the LspA proteins led us to examine whether small Rho GTPases in macrophages could be affected by wild-type *H. ducreyi*. However, if the LspA proteins acted similarly to YopT from *Yersinia* species, then this would support the second hypothesis in which the LspA proteins somehow enter or penetrate into the macrophage. The observed changes in total membrane-bound Cdc42 (Chapter Seven, Fig. 36) and decreased active Rac levels (Chapter Seven, Fig. 37) are most likely downstream effects related to the decreased level of active phospho-Src. I also considered that the YopT-like region may cleave Src family members in a manner similar to how YopT cleaves the small Rho GTPases Rho, Rac and Cdc42. However, experiments designed to test this hypothesis showed no change in the level of membrane-bound Hck regardless of whether the macrophages were incubated with wild-type *H. ducreyi* or the *lspA1 lspA2* mutant (Chapter Seven, Fig. 38). Taken together with the small Rho GTPase data, these findings indicate the LspA proteins likely use a mechanism to inhibit phagocytosis that is different from that used by YopT from *Yersinia* species.

Two lines of evidence support the first hypothesis in which the LspA proteins interact with an immune cell specific receptor, leading to a negative signal for phagocytosis. The level of active phospho-Src PTKs in all four phagocytic cell types (J774A.1, RAW264.7, HL-60 and DC2.4) tested in this study were reduced by exposure to wild-type *H. ducreyi*, whereas phospho-Src PTK levels in HeLa cells appeared to be unaffected (Chapter Six, Fig. 31A). Further characterization of other immune cell types demonstrated that the effect of the LspA proteins was only found in the T cell-like Jurkat cells and not in the B cell-like Daudi cells or mast cell-like RBL-1 cells. These findings

raise the possibility that a surface component present in some immune cell lineages may interact with the LspA proteins, resulting in a negative signaling event. This possibility is reinforced by the finding that proteinase K treatment of J774A.1 macrophages eliminated the ability of wild-type *H. ducreyi* to reduce levels of active phospho-Src PTKs (Chapter Seven, Fig. 35). At this time, we cannot exclude the possibility that LspA proteins enter the macrophage via an endocytic process and exert their function in the cytoplasm, but it is unclear how these proteins would survive endosomal proteolysis and exit into the cytoplasm. Below is a schematic of our favored hypothesis (Fig. 50).

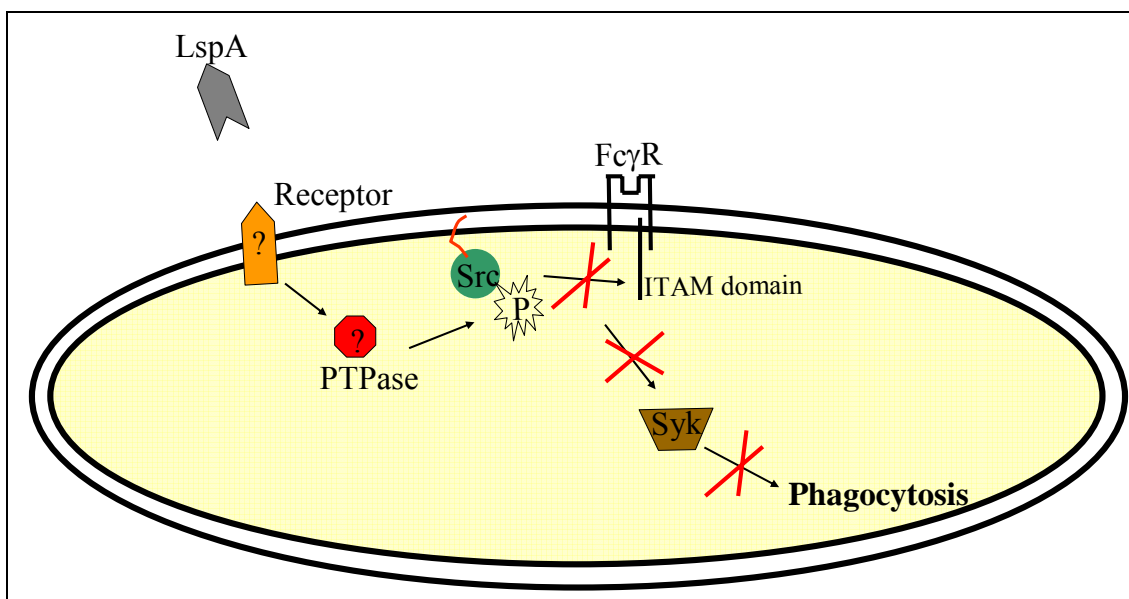


**Figure 50.** Schematic of the hypothesis for a receptor-mediated inhibition of Src PTK activity by the LspA proteins.

Efforts to clone full-length *H. ducreyi* *lspA* genes into *E. coli* or purify LspA proteins from spent *H. ducreyi* culture medium have been unsuccessful to date. However, these efforts have brought our laboratory closer to obtaining purified LspA1 protein. My



finding that the YopT-like region likely functions in autocatalytic cleavage of LspA1 suggests that the soluble LspA1 protein is the ultimate functional form of this protein. However, this does raise the question of which is the most active form of LspA1. Is it the soluble supernatant form or is some cell-bound form more active? My published experiments using PMN-like HL-60 cells showed that wild-type *H. ducreyi* CCS could inhibit the phagocytic activity of these cells (Chapter Six, Fig. 28) (141). This finding indicated that active LspA protein was present in soluble form in CCS.

It is also unclear whether the LspA proteins are members of the YopT cysteine protease family due to the findings that the C2937 residue and the C2941 residue in LspA1 are not involved in processing. It is possible that the LspA proteins are serine proteases and may be members of a novel protease family. Further work is necessary to determine this. It is also important to note that, once the type of specific protease is determined, then work will need to be performed with inhibitors to determine whether this protease activity is necessary for phagocytic inhibition. Lastly, work is ongoing to determine the exact cleavage site that is affected by this YopT-like region by determining the N-terminal sequence of the C-terminal cleaved product. Determining the exact cleavage site will help facilitate efforts to further confirm the autocatalytic activity of the LspA proteins and to correctly purify processed forms of the LspA1 proteins. This may also allow for fusion proteins to be tested to determine if they alone inhibit Src family PTK activity. More importantly, knowing the exact amino acid sequence of the cleavage site in LspA1 may

help find macrophage proteins with similar sequences that could be cleaved and involved in the LspA proteins' inhibition of phagocytic activity.

How the LspA proteins reduce the catalytic activity of the Src PTKs remains to be determined, but based on some of the data described above, it is possible that a specific immune cell inhibitory receptor is involved (Fig. 50). Furthermore, the finding that only the active phosphotyrosine (pY418) level is decreased in macrophages, and not the levels of inactive phosphotyrosine (pY529) (Chapter Six, Fig. 31A), suggests that a specific phosphatase activity may be upregulated in macrophages exposed to the LspA proteins and this effect is mediated via a membrane receptor. Protein-tyrosine phosphatases (PTPases) function in regulating phosphorylation levels in mammalian cells, and their activity in balancing these levels plays an important role in cell signaling. I have attempted to determine if there is an increase in some type of PTPase activity in macrophages exposed to the wild-type *H. ducreyi* strain relative to macrophages exposed to the *lspA1 lspA2* mutant. Macrophage cellular fractions were prepared and utilized in assays measuring PTPase activity. In two fractions from macrophages incubated with the wild-type *H. ducreyi* strain, there appeared to be a two-fold increase in PTPase activity when compared to the equivalent fractions from macrophages that had been incubated with the *lspA1 lspA2* mutant (Chapter Seven, Fig. 40A and 40B). When these fractions were probed with antibodies to known PTPases (i.e., CD45, PTP $\alpha$ , SIRP $\alpha$ , and SHP-1), only SHP-1 appeared to be present in these two fractions (Chapter Seven, Fig. 40C). While it has been reported that SHP-1 functions mostly in the dephosphorylation of the inactive phosphotyrosine

(pY529) residue (188), it is possible that SHP-1 activity toward the active pY418 residue is increased by the immune cell's interaction with the LspA proteins. Further experiments measuring SHP-1 activity in in vitro PTPase assays are planned and should hopefully answer these questions. It is also possible that another PTPase is responsible for this increase in activity and further biochemical characterization will be necessary to address this.

If the LspA proteins do interact with a specific receptor, then there are many experimental options available to identify the exact receptor; however, the majority of these approaches will require purified LspA protein. Attempting to purify recombinant LspA1 has been a major focus of my work during the last several years, and is described in detail in Chapter Eight. Having purified protein will permit a precise determination of whether the LspA proteins are directly responsible for phagocytic inhibition by *H. ducreyi*. The availability of purified LspA1 will also allow further biochemical characterization and allow experiments to look for interaction with immune cell surface components.

Exactly how the LspA proteins are involved in the observed reduction in the catalytic activity of the Src family protein tyrosine kinases remains to be determined. At this time, I cannot formally exclude the possibility that another, as yet unidentified *H. ducreyi* gene product works in concert with the LspA proteins to inhibit phagocytosis. These ongoing efforts will hopefully increase our knowledge about a major virulence mechanism of *H. ducreyi*, contribute to our understanding of the pathogenesis of chancroid,

and contribute to our knowledge of phagocytosis and the signaling pathways involved in this crucial host defense mechanism.

## Reference List

1. **Abdullah, M., I. Nepluev, G. Afonina, S. Ram, P. Rice, W. Cade, and C. Elkins.** 2005. Killing of *dsrA* Mutants of *Haemophilus ducreyi* by Normal Human Serum Occurs via the Classical Complement Pathway and Is Initiated by Immunoglobulin M Binding. *Infect. Immun.* **73**:3431-3439.
2. **Abeck, D., A. L. Freinkel, H. C. Korting, R.-M. Szeimis, and R. C. Ballard.** 1997. Immunohistochemical investigations of genital ulcers caused by *Haemophilus ducreyi*. *Int. J. STD & AIDS* **8**:585-588.
3. **Aderem, A.** 2003. Phagocytosis and the inflammatory response. *J. Infect. Dis.* **187 Suppl 2**:S340-S345.
4. **Afonina, G., I. Leduc, I. Nepluev, C. Jeter, P. Routh, G. Almond, P. E. Orndorff, M. Hobbs, and C. Elkins.** 2006. Immunization with the *Haemophilus ducreyi* hemoglobin receptor HgbA protects against infection in the swine model of chancroid. *Infect. Immun.* **74**:2224-2232.
5. **Ahmed, H. J., S. Borrelli, J. Jonasson, L. Eriksson, S. Hanson, B. Hojer, M. Sunkuntu, E. Musaba, E. L. Roggen, T. Lagergard, and A. A. Lindberg.** 1995. Monoclonal antibodies against *Haemophilus ducreyi* lipooligosaccharide and their diagnostic usefulness. *Eur. J. Clin. Microbiol. Infect. Dis.* **14**:892-898.
6. **Ahmed, H. J., C. Johansson, L. A. Svensson, K. Ahlman, M. Verdrengh, and T. Lagergard.** 2002. In vitro and in vivo interactions of *Haemophilus ducreyi* with host phagocytes. *Infect. Immun.* **70**:899-908.
7. **Al Tawfiq, J. A., K. R. Fortney, B. P. Katz, A. F. Hood, C. Elkins, and S. M. Spinola.** 2000. An isogenic hemoglobin receptor-deficient mutant of *Haemophilus ducreyi* is attenuated in the human model of experimental infection. *J. Infect. Dis.* **181**:1049-1054.
8. **Al-Tawfiq, J. A., M. E. Bauer, K. R. Fortney, B. P. Katz, A. F. Hood, M. Ketterer, M. A. Apicella, and S. M. Spinola.** 2000. A pilus-deficient mutant of *Haemophilus ducreyi* is virulent in the human model of experimental infection. *J. Infect. Dis.* **181**:1176-1179.
9. **Al-Tawfiq, J. A., K. R. Fortney, B. P. Katz, C. Elkins, and S. M. Spinola.** 1999. An isogenic hemoglobin receptor-deficient mutant of *Haemophilus ducreyi* is attenuated in the human model of experimental infection, p. 213. *In* .
10. **Al-Tawfiq, J. A., K. L. Palmer, C.-Y. Chen, J. C. Haley, B. P. Katz, A. F. Hood, and S. M. Spinola.** 1999. Experimental infection of human volunteers with

- Haemophilus ducreyi* does not confer protection against subsequent challenge. J. Infect. Dis. **179**:1283-1287.
11. **Al-Tawfiq, J. A., A. C. Thornton, B. P. Katz, K. R. Fortney, K. D. Todd, A. F. Hood, and S. M. Spinola.** 1998. Standardization of the experimental model of *Haemophilus ducreyi* infection in human subjects. J. Infect. Dis. **178**:1684-1687.
  12. **Albritton, W. L.** 1989. Biology of *Haemophilus ducreyi*. Microbiol. Rev. **53**:377-389.
  13. **Albritton, W. L., J. L. Brunton, L. Slaney, and I. W. MacLean.** 1982. Plasmid-mediated sulfonamide resistance in *Haemophilus ducreyi*. Antimicrob. Agents Chemother. **21**:159-165.
  14. **Albritton, W. L., I. W. MacLean, P. D. Bertram, and A. R. Ronald.** 1981. Haemin requirements in *Haemophilus* with special reference to *H. ducreyi*, p. 75-82. In M. Kilian, W. Frederiksen, and E. L. Biberstein (ed.), *Haemophilus, Pasteurella, and Actinobacillus*. Academic Press, London.
  15. **Alfa, M. J. and P. Degagne.** 1997. Attachment of *Haemophilus ducreyi* to human foreskin fibroblasts involves LOS and fibronectin. Microb. Pathog. **22**:39-46.
  16. **Alfa, M. J., P. Degagne, and P. A. Totten.** 1996. *Haemophilus ducreyi* hemolysin acts as a contact cytotoxin and damages human foreskin fibroblasts in cell culture. Infect. Immun. **64**:2349-2352.
  17. **Altincicek, B., A. K. Kollas, S. Sanderbrand, J. Wiesner, M. Hintz, E. Beck, and H. Jomaa.** 2001. GcpE is involved in the 2-C-methyl-D-erythritol 4-phosphate pathway of isoprenoid biosynthesis in *Escherichia coli*. J. Bacteriol. **183**:2411-2416.
  18. **Arko, R. J.** 1972. *Neisseria gonorrhoeae*: experimental infection of laboratory animals. Science **177**:1200-1201.
  19. **Arko, R. J.** 1973. Implantation and use of a subcutaneous culture chamber in laboratory animals. Lab Anim Sci. **23**:105-106.
  20. **Badger, J. L. and V. L. Miller.** 1998. Expression of invasins and motility are coordinately regulated in *Yersinia enterocolitica*. J. Bacteriol. **180**:793-800.
  21. **Baron, G. S. and F. E. Nano.** 1998. MglA and MglB are required for the intramacrophage growth of *Francisella novicida*. Mol. Microbiol. **29**:247-259.
  22. **Bateman, A.** 1999. The SIS domain: a phosphosugar-binding domain. Trends Biochem. Sci. **24**:94-95.

23. **Bauer, B. A., S. R. Lumbley, and E. J. Hansen.** 1999. Characterization of a WaaF (RfaF) homolog expressed by *Haemophilus ducreyi*. *Infect. Immun.* **67**:899-907.
24. **Bauer, B. A., M. K. Stevens, and E. J. Hansen.** 1998. Involvement of the *Haemophilus ducreyi gmhA* gene product in lipooligosaccharide expression and virulence. *Infect. Immun.* **66**:4290-4298.
25. **Bauer, M. E., M. P. Goheen, C. A. Townsend, and S. M. Spinola.** 2001. *Haemophilus ducreyi* associates with phagocytes, collagen, and fibrin and remains extracellular throughout infection of human volunteers. *Infect. Immun.* **69**:2549-2557.
26. **Bauer, M. E. and S. M. Spinola.** 1999. Binding of *Haemophilus ducreyi* to extracellular matrix proteins. *Infect. Immun.* **67**:2649-2652.
27. **Bauer, M. E. and S. M. Spinola.** 2000. Localization of *Haemophilus ducreyi* at the pustular stage of disease in the human model of infection. *Infect. Immun.* **68**:2309-2314.
28. **Baumler, A. J., J. G. Kusters, I. Stojiljkovic, and F. Heffron.** 1994. *Salmonella typhimurium* loci involved in survival within macrophages. *Infect. Immun.* **62**:1623-1630.
29. **Bezancon, F., V. Griffon, and L. Le Sourd.** 1900. Culture du bacille du chancre mou. *C. R. Soc. Biol.* **52**:1048-1051.
30. **Blackmore, C. A., K. Limpakarnjanarat, J. G. Rigau Perez, W. L. Albritton, and J. R. Greenwood.** 1985. An outbreak of chancroid in Orange County, California: descriptive epidemiology and disease-control measures. *J. Infect. Dis.* **151**:840-844.
31. **Blander, J. M. and R. Medzhitov.** 2004. Regulation of phagosome maturation by signals from toll-like receptors. *Science* **304**:1014-1018.
32. **Blick, R. J.** 2001. Investigation of Differential Gene Regulation in *Haemophilus ducreyi*. Master of Science University of Texas Southwestern Medical Center at Dallas.
33. **Blick, R. J., A. T. Revel, and E. J. Hansen.** 2003. FindGDPs: identification of primers for labeling microbial transcriptomes for DNA microarray analysis. *Bioinformatics.* **19**:1718-1719.
34. **Bolon, D. N., R. A. Grant, T. A. Baker, and R. T. Sauer.** 2004. Nucleotide-dependent substrate handoff from the SspB adaptor to the AAA+ ClpXP protease. *Mol. Cell* **16**:343-350.

35. **Bong, C. T., K. R. Fortney, B. P. Katz, A. F. Hood, L. R. San Mateo, T. H. Kawula, and S. M. Spinola.** 2002. A superoxide dismutase C mutant of *Haemophilus ducreyi* is virulent in human volunteers. *Infect. Immun.* **70**:1367-1371.
36. **Bong, C. T., J. Harezlak, B. P. Katz, and S. M. Spinola.** 2002. Men are more susceptible than women to pustule formation in the experimental model of *Haemophilus ducreyi* infection. *Sex Transm. Dis.* **29**:114-118.
37. **Bong, C. T., R. E. Throm, K. R. Fortney, B. P. Katz, A. F. Hood, C. Elkins, and S. M. Spinola.** 2001. DsrA-deficient mutant of *Haemophilus ducreyi* is impaired in its ability to infect human volunteers. *Infect. Immun.* **69**:1488-1491.
38. **Bozue, J. A., L. Tarantino, and R. S. Munson, Jr.** 1998. Facile construction of mutations in *Haemophilus ducreyi* using *lacZ* as a counter-selectable marker. *FEMS Microbiol. Lett.* **164**:269-273.
39. **Bozue, J. A., M. V. Tullius, J. Wang, B. W. Gibson, and R. S. Munson, Jr.** 1999. *Haemophilus ducreyi* produces a novel sialyltransferase. Identification of the sialyltransferase gene and construction of mutants deficient in the production of the sialic acid-containing glycoform of the lipooligosaccharide. *J. Biol. Chem.* **274**:4106-4114.
40. **Brentjens, R. J., M. Ketterer, M. A. Apicella, and S. M. Spinola.** 1996. Fine tangled pili expressed by *Haemophilus ducreyi* are a novel class of pili. *J. Bacteriol.* **178**:808-816.
41. **Brown, T. J., R. C. Ballard, and C. A. Ison.** 1995. Specificity of the immune response to *Haemophilus ducreyi*. *Microb. Pathog.* **19**:31-38.
42. **Carlone, G. M., W. O. Schalla, C. W. Moss, D. L. Ashley, D. M. Fast, J. S. Holler, and B. D. Plikaytis.** 1988. *Haemophilus ducreyi* isoprenoid quinone content and structure determination. *Int. J. Syst. Bacteriol.* **38**:249-253.
43. **Caron, E. and A. Hall.** 1998. Identification of two distinct mechanisms of phagocytosis controlled by different Rho GTPases. *Science* **282**:1717-1721.
44. **Casin, I., F. Grimont, and P. A. Grimont.** 1986. Deoxyribonucleic acid relatedness between *Haemophilus aegyptius* and *Haemophilus influenzae*. *Ann. Inst. Pasteur Microbiol.* **137B**:155-163.
45. **Casin, I., F. Grimont, P. A. D. Grimont, and M.-J. Sanson-Le Pors.** 1985. Lack of deoxyribonucleic acid relatedness between *Haemophilus ducreyi* and other *Haemophilus* species. *Int. J. Syst. Bacteriol.* **35**:23-25.



46. **Chang, A. C. Y. and S. N. Cohen.** 1978. Construction and characterization of amplifiable multicopy DNA cloning vehicles derived from the P15A cryptic miniplasmid. *J. Bacteriol.* **134**:1141-1156.
47. **Chen, C.-Y., K. J. Mertz, S. M. Spinola, and S. A. Morse.** 1997. Comparison of enzyme immunoassays for antibodies to *Haemophilus ducreyi* in a community outbreak of chancroid in the United States. *J. Infect. Dis.* **175**:1390-1395.
48. **Chui, L., W. Albbritton, B. Paster, I. W. MacLean, and R. Marusyk.** 1993. Development of the polymerase chain reaction for diagnosis of chancroid. *J. Clin. Microbiol.* **31**:659-664.
49. **Cole, L. E.** 2004. Host Association Mechanisms of *Haemophilus ducreyi*. PhD University of North Carolina.
50. **Cole, L. E., T. H. Kawula, K. L. Toffer, and C. Elkins.** 2002. The *Haemophilus ducreyi* serum resistance antigen DsrA confers attachment to human keratinocytes. *Infect. Immun.* **70**:6158-6165.
51. **Cooney, D. S., H. Phee, A. Jacob, and K. M. Coggeshall.** 2001. Signal transduction by human-restricted Fc gamma RIIa involves three distinct cytoplasmic kinase families leading to phagocytosis. *J. Immunol.* **167**:844-854.
52. **Cope, L. D., S. R. Lumbley, J. L. Latimer, J. Klesney-Tait, M. K. Stevens, L. S. Johnson, M. Purven, R. S. Munson, Jr., T. Lagergard, J. D. Radolf, and E. J. Hansen.** 1997. A diffusible cytotoxin of *Haemophilus ducreyi*. *Proc. Natl. Acad. Sci. USA* **94**:4056-4061.
53. **Cortes-Bratti, X., T. Frisan, and M. Thelestam.** 2001. The cytolethal distending toxins induce DNA damage and cell cycle arrest. *Toxicon* **39**:1729-1736.
54. **Cortes-Bratti, X., C. Karlsson, T. Lagergard, M. Thelestam, and T. Frisan.** 2001. The *Haemophilus ducreyi* cytolethal distending toxin induces cell cycle arrest and apoptosis via the DNA damage checkpoint pathways. *J. Biol. Chem.* **276**:5296-5302.
55. **Crowley, M. T., P. S. Costello, C. J. Fitzer-Attas, M. Turner, F. Meng, C. Lowell, V. L. Tybulewicz, and A. L. DeFranco.** 1997. A critical role for Syk in signal transduction and phagocytosis mediated by Fcγ receptors on macrophages. *J. Exp. Med.* **186**:1027-1039.
56. **Danese, P. N. and T. J. Silhavy.** 1997. The sigma<sup>E</sup> and the Cpx signal transduction systems control the synthesis of periplasmic protein-folding enzymes in *Escherichia coli*. *Genes Develop.* **11**:1183-1193.

57. **Danese, P. N., W. B. Snyder, C. L. Cosma, L. J. B. Davis, and T. J. Silhavy.** 1995. The Cpx two-component signal transduction pathway of *Escherichia coli* regulates transcription of the gene specifying the stress-inducible periplasmic protease, DegP. *Genes Develop.* **9**:387-398.
58. **Dangor, Y., R. C. Ballard, F. da L. Exposto, G. Fehler, S. D. Miller, and H. J. Koornhof.** 1990. Accuracy of clinical diagnosis of genital ulcer disease. *Sex. Transm. Inf.* **17**:184-189.
59. **De Ley, J., W. Mannheim, R. Mutters, K. Peichulla, R. Tytgat, P. Segers, M. Bisgaard, W. Frederiksen, K.-H. Hinz, and M. Vanhoucke.** 1990. Inter- and intrafamilial similarities of rRNA cistrons of the *Pasteurellaceae*. *Int. J. Syst. Bacteriol.* **40**:126-137.
60. **Desjardins, M., L. G. Fillion, S. Robertson, and D. W. Cameron.** 1995. Inducible immunity with a pilus preparation booster vaccination in an animal model of *Haemophilus ducreyi* infection and disease. *Infect. Immun.* **63**:2012-2020.
61. **Dewhirst, F. E., B. J. Paster, I. Olsen, and G. J. Fraser.** 1992. Phylogeny of 54 representative strains of species in the family *Pasteurellaceae* as determined by comparison of 16S rRNA sequences. *J. Bacteriol.* **174**:2002-2013.
62. **DiCarlo, R. P., B. S. Armentor, and D. H. Martin.** 1995. Chancroid epidemiology in New Orleans men. *J. Infect. Dis.* **172**:446-452.
63. **DiCarlo, R. P. and D. H. Martin.** 1997. The clinical diagnosis of genital ulcer disease in men. *Clin. Infect. Dis.* **25**:292-298.
64. **Dixon, L. G., W. L. Albritton, and P. J. Willson.** 1994. An analysis of the complete nucleotide sequence of the *Haemophilus ducreyi* broad-host-range plasmid pLS88. *Plasmid* **32**:228-232.
65. **Doyle, S. E., R. M. O'Connell, G. A. Miranda, S. A. Vaidya, E. K. Chow, P. T. Liu, S. Suzuki, N. Suzuki, R. L. Modlin, W. C. Yeh, T. F. Lane, and G. Cheng.** 2004. Toll-like receptors induce a phagocytic gene program through p38. *J. Exp. Med.* **199**:81-90.
66. **Ducrey, A.** 1889. Experimentelle Untersuchungen uber den Ansteckungsstof des weichen Schankers und uber die Bubonen. *Monatsh. Prakt. Dermatol.* **9**:387-405.
67. **Dutro, S. M., G. E. Wood, and P. A. Totten.** 1999. Prevalence of, antibody response to, and immunity induced by *Haemophilus ducreyi* hemolysin. *Infect. Immun.* **67**:3317-3328.

68. **Elkins, C.** 1995. Identification and purification of a conserved heme-regulated hemoglobin-binding outer membrane protein from *Haemophilus ducreyi*. *Infect. Immun.* **63**:1241-1245.
69. **Elkins, C., C.-J. Chen, and C. E. Thomas.** 1995. Characterization of the *hgbA* locus encoding a hemoglobin receptor from *Haemophilus ducreyi*. *Infect. Immun.* **63**:2194-2200.
70. **Elkins, C., K. J. Morrow, Jr., and B. Olsen.** 2000. Serum resistance in *Haemophilus ducreyi* requires outer membrane protein DsrA. *Infect. Immun.* **68**:1608-1619.
71. **Elkins, C., P. A. Totten, B. Olesen, and C. E. Thomas.** 1998. Role of the *Haemophilus ducreyi* Ton system in internalization of heme from hemoglobin. *Infect. Immun.* **66**:151-160.
72. **Fellay, R., J. Frey, and H. M. Krisch.** 1987. Interposon mutagenesis of soil and water bacteria: a family of DNA fragments designed for in vitro insertional mutagenesis of Gram negative bacteria. *Gene* **52**:147-152.
73. **Filip, C., G. Fletcher, J. L. Wulff, and C. F. Earhart.** 1973. Solubilization of the cytoplasmic membrane of *Escherichia coli* by the ionic detergent sodium-lauryl sarcosinate. *J. Bacteriol.* **115**:717-722.
74. **Fitzer-Attas, C. J., M. Lowry, M. T. Crowley, A. J. Finn, F. Meng, A. L. DeFranco, and C. A. Lowell.** 2000. Fcγ receptor-mediated phagocytosis in macrophages lacking the Src family tyrosine kinases Hck, Fgr, and Lyn. *J. Exp. Med.* **191**:669-682.
75. **Fleming, D. T. and J. N. Wasserheit.** 1999. From epidemiological synergy to public health policy and practice: the contribution of other sexually transmitted diseases to sexual transmission of HIV infection. *Sex. Transm. Inf.* **75**:3-17.
76. **Fortney, K. R., R. S. Young, M. E. Bauer, B. P. Katz, A. F. Hood, R. S. Munson, Jr., and S. M. Spinola.** 2000. Expression of peptidoglycan-associated lipoprotein is required for virulence in the human model of *Haemophilus ducreyi* infection. *Infect. Immun.* **68**:6441-6448.
77. **Freinkel, A. L.** 1987. Histological aspects of sexually transmitted genital lesions. *Histopath.* **11**:818-831.
78. **Fullner, K. J. and J. J. Mekalanos.** 2000. In vivo covalent cross-linking of cellular actin by the *Vibrio cholerae* RTX toxin. *EMBO J.* **19**:5315-5323.

79. **Gelfanova, V., E. J. Hansen, and S. M. Spinola.** 1999. Cytolethal distending toxin of *Haemophilus ducreyi* induces apoptotic death of Jurkat T cells. *Infect. Immun.* **67**:6394-6402.
80. **Gelfanova, V., T. L. Humphreys, and S. M. Spinola.** 2001. Characterization of *Haemophilus ducreyi*-specific T-cell lines from lesions of experimentally infected human subjects. *Infect. Immun.* **69**:4224-4231.
81. **Gibson, B. W., A. A. Campagnari, W. Melaugh, N. J. Phillips, M. A. Apicella, S. Grass, J. Wang, K. L. Palmer, and R. S. Munson, Jr.** 1997. Characterization of a transposon Tn916-generated mutant of *Haemophilus ducreyi* 35000 defective in lipooligosaccharide biosynthesis. *J. Bacteriol.* **179**:5062-5071.
82. **Grass, S. and G. J. St, III.** 2000. Maturation and secretion of the non-typable *Haemophilus influenzae* HMW1 adhesin: roles of the N-terminal and C-terminal domains. *Mol. Microbiol.* **36**:55-67.
83. **Gray, R. H., M. J. Wawer, R. Brookmeyer, N. K. Sewankambo, D. Serwadda, F. Wabwire-Mangen, T. Lutalo, X. Li, T. vanCott, and T. C. Quinn.** 2001. Probability of HIV-1 transmission per coital act in monogamous, heterosexual, HIV-1-discordant couples in Rakai, Uganda. *Lancet* **357**:1149-1153.
84. **Greenberg, S.** 2001. Diversity in phagocytic signalling. *J. Cell Sci.* **114**:1039-1040.
85. **Greenberg, S., K. Burridge, and S. C. Silverstein.** 1990. Colocalization of F-actin and talin during Fc receptor-mediated phagocytosis in mouse macrophages. *J. Exp. Med.* **172**:1853-1856.
86. **Greenberg, S., J. el Khoury, F. Di Virgilio, E. M. Kaplan, and S. C. Silverstein.** 1991. Ca(2+)-independent F-actin assembly and disassembly during Fc receptor-mediated phagocytosis in mouse macrophages. *J. Cell Biol.* **113**:757-767.
87. **Greenberg, S. and S. Grinstein.** 2002. Phagocytosis and innate immunity. *Curr. Opin. Immunol.* **14**:136-145.
88. **Gresham, H. D., B. M. Dale, J. W. Potter, P. W. Chang, C. M. Vines, C. A. Lowell, C. F. Lagenaur, and C. L. Willman.** 2000. Negative regulation of phagocytosis in murine macrophages by the Src kinase family member, Fgr. *J. Exp. Med.* **191**:515-528.
89. **Gulig, P. A., G. H. McCracken, Jr., C. F. Frisch, K. H. Johnston, and E. J. Hansen.** 1982. Antibody response of infants to cell surface-exposed outer membrane proteins of *Haemophilus influenzae* type b after systemic *Haemophilus* disease. *Infect. Immun.* **37**:82-88.

90. **Haine, V., A. Sinon, S. F. Van, S. Rousseau, M. Dozot, P. Lestrade, C. Lambert, J. J. Letesson, and B. De, X.** 2005. Systematic targeted mutagenesis of *Brucella melitensis* 16M reveals a major role for GntR regulators in the control of virulence. *Infect. Immun.* **73**:5578-5586.
91. **Hammond, G. W.** 1996. A history of the detection of *Haemophilus ducreyi*, 1889-1979. *Sex. Transm. Inf.* **23**:93-96.
92. **Hammond, G. W., C. J. Lian, J. C. Wilt, W. L. Albritton, and A. R. Ronald.** 1978. Determination of the hemin requirement of *Haemophilus ducreyi*: evaluation of the porphyrin test and media used in the satellite growth test. *J. Clin. Microbiol.* **7**:243-246.
93. **Hammond, G. W., C. J. Lian, J. C. Wilt, and A. R. Ronald.** 1978. Comparison of specimen collection and laboratory techniques for isolation of *Haemophilus ducreyi*. *J. Clin. Microbiol.* **7**:39-43.
94. **Hammond, G. W., C. J. Lian, J. C. Wilt, and A. R. Ronald.** 1978. Antimicrobial susceptibility of *Haemophilus ducreyi*. *Antimicrob. Agents Chemother.* **13**:608-612.
95. **Hammond, G. W., M. Slutchuk, J. Scatliff, E. Sherman, J. C. Wilt, and A. R. Ronald.** 1980. Epidemiologic, clinical, laboratory, and therapeutic features of an urban outbreak of chancroid in North America. *Rev. Infect. Dis.* **2**:867-879.
96. **Hansen, A. M., H. Lehnher, X. Wang, V. Mobley, and D. J. Jin.** 2003. *Escherichia coli* SspA is a transcription activator for bacteriophage P1 late genes. *Mol. Microbiol.* **48**:1621-1631.
97. **Hansen, A. M., Y. Qiu, N. Yeh, F. R. Blattner, T. Durfee, and D. J. Jin.** 2005. SspA is required for acid resistance in stationary phase by downregulation of H-NS in *Escherichia coli*. *Mol. Microbiol.* **56**:719-734.
98. **Hansen, E. J., J. L. Latimer, S. E. Thomas, M. Helminen, W. L. Albritton, and J. D. Radolf.** 1992. Use of electroporation to construct isogenic mutants of *Haemophilus ducreyi*. *J. Bacteriol.* **174**:5442-5449.
99. **Hansen, E. J., S. R. Lumbley, J. A. Richardson, B. K. Purcell, M. K. Stevens, L. D. Cope, J. Datte, and J. D. Radolf.** 1994. Induction of protective immunity to *Haemophilus ducreyi* in the temperature-dependent rabbit model of experimental chancroid. *J. Immunol.* **152**:184-192.
100. **Hansen, E. J., S. R. Lumbley, H. Saxen, K. Kern, L. D. Cope, and J. D. Radolf.** 1995. Detection of *Haemophilus ducreyi* lipooligosaccharide by means of an immunolimus assay. *J. Immunol. Methods* **185**:225-235.

101. **Haydock, A. K., D. H. Martin, S. A. Morse, C. Cammarata, K. J. Mertz, and P. A. Totten.** 1999. Molecular characterization of *Haemophilus ducreyi* strains from Jackson, Mississippi and New Orleans, Louisiana. *J. Infect. Dis.* **179**:1423-1432.
102. **Hayes, R. J., K. F. Schulz, and F. A. Plummer.** 1995. The cofactor effect of genital ulcers on the per-exposure risk of HIV transmission in sub-Saharan Africa. *J. Trop. Med. Hyg.* **98**:1-8.
103. **Hiltke, T. J., M. E. Bauer, J. Klesney-Tait, E. J. Hansen, R. S. Munson, Jr., and S. M. Spinola.** 1999. Effect of normal and immune sera on *Haemophilus ducreyi* 35000HP and its isogenic MOMP and LOS mutants. *Microb. Pathog.* **26**:93-102.
104. **Hobbs, M. M., L. R. San Mateo, P. E. Orndorff, G. Almond, and T. H. Kawula.** 1995. Swine model of *Haemophilus ducreyi* infection. *Infect. Immun.* **63**:3094-3100.
105. **Humphreys, T. L., C. T. Schnizlein-Bick, B. P. Katz, L. A. Baldrige, A. F. Hood, R. A. Hromas, and S. M. Spinola.** 2002. Evolution of the cutaneous immune response to experimental *Haemophilus ducreyi* infection and its relevance to HIV-1 acquisition. *J. Immunol.* **169**:6316-6323.
106. **Jacob-Dubuisson, F., C. Buisine, N. Mielcarek, E. Clement, F. D. Menozzi, and C. Locht.** 1996. Amino-terminal maturation of the *Bordetella pertussis* filamentous haemagglutinin. *Mol. Microbiol.* **19**:65-78.
107. **Jacob-Dubuisson, F., C. El Hamel, N. Saint, S. Guedin, E. Willery, G. Molle, and C. Locht.** 1999. Channel formation by FhaC, the outer membrane protein involved in the secretion of the *Bordetella pertussis* filamentous hemagglutinin. *J. Biol. Chem.* **274**:37731-37735.
108. **Jacob-Dubuisson, F., B. Kehoe, E. Willery, N. Reveneau, C. Locht, and D. A. Relman.** 2000. Molecular characterization of *Bordetella bronchiseptica* filamentous haemagglutinin and its secretion machinery. *Microbiology* **146** ( Pt 5):1211-1221.
109. **Jacob-Dubuisson, F., C. Locht, and R. Antoine.** 2001. Two-partner secretion in Gram-negative bacteria: a thrifty, specific pathway for large virulence proteins. *Mol. Microbiol.* **40**:306-313.
110. **Janowicz, D., I. Leduc, K. R. Fortney, B. P. Katz, C. Elkins, and S. M. Spinola.** 2006. A DltA mutant of *Haemophilus ducreyi* Is partially attenuated in its ability to cause pustules in human volunteers. *Infect. Immun.* **74**:1394-1397.
111. **Janowicz, D., N. R. Luke, K. R. Fortney, B. P. Katz, A. A. Campagnari, and S. M. Spinola.** 2006. Expression of OmpP2A and OmpP2B is not required for pustule formation by *Haemophilus ducreyi* in human volunteers. *Microb. Pathog.* **40**:110-115.

112. **Janowicz, D. M., K. R. Fortney, B. P. Katz, J. L. Latimer, K. Deng, E. J. Hansen, and S. M. Spinola.** 2004. Expression of the LspA1 and LspA2 proteins by *Haemophilus ducreyi* is required for virulence in human volunteers. *Infect. Immun.* **72**:4528-4533.
113. **Jarrige, A., D. Brechemier-Baey, N. Mathy, O. Duche, and C. Portier.** 2002. Mutational analysis of polynucleotide phosphorylase from *Escherichia coli*. *J. Mol. Biol.* **321**:397-409.
114. **Jessamine, P. G., F. A. Plummer, J. O. Ndinya-Achola, M. A. Wainberg, I. Wamola, L. J. D'Costa, D. W. Cameron, J. N. Simonsen, P. Plourde, and A. R. Ronald.** 1990. Human immunodeficiency virus, genital ulcers and the male foreskin: synergism in HIV-1 transmission. *Scand. J. Infect. Dis.* **69,Suppl.**:181-186.
115. **Jessamine, P. G. and A. R. Ronald.** 1990. Chancroid and the role of genital ulcer disease in the spread of human retroviruses. *Med. Clin. North. Am.* **74**:1417-1431.
116. **Johnson, S. R., D. H. Martin, C. Cammarata, and S. A. Morse.** 1994. Development of a polymerase chain reaction assay for the detection of *Haemophilus ducreyi*. *Sex. Transm. Inf.* **21**:13-23.
117. **Jutras, I. and M. Desjardins.** 2005. Phagocytosis: at the crossroads of innate and adaptive immunity. *Annu. Rev. Cell Dev. Biol.* **21**:511-527.
118. **Karim, Q. N., G. Y. Finn, C. S. F. Easmon, Y. Dangor, D. A. B. Dance, Y. F. Ngeow, and R. C. Ballard.** 1989. Rapid detection of *Haemophilus ducreyi* in clinical and experimental infections using monoclonal antibody: a preliminary evaluation. *Genitourin. Med.* **65**:361-365.
119. **King, R., J. Gough, A. R. Ronald, J. Nasio, J. O. Ndinyaachola, F. Plummer, and J. A. Wilkins.** 1996. An immunohistochemical analysis of naturally occurring chancroid. *J. Infect. Dis.* **174**:427-430.
120. **Klesney-Tait, J., T. J. Hiltke, I. Maciver, S. M. Spinola, J. D. Radolf, and E. J. Hansen.** 1997. The major outer membrane protein of *Haemophilus ducreyi* consists of two OmpA homologs. *J. Bacteriol.* **179**:1764-1773.
121. **Kroll, J. S., P. R. Langford, K. E. Wilks, and A. D. Keil.** 1995. Bacterial [Cu,Zn]-superoxide dismutase: phylogenically distinct from the eukaryotic enzyme, and not so rare after all! *Microbiology* **141**:2271-2279.
122. **Lagergard, T. and M. Purven.** 1993. Neutralizing antibodies to *Haemophilus ducreyi* cytotoxin. *Infect. Immun.* **61**:1589-1592.

123. **Langford, P. R. and J. S. Kroll.** 1997. Distribution, cloning, characterization and mutagenesis of *sodC*, the gene encoding copper/zinc superoxide dismutase, a potential determinant of virulence in *Haemophilus ducreyi*. FEMS Immunol. Med. Microbiol. **17**:235-242.
124. **Lara-Tejero, M. and J. E. Galan.** 2000. A bacterial toxin that controls cell cycle progression as a deoxyribonuclease I-like protein. Science **290**:354-357.
125. **Leduc, I., P. Richards, C. Davis, B. Schilling, and C. Elkins.** 2004. A novel lectin, DltA, is required for expression of a full serum resistance phenotype in *Haemophilus ducreyi*. Infect. Immun. **72**:3418-3428.
126. **Lee, B. C.** 1991. Iron sources for *Haemophilus ducreyi*. J. Med. Microbiol. **34**:317-322.
127. **Lee, E. H., H. Masai, G. C. Allen, Jr., and A. Kornberg.** 1990. The priA gene encoding the primosomal replicative n' protein of *Escherichia coli*. Proc. Natl. Acad. Sci. U. S. A **87**:4620-4624.
128. **Levchenko, I., M. Seidel, R. T. Sauer, and T. A. Baker.** 2000. A specificity-enhancing factor for the ClpXP degradation machine. Science **289**:2354-2356.
129. **Lewis, D. A.** 1999. The use of experimental animal and human models in the study of chancroid pathogenesis. Int. J. STD AIDS **10**:71-79.
130. **Lewis, D. A.** 2000. Diagnostic tests for chancroid. Sex Transm. Infect. **76**:137-141.
131. **Lewis, D. A.** 2003. Chancroid: clinical manifestations, diagnosis, and management. Sex Transm. Infect. **79**:68-71.
132. **Lewis, D. A., M. K. Stevens, J. L. Latimer, C. K. Ward, K. Deng, R. Blick, S. R. Lumbley, C. A. Ison, and E. J. Hansen.** 2001. Characterization of *Haemophilus ducreyi* cdtA, cdtB, and cdtC mutants in in vitro and in vivo systems. Infect. Immun. **69**:5626-5634.
133. **Li, L., A. Sharipo, E. Chaves-Olarte, M. G. Masucci, V. Levitsky, M. Thelestam, and T. Frisan.** 2002. The *Haemophilus ducreyi* cytolethal distending toxin activates sensors of DNA damage and repair complexes in proliferating and non-proliferating cells. Cell Microbiol **4**:87-99.
134. **Lowell, C. A.** 2004. Src-family kinases: rheostats of immune cell signaling. Mol. Immunol. **41**:631-643.
135. **Lukomski, S., N. P. Hoe, I. Abdi, J. Rurangirwa, P. Kordari, M. Liu, S. J. Dou, G. G. Adams, and J. M. Musser.** 2000. Nonpolar inactivation of the hypervariable streptococcal inhibitor of complement gene (sic) in serotype M1 *Streptococcus*



- pyogenes* significantly decreases mouse mucosal colonization. Infect. Immun. **68**:535-542.
136. **Manes, S., G. del Real, and A. Martinez.** 2003. Pathogens: raft hijackers. Nat. Rev. Immunol. **3**:557-568.
  137. **Martin, G. S.** 2001. The hunting of the Src. Nat. Rev. Mol. Cell Biol. **2**:467-475.
  138. **Merkel, T. J., S. Stibitz, J. M. Keith, M. Leef, and R. Shahin.** 1998. Contribution of regulation by the bvg locus to respiratory infection of mice by *Bordetella pertussis*. Infect. Immun. **66**:4367-4373.
  139. **Mertz, K. J., D. L. Trees, W. c. Levine, J. S. Lewis, B. Litchfield, K. S. Pettus, S. A. Morse, St Louis ME, J. B. Weiss, J. Schwebke, J. Dickes, R. Kee, J. Reynolds, D. Hutcheson, D. Green, I. Dyer, G. A. Richwald, J. Novotny, M. Goldberg, J. A. O'Donnell, and R. Knaup.** 1998. Etiology of genital ulcers and prevalence of human immunodeficiency virus coinfection in 10 US cities. J. Infect. Dis. **178**:1795-1798.
  140. **Miller, W. G. and S. E. Lindow.** 1997. An improved GFP cloning cassette designed for prokaryotic transcriptional fusions. Gene **191**:149-153.
  141. **Mock, J. R., M. Vakevainen, K. Deng, J. L. Latimer, J. A. Young, N. S. van Oers, S. Greenberg, and E. J. Hansen.** 2005. *Haemophilus ducreyi* targets Src family protein tyrosine kinases to inhibit phagocytic signaling. Infect. Immun. **73**:7808-7816.
  142. **Morse, S. A.** 1989. Chancroid and *Haemophilus ducreyi*. Clin. Microbiol. Rev. **2**:137-157.
  143. **Morse, S. A., D. L. Trees, Y. Htun, F. Radebe, K. A. Orle, Y. Dangor, C. M. Beck-Sague, S. Schmid, G. Fehler, J. B. Weiss, and R. C. Ballard.** 1997. Comparison of clinical diagnosis and standard laboratory and molecular methods of the diagnosis of genital ulcer disease in Lesotho: Association with human immunodeficiency virus infection. J. Infect. Dis. **175**:583-589.
  144. **Munson, R. S., Jr., H. Zhong, R. Mungur, W. C. Ray, R. J. Shea, G. G. Mahairas, and M. H. Mulks.** 2004. *Haemophilus ducreyi* strain ATCC 27722 contains a genetic element with homology to the vibrio RS1 element that can replicate as a plasmid and confer NAD independence on haemophilus influenzae. Infect. Immun. **72**:1143-1146.
  145. **Museyi, K., E. Van Dyck, T. Vervoort, D. Taylor, C. Hoge, and P. Piot.** 1988. Use of an enzyme immunoassay to detect serum IgG antibodies to *Haemophilus ducreyi*. J. Infect. Dis. **157**:1039-1043.

146. **Nesic, D., Y. Hsu, and C. E. Stebbins.** 2004. Assembly and function of a bacterial genotoxin. *Nature* **429**:429-433.
147. **Nika, J. R., J. L. Latimer, C. K. Ward, R. J. Blick, N. J. Wagner, L. D. Cope, G. G. Mahairas, R. S. Munson, Jr., and E. J. Hansen.** 2002. *Haemophilus ducreyi* requires the *flp* gene cluster for microcolony formation in vitro. *Infect. Immun.* **70**:2965-2975.
148. **Nurse, P., K. H. Zavitz, and K. J. Marians.** 1991. Inactivation of the *Escherichia coli* priA DNA replication protein induces the SOS response. *J. Bacteriol.* **173**:6686-6693.
149. **Odenbreit, S., B. Gebert, J. Puls, W. Fischer, and R. Haas.** 2001. Interaction of *Helicobacter pylori* with professional phagocytes: role of the cag pathogenicity island and translocation, phosphorylation and processing of CagA. *Cell Microbiol* **3**:21-31.
150. **Odumeru, J. A., G. M. Wiseman, and A. R. Ronald.** 1984. Virulence factors of *Haemophilus ducreyi*. *Infect. Immun.* **43**:607-611.
151. **Odumeru, J. A., G. M. Wiseman, and A. R. Ronald.** 1985. Role of lipopolysaccharide and complement in susceptibility of *Haemophilus ducreyi* to human serum. *Infect. Immun.* **50**:495-499.
152. **Oldenborg, P. A., H. D. Gresham, and F. P. Lindberg.** 2001. CD47-signal regulatory protein  $\alpha$  (SIRP $\alpha$ ) regulates Fc $\gamma$  and complement receptor-mediated phagocytosis. *J. Exp. Med.* **193**:855-862.
153. **Orle, K. A., C. A. Gates, D. H. Martin, B. A. Body, and J. B. Weiss.** 1996. Simultaneous PCR detection of *Haemophilus ducreyi*, *Treponema pallidum*, and Herpes simplex virus types 1 and 2 from genital ulcers. *J. Clin. Microbiol.* **34**:49-54.
154. **Pacello, F., P. R. Langford, J. S. Kroll, C. Indiani, G. Smulevich, A. Desideri, G. Rotilio, and A. Battistoni.** 2001. A novel heme protein, the Cu,Zn-superoxide dismutase from *Haemophilus ducreyi*. *J. Biol. Chem.* **276**:30326-30334.
155. **Palmer, K. L., W. E. Goldman, and R. S. Munson, Jr.** 1996. An isogenic haemolysin-deficient mutant of *Haemophilus ducreyi* lacks the ability to produce cytopathic effects on human foreskin fibroblasts. *Mol. Microbiol.* **21**:13-19.
156. **Palmer, K. L., S. Grass, and R. S. Munson, Jr.** 1994. Identification of a hemolytic activity elaborated by *Haemophilus ducreyi*. *Infect. Immun.* **62**:3041-3043.
157. **Palmer, K. L. and R. S. Munson, Jr.** 1993. Identification of a hemolysin produced by *Haemophilus ducreyi* and isolation of a Tn916 transposon mutant, p. 75. *In* .

158. **Palmer, K. L. and R. S. Munson, Jr.** 1995. Cloning and characterization of the genes encoding the haemolysin of *Haemophilus ducreyi*. *Mol. Microbiol.* **18**:821-830.
159. **Palmer, K. L., C. T. Schnizlein-Bick, A. Orazi, K. John, C. Y. Chen, A. F. Hood, and S. M. Spinola.** 1998. The immune response to *Haemophilus ducreyi* resembles a delayed-type hypersensitivity reaction throughout experimental infection of human subjects. *J. Infect. Dis.* **178**:1688-1697.
160. **Palmer, K. L., A. C. Thornton, K. R. Fortney, R. S. Munson, Jr., and S. M. Spinola.** 1998. Evaluation of an isogenic hemolysin-deficient mutant in the human model of *Haemophilus ducreyi* infection. *J. Infect. Dis.* **178**:191-199.
161. **Parsons, N. J., P. V. Patel, E. L. Tan, J. R. C. Andrade, C. A. Nairn, M. Goldner, J. A. Cole, and H. Smith.** 1988. Cytidine 5'-monophospho-N-acetyl neuraminic acid and a low molecular weight factor from human blood cells induce lipopolysaccharide alteration in gonococci when conferring resistance to killing by human serum. *Microb. Pathog.* **5**:303-309.
162. **Pickett, C. L. and C. A. Whitehouse.** 1999. The cytolethal distending toxin family. *Trends Microbiol.* **7**:292-297.
163. **Plummer, F. A., J. N. Simonsen, D. W. Cameron, J. O. Ndinya-Achola, J. K. Kreiss, M. N. Gakinya, P. Waiyaki, M. Cheang, P. Piot, A. R. Ronald, and E. N. Ngugi.** 1991. Cofactors in male-female sexual transmission of human immunodeficiency virus type 1. *J. Infect. Dis.* **163**:233-239.
164. **Post, D. M., R. Mungur, B. W. Gibson, and R. S. Munson, Jr.** 2005. Identification of a novel sialic acid transporter in *Haemophilus ducreyi*. *Infect. Immun.* **73**:6727-6735.
165. **Prather, D. T., M. Bains, R. E. Hancock, M. J. Filiatrault, and A. A. Campagnari.** 2004. Differential expression of porins OmpP2A and OmpP2B of *Haemophilus ducreyi*. *Infect. Immun.* **72**:6271-6278.
166. **Purcell, B. K., J. A. Richardson, J. D. Radolf, and E. J. Hansen.** 1991. A temperature-dependent rabbit model for production of dermal lesions by *Haemophilus ducreyi*. *J. Infect. Dis.* **164**:359-367.
167. **Purven, M., E. Falsen, and T. Lagergard.** 1995. Cytotoxin production in 100 strains of *Haemophilus ducreyi* from different geographic locations. *FEMS Microbiol. Lett.* **129**:221-224.
168. **Purven, M. and T. Lagergard.** 1992. *Haemophilus ducreyi*, a cytotoxin-producing bacterium. *Infect. Immun.* **60**:1156-1162.

169. **Raivio, T. L. and T. J. Silhavy.** 1997. Transduction of envelope stress in *Escherichia coli* by the Cpx two-component system. *J. Bacteriol.* **179**:7724-7733.
170. **Raivio, T. L. and T. J. Silhavy.** 1999. The  $\sigma$ E and Cpx regulatory pathways: overlapping but distinct envelope stress responses. *Curr. Opin. Microbiol* **2**:159-165.
171. **Ramarao, N., S. D. Gray-Owen, S. Backert, and T. F. Meyer.** 2000. *Helicobacter pylori* inhibits phagocytosis by professional phagocytes involving type IV secretion components. *Mol. Microbiol* **37**:1389-1404.
172. **Rather, P. N., K. A. Solinsky, M. R. Paradise, and M. M. Parojcic.** 1997. aarC, an essential gene involved in density-dependent regulation of the 2'-N-acetyltransferase in *Providencia stuartii*. *J. Bacteriol.* **179**:2267-2273.
173. **Robinson, N. J., D. W. Mulder, B. Auvert, and R. J. Hayes.** 1997. Proportion of HIV infections attributable to other sexually transmitted diseases in a rural Ugandan population: simulation model estimates. *Int. J. Epidemiol.* **26**:180-189.
174. **Ronald, A. R. and F. A. Plummer.** 1985. Chancroid and *Haemophilus ducreyi*. *Ann. Intern. Med.* **102**:705-707.
175. **Rosenberger, C. M. and B. B. Finlay.** 2003. Phagocyte sabotage: disruption of macrophage signalling by bacterial pathogens. *Nat. Rev. Mol. Cell Biol.* **4**:385-396.
176. **Sambrook, J., E. F. Fritsch, and T. Maniatis.** 1989. Molecular cloning - a laboratory manual, 2nd Edition. Cold Spring Harbor Laboratory Press, Cold Spring Harbor, N.Y.
177. **San Mateo, L. R., M. M. Hobbs, and T. H. Kawula.** 1998. Periplasmic copper-zinc superoxide dismutase protects *Haemophilus ducreyi* from exogenous superoxide. *Mol. Microbiol.* **27**:391-404.
178. **San Mateo, L. R., K. L. Toffer, P. E. Orndorff, and T. H. Kawula.** 1999. Immune cells are required for cutaneous ulceration in a swine model of chancroid. *Infect. Immun.* **67**:4963-4967.
179. **San Mateo, L. R., K. L. Toffer, P. E. Orndorff, and T. H. Kawula.** 1999. Neutropenia restores virulence to an attenuated Cu,Zn superoxide dismutase-deficient *Haemophilus ducreyi* strain in the swine model of chancroid. *Infect. Immun.* **67**:5345-5351.
180. **Sarafian, S. K., T. C. Woods, J. S. Knapp, B. Swaminathan, and S. A. Morse.** 1991. Molecular characterization of *Haemophilus ducreyi* by ribosomal DNA fingerprinting. *J. Clin. Microbiol.* **29**:1949-1954.

181. **Segura, M., M. Gottschalk, and M. Olivier.** 2004. Encapsulated *Streptococcus suis* inhibits activation of signaling pathways involved in phagocytosis. *Infect. Immun.* **72**:5322-5330.
182. **Selbach, M., S. Moese, R. Hurwitz, C. R. Hauck, T. F. Meyer, and S. Backert.** 2003. The *Helicobacter pylori* CagA protein induces cortactin dephosphorylation and actin rearrangement by c-Src inactivation. *EMBO J.* **22**:515-528.
183. **Sell, S. and S. J. Norris.** 1983. The biology, pathology, and immunology of syphilis. *Int. Rev. Exp. Pathol.* **24**:203-276.
184. **Shao, F., P. M. Merritt, Z. Bao, R. W. Innes, and J. E. Dixon.** 2002. A *Yersinia* effector and a *Pseudomonas* avirulence protein define a family of cysteine proteases functioning in bacterial pathogenesis. *Cell* **109**:575-588.
185. **Shao, F., P. O. Vacratsis, Z. Bao, K. E. Bowers, C. A. Fierke, and J. E. Dixon.** 2003. Biochemical characterization of the *Yersinia* YopT protease: cleavage site and recognition elements in Rho GTPases. *Proc. Natl. Acad. Sci. U. S. A* **100**:904-909.
186. **Sheahan, K. L., C. L. Cordero, and K. J. Fullner Satchell.** 2004. Identification of a domain within the multifunctional *Vibrio cholerae* RTX toxin that covalently cross-links actin. *Proc. Natl. Acad. Sci. U. S. A* **101**:9798-9803.
187. **Sheldon, W. H. and A. Heyman.** 1946. Studies on chancroid: I. Observations on the histology with an evaluation of biopsy as a diagnostic procedure. *Am. J. Pathol.* **22**:415-425.
188. **Somani, A. K., J. S. Bignon, G. B. Mills, K. A. Siminovitch, and D. R. Branch.** 1997. Src kinase activity is regulated by the SHP-1 protein-tyrosine phosphatase. *J. Biol. Chem.* **272**:21113-21119.
189. **Sorensen, K. I. and B. Hove-Jensen.** 1996. Ribose catabolism of *Escherichia coli*: characterization of the rpiB gene encoding ribose phosphate isomerase B and of the rpiR gene, which is involved in regulation of rpiB expression. *J. Bacteriol.* **178**:1003-1011.
190. **Sozio, M. S., M. A. Mathis, J. A. Young, S. Walchli, L. A. Pitcher, P. C. Wrage, B. Bartok, A. Campbell, J. D. Watts, R. Aebersold, R. H. Van Huijsduijnen, and N. S. van Oers.** 2004. PTPH1 is a predominant protein-tyrosine phosphatase capable of interacting with and dephosphorylating the T cell receptor  $\zeta$  subunit. *J. Biol. Chem.* **279**:7760-7769.
191. **Spinola, S. M., M. E. Bauer, and R. S. Munson, Jr.** 2002. Immunopathogenesis of *Haemophilus ducreyi* infection (chancroid). *Infect. Immun.* **70**:1667-1676.

192. **Spinola, S. M., C. T. Bong, A. L. Faber, K. R. Fortney, S. L. Bennett, C. A. Townsend, B. E. Zwickl, S. D. Billings, T. L. Humphreys, M. E. Bauer, and B. P. Katz.** 2003. Differences in host susceptibility to disease progression in the human challenge model of *Haemophilus ducreyi* infection. *Infect. Immun.* **71**:6658-6663.
193. **Spinola, S. M., A. Castellazzo, M. Shero, and M. A. Apicella.** 1990. Characterization of pili expressed by *Haemophilus ducreyi*. *Microb. Pathog.* **9**:417-426.
194. **Spinola, S. M., K. R. Fortney, B. P. Katz, J. L. Latimer, J. R. Mock, M. Vakevainen, and E. J. Hansen.** 2003. *Haemophilus ducreyi* requires an intact *flp* gene cluster for virulence in humans. *Infect. Immun.* **71**:7178-7182.
195. **Spinola, S. M., T. J. Hiltke, K. R. Fortney, and K. L. Shanks.** 1996. The conserved 18,000-molecular-weight outer membrane protein of *Haemophilus ducreyi* has homology to PAL. *Infect. Immun.* **64**:1950-1955.
196. **Spinola, S. M., A. Orazi, J. N. Arno, K. R. Fortney, P. Kotylo, C.-Y. Chen, A. A. Campagnari, and A. F. Hood.** 1996. *Haemophilus ducreyi* elicits a cutaneous infiltrate of CD4 cells during experimental human infection. *J. Infect. Dis.* **173**:394-402.
197. **Spinola, S. M., L. M. Wild, M. A. Apicella, A. A. Gaspari, and A. A. Campagnari.** 1994. Experimental human infection with *Haemophilus ducreyi*. *J. Infect. Dis.* **169**:1146-1150.
198. **Stevens, M. K., L. D. Cope, J. D. Radolf, and E. J. Hansen.** 1995. A system for generalized mutagenesis of *Haemophilus ducreyi*. *Infect. Immun.* **63**:2976-2982.
199. **Stevens, M. K., D. J. Hassett, J. D. Radolf, and E. J. Hansen.** 1996. Cloning and sequencing of the gene encoding the Cu,Zn-superoxide dismutase of *Haemophilus ducreyi*. *Gene* **183**:35-40.
200. **Stevens, M. K., J. Klesney-Tait, S. R. Lumbley, K. A. Walters, A. M. Joffe, J. D. Radolf, and E. J. Hansen.** 1997. Identification of tandem genes involved in lipooligosaccharide expression by *Haemophilus ducreyi*. *Infect. Immun.* **65**:651-660.
201. **Stevens, M. K., S. Porcella, J. Klesney-Tait, S. R. Lumbley, S. E. Thomas, M. V. Norgard, J. D. Radolf, and E. J. Hansen.** 1996. A hemoglobin-binding outer membrane protein is involved in virulence expression by *Haemophilus ducreyi* in an animal model. *Infect. Immun.* **64**:1724-1735.
202. **Sun, J. and J. T. Barbieri.** 2003. *Pseudomonas aeruginosa* ExoT ADP-ribosylates CT10 regulator of kinase (Crk) proteins. *J. Biol. Chem.* **278**:32794-32800.

203. **Svensson, L. A., A. Tarkowski, M. Thelestam, and T. Lagergard.** 2001. The impact of *Haemophilus ducreyi* cytolethal distending toxin on cells involved in immune response. *Microb. Pathog.* **30**:157-166.
204. **Swanson, J. A. and A. D. Hoppe.** 2004. The coordination of signaling during Fc receptor-mediated phagocytosis. *J. Leukoc. Biol.* **76**:1093-1103.
205. **Throm, R. E., J. A. Al Tawfiq, K. R. Fortney, B. P. Katz, A. F. Hood, C. A. Slaughter, E. J. Hansen, and S. M. Spinola.** 2000. Evaluation of an isogenic major outer membrane protein-deficient mutant in the human model of *Haemophilus ducreyi* infection. *Infect. Immun.* **68**:2602-2607.
206. **Throm, R. E. and S. M. Spinola.** 2001. Transcription of candidate virulence genes of *Haemophilus ducreyi* during infection of human volunteers. *Infect. Immun.* **69**:1483-1487.
207. **Totten, P. A., W. R. Morton, A. M. Clark, G. H. Knitter, K. L. Eiffert, and W. E. Stamm.** 1993. Development of a primate model for chancroid, p. 200. *In* .
208. **Totten, P. A., D. V. Norn, and W. E. Stamm.** 1995. Characterization of the hemolytic activity of *Haemophilus ducreyi*. *Infect. Immun.* **63**:4409-4416.
209. **Towbin, H., T. Staehelin, and J. Gordon.** 1979. Electrophoretic transfer of proteins from acrylamide gels to nitrocellulose sheets: procedure and some applications. *Proc. Natl. Acad. Sci. USA* **76**:4350-4354.
210. **Trees, D. L., R. J. Arko, and S. A. Morse.** 1991. Mouse subcutaneous chamber model for *in vivo* growth of *Haemophilus ducreyi*. *Microb. Pathog.* **11**:387-390.
211. **Trees, D. L. and S. A. Morse.** 1995. Chancroid and *Haemophilus ducreyi*: an update. *Clin. Microbiol. Rev.* **8**:357-375.
212. **Tsutsumi, R., H. Higashi, M. Higuchi, M. Okada, and M. Hatakeyama.** 2003. Attenuation of *Helicobacter pylori* CagA x SHP-2 signaling by interaction between CagA and C-terminal Src kinase. *J. Biol. Chem.* **278**:3664-3670.
213. **Tyndall, M., P. J. Plourde, E. F. A. Agoki, W. Malisa, J. O. Ndinya-Achola, F. A. Plummer, and A. R. Ronald.** 1993. Ferozacin in the treatment of chancroid: an open study in men seropositive or seronegative for the human immunodeficiency virus type 1. *Am. J. Med.* **94**:85S-88S.
214. **UNAIDS.** 1997. Sexually transmitted diseases: policies and principles for prevention and care. World Health Organization, New York, N.Y.

215. **Vakevainen, M., S. Greenberg, and E. J. Hansen.** 2003. Inhibition of phagocytosis by *Haemophilus ducreyi* requires expression of the LspA1 and LspA2 proteins. *Infect. Immun.* **71**:5994-6003.
216. **van Oers, N. S., H. von Boehmer, and A. Weiss.** 1995. The pre-T cell receptor (TCR) complex is functionally coupled to the TCR-zeta subunit. *J. Exp. Med.* **182**:1585-1590.
217. **Wan, J. S. and M. G. Erlander.** 1998. Cloning differentially expressed genes by using differential display and subtractive hybridization, p. 45-68. *In* P. Liang and A. B. Pardee (ed.), *Differential Display Methods and Protocols*, vol. 85. Humana press, Inc., Totowa, NJ.
218. **Ward, C. K., J. L. Latimer, J. R. Nika, M. Vakevainen, J. R. Mock, K. Deng, R. J. Blick, and E. H. Hansen.** 2003. Mutations in the *lspA1* and *lspA2* genes of *Haemophilus ducreyi* affect the virulence of this pathogen in an animal model system. *Infect. Immun.* **71**:2478-2486.
219. **Ward, C. K., S. R. Lumbley, J. L. Latimer, L. D. Cope, and E. J. Hansen.** 1998. *Haemophilus ducreyi* secretes a filamentous hemagglutinin-like protein. *J. Bacteriol.* **180**:6013-6022.
220. **Ward, C. K., J. R. Mock, and E. J. Hansen.** 2004. The LspB Protein Is Involved in the Secretion of the LspA1 and LspA2 Proteins by *Haemophilus ducreyi*. *Infect. Immun.* **72**:1874-1884.
221. **Weiser, J. N. and E. C. Gotschlich.** 1991. Outer membrane protein A (OmpA) contributes to serum resistance and pathogenicity of *Escherichia coli* K-1. *Infect. Immun.* **59**:2252-2258.
222. **Wood, G. E., S. M. Dutro, and P. A. Totten.** 1999. Target cell range of *Haemophilus ducreyi* hemolysin and its involvement in invasion of human epithelial cells. *Infect. Immun.* **67**:3740-3749.
223. **Wood, G. E., S. M. Dutro, and P. A. Totten.** 2001. *Haemophilus ducreyi* inhibits phagocytosis by U-937 cells, a human macrophage-like cell line. *Infect. Immun.* **69**:4726-4733.
224. **Yanofsky, C.** 2004. The different roles of tryptophan transfer RNA in regulating trp operon expression in *E. coli* versus *B. subtilis*. *Trends Genet.* **20**:367-374.
225. **Young, R. S., K. Fortney, J. C. Haley, A. F. Hood, A. A. Campagnari, J. Wang, J. A. Bozue, R. S. Munson, Jr., and S. M. Spinola.** 1999. Expression of sialylated or paragloboside-like lipooligosaccharides are not required for pustule formation by *Haemophilus ducreyi* in human volunteers. *Infect. Immun.* **67**:6335-6340.



226. **Young, R. S., K. R. Fortney, V. Gelfanova, C. L. Phillips, B. P. Katz, A. F. Hood, J. L. Latimer, R. S. Munson, E. J. Hansen, and S. M. Spinola.** 2001. Expression of cytolethal distending toxin and hemolysin is not required for pustule formation by *Haemophilus ducreyi* in human volunteers. *Infect. Immun.* **69**:1938-1942.
227. **Zhu, M., F. Shao, R. W. Innes, J. E. Dixon, and Z. Xu.** 2004. The crystal structure of *Pseudomonas* avirulence protein AvrPphB: a papain-like fold with a distinct substrate-binding site. *Proc. Natl. Acad. Sci. U. S. A* **101**:302-307.

## VITAE

Jason Robert Mock was born on February 7, 1977 in Urbana, Illinois, the son of Mary Ann Mock and Richard Edwin Mock. At the age of five, Jason moved from Philo, Illinois to Amarillo, Texas where he began school shortly after his younger sister, Cynthia, was born. After the first day of kindergarten, he demonstrated his interest in higher education by expressing to his mother that he was worried that “I don’t know, mom, college is going to be really hard”. However, these early concerns aside he graduated from Amarillo High School in 1995, and received his Bachelor of Science degree in Genetics *summa cum laude* from Texas A&M University in 1999. During his senior year, he received the first annual Student Worker of the Year Award. Since 1999, he has been enrolled at the University of Texas Southwestern Medical Center. During his studies, he has served as a teaching assistant for the Medical Microbiology laboratory course, and as a lecturer at the Dallas County HIV and STD prevention center. He currently lives in Dallas, Texas.

Permanent Address: 7920 Fenley  
Amarillo, Texas 79121